Polyatomic London Dispersion Forces and NMR Gas-to-Liquid Chemical Shifts

By

Mansur Sultan-Mohammadi, B.Sc., M.Sc. (Tehran), M.Sc. (B'ham)

A thesis presented for the degree of Ph.D of
Aston University.

May, 1986.

A Thesis Presented for the Degree of Doctor of Philosophy
By

Mansur Sultan-Mohammadi

May 1986

One of the most recent attempts to characterize inter-molecular dipersion forces is due to Homer and Percival, who used a modified Onsager-type reaction field approach coupled with the "buffeting" theory which accounts for the intimate effects of molecular encounters. In this thesis their overall approach is evaluated and compared with the theories of other workers that have been used to characterize NMR gas-to-solution chemical shifts. It is shown that an extended "buffeting" concept, based on their approach, renders the reaction field part of their theorem obsolete.

A completely novel generalized expression for London dispersion forces is deduced by accounting for all the inter-molecular atom-atom dispersion interactions. In arriving at this expression three fundamental problems are resolved. First, a general order relationship between the mean squares of the fluctuating input and output of any system is derived to permit transformation of electrostatic expressions to electrodynamic situations. Second, a novel method is presented for characterizing the ionization potentials and polarizabilities of bonded atoms in terms of the corresponding properties of the appropriate inert atoms. Third, the average of the inverse-sixth-power of the inter-molecular atomic separation that governs dispersion forces is evaluated for molecules that are subject to random thermal motion in the liquid state; the explicit analytical expression so obtained is confirmed by the MONTE CARLO technique.

The principles implicit in resolving the three stated problems are embodied in a theorem that enables the characterization of polyatomic inter-molecular mean-square fluctuating fields and the corresponding potential energies. The resulting equations are tested exhaustively and shown to enable the precise characterizations of NMR gas-to-solution shifts and latent heats of vaporization. Moreover, the equations are used to explain the relative solubilities of various gases in selected solvents and the corresponding activity coefficients.

The limitations of the general approach to slowly rotating large molecules are recognized and evidence is given for the fact that for this type of molecules the inter-molecular potentials can be calculated using a simple solute-(solvent)atom additivity principle.

Key Words

NMR van der Waals-Nuclear Screening
Generalized Reaction Field Theory
Generalized London Dispersion Potential or Buffeting Potential
Inert-Atom Additivity Rule for Molecular Ionization Potential
Heat of Vaporization

Acknowledgments

I would like to thank the following people who helped to make this work possible.

For help, perpetual encouragement, and problem-solving comments my supervisor Dr. J. Homer.

For much patience, love, moral support, and the design of the Greek letters my wife Soheyla.

For constructive criticism and rendering of the graphs Dr. F. Zamani.

For Z80-Machine Code version of the MONTE CARLO program, equations and graphs of Appendices 3 and 4 Mr. E. Creighton (from EVODE Ltd. Stafford).

For help and computer time Mr. R. Withwood (from EVODE Ltd.).

For careful editing of the manuscript Miss P. Clifford, and for help Mrs. S. Dirdin.

For proof-reading and editorial suggestions Mr. A. Kendall.

For encouragement and help my colleagues (in particular Mr. S. Patel, and Mr. J. Roberts) in the NMR laboratory.

I wish also to express my sincere gratitude for the vital financial support given to me by the International Family Service (in particular Mrs. J. Jones, the Director), and EVODE Ltd. Stafford.

Thanks are also due to then Department of Chemistry, Aston University, for financial support following the period of ORS support during the early stages of the work.

<u>Contents</u>

Chapter 1

Generalized Reaction Field Theory

Chapter 2

Reaction Field Characterization of the van der Waals Screening Constant

Chapter 3

Polyatomic London Potential

Chapter 4

Comparison between the Site-Factor and Buffeting Theories of the van der Waals Nuclear Screening

Chapter 5

Polyatomic Dispersion Field and van der Waals Nuclear Screening Constant

Chapter 6

The Buffeting Interaction and Solubility of Gases in Liquids

Appendices

Tables

Illustrations

Chapter 1

Generalized Reaction Field Theory

Introduction

The reaction field characterization of the van der Waals nuclear screening constant brings out an interesting enigma concerning the equality of the Onsager's electrostatic reaction field formula with a corresponding electrodynanic formulation.

This enigma in turn triggers a more general question about the identity of *electrostatic* expressions with corresponding *dynamic* ones. The question arises whether or not the dipole-static field potential energy is equivalent to the dipole-oscillating field potential energy.

This chapter deals with finding the ever-elusive answer to this enigma, by grafting three pieces of text-book mathematics, the Green's function or convolution integral solution of a linear differential equation, the Fourier Transform, and the Hilbert Space.

Manipulation of these three well-known theories in the time domain leads to a new general inequality between the mean squares of the causes (inputs) and effects (outputs), which for reaction field reads $\langle R^2 \rangle \leqslant g^2 \langle m^2 \rangle$. The shortcomings of the inequality are offset by the simplicity and more importantly the generality of the method.

The inequality is a direct consequence of working in the time domain. The frequency domain solution of this problem, which should result in an equality, is quite a formidable task considering the fact that integrals involved are quadratic in 'g', the <u>transfer function</u> of the system. This is why Linder, who pioneered the dynamic reaction field (RF) work, uses the RF-moment correlation function, $\langle R(t).m(t)\rangle$, instead of the RF auto-correlation function, $\langle R(t).R(t')\rangle$, which results in a straightforward RF-moment relation.

The stated equality is found by defining a mean potential energy for dynamic processes, based on the inequality, and equating it to Linder's or London's potential formula. For RF this procedure works out as, $\langle R^2\rangle = (1/16)g^2 \langle m^2\rangle$.

The factor of 1/16 is the answer to the enigma, in that the use of Onsager's static RF formula for an oscillating dipole over-estimates the calculated values of van der Waals screening constant $\sigma_w = - B \langle R^2\rangle$ by a factor of 16. This is a setback for the RF characterization of σ_w which is already suffering a shortfall from the experimental values by about one order of magnitude.

It is shown that the orthodox supposition that potential energy, being a static quantity, justifies the use of electrostatic expressions in place of an electrodynamic one is groundless.

It is also shown that London's dispersion potential formula can be derived from two expressins only.

The inequality is used further for some general fluctuation problems including Brownian motion and thermal noise in electrical systems.

Note that the vector quantities are not denoted unless the results could be affected by the absence of a vector sign.

1.1. Historical Background

This section aims at a non-mathematical introduction of the reaction field notion by a chronicle of the developments and shortcomings of dielectric theories.

1.1.1 Onsager Reaction Field Theory of polar molecules

Studies and experiments on dielectric materials stimulated attempts to correlate the dielectric constant, $\varepsilon > 1$, with the microscopic structure of matter.

In 1836, Mossotti[1] -after Faraday[2] who considered insulating materials (coined by him as dielectrics) as conducting spheres in a non-conducting medium- assumed molecules to be equivalent to conducting spheres of radius 'a'. Under the influence of an applied electrostatic field E_o, the charge on the sphere would readjust or polarize itself inducing a non-zero electric dipole moment, $\mu_{in} = \alpha E_o$, where α is the (volume) polarizability.

He derived a relationship between the dielectric constant ε, and the polarizability of molecules, which was derived again in 1879 by Clausius[3,4];

$$V \frac{(\varepsilon - 1)}{(\varepsilon + 2)} = (4\pi/3)L\,\alpha \qquad \text{Mossotti-Clausius Eq.} \qquad (1.1)$$

where V and L are respectively molar volume and Avogadro's number. Physically, this expression means that the departure of ε of materials from unity is caused by the polarization of their molecules.

A corresponding expression for refractive index, 'n', given by Lorenz[2] in Denmark (1880), and Lorentz[2,5] in Holland (1880) proved its validity by using Drude's oscillatory model of electrons[6, see sec. 1.8];

$$V \frac{(n^2 - 1)}{(n^2 + 2)} = (4\pi/3)L\,\alpha \qquad \text{Lorentz-Lorenz Eq.} \qquad (1.2)$$

Fundamental to the derivation of (1.1) and (1.2) are two concepts. First the <u>local field</u>[1] or the field at the site of a molecule[7,8] in a spherical cavity, E_L (further details of which are given in the following chapter);

$$E_L = E_o + (4\pi/3)P \qquad (1.3)$$

where P is the polarization caused by the external field E_o. Second, the additivity rule (due to Lorentz) which states that polarization equals the sum of all the molecular induced dipoles;

$$P = L\,E_L\alpha/V \qquad (1.4)$$

Comparison with the experimental data showed that the right-hand side of (1.2) is a true constant for a particular molecule, namely independent of temperature, but the right-side of (1.1) is not in general a constant and in some cases it depends on temperature[4]. Experiments also confirmed the correction term of $(4\pi/3)P$ for the local field.

Amongst the proposed suggestions to explain the invalidity of

(1.1) for some compounds, the most useful proved to be Debye's (1912) idea of attributing a permanent electric dipole moment, to molecules[1,2,4,9]. The electric dipole is not solely due to the distortion of electrons by E_o, namely μ_{in}, but if the molecule has a permanent dipole μ in the absence of E_o, then the temperature dependence of (1.1) can be satisfactorily explained.

A magnetic susceptibility due entirely to the orientation of permanent dipoles was suggested in 1905 by Langevin[1,2]. Debye took the local field approach and adapted the Langevin formula for the electric case to arrive at;

$$V \frac{(\varepsilon - 1)}{(\varepsilon + 2)} = (4\pi/3)L\ (\alpha + \mu^2/3kT) \qquad \text{Debye's Eq.}\ (1.5)$$

We, therefore, deduce the existence of two kinds of polarizability, namely electronic α, and, orientational due to the thermal motion of molecules, $\alpha_{OR} = \mu^2/3kT$.

Quantum mechanical (QM) calculations essentially confirmed Debye's Eq.[1,4,10,11];

$$V \frac{(\varepsilon - 1)}{(\varepsilon + 2)} = (4\pi/3)L\ [\alpha + (\mu^2/3kT)(1 - f(T))] \qquad \text{QM Eq.}$$

where the correction factor f(T) is negligible except at extremely low temperatures.

The Debye's Eq. did not work for polar liquids in which the molecules are so close together that the orientation in E_o is restricted by the mutual interaction of their dipoles. The molar polarizabilities of O_2 and N_2 gases, for example, are 3.869 and 4.395 cm^3/mole with the corresponding liquid state values of 3.878 and 4.396[12], whereas they are 4 and 18 for vapour and liquid water respectively. The discrepancy for water in the two states is nevertheless only about 10%[1] for Lorentz-Lorenz Eq.

van Arkel and Snoek[13] added a term to 3kT in Debye's Eq. to arrive at;

$$V \frac{(\varepsilon - 1)}{(\varepsilon + 2)} = (4\pi/3)L\ [\alpha + \mu^2/(3kT + CL\mu^2)] \qquad (1.6)$$

where C is a constant. This expression was found to agree with experiments for all concentrations[4]. However, it did not work for a number of compounds supposed to undergo association, including alcohols, acids, and amines.

In 1936, Onsager[14] explained the deviation of polar liquids from the original Debye's theory by a fundamental change in (1.1). He assumed that part of the local field (1.3) which acts on the dipole, is in fact produced by induction in the surrounding dielectric by the dipole itself. This part of the local field which has come to be called the Reaction Field (RF), R does not act in the direction of the external field E_o, but it acts in the direction of the inducing dipole μ. Therefore it cannot give a torque on the original dipole. In other words the RF is not effective in the orientation of the permanent dipole. Therefore the directing or orientating field to be used in Debye's approach is not E_L, but E_d;

$$E_d = E_L - R \cos \theta$$

where θ is an average angle between μ and E_o. The use of E_d in Debye's method now gives;

$$V \frac{(\varepsilon - 1)}{(\varepsilon + 2)} = (4\pi/3)L\ [\alpha + \mu^2/(3kT + \mu R)] \qquad (1.7)$$

This is of the same form as (1.6) with $\mu R = CL\mu^2$. Onsager deduced the value of R for a molecule with a rigid permanent dipole μ, in a spherical cavity of radius 'a' (see Chapter 2) to be[3,4];

$$R = g\ \mu \tag{1.8}$$

where 'g', the RF parameter is given by;

$$g = \frac{2(\varepsilon - 1)}{(2\varepsilon + 1)} \frac{1}{a^3} \tag{1.9}$$

The formalism of the RF was greatly simplified by using the continuum model, developed by Martin and Bell[15]. In this model the permanent dipole at the centre of a spherical cavity interacts with its entire surrounding, which is viewed as a continuous medium. The field of the dipole polarizes the continuum giving rise to R which is proportional to the dipole.

1.1.2. Reaction Field Theory of Non-polar Molecules

Finding the RF technique restricted to polar compounds and therefore restricted to the electrostatic interactions, Linder[16] in 1960 developed a continuum model for non-polar molecules $\mu = 0$ which enabled the RF technique to characterize dispersion interactions.

He considered a spherical molecule of radius 'a' in which the rapid oscillations of the electrons about the nuclei give rise to an instantaneous dipole moment m(t), the mean value of which is zero, $\langle m(t) \rangle = 0$. The field associated with m(t) polarizes the uniform dielectric medium which surrounds the molecule. The degree of the polarization depends on the dielectric constant ε which is now different for static and time-dependent fields. By assuming that, m(t) oscillates with frequency ω_i, the molecules of the dielectric all oscillate with frequency ω_j, and the fields induced in the molecules of the medium are additive (1.4) Linder found;

$$R(t) = g_j m_i(t) \frac{\omega_j^2}{(\omega_j^2 - \omega_i^2)} \tag{1.10}$$

where g_j is given by (1.9). The oscillating RF, R(t), has a vanishing mean value because $\langle m(t) \rangle = 0$, but the mean of the square of R(t), namely $\langle R^2(t) \rangle$, is finite.

The expression of such a mean-square RF for oscillating moment however is not given by Linder. As Rummens[17] puts it "... one might ask why Linder, having arrived at (1.10), did not simply square it to obtain a useable $\langle R^2 \rangle$. The reason appears to be that averaging over the frequency distributions becomes quite intractable. It is only in the expression for the work 'W' that a neat trick ($\alpha_i g_j \simeq \alpha_j g_i$) makes this averaging feasible".

Linder[16,18,19] arrives at a new unorthodox relationship for the dynamic potential energy betwwen an oscillating moment and its induced RF;

$$W = -(1/2)\ y \langle m^2 \rangle\ g \qquad \text{where} \quad y = 1/4 \tag{1.11}$$

This result is in sharp contrast to the orthodox view[3,20] that potential energy as a static quantity justifies the use of electrostatic potential energy, namely $-(1/2) \langle m^2 \rangle$ g.

The interpretation of (1.11) is straightforward. A direct "mapping" or transformation of an electrostatic expression ($y = 1$) into a dynamic one ($y < 1$) is erroneous.

1.1.3. Reaction Field of Non-polar molecules in NMR

The RF technique finds its own use in a variety of problems including the solvent effects studies in NMR, biochemistry[21], spectral shifts[22], and bond intensities[23]. Consequently the lack of a dynamic R(t)-m(t) relationship, analogous to the static expression (1.8), is more and more evident.

The lack of such relationship for the RF characterization of the van der Waals nuclear screening constant according to $\sigma_w = - B \langle R^2 \rangle$ (see Chapter 2) in NMR studies, is circumvented by either of the two following methods:

(a) Equating Linder's work function (1.11) with the potential energy of a polarizable molecule in a static field[24,25];
$U = -(1/2)\ \alpha E_0^2$
This expression is assumed by Linder to hold for the dynamic field -in contradiction of his own result on 'W'- provided that E_0^2 is disguised as a mean-square field, $\langle E^2 \rangle$ to obtain the erroneous expression $\langle E^2 \rangle = (1/4)\ g\ \langle m^2 \rangle / \alpha$, which is used in place of $\langle R^2 \rangle$.

(b) Direct mapping of the static relationship (1.8) into the dynamic one[26-29]; that is $\langle R^2 \rangle = g^2\ \langle m^2 \rangle$. This is obtained by squaring (1.8), and using m for μ and the averaging sign $\langle \rangle$. As (1.10) shows, such mapping appears to be invalid unless the mean of the square of the frequency function becomes unity.

The purpose of this chapter is therefore to investigate rigorously the validity of the direct mapping.

1.2. Generalized Reaction Field Formula

It is well-known that for any arbitrary variable electric field the conventional electrostatic definition of the dielectric constant, $D = \varepsilon_o E_o$, is no longer valid and has to be superseded by a general expression which accommodates the fact that the electric polarization of matter cannot keep pace with the change in the field[3,20,30,31];

$$D(t) = E(t) + \int_{-\infty}^{\infty} E(\tau) f(t - \tau) d\tau \qquad (1.12)$$

where the Fourier Transform of f(t) is the frequency-dependent dielectric constant $\varepsilon(\omega)$. This relationship states that the value of D at any given instant 't' is determined not only by the value of E(t) at that instant, but depends on the values of E(t) at every previous instant.

This section is devoted to the derivation of a similiar relationship for RF, when the moment varies with time. We begin with the barest essential, a differential equation, and develop it into a general expression for R.

1.2.1. Linear Systems and Differential Equations

Many physical systems are governed by a class of equations called Linear Differential Equations with constant coefficients;

$$\sum_n a_n \frac{d^n Y(t)}{dt^n} = X(t) \qquad (1.13)$$

Forced oscillations, Y(t), of a body of mass 'm' on a spring of spring constant 'k' and damping 'h', for example, can be written as[32,33];

$$m \frac{d^2 Y(t)}{dt^2} + h \frac{dY(t)}{dt} + k\, Y(t) = X(t) \qquad (1.14)$$

Further examples are:

$$L \frac{d^2q(t)}{dt^2} + R \frac{dq(t)}{dt} + \frac{1}{C} q(t) = V(t) \tag{1.14a}$$

D.Eq. for the charge q in RLC-circuit[33].

$$ml \frac{d^2\theta(t)}{dt^2} + h \frac{d\theta(t)}{dt} + mg\, \theta(t) = 0 \tag{1.14b}$$

D.Eq. for the small oscillations, θ, of a simple pendulum[33].

$$m \frac{d^2X(t)}{dt^2} + h \frac{dX(t)}{dt} + \omega_o m\, Y(t) = eE(t) \tag{1.14c}$$

D.Eq. for the oscillations, X, of electrons under oscillating electric field of light E(t)[32].

If X(t) in (1.13) is regarded as an external force or input, which drives the system, and Y(t) as the response or output of the system, the left-side of the equation embodies the internal physical properties and charactaristics of the system. In fact the amount by which the system responds to an external or driving force is embodied in operator $\sum_n a_n d^n/dt^n$.

Sometimes sufficient information about the system allows its accurate modelling by a D.Eq., but more often a system is available only as a black box in such way that the relationship between the input and output cannot be so derived.

The back box representations of the continuum (as a system) in the RF theory and that in (1.13), for example, are depicted in Fig. 1.1.

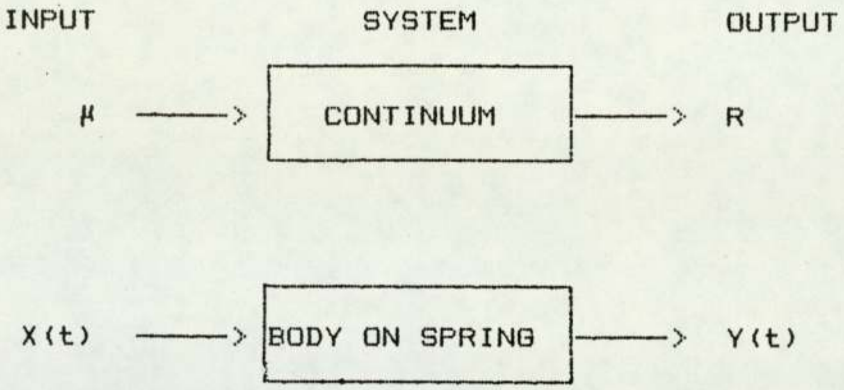

Fig. 1.1. Black Box Representation of a System.

1.2.2. Solution of the Linear Differential Equation

The steady-state solution of (1.14) in terms of the response or Green's function of the system, G(t), can be written as[35-40];

$$Y(t) = \int_{-\infty}^{\infty} G(t - \tau)X(\tau)\, d\tau$$

where the Green's function can be thought of as a weighting factor which describes how much the past input, $X(\tau)$, $-\infty < \tau < t$, influences the present output Y(t).

This interpretation is parallel to the one given for (1.12) at the onset of this section. This Eq. is the integral form of (1.14) which is particularly useful when the internal elements and the physical laws that relate them cannot be analysed and used to derive the D.Eq. of the system. In other words the integral or convolution form of a D.Eq. is useful when the system is known only as a black box, like the continuum system.

A time-varying electric moment, m(t), acts on the continuum as a driving force or input and results in an output, R(t), which is therefore of the form;

$$R(t) = \int_{-\infty}^{\infty} G(t - \tau) m(\tau) d\tau \qquad (1.15)$$

This type of expression conveys a simple message. It states that for a time-varying dipole the Onsager's RF, in contrast to the static case (1.8), takes the form of $R(t) = g(\omega)\ m(t)$, where $g(\omega)$ is the frequency-dependent RF parameter (see sec. 1.8).

This is analogous to an electric system with alternative current input $I(t)$, in which the Ohm's law (equivalent of Onsager's RF) is no longer $V = R\ I$, but $V(t) = Z(\omega)\ I(t)$, where $Z(\omega)$ is the system impedence, Fig. 1.2.

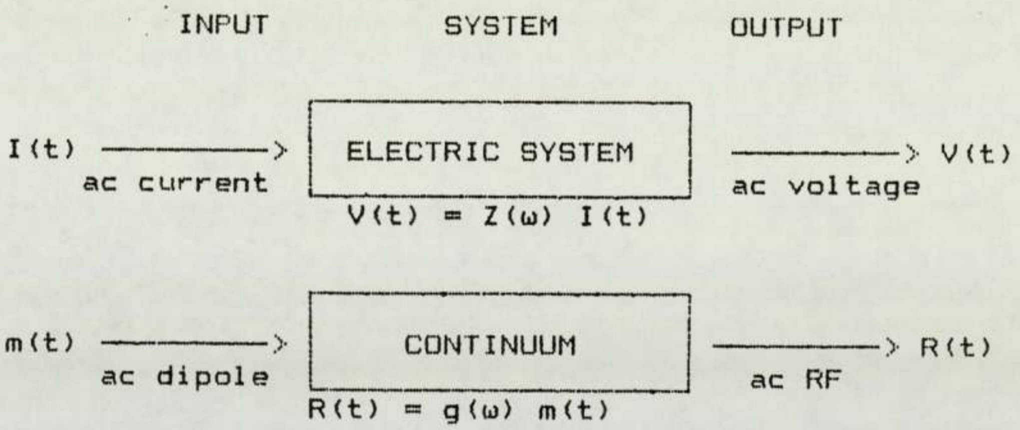

Fig. 1.2. Black Box Representation of Electric and Continuum Systems.

The input-output of any Linear system can be described by (1.15) which here is the <u>generalized reaction field</u> formula and has been used by Linder in his RF theory[18,19].

The underlying assumption of this Eq. is the linearity of the system. That is, the independence of the behaviour of the system and the magnitude of the input, $m(t)$, which of course is an idealization but often a good one[34]. To proceed further the Fourier Integrals have to be introduced.

1.3. Fourier Transform of the Generalized RF formula

Amongst different definitions of Fourier Integrals[42,43,44], the Pippard[42] and Lifshitz-Pitaevskii[43] forms are adopted here to resolve the time-dependent input, output, and the Green's function into their Fourier Transforms (FT);

$$F(t) = (1/2\pi) \int_{-\infty}^{\infty} F(\omega)\, e^{-i\omega t}\, d\omega \qquad (1.16)$$

$$F(\omega) = \int_{-\infty}^{\infty} F(t)\, e^{i\omega t}\, dt \qquad (1.17)$$

Hereafter, it is understood that the lower and the upper limits on the intgrals are respectively $-\infty$ and $+\infty$.

Any function like F(t) can be considered as a superposition of harmonics ($e^{-i\omega t} = \exp(-i\omega t) = \cos \omega t - i \sin \omega t$) with different amplitudes, a_k, and frequencies, ω_k, such that;

$F(t) = \Sigma\, a_k \exp(-i\omega_k t)$

where the set of frequencies, ω_k, is called the spectrum of the function F(t). Expression (1.16) is the continuous form of this sum, where $F(\omega)d\omega$ represents the amplitude corresponding to the frequency interval $d\omega$. That is why the function $F(\omega)$ has come to be called the 'spectral density' of F(t).

Now, the FT of R(t), m(t), and G(t) can be written as;

$$R(t) = (1/2\pi) \int R(\omega) \exp(-i\omega t)\, d\omega \qquad (1.18)$$

$$R(\omega) = \int R(t) \exp(i\omega t)\, dt \qquad (1.19)$$

$$m(t) = (1/2\pi) \int m(\omega) \exp(-i\omega t)\, d\omega \qquad (1.20)$$

$$m(\omega) = \int m(t) \exp(i\omega t)\, dt \qquad (1.21)$$

$$G(t) = (1/2\pi) \int g(\omega) \exp(-i\omega t)\, d\omega \qquad (1.22)$$

$$g(\omega) = \int G(t) \exp(i\omega t)\, dt \qquad (1.23)$$

The Onsager's RF formula can be retrieved from (1.15) by setting $m(t) = \mu$ and using (1.23);

$$R(t) = \int m(\tau)\, G(t - \tau)\, d\tau = \mu \int G(t - \tau)\, d\tau$$

Letting $t - \tau = s$, so that $d\tau = -ds$, one gets;

$$R(t) = \mu \int G(s)\, ds$$

(Note that the integral limits reverse when s changes to τ, because τ is equivalent to -s)

The integral is $g(\omega = 0)$, because from (1.23);

$$g(0) = \int G(s) \exp(it0)\, ds = \int G(s) ds \qquad (1.24)$$

so that R(t) becomes;

$$R(t) = R\, \mu\, g(0) = \mu\, g$$

From this result (1.9), in terms of the frequency dependent, and static dielectric constants can be written as;

$$g = g(0) = \frac{2(\varepsilon_o - 1)}{(2\varepsilon_o + 1)\, a^3} \quad ; \; g(w) = \frac{2(\varepsilon(\omega) - 1)}{(2\varepsilon(\omega) + 1)\, a^3} \qquad (1.25)$$

where $g(\omega)$, the FT of G(t) according to (1.23), is called the <u>Transfer Function</u> of the system.

We seek a relationship between the mean squares of R, $\langle R^2 \rangle$, and m, $\langle m^2 \rangle$, which entails the knowledge of the Fourier Transform of these quantities presented in the next section.

1.4. Concept of Fluctuation

The basic concepts of the mean and mean-square of fluctuation, and their FT are outlined here to form the cornerstone of the R-m relationship.

1.4.1. Definition of Fluctuation

Experiments designed to measure the same physical quantity, which describes a system in equilibrium, almost always give the mean value of that quantity. Nevertheless, regardless of the nature of the measurements there will be deviations from, or fluctuations about the mean value[43,45].

Let us throughout this section, consider the generalized RF, R(t), as fluctuating or random variable quantity related to the macroscopic continuum system. At any instance of time R(t) fluctuates about its mean value, $\langle R\rangle$, so that;

$$\Delta R(t) = R(t) - \langle R\rangle \qquad (1.26)$$

denotes the fluctuations of R . The mean of these fluctuations $\langle \Delta R(t)\rangle$ is zero because $\Delta R(t)$ can be both positive and negative. The square of the fluctuations, $(\Delta R(t))^2$, however, is always positive, so its mean value, $\langle (\Delta R)^2\rangle$, forms a suitable measure of the mean of the fluctuations;

$$\langle (\Delta R)^2\rangle = \langle\ (R(t) - \langle R\rangle)^2\ \rangle = \langle\ R(t)^2 + \langle R\rangle^2 - 2R(t)\langle R\rangle\ \rangle$$

$$\langle (\Delta R)^2\rangle = \langle R^2\rangle + \langle R\rangle^2 - 2\langle R\rangle\langle R\rangle = \langle R^2\rangle - \langle R\rangle^2 \qquad (1.27)$$

This mean-square quantity is an average of second order[46] which is also called the second moment of R(t) about its mean because of the analogy between this and the moment of inertia in mechanics[47,48].

The mean value of a time function R(t) is defined as;

$$\langle R(t)\rangle = \lim_{T\to\infty} \frac{1}{2T} \int_{-T}^{T} R(t)dt \qquad (1.28)$$

It is simply the area under the R(t)-t curve in the interval; -T to +T, divided by the length of the interval, 2T, as the length of the interval becomes infinite. Substituting for R(t) from (1.15) into (1.28);

$$\langle R(t)\rangle = \lim_{T\to\infty} \frac{1}{2T} \int_{-T}^{T} dt \int G(t - \tau)\, m(\tau)d\tau$$

which can be written as (convolution is commutative[34]);

$$\langle R(t)\rangle = \lim_{T\to\infty} \frac{1}{2T} \int_{-T}^{T} dt \int G(\tau)\, m(t - \tau)d\tau$$

The rearranging of the integrals gives;

$$\langle R(t)\rangle = \lim_{T\to\infty} \frac{1}{2T} \int_{-T}^{T} m(t - \tau)dt \int G(\tau)d\tau$$

The value of the first integral is $\langle m(t)\rangle$, the mean value of m(t), by analogy with (1.28). This is so because a translation of m(t) by an amount τ does not affect its mean value. The second integral is the static RF parameter g(0), according to (1.24), therefore;

$$\langle R(t)\rangle = \langle m(t)\rangle\, g(0) \qquad (1.29)$$

where $\langle m(t)\rangle = 0$, and as a result, $\langle R(t)\rangle = 0$.

According to (1.29) the mean value of the output of a Linear system equals the mean value of the input times the static transfer function of the system, or, using electrical engineering terminology, the dc gain of the system[34].

Substituting $\langle R\rangle = 0$ into (1.27) gives; $\langle(\Delta R)^2\rangle = \langle R^2\rangle$, stating that for zero mean value the mean of the square of fluctuations is equivalent to the mean-square value, $\langle R^2\rangle$.

This, of course, does not mean that in the presence of mean values the fluctuations lack any physical significance. Fluctuations in density, and fluctuations in internal energy, for example, account respectively, for the scattering of light and the anomalous large specific heats at constant volume near the critical points[49].

1.4.2. Fourier Analysis of Mean-square quantities

The mean-square values of $R(t)$ and $m(t)$ are related to their spectral densities $R(\omega)$ and $m(\omega)$ by[43,47];

$$\langle R^2\rangle = (1/2\pi) \int |R(\omega)|^2 \, d\omega$$

$$\langle m^2\rangle = (1/2\pi) \int |m(\omega)|^2 \, d\omega \qquad (1.30)$$

The proof of (1.30), which is avoided here because it entails the mathematics of Dirac Delta function[36,50-52], is given by Lifshitz and Pitavskii[43].

A physical interpretation of (1.30) may be given if $R(t)$ or $m(t)$ is considered as wave or voltage wave forms. Classically the energy in a wave is proportional to the square of its amplitude or as Ditchburn[53] puts it, the energy associated with the frequency range $d\omega$ is;

$$E(\omega)d\omega = (1/2\pi) \, |R(\omega)|^2 \, d\omega$$

$$E(\omega)d\omega = (1/2\pi) \, |m(\omega)|^2 \, d\omega \qquad (1.31)$$

The integration of (1.31) for all frequencies reproduces (1.30).

Considering R(t) or m(t) as voltage wave forms applied across a one Ohm resistor; $\langle R^2 \rangle$ or $\langle m^2 \rangle$ are then equivalent to the mean power dissipated by the resistor[34]. Note that this generalized definition of mean power is the same whether R(t) is accelerator, voltage, displacement, and so forth[54].

The mean-square values are also related to their time functions by Parsaval's or Rayleigh's theorem[44,53,55];

$$\int |R(t)|^2 \, dt = (1/2\pi) \int |R(\omega)|^2 \, d\omega$$

$$\int |R(t)|^2 \, dt = (1/2\pi) \int |R(\omega)|^2 \, d\omega \qquad (1.32)$$

Relationships of this form were first used by Rayleigh[56] in his study of black-body radiation. Comparison between (1.30) and (1.32) gives;

$$\langle R^2 \rangle = \int |R(t)|^2 \, dt$$

$$\langle m^2 \rangle = \int |m(t)|^2 \, dt \qquad (1.33)$$

to be used in the time-domain analysis in section 1.6. First a brief account of Hilbert space is required.

1.5. Hilbert Space and the Buniakauski Inequality

In the ordinary 3-dimensional Cartesian space, the scalar product of two vectors is given by;

$\overline{r}_1 . \overline{r}_2 = |r_1| \; |r_2| \cos \theta$

where θ is the angle between the two vectors. As $|\cos \theta| \leqslant 1$ one may rewrite this equality in the form of an order relation known as Schwarz's inequality[57];

$\bar{r}_1.\bar{r}_2 \leqslant |r_1|\cdot|r_2|$

In terms of the components of the vectors;

$r_1 = \{x_1, x_2, x_3\}$; $r_2 = \{y_1, y_2, y_3\}$

the inequality reads;

$$\bar{r}_1.\bar{r}_2 = \sum_{i=1}^{3} x_i\ y_i \leqslant \sum_{i=1}^{3} (x_i^2)^{1/2} \sum_{i=1}^{3} (y_i^2)^{1/2}$$

Squaring both sides of the last relation gives;

$$[\sum_{1}^{3} x_i\ y_i\ ]^2 \leqslant \sum_{1}^{3} x_i^2 \sum_{1}^{3} y_i^2$$

Now in an imaginative n-dimensional space where vectors r_1 and r_2 have n components, the square of their scalar product is given by[37,57,58];

$$[\sum_{1}^{n} x_i\ y_i\ ]^2 \leqslant \sum_{1}^{n} x_i^2 \sum_{1}^{n} y_i^2 \qquad (1.3\ 4)$$

In <u>Hilbert space</u> -an abstract generalization of the ordinary 3-dimensional vector space[59]- which is defined as an infinite dimentional space (1.34) becomes;

$$[\sum_{1}^{\infty} x_i\ y_i\ ]^2 \leqslant \sum_{1}^{\infty} x_i^2 \sum_{1}^{\infty} y_i^2$$

Every function, in any domain, can be envisaged as a vector in Hilbert space, like Schrodinger's vector-valued state function $\psi(t)$ which assumes values from an infinite-dimensional complex Euclidean space bearing the name of Hilbert space. Thus we can introduce the scalar product of two functions in this space as[58,60];

$$| \int f(x)\ q(x)\ dx\ |^2 \leqslant \int |f(x)|^2\ dx \int |q(x)|^2\ dx \qquad (1.35)$$

where $\int |f|^2\ dx$ and $\int |q|^2\ dx < \infty$. This condition implies that the functions must be square integrable[55,61], like (1.33).

Expression (1.35), the generalization of the Schwarz's order relation, is called the Buniakauski inequality. It can be used for estimation of the solution of formidable integrals by parting them into two simpler forms[62]. It is also used in quantum mechanics for the derivation of the general uncertainty relationship[63].

It is worth noting that the equality sign of (1.35) holds if the quotient $f(x)/q(x)$ is a constant everywhere in $(-\infty, +\infty)$. In other words the equality holds if $f(x)$ and $q(x)$ are colinear; $f(x)/q(x) = y$, where y is a scalar[64,65]. The equality sign is used for minimum wave packet wave function, coherent states[63] -linearly dependent states-, and for matched filter in control system theory, where the Green's function and input are linearly dependent to maximize the signal to noise ratio[65].

1.6. The RF-m relationship

Combination of (1.15), (1.24), (1.33), (1.35), and a method due to Titchmarsh[55, p.91], leads to the sought-for $\langle R^2\rangle$-$\langle m^2\rangle$ relationship;

$$R(t) = \int G(t - \tau)\ m(\tau)d\tau$$

$$|R(t)|^2 = | \int G(t - \tau)\ m(\tau)d\tau\ |^2$$

dissecting the integral into two parts according to (1.35);

$$|R(t)|^2 \leqslant \int |m(\tau)|^2\ d\tau \int |G(t - \tau)|^2\ d\tau$$

$$\leqslant \int |m(\tau)|^2 G(t - \tau)\, d\tau \int G(t - \tau)\, d\tau$$

a change of argument $t - \tau = s$, and then $ds = -d\tau$ gives;

$$|R(t)|^2 \leqslant \int |m(\tau)|^2 G(t - \tau)\, d\tau \int G(s)\, ds$$

rearranging and integrating both sides with respect to t;

$$\int |R(t)|^2\, dt \leqslant \int G(s)\, ds \int G(t - \tau)\, dt \int |m(\tau)|^2\, d\tau$$

replacing the integral on the extreme left by (1.33) and changing the argument again, $t - \tau = s$, $ds = dt$, results in;

$$\langle R^2 \rangle \leqslant \int G(s)\, ds \int G(s)\, ds \int |m(\tau)|^2\, d\tau \text{ , or}$$

$$\langle R^2 \rangle \leqslant \left[\int G(s)\, ds \right]^2 \int |m(\tau)|^2\, d\tau$$

The first and the second integrals are $g(0)$ and $\langle m^2 \rangle$ from (1.24) and (1.33) respectively;

$$\langle R^2 \rangle \leqslant g^2(0)\ \langle m^2 \rangle \qquad (1.36)$$

This is the sought-for relationship between mean squares of R and m. As no specific properties of input, output, or the transfer function, 'g', of the RF system are used, (1.36) embodies a *general* input-output relationship for Linear systems.

It states that the mean-square of the output can be estimated from a knowledge of the mean-square of the input and the transfer function of the system at zero frequency, g(0), see Fig. 1.3.

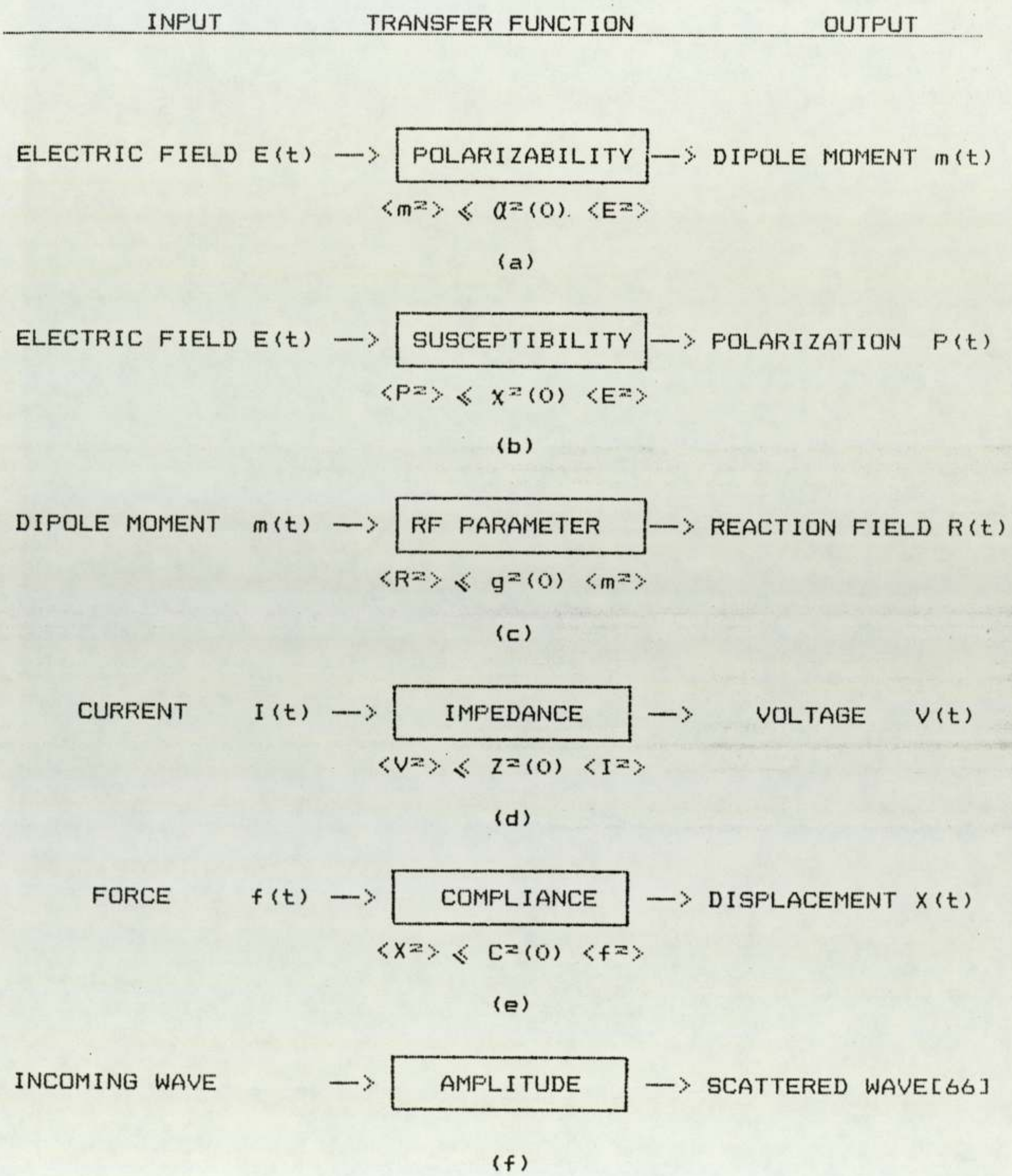

Fig. 1.3. The input- output relationship based on (1.36).

It must be emphasised that the generalized RF theory provides no information on the functional forms of g or $\langle m^2 \rangle$. These quantities are to be predetermined by other methods, if the explicit form of the output is required.

As regards the RF theory, (1.36) states that the static and dynamic RF formulas are not necessarily directly interchangable. The reminder of this chapter is devoted to the equalization of (1.36) for special cases.

1.7. Equalizing the Order Relation for RF

It is well-known that potential energy between a permanent electric dipole, μ, and a static electric field is given by;

$$U = - \mu \, . \, E_0$$

If the induction effect of the field creates the dipole, this Eq. becomes[2,4,32];

$$U = - \int_0^\mu E . d\mu \qquad (1.37)$$

or, using $\mu_{in} = \alpha(0) \, E_0$;

$$U = - (1/\alpha) \int_0^\mu \mu . d\mu = - (1/2) \, \alpha(0) \, E_0^2 \qquad (1.38)$$

Linder sets off with (1.37) and rightly assumes that the instantaneous potential between an oscillating dipole m(t) and its induced RF (RF is zero and reaches R by induction) is of the same form;

$$U(inst.) = - (1/2) \, m(t).R(t)$$

By using $R(t) = g(\omega) \, m(t)$, this expression becomes;

$$U(inst.) = - (1/2) \, g(\omega) \, m(t).m(t) \qquad (1.39)$$

The symbols are persistently indexed to avoid mis-derivations.

Without indices, (1.39) for example, can be written as; $U = -(1/2)\ g\ m^2$, which under the disguise of an averaging sign becomes;

$$U = -(1/2)\ g\ \langle m^2 \rangle \qquad (1.40)$$

which appears to prove that the potential between a dynamic RF and a dynamic moment equals the static potential of; $U = -(1/2)\ g\ \mu^2$.

Linder's work diverges from this convention by proper averaging of (1.39) as;

$$U_{av} = \langle U(\text{inst.}) \rangle = -(1/2)\ \langle g(\omega)\ m(t).m(t) \rangle$$

This is the gist of Linder's generalized RF work[18,19]. He shows that the meam dynamic potential, after all, turns out to be similar to (1.40), only four times smaller;

$$U_{av} = -(1/2)(1/4)\ g(0)\ \langle m^2 \rangle \qquad (1.41)$$

This, like (1.36), is a general result independent of the specific properties of the RF system, and therefore can be used for other similar cases (see sec. 1.8).

To equalize (1.36) for the RF, one can deduce a mean potential expression from (1.36) and equate it to (1.41). In terms of the root-mean-square (rms) moment, $\Delta m = \langle m^2 \rangle^{1/2}$, and RF, $\Delta R = \langle R^2 \rangle^{1/2}$ such expression reads;

$$U_{av} = -(1/2)\ \Delta m.\Delta R \qquad (1.42)$$

Inequality (1.36) in terms of rms's becomes;

$$\Delta R = y^{1/2}\ g(0)\ \Delta m$$

where y is an equalizing factor. Substituting for ΔR in (1.42) from this expression gives;

$U_{av} = -(1/2)\ y^{1/2}\ g(0)\ \Delta m.\Delta m$, or;

$$U_{av} = -(1/2)\ y^{1/2}\ g(0)\ \langle m^2 \rangle \qquad (1.43)$$

Comparison between (1.41) and (1.43) shows that, $y^{1/2} = 1/4$, or $y = 1/16$. Therefore (1.36) for the RF becomes;

$\langle R^2 \rangle = y\ g^2(0)\ \langle m^2 \rangle$, or ;

$$\langle R^2 \rangle = (1/16)\ g^2(0)\ \langle m^2 \rangle \qquad (1.44)$$

The equalizing factor of 1/16 could be deduced without defining (1.42) by arguing that the square dependence of 'g' in (1.36) demands the square of Linder's factor in (1.41) which is 1/16.

The message of (1.44) is clear, a direct mapping of the static RF expression into the dynamic situation is invalid and results in the over-estimation of the calculated values by a factor of 1/16. This is further discussed in the next chapter in the NMR context.

1.8. Potential Energy of an Induced Moment in a Varying Field

The dynamic form of (1.37), when an oscillating field induces a moment can be written as;

$U(\text{inst.}) = -(1/2)\ m_{in}(t).E(t)$

where on using $m_{in} = \alpha(\omega)\ E(t)$, and averaging gives;

$$U_{av} = \langle U(\text{inst.}) \rangle = -(1/2)\ \langle \alpha(\omega)\ E(t).E(t) \rangle$$

The outcome of this averaging, in principle, should be similar to Linder's potential (1.41), as there is no difference in the treatment of a field, E(t), inducing a moment, m(t), or a moment m(t), inducing a field, R(t);

$$U_{av} = -(1/2)(1/4)\ \alpha(0)\ \langle E^2 \rangle \tag{1.45}$$

As the survey in the next section shows, with the exception of London, almost every author, including Linder, has used the static expression (1.38) for the dynamic situation.

The form of the frequency dependence of polarizability $\alpha(\omega)$ can be found using Drude's[2,5,6,32,49] oscillatory model of light dispersion. In this model the D.Eq. that governs the interaction between light -the oscillatory electric field of light E(t)- and matter -the electrons of matter with natural frequency ω_o and spring constant $k = \omega_o^2 m$- is given by (1.14c). In other words, the system is not a black box. The workability of this model has been verified by QM[53,67,68].

The procedure of deriving the Transfer Function of the system, α, from its D.Eq., as given here, will be used later (sec.1.11). Substituting for the electron's displacement X(t) its FT from (1.16) into (1.14c) one obtains;

$$(1/2\pi)\ [-m\omega^2 - ih\omega + m\omega_o^2]\ \int X(\omega)\ \exp(-i\omega t)\ d\omega = e\ E(t)$$

or in terms of the original X(t);

$$[-m\omega^2 - ih\omega + m\omega_o^2]\ X(t) = e\ E(t)$$

where ω is the frequency of the oscillations of the driving field E(t). Therefore the oscillations of the electrons and conscequently the induced electric moment, $m_{in}(t) = e\ X(t)$, can be written as;

$$m_{in}(t) = e\,X(t) = \frac{e^2}{(m\omega_o^2 - m\omega^2 - ih\omega)}\,E(t) \qquad (1.46)$$

where the Transfer function of the system is;

$$\alpha(\omega) = \frac{e^2}{(m\omega_o^2 - m\omega^2 - ih\omega)}$$

For the static field $\omega = 0$, one gets the static polarizability[32,69];

$$\alpha(0) = e^2/(m\omega_o^2) \qquad (1.47)$$

Expression (1.46) therefore may be cast into the text-book form[32,70];

$m(t) = \alpha(\omega)\;E(t)$,

which is the input-output relationship for a Linear system as was given previously. The polarizability being a complex number embodies the fact that the induced moment lags behind the electric field, or it is shifted in phase to some extent. It will be recalled that this is the interpretation given for (1.12) and (1.15).

1.9. A Survey of the Static-to-Dynamic Direct Mapping

It was proved in the preceding section that the static potential (1.38) and the dynamic one (1.45) are not interchangable without the mapping factor of 1/4. Nevertheless almost always the static expression is used for the dynamic situation.

Margenau[71] for the time-varying field (thermal fluctuations) uses (1.38). As is shown in the next section for fluctuations of thermal origin, this appears be permissible.

Prosen[72] in treatment of the interaction between molecules and metallic surfaces, uses (1.38) for the instantaneous molecular field.

Slater[73], Mott[74], Buckingham[75], Bothner-By[76], Yonemoto[77], Raynes et al[78], Bernstein and Raynes[79], Rummens and Bernstein[80], and even Linder[24], all use (1.38) for time-varying field.

The crux of the Frohlich[20, pp. 40,42,177] and Bottcher[3, Chap. 4] argument in this connection is that potantial energy as a static entity justifies the use of static potential for any time-varying field.

The only exception appears to be London, that in his famous paper on the general theory of molecular forces[81], distinguishes between the static and dynamic potential by using $U = - (1/2)\ \alpha(\omega)\ F_0^2$, for the latter and (1.38) for the former where F_0 is the amplitude of the field oscillating with ω.

In the following sections the inequality is used for the study of London's dispersion formula and Brownian motion of electrons and particles.

1.10. The Inequality and London's Potential Formula

London's potential energy between two identical spheres (atoms) with polarizabilities α and fluctuating dipoles $m(t)$, a distance R apart is given by[67,68,81];

$U_L = - (3/4)\ h\nu\ \alpha^2(0)\ R^{-6}$

where the dipolar fluctuations are of quantum origin with frequency ν and a mean-square value of $\langle m^2 \rangle = (3/2)\ h\nu\ \alpha(0)$ (see Appendix 1, Eq. A1.4). In terms of the mean-square dipole, U_L becomes;

$$U_L = -\ (1/2)\ \alpha(0)\ \langle m^2 \rangle\ R^{-6} \qquad (1.48)$$

To derive (1.48) using the inequality (1.36) as given in Fig. 1.3a, the relationship between $\langle E^2 \rangle$ and $\langle m^2 \rangle$ should be found first.

The field of a permanent dipole μ at a point a distance R away from the centre of the dipole is given in <u>electrostatics</u> as[3,70,82,83];

$$\bar{E}_0 = \frac{3\ (\bar{\mu}.\bar{R})\ \bar{R}}{R^5} - \frac{\bar{\mu}}{R^3}$$

Provided that R is small, electrodynamic calculations show that the same expression holds for an oscillating dipole[70,82,83];

$$\bar{E}(t) = \frac{3\ (\bar{m}(t).\bar{R})\ \bar{R}}{R^5} - \frac{\bar{m}(t)}{R^3} \qquad (1.49)$$

Under the same condition the magnetic field of such a dipole vanishes[83] justifying the characterization of σ_w by electric field only.

Referring to Fig. 1.4, the dipolar oscillations of each atom produces, according to (1.49), an oscillating field at the site of the other atom, the mean value of which is zero because $\langle m(t) \rangle = 0$. The mean-square field, however has a finite value which in terms of the mean-square dipole is given by (Appendix 2 Eq. A2.1);

$$\langle E^2 \rangle = 2 \langle m^2 \rangle R^{-6} \qquad (1.50)$$

The method of deriving this relation is due to Hirschfelder and Meath[84] and the result agrees with that of Mott[74] arrived at by a different method.

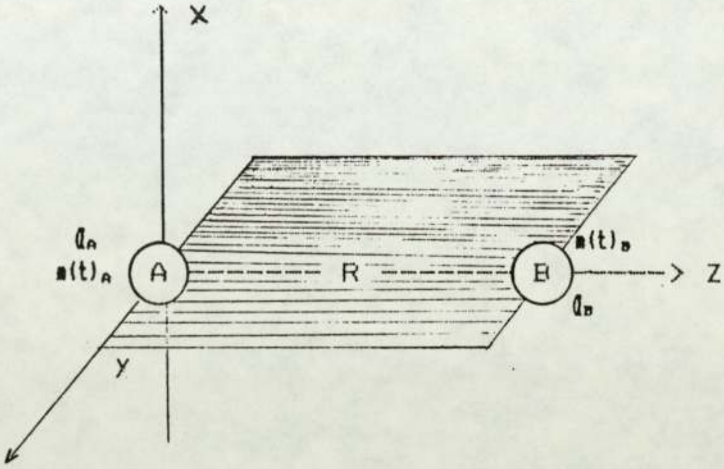

Fig. 1.4. Interaction between two non-polar atoms.

Now, the instantaneous potentials between the field of A and the moment that it induces in B, U(inst.,AB), and that of B on A, U(inst.,BA), can be written as;

$$U(\text{inst.})_{AB} = -\ (1/2)\ m_{in}(t)_B . E(t)_A$$
$$U(\text{inst.})_{BA} = -\ (1/2)\ m_{in}(t)_A . E(t)_B$$

The total <u>mutual</u> potential for the identical atoms is thus;

$$U(\text{inst.}) = -\ m_{in}(t).E(t)$$

the average of which according to the previous discussions is;

$$U_{Av} = -\ y^{1/2}\ \alpha(0)\ \langle E^2 \rangle, \text{ where } y = 1/16 \qquad (1.51)$$

Substituting for $\langle E^2 \rangle$ from (1.50) into (1.51) gives London's potential (1.48). The ease with which London's potential is obtained using two expressions only, (1.50) and (1.51), is noteworthy. Expressions (1.50) and (1.51) have a predominant role in the generalization of the London potential for polyatomic molecules at small separations (see Chapter 3).

1.11. The Inequality and Thermal Fluctuations

The equalizing factor of 1/16 was found for fluctuations of quantum nature, that is the zero-point oscillations of electrons in atoms or molecules which give rise to the time varying input, m(t). This input in turn produced the outputs R(t) or E(t) in the RF or dispersion theories respectively.

This section deals with fluctuations of thermal origin that are of practical importance. Brownian motion and thermal noise in electrical systems, known to vacuum tube amplifier technicians as tube noise, are two examples.

1.11.1 Thermal or Johnson Noise

Electrons in a length of copper wire are in random motion like the molecules of gas confined in a container. They have no net direct motion along the wire, but because the number of electrons is finite, there will be small fluctuations in the rate of the passage of them through a cross-section of wire. Therefore, conductors will contain a small rapid fluctuating current even though, averaged over a long time the net current is zero. These fluctuations give rise to a fluctuating voltage across the wire which is called electrical or thermal noise and can be measured by suitable instruments[85].

Johnson discovered[86] and measured[87] this electromotive force (fluctuating voltage) in conductors, which is related in a simple way to the absolute temperature T and resistance R of the conductor only. Johnson attributed this voltage to the thermal agitations of the electrons in conductors[87].

This phenomenon was immediately explained by Nyquist[88], and the result, known as the Nyquist theorem, is[88,89,90];

$$\langle V^2\rangle = 4\ kT\ R \tag{1.52}$$

where $\langle V^2\rangle$ is the mean-square voltage.

The inequality (1.36) for the potential between the two terminals of a conductor of resistance R reads (Fig. 1.3d);

$$\langle V^2\rangle = y_T\ Z^2(0)\ \langle I^2\rangle; \quad \text{or,}$$

$$\langle V^2\rangle = y_T\ R^2\ \langle I^2\rangle \tag{1.53}$$

where y_T is the equalizing factor of thermal fluctuations. Replacing the explicit form of the mean-square current[89,91];

$$\langle I^2\rangle = 4\ kT/R$$

into (1.53) and comparing the result with (1.52) gives, $y_T = 1$

Experiments[87] show that aqueous solutions of NaCl, K_2CrO_4, $CuSO_4$, and $Ca(NO_3)_2$, or, a carbon filament of the same resistance of 1.17×10^6 Ohms generate equal (rms) voltages of 1.14 microvolts at room temperature as (1.52) embodies.

In NMR experiments on living systems[92], which have a fairly high concentration of ions, for example, the sample itself can generate a significant amount of thermal noise, thus decreasing the effective signal-to-noise ratio[93,94].

1.11.2. Brownian Motion

The chaotic motion of a macroscopic visible particle, such as smoke particles in air or a pollen suspended in a drop of liquid which reflects the random motion of the molecules of the medium, is called Brownian motion[95-97].

A probabilistic description of this phenomenon was first given by Einstein in 1905[97], but we use a stochastic approach due to Langevin[47,89]. His method is more akin to the D.Eq. method given here.

The D.Eq. governing the displacement $X(t)$ of the suspended particle is given by (1.14) without the restoring force, $k = 0$. This Eq. in terms of the velocity of the particle $v(t)$ is known as Langevin's Eq.;

$$m \, dv(t)/dt + h \, v(t) = f(t) \qquad (1.54)$$

where h and f are respectively the friction constant and the random force representing the interactions between the particle and the molecules of the medium, $\langle f(t) \rangle = 0$.

The friction or damping constant is related to the viscosity of the liquid η the radius of the particle 'r' and, the diffusion coefficient D, by Stocke's $h = 6\pi\eta r$, or Einstein's $D = kT/h$ relationships.

By using the equipartition theorem[98]; $m \langle v^2 \rangle = kT$, and (1.54) one can readily show that over a long period of time when the particle undergoes myriads of collisions ($t \gg m/h$) the amount by which the particle spreads around, $\langle x^2 \rangle$, is given by[47,89];

$\langle x^2 \rangle = 2\ kT\ t/h$; or $\langle x^2 \rangle = 2\ D\ t$ (1.55)

Now, the inequality (1.36) for (1.54) gives;

$\langle v^2 \rangle = y_T\ L^2(0)\ \langle f^2 \rangle$ (1.56)

To compare this with (1.55) the form of the transfer function $L(0)$, and the mean-square force must be known.
Treating (1.54) according to the procedure of sec. 1.8 for obtaining the transfer function results in;

$L(\omega) = 1/(h - i\omega m)$; or $L(0) = 1/h$

Substituting for $L(0)$ and $y_T = 1$, which was found for the Brownian motion of electrons, into (1.56) gives;
$\langle v^2 \rangle = \langle f^2 \rangle / h^2$

For $\langle v^2 \rangle$, kT/m from the equipartition theorem can be used when the particle performs a random walk, that is when $t \gg m/h$. Therefore, the mean-square force becomes;

$\langle f^2 \rangle = kT\ h^2/m$
which in terms of the particle's relaxation time, $s = m/h$ and the viscosity of the liquid may be written as;

$\langle f^2 \rangle = 6\pi\ r\eta\ kT/s$ (1.57)

Reif[47] and Kubo[99], using the Fluctuation-Dissipation theorem (FDT), express the auto-correlation of the force respectively as;

$2\ kT\ h = \int \langle f(t).f(t')\rangle\ d(t-t')$, and;

$$2\ kT\ h\ \delta(t-t') = \langle f(t).f(t')\rangle \qquad (1.58)$$

where $\delta(t)$ is the Dirac Delta function. It is intriguing that the mean-square form of a flutuating quantity is not explicitly provided by the FDT.

We note that the inequality provides the explicit form of the mean-square force using the value of unity found for y_T from the thermal noise.

The phenomena of thermal noise and Brownian motion are closely related, and so the Nyquist theorem can be greatly generalized. Such generalization was first stated by Callen and Walton[100]. The generalized theorem is called the FDT[101], because it relates the fluctuations of a physical quantity of a system in equilibrium to a dissipation process, similar to (1.57) where $\langle f(t).f(t)\rangle = \langle f^2\rangle$ is related to h.

Expression (1.55) has wide variety of uses including the motion of colloidal particle, chemical reactions, hydrodynamic, and many-particle systems.

Perrin[101] in 1910 by measuring $\langle x^2\rangle$ for gamboge particles found a value of 6.73×10^{23} $mole^{-1}$ for Avogadro's number. Kappler[103] in 1931, by the study of the fluctuations of a light spot reflected from a galvometer mirror, which responds to Brownian motion under the action of air molecules no matter how efficiently evacuated[45], found a value of 6.063×10^{23} for Avogadro's number. The accepted value is 6.022×10^{23} $mole^{-1}$.

The inequality may be useful in linking the fluctuations of thermodynamic variables, such as entropy $\langle \Delta S^2 \rangle = kC_p$[104] and volume $\langle V^2 \rangle$ with the fluctuations of the cause (input).

More subtle problems can also be simplified by the inequality. For example, the quantum electrodynamic problem of fluctuations in the position of a free electron, which may be thought of as Brownian motion of electrons in equilibrium with zero-point fluctuations of the electric and magnetic fields in empty space[105]. The non-relativistic classical Eq. of motion of a free electron under the electric field $E(t)$ is given by (1.14c) for $k = 0$. The transfer function of such system is;

$T(\omega) = 1/(m\omega^2)$, or , $T(0) = \infty$

The inequality between the output $x(t)$ and the input $E(t)$ is then;

$\langle x^2 \rangle \leqslant T(0) \langle E^2 \rangle$, or ,$\langle x^2 \rangle = \infty$

which is in agreement with the Welton[105] result. The quantum treatment of this problem gives finite value for $\langle x^2 \rangle$, by which the zero-point fluctuations in the electric field in empty space can be easily found using $y = 1/16$ and the inequality, without resort to other complicated quantum electrodynamic methods.

1.12. Reaction Field and the Heat of Vaporization

The equalizing factor of less than unity for quantum effects can be verified directly by the calculation of heats of vaporization for non-polar compounds.

Linder[16] has shown that the potential energy between the moment and RF roughly characterizes the heat of vaporization, H_v. For one mole of a pure non-polar compound using (1.43) one can write[16];

$H_v = -(1/2)\, y^{1/2} L \langle m^2 \rangle g(0)$;   where $y = 1/16$

By using (A1.4) for $\langle m^2 \rangle$[16,18], (1.25) for $g(0)$, Maxwell's relation $\varepsilon = n^2$ for dielectric constant, Onsager's relation $(4\pi/3)\, a^3 L = V$ for the cavity size, and Bottcher's relation $\alpha(0) = a^3 (n^2 - 1)/(n^2 + 2)$ for polarizability, the expression of H_v becomes;

$$H_v(\mathrm{KJ/mole}) = -144\, y^{1/2}\, I(\mathrm{ev}) \frac{(n^2-1)^2}{(2n^2 + 1)(n^2 + 2)} \qquad (1.59)$$

To avoid duplication, the experimental and calculated heats of vaporization from Linder's work are only graphically compared in Fig. 1.5.

The purpose of this comparison is to reinforce the equalizing factor of less than unity which gives the right order of magnitude of the experimental values. We note that for $y = 1$, implying the correspondence of static and dynamic relationships the calculated values of H_v would be four times larger than those given in Fig. 1.4.

Expression (1.59) has also been used for the heats of sublimation of solid argon and iodine. For both solids (1.59) gives values twice larger than the experimental ones; 121.7 and 13.2 KJ/mole as compared to the experimental values of 64.4 and 6.6 for I_2 and Ar respectively. For $y = 1$, the discrepancies increase four-fold.

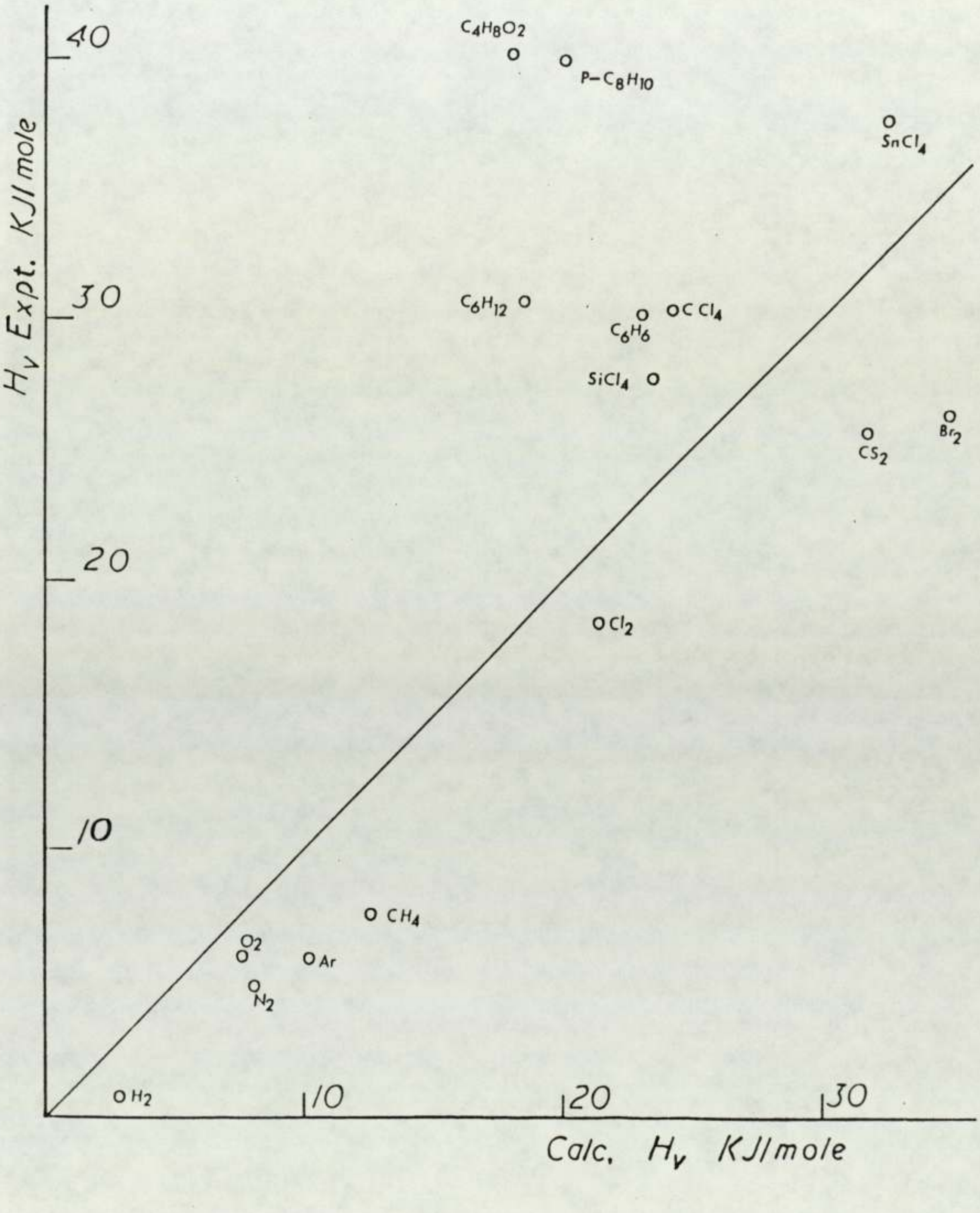

Fig. 1.5 A comparison between the experimental and calculated heats of vaporization by the RF model (from Ref. 16).

1.13. Conclusions

The dynamic RF formula turned out to be a specific form of a general inequality . Physically speaking the inequality results from the fact that the total output energy, $\langle R^2 \rangle$, cannot exceed the total input energy, so that $\langle R^2 \rangle \leqslant g^2 \langle m^2 \rangle$.

A serious criticism of the Onsager's static RF that has been raised concerns the effect of thermal re-orientation of the solute molecule and as a result the fluctuations of its permanent dipole μ. The direction of μ is assumed to be fixed in Onsager's theory. However, $y_T = 1$ for thermal fluctuations shows that such a criticism is invalid and thermal motion does not affect Onsager's RF, because $\langle R^2 \rangle = g^2 \langle \mu^2 \rangle$. This is in agreement with Linder's finding[19].

It is tempting to add a correction term to (1.2), in the same line with the Debye correction to (1.1). We may informally, by analogy with (1.7), write;

$f(n) = [\ \alpha(\text{gas}) + X \langle m^2 \rangle / (3/2\ h\nu + \langle R.m \rangle)\ ]$

where $f(n)$ is used for all the parameters of (1.2) except for α, and 'X' is a numerical factor to be determined. Note that $(3/2)h\nu$ is used as the quantum counterpart of $3kT$[106,107], and $\alpha(\text{gas})$ for α to emphasize that it is the gas phase polarizability.

By using $\langle m^2 \rangle = (3/2)h\nu\ \alpha(\text{gas})$, Bottcher's relation of the last section for $\alpha(\text{gas})$, and Linder's relation $\langle R.m \rangle = (1/4)\ g \langle m^2 \rangle$ this expression may be written as;

$$f(n) = [\alpha(\text{gas}) + X \frac{a^3}{(n^2 + 2)/(n^2 - 1) + (n^2 - 1)/(4n^2 + 2)}\ ]$$

This is somewhat similar to the Raman and Krishnan[4] correction term for (1.2) which they added on the grounds that liquids are really anisotropic;

$$f(n) = [\ \alpha + \frac{(\varepsilon - 1)}{(\varepsilon + 2)}\Phi]\qquad\qquad \text{Raman-Krishnan Eq.}$$

where Φ is a molecular constant. This extra term explains why the $(n^2 - 1)/(n^2 + 2)$ factor usually decreases with increase in density.

Let us see if the informal correction rectifies the slight discrepancies observed in using (1.2) for water and benzene. For water ($n = 1.3325$, $V = 18$ cm^3/mole) the correction term works out to X1.43 A^3. The polarizability of water is, 1.44 A^3, therefore, the 10% discrepancy observed for water[1] would be explained if X = 1/10. This adds .143 A^3 to the gas phase polarizability.

For benzene ($n = 1.5$, $V = 89$ cm^3/mole) the correction term gives 1 A^3, for X = 1/10 found from water data, which is 10% of 10.4 A^3, the polarizability of benzene. This exceeds the observed 3.8%[4] discrepancy . Therefore, judging by these data, X appears to be a variable and probably a function of molecular parameters, the exact nature of which requires scrutiny.

The inequality may prove useful in other fields including the interaction of micro or ultrasonic wave with matter, the noise problems in light fibers communication and the rotational Brownian motion which is related to dielectric and NMR relaxation processes[108].

Chapter 2

Reaction Field Characterization of the van der Waals Screening Constant

Introdution

The study of NMR chemical shifts has revived dormant electromagnetic problems including the difference between corresponding electrostatic and electrodynamic quantities which was studied in the previous chapter.

This chapter deals with the effects of solvent (medium) on the NMR chemical shift and this again activates problems of the Lorentz local field, the Lorentz inner field, the Onsager cavity size, and the demagnetization field (the characteristic of ferromagnetic materials).

The solvent or the medium nuclear screening constant of a species is recognized to be caused by at least five effects;

$\sigma_m = \sigma_a + \sigma_b + \sigma_w + \sigma_E + \sigma_R + \ldots$

The origin and the meaning of these terms are traced, and the characterization of the van der Waals term, σ_w, by the reaction field technique is considered.

In the search for a universal reaction field formulation for σ_w the Homer and Percival reaction field model is tested on over 200 available solute-solvent ^{1}H, ^{19}F, ^{31}P, and ^{129}Xe systems.

It is shown that their reaction field (RF) model overcomes the two cardinal problems of any pure reaction field model, namely the Onsager cavity size and the shortfall from the experimental values. This is achieved at the expense of prominent intercepts in the RF-σ_w relationship.

The existence of the intercepts necessitates the inclusion of pairwise interactions in the characterization of σ_w, which leads to the inference that no pure RF model is capable of an adequate formulation of σ_w.

Based on the Homer and Percival RF model a B value for ^{31}P, and that of ^{129}Xe are calculated in agreement with some theoretical values.

Moreover, the study of dynamic and static B ^{1}H once more validates the general inequality of the previous chapter.

2.1. Historical Background

In this section an adaptation of Dickinson's work on the time average magnetic field at a nucleus in a NMR experiment serves to describe the nature of the van der Waals (vdW) nuclear screening.

2.1.1. What is the vdW nuclear screening

The first effect of the medium in the chemical shift was dicovered in 1951 by Dickinson[109]. By analogy with the electrostaticsof a local field (Eq. 1.3), Dickinson argues that for a macroscopic sample of matter which is used in the NMR experiment, the effective magnetic field to which the resonating nuclei are exposed will not be exactly the same as the externally applied field. The time average (local) field at a <u>nucleus</u> consists of three significant components;

$$H_L = H_o + H' + H'' \tag{2.1}$$

1- H_o is the external magnetic field.

2- H', an <u>intra-molecular</u> field, is the magnetic shielding field at the nucleus due to the molecule cotaining the nucleus. According to Dickinson[110] this term is proportional to the external field, pH_o. Using the result of Anderson's[111] work on H_2, he finds that p is negative and of the order of 10^{-5}. Therefore, hereafter H' is denoted by $-pH_o$.

3- H'' is the magnetization field due to <u>paramagnetic</u> ions that might be added to the sample for shortening the spin lattice relaxation time.

Following the Debye's method for electric dipoles[9,112] he divides H'' into two parts;

$$H'' = (4\pi/3)M - sM \tag{2.2}$$

where the first term is the familiar Lorentz[5] term for local fields, namely the contribution of the outer region of a (semi-)macroscopic spherical cavity on the molecule inside the cavity. The second term, however, is the <u>demagnetization</u> field or, the amount by which the field in the sample is less than the external one. The demagnetization expresses the effects of magnetic poles on the outer surface of the sample[113], so it depends on the shape of the sample. On combining (2.1) and (2.2) one gets;

$$H_L = H_o - pH_o + (4\pi/3)M - sM \qquad (2.3)$$

Fig. 2.1 depicts this expression apart from the intra-molecular term, $-pH_o$.

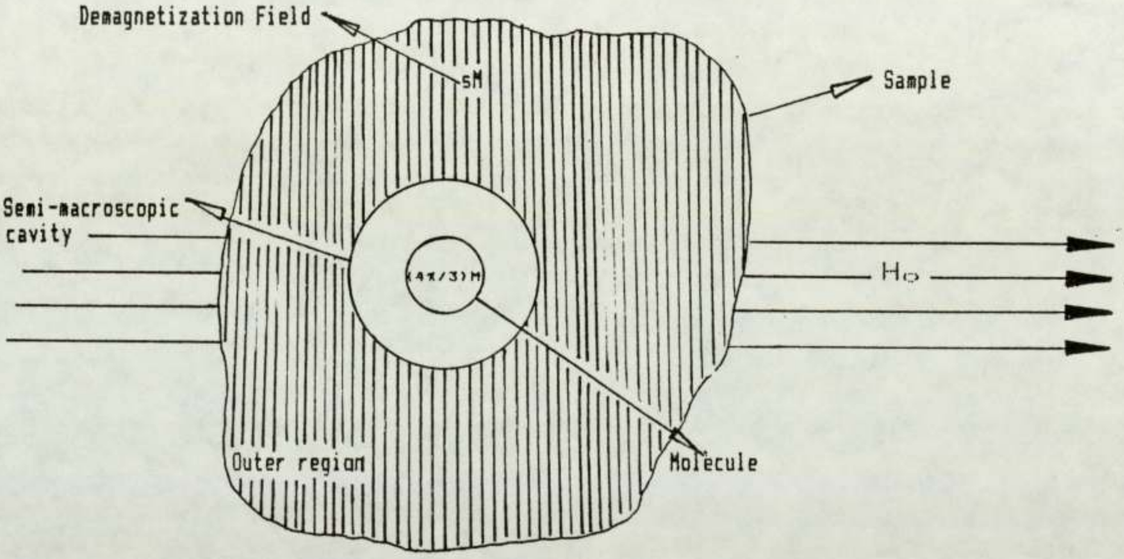

Fig. 2.1. The Lorentz local field for a paramagnetic specimen.

Note that the electric equivalent of $-pH_o$, that is $-pE_o$, could have been included in the expression for E_L (Eq. 1.3) if the local field at an <u>atom</u> in the central molecule were needed. Therefore the true difference between the forms of E_L and H_L is in the demagnetization field.

It is worth noting here that in dielectric theories of local fields there is no mention of a depolarization or shape dependent field[7,8,114], even when the shape of the sample is explicit in the treatment of the local electric or magnetic fields for dielectic and diamagnetic materials[49].

Apparently the demagnetization or shape correction is characteristic of ferromagnetic materials because of their high magnetic susceptibilities[115-120]. This correction however has become quite important for diamagnetic materials in high resolution NMR, where shifts of accuracy of less than 1 ppm can be detected.

Dickinson[109] using spherical and cylindrical (length to diameter ratio of at least 10:1) sample tubes, for which the shape factors* are $s = (4\pi/3)$ and 2π respectively[120], found that the factor $(4\pi/3)M - sM$ is in general not correct and that the actual factor may be several times larger or smaller or may even be of the opposite sign[121].

A suggested explanation of this anomaly was put forward by Bloembergen and Dickinson[122], and Ayant[123] who considered that the contribution to the local field from the region within the spherical cavity is, in this case, not zero. Therefore, for the demagnetization or shape factor to be valid another term must be added to (2.2). This term was assumed to be zero by Dickinson on the basis of electromagnetism[124];

$$H'' = (4\pi/3)M - sM + qM \qquad (2.4)$$

Dickinson defines q in the qM term as an interaction factor. This is a familiar and contentious term in electromagnetism where it is called the inner Lorentz field and arises from the polarization P, or magnetization M, of the molecules within the spherical cavity. It was proved to be zero by Lorentz[5] for a

---

*: Eperiments show that the shape factor s depends somewhat on the permeability of the specimen as well as its shape[120].

cubic lattice or for complete disorder of the molecules inside the semi-macroscopic cavity[8,114,124], although the assumption that $q = 0$ may be apt for gases, but it is not true for liquids[125]. There have been extensive arguments on this matter going on for years[9,125,126], thanks are due to high resolution MNR for reviving the subject. Expression (2.4) is depicted in Fig. 2.2.

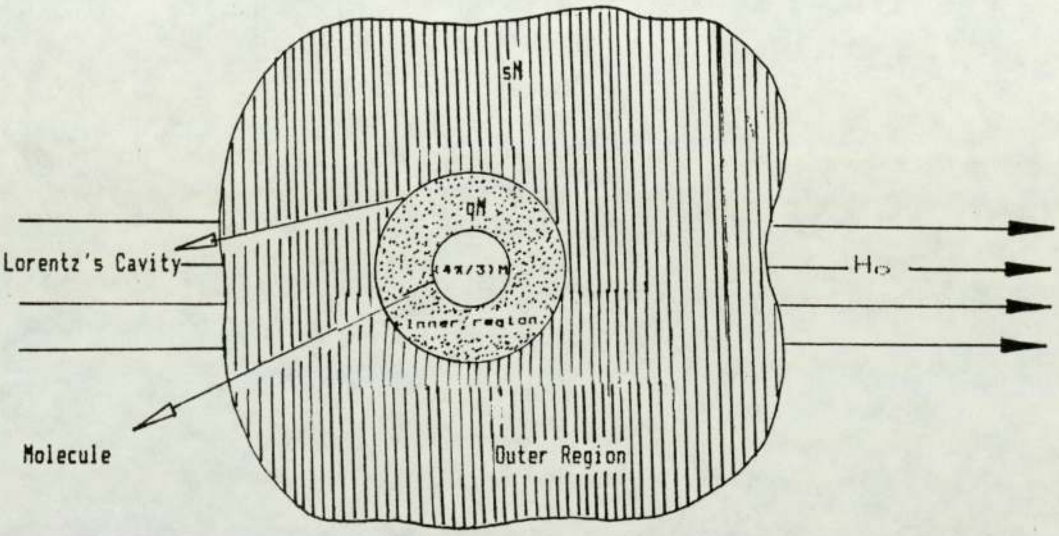

Fig. 2.2. The Lorentz local field for a diamagnetic material in the high resolution NMR experiment.

The gist of this new term, qM, is that it reflects the effect of interactions between the central and individual molecules of the inner region. In this, it may be regarded as the genesis of the vdW chemical shift. The expression for the local field for cylindrical sample shape transverse to H_o; $s = 2\pi$, now becomes;

$$H_L = H_o - pH_o + (4\pi/3)M - 2\pi M - qM, \text{ or}$$

$$H_L = H_o - pH_o - (2\pi/3)M - qM \qquad (2.5)$$

where for the purpose of this historical introduction $-qM$ is used (Dickinson finds both positive and negative q values; see table 7 in Ref.[109]). The manipulation of (2.5) results in an expression for the screening constant, as follows.

The magnetization M similar to the polarization, $P = L E_L \alpha/V$ (Eq. 1.4), is $M = \chi H_L$, which on substitution for the local field from (2.5) gives;

$$M = \frac{\chi H_o(1 - p)}{(1 + (2\pi/3)\chi + q\chi)} = \chi H_o \text{ , for } \chi \text{ and } p \ll 1$$

replacing this back into (2.5) gives;

$$H_L = H_o - pH_o - (2\pi/3)\chi H_o - q\chi H_o\text{, or,}$$
$$H_L = H_o [1 - (p + (2\pi/3)\chi + q\chi)] \qquad (2.6)$$

A comparison between (2.6) and the general NMR expression; $H = H_o (1 - \sigma)$, shows that;

$$\sigma = p + (2\pi/3)\chi + q\chi \qquad (2.7)$$

where σ is the nuclear screening constant.

It took some ten years for the screening constant to be recognized in this form in NMR studies. This came about by attempts to justify the cylindrical sample factor of $2\pi/3 = 2.09$ Bothner-By and Glick were the first to investigate this factor. They found excellent linear relationship between chemical shifts and volume magnetic susceptibilities χ_v, with the proportionality constant ranging from 2.3 to 3.0 (mean = 2.6) rather than 2.09[127]. Their further work on aromatic solvents showed that they behave quite differently and this anomaly was attributed to the magnetic anisotropy of aromatics[128,129], which is the origin of the neighbour anisotropy effect, σ_a. Others also found anomalies in this factor[130-132].

Nevertheless the faith in $2\pi/3$ was so deep that it was fixed at this value and the anomalies were attributed to other effects such as vdW interactions by Glick and Eherson[133].

There was a muddle over the subject for some time during which the chemical screening was not yet recognized as (2.7) until finally Bothner-By[134] made a breakthrough. He determined the effect of medium for each solute by measuring the solute, first in the gas phase, so finding the <u>intra-molecular</u> effects, σ_g and then at infinite dilution in a solvent, σ. The difference between the two screening constant $(\sigma - \sigma_g)$ is then the gas-to-solution medium screening of that solute. This was accepted to be proportional to $(2\pi/3)\chi_v$ plus another term to explain the anomalies, namely the vdW interaction term;

$$\sigma - \sigma_g = (2\pi/3)\chi_v + \sigma(\text{vdW}), \text{ or,}$$

$$\sigma = \sigma_g + (2\pi/3)\chi_v + \sigma(\text{vdW})$$

This in fact is re-discovered (2.7) because as Dickinson showed, p is related to the <u>intra-molecular</u> effects of the solute which is the same as σ_g, and $\sigma(\text{vdW})$ is the interaction term surmised by him.

Note the proportionality of the Dickinson interaction term qM with the magnetic susceptibility χ. This fact quite puzzled investigators when they found that the excess of the screening corrected for the bulk susceptibility, namely;

$$(\sigma - \sigma_g) - (2\pi/3)\ \chi_v = \sigma(\mathrm{vdW})$$

was still proportional to χ_v.

Bothner-By found that $(\sigma - \sigma_g - (2\pi/3)\chi_v)$ was negative (for non-aromatic solvents with $\sigma_a = 0$) namely, the excess screening is down-field. This was established as the vdW screening constant σ_w, arising from the interaction between the solute and the solvent. One can therefore, in the presence of magnetically anisotropic solvents write;

$$\sigma_m = (\sigma - \sigma_g) = \sigma_a + \sigma_b + \sigma_w \tag{2.8}$$

The purpose of the remainder of this chapter is to show the characterization of σ_w by the RF model.

2.1.2. Characterization of σ_w, and the B parameter

An RF formulation of σ_w entails a knowledge of some sort of relationship between this quantity and a (reaction) field. The work of Marshall and Pople[135] provides such knowledge.

They have calculated the shielding of an isolated hydrogen atom that is, (besides H_o) simultaneously subjected to a uniform static electric field. Their 2nd order perturbation theory showed that a static field either perpendicular or parallel to the magnetic field H_o will cause de-shielding proportional to E_o^2;

$$\sigma = -\frac{881\ a_o^2}{216\ mc^2} E_o^2 \tag{2.9}$$

where a_o, m, and c are respectively the Bohr radius (.529 A), the electron mass (9.109×10^{-28} gr), and the speed of light (2.998×10^{10} cm/s). Inserting these values into (2.9);

$$\sigma = - .738\times10^{-18}(\mathrm{cm}^3/\mathrm{erg})\ E_o^2$$

This expression, for the first time, linked the screening with an external perturber (input) other than H_o. It can be written as;

$$\sigma = - B_o\ E_o^2 \tag{2.10}$$

where $B_o = .738\times10^{-18}\ \mathrm{cm}^3/\mathrm{erg}$.

Stephen[136] suggested that rapidly fluctuating electric fields of neighbouring non-polar molecules can give rise to vdW forces and therefore generate de-shielding that (note the direct static-to-dynamic mapping) by analogy with (2.10) should be;

$$\sigma_w = - B_o\ \langle E^2\rangle$$

where $\langle E^2\rangle$ is the non-zero mean-square of the fluctuating field Let us rewrite this as;

$$\sigma_w = - B\ \langle E^2\rangle \tag{2.11}$$

where B is the dynamic counterpart of B_o.

There was no theoretical work on the σ_w-$\langle E^2\rangle$ relationship until Marshall and Pople[137] published the result of their study on two interacting H atoms, a case more akin to the Stephen suggestion. They found that the vdW forces decrease the screening (in the absence of overlap forces) so that the shielding in one H atom caused by the neighbouring one is given by;

$$\sigma_w = - \frac{23.86\ \hbar^2 a_o^4}{3\ m^2 c^2}\ R^{-6} \tag{2.12}$$

To extract a B parameter from this, which is inexplicit in terms of the field, one has to find a field expression as a function of R^{-6} and compare the two. Combining the London potential Eq., $U_L = -(3/4) I \alpha^2 R^{-6}$ for two interacting H atoms a distance R apart, with Eq. (1.51), $U = -(1/4)\alpha\langle E^2\rangle$ one gets;

$$\langle E^2\rangle = 3\ I\ \alpha\ R^{-6} \qquad (2.13)$$

Replacing $\langle E^2\rangle$ in (2.11) by (2.13);

$$\sigma_w = -\ 3\ B\ I\ \alpha\ R^{-6} \qquad (2.14)$$

and then comparing (2.12) with (2.14) gives the expression for B;

$$B = \frac{23.86\ \hbar^2 a_0^4}{9\ m^2c^2\ \alpha I} \qquad (2.15)$$

Inserting for $\alpha_H = .6668\ A^3$, $I_H = 13.5$ eV, and other constants in this, one obtains, $B = .1908\times10^{-18}\ cm^3/erg$.

This value for the fluctuating field of H atom is about four times smaller than B_o of the static field. One notes the emergence of the now familiar dynamic-static relationship as was discussed in the previous chapter. The static expression for an observable;

$$\sigma(\text{output}) = -\ B_o\ E_0^2(\text{input})$$

can be transposed into its dynamic one (2.11) by a numerical factor less than unity, $y < 1$;

$$\sigma_{output} = -\ y^{1/2}\ B_o\ \langle E^2(t)\rangle_{input}$$

where $y^{1/2}B_o = .1908\times10^{-18}$ equals the dynamic B for $y^{1/2} \simeq 1/4$, in agreement with $y^{1/2} = 1/4$ found for quantum effects when the transfer function of the system is not quadratic.

The fact that $B_o > B$ is attributed by Rummens[17] partly to the use of (2.13) which has been derived by Raynes et al[78] on the basis of $U = -(1/2)\alpha\langle E^2\rangle$, rather than $U = -(1/4)\alpha\langle E^2\rangle$. They arrived at the same expression as (2.13) because of the use of $h\nu = 2I$ in the London potential formula (see sec. 2.3.2).

The quantum theory of Kromhout and Linder[138] on B also supports the Marshall and Pople value of $.19\times10^{-18}$. They give the following B (dynamic) values;

X...X interaction	H...H	He...He	Ne...Ne	Kr...Kr	Xe...Xe	CH_4...CH_4	CF_4...CF_4
$B\times10^{18}$ cm^3/erg	.21	.17	4.1	252	914	.59	18

The work of Jameson et al[139] on B_o of hydrogen and inert atoms in a static field E_o generally gives lower values compared to those of Kromhout and Linder. For helium for example, their B_o is low by a factor of two, and, the same factor increases their B_o for H near to the Marshall and Pople value of .74;

X...E_o interaction	H	He	Ne	Ar	Kr	Xe
$B_o\times10^{18}$ cm^3/erg	.35	.075	5.6	41.3	124.7	337.3

According to Rummens[17] the nature of the approximations in the Jameson (et al) procedure makes their B_o values for light atoms less reliable, though they might be quite good for heavy atoms.

We infer from the evidence in this section that the link between the vdW screening and some form of a fluctuating field is provided by a parameter B which mainly depends on the resonant nucleus and the interacting solute-solvent system. In terms of the RF such a relationship reads;

$$\sigma_w = - B \langle R^2 \rangle$$

substituting for $\langle R^2 \rangle$ from (1.44) one finds;

$$\sigma_w = - B\, y\, g^2 \langle m^2 \rangle, \text{ or,}$$

$$\sigma_w = - B\, y \frac{(2n^2 - 2)^2}{(2n^2 + 1)^2 a^6} \langle m^2 \rangle \qquad (2.16)$$

where 'a' is the cavity size and $y = 1/16$. Note that there exists a direct relationship between $\langle m^2 \rangle = \sum e^2 \langle r_i{}^2 \rangle$ and χ. The molar susceptibility of an atom may be written as[1];

$$\chi = - (e^2 L/6mc^2) \sum \langle r_i{}^2 \rangle$$

so that (2.16) becomes;

$$\sigma_w = q\, \chi, \text{ and,} \qquad q = \frac{6\, By\, mc^2}{L} \frac{(2n^2 - 2)^2}{(2n^2 + 1)^2 a^6}$$

where $q\, \chi$ is the Dickinson interaction term.

2.2. Problems with the RF model of σ_w

The argument in the historical background suggests the interactions between the central molecule and those of the inner region as the cause of the vdW shift (see Fig. 2.2). In other words, it has been recognized that[76,136] σ_w arises from the interactions between the nearest neighbours. The continuum, or the RF model, as it is known, characterizes the effects of interactions between the central molecule and those of the outer region, the continuum.

2.2.1. The Problem of the First Molecular Shell

Linder[19] believes that the RF model is highly artificial when used at the molecular level because in this model the molecules that surround a specific molecule at the centre of a cavity must form a uniform dielectric. To achieve this uniformity the cavity must be of semi-macroscopic size[3,14] as shown in Fig. 2.2. In other words, surrounding molecules appear uniform to the central one at some distance away from the nearest neighbours[140]. The individuality of the molecules in this model is "smeared out" by using the refractive index, a bulk property. The nearest neighbours interaction which identifies σ_w is totally nonexistent in this theory. It is therefore not far from reality to say that the RF models another bulk effect.

2.2.2. The Problem of the Cavity size

If the validity of this model is to be tested, by using (2.16), the true size of the cavity must be known.

A much criticized[4,17,19] expression is what has come to be called Onsager's approximation, $(4\pi/3)\ L\ a^3 = V$, which was used in section 1.11 for finding heats of vaporization. This expression is supported by the fact that it reduces the Bottcher-Onsager formula[3] for dipolar liquids to the Mossotti-Clausiuss formula which works so well for non-polar compounds.

Accepting Onsager's cavity size, however, is tantamount to shrinking the semi-macroscopic cavity into molecular sizes. Some authors[19,80] regard this as the root of RF model problems. Others notably Kirkwood[141] and Chelkowski[124] believe that Onsager's cavity is a real cavity and differs from that of Lorentz which is filled with material of the dielectric.

The most serious defect of this model, Kirkwood continues, lies in the assumption of a uniform local dielectric which is identical to the macroscopic dielectric of the medium.

However, not much has been done to improve this so-called approximation. Linder[19], links 'a' to the radial distribution function, a notorious mathematically untractable quantity available by experiment. Using x-ray scattering data for Xe at −110 °C, he finds roughly that a = 3.28 A; the Onsager's value is 2.57 A for $V = 42.7$ cm^3/mole at −110 °C.

Jaffe[142] has used the Hertz expression (see sec. 3.3.3) for random distribution of points to remove this objectionable feature of Onsager's theory. His work offers no direct expression that can be used for 'a'. As it is shown in Chapter 3 the cavity size obtained from the Hertz expression is smaller than that of Onsager's.

Therefore, we will use Onsager's cavity size, and consider the problem of the first shell of molecules as a serious setback to the RF model of σ_w.

2.3. Correlational Analysis of $\langle R^2 \rangle$-σ_w relationship

In this section the suitability of the RF model of σ_w is analysed by the study of the linear relationship between calculated values of $\langle R^2 \rangle$ and experimental values of σ_w.
For computational purposes (2.16) may be written as;

$$\langle R^2 \rangle(\mathrm{erg/cm^3}) = y\ 61.2\times 10^{12}\ \frac{(n_v^2 - 1)^2}{(2n_v^2 + 1)^2}\ \frac{I_u(\mathrm{ev})\ \alpha_u(\mathrm{A^3})}{V_u^2(\mathrm{cm^3/mole})} \qquad (2.17)$$

where Onsager's expression for 'a', Eq. (A1.4) for $\langle m^2 \rangle$, u for the solute and v for the solvent are used.

It is customery[24,25,27,29,143,144-147] to use the volume of solute, or central molecule, V_u, for the cavity size as used in (2.17). When the tabulated values of I, α, and V are inserted in (2.17), and the result is multiplied by the value of B in ppm cm^3/erg that is $B \times 10^6$, σ_w(cal.) would be in ppm

$$\sigma_w(\text{cal.}) = \sigma_{RF}(\text{ppm}) = - y\, B(\text{ppm cm}^3/\text{erg}) \langle R^2 \rangle (\text{erg/cm}^3) \qquad (2.18)$$

For the initial test the experimental σ_w(expt.) values of the tetramethyl compounds are used. The calculated values of RF according to (2.17) for y = 1 are denoted by RFu in table 2.1. The correlation coefficients for the linear relationship between RFu and σ_w(expt.) with their slopes -showing the B values according to (2.18)- are also given at the bottom of the table.

Note that this analysis is for a given solute in a series of solvents. This is because the bulk susceptibility correction, σ_b, is done on this basis, and as Glick et al[130] found the excellent linear relation between σ_m and χ_v exists in this way only. Rummens[27] says that using a series of solvents will eliminate at least part of the experimental errors and model errors.

Table 2.1 shows that on the one hand, the correlations are poor (the significance level, a measure of the accidental correlation, is more than 5%), and, on the other hand, the calculated values on the basis of B_o = .74, would be an order

Table 2.1. Comparison between Experimental* and calculated σ_m

Solvent	$\langle R^2 \rangle$x10^{-12} erg/cm^3 (2.18)	Solute CMe_4	 $SiMe_4$	 $GeMe_4$	 $SnMe_4$	 $PbMe_4$
CMe_4	RFu	.0111	.0109	.0112	.0113	.0129
	RFv	.0111	.0123	.0123	.0127	.0138
$SiMe_4$	RFu	.0118	.0115	.0119	.0119	.0137
	RFv	.0105	.0115	.0116	.0119	.0130
$GeMe_4$	RFu	.0133	.0130	.0134	.0135	.0154
	RFv	.0120	.0133	.0134	.0137	.0149
$SnMe_4$	RFu	.0159	.0156	.0160	.0161	.0185
	RFv	.0141	.0156	.0157	.0161	.0175
$PbMe_4$	RFu	.0196	.0191	.0197	.0198	.0227
	RFv	.0183	.0202	.0203	.0208	.0227
CC+	RFu-σ_m	.878	.917	.909	.923	.925
Slope = B		8.45	9.35	9.27	9.76	8.56
CC	RFv-σ_m	.946	.969	.965	.974	.977
Slope = B		9.99	9.52	9.71	10.02	9.25

*: Given in table 2.4.

+: Correlation coefficient.

of magnitude smaller than the experimental ones. This is apparent from the slopes of about 10 times larger than $.74\times10^{-12}$ ppm cm^3/erg. Note that for the actual value of $y = 1/16$ the calculated screenings fall short of the observed ones by two orders of manitude.

2.3.1. The Idea of the Solvent Cavity Size

The RF-σ_w correlation can be improved if the solute cavity size in (2.17) is changed for a more realistic cavity size.

It is more likely that the solute molecules fit into the empty sites of the solvent medium. The size of these empty sites or holes according to the "significant structure model"[148] of liquids is naturally determined by the solvent. On this account the size of the cavity for binary systems, should be related to the solvent and not the solute. This idea is tested by finding the RF values, denoted by RFv, with V_u in (2.17) replaced by V_v.

Table 2.1 shows the increase in the correlation coefficients (with improved significance levels, < 5%) of RFv-σ_w(expt.) relationship for tetramethyl systems. Table 2.2 highlights the superiority of the solvent cavity size to that of solute (save for P_4 which shows a negative intercept) by selecting systems in which the volumes vary by a factor of seven.

Rummens[27] on the basis of a "site-factor" RF model, argues that the cavity size appears to be independent of the size of the solvent molecules, but on the other hand, he continues, a simple proportionality between 'a' and V_u is not satisfactory either. The fact that the incorporated site-factor

Table 2.2. Comparison between the Solute Cavity RF, RFu, and the Solvent Cavity RF, RFv

Solute	$\langle R^2 \rangle \times 10^{-12}$ erg/cm^3 (2.18)	Solvent							RF-σ_w* CC
		$Si(OEt)_4$	$Si(OMe)_4$	$SiEt_4$	$SnEt_4$	$SnMe_4$	$SiCl_4$	CCl_4	
CH_4	RFu	.0630	.0570	.0750	.0830	.0760	.0710	.0810	.469
	RFv	.0014	.0028	.0023	.0024	.0044	.0058	.0095	.951
CF_4	RFu	.0197	.0179	.0235	.0262	.0240	.0223	.0256	.666
	RFv	.0017	.0035	.0028	.0029	.0055	.0072	.0118	.903
$Si(OEt)_4$	RFu	.0080	.0073	.0096	.0107	.0098	.0091	.0104	.514
	RFv	.0080	.0162	.0162	.0132	.0250	.0330	.0543	.934
		$n-C_5H_{12}$	C_6H_{12}	C_6H_6	CCl_4	CS_2	P_4		
P_4	RFu	.0442	.0563	.0700	.0620	.0944	.1700		.991+
	RFv	.0152	.0220	.0410	.0301	.1210	.1700		.915

---

*: σ_w (Expt.) are given in tables 2.5, 2.7, and 2.9.

+: The intercept is negative - 6.7 ppm.

(see Chapters 3 and 4) has a strong effect on the RF model discredits his conclusion. In practice he finds a cavity size larger than the size of the benzene molecule and of the same size as $C(CH_3)_4$ for CH_4. This shows that the cavity size of CH_4 is more akin to the holes in solvents rather than its molecular size.

2.3.2. Homer and Percival RF model

In general any RF model is plagued with the two afore-mentioned problems, namely the poor correlation, and, the shortfall of experimental values.

Rummens in his comprehensive RF work[27] has, to some extent, circumvented the former by incorporating the solute-site-factor idea into the RF work frame. The latter shortcoming however, has not been overcome and different factors for different solutes have been used to "scale" the calculated values up to the experimental ones. He has found that the scale factors range from 6 for CH_4 to 16 for $Ge(CH_3)_4$ (this is for B_0 = .74 and y = 1). Rummens has made an attempt to relate this shortcoming to the Onsager's approximation for the cavity size.

It is shown in chapter four that the need for a scale factor partly arises from the lack of the "solvent-site-factor" in his model. The nature of the RF model, that is the exclusion of the first molecular shell, chiefly necessitates the use of a scale factor.

Demontgolfier's RF model (y = 1) for CH_4 and C_5H_{10} requires scale factors of 3.4[144,149] and 13.5[144] respectively.

Homer and Percival[29] have recently proposed a new RF model that overcomes the two mentioned problems. The gist of their argument is as follows.

As the solute moment $m_u(t)$ polarizes the continuum and produces an RF on itself $\langle R^2 \rangle_u$, likewise an RF can be assigned to every solvent molecule of the <u>first shell</u> surrounding the solute. These macroscopic solvent fields $\langle R^2 \rangle_v$ are constant over the microscopic solvent cavity accommodating the solute molecule, and will not be diminished in reaching the solute, or at least its peripheral atoms. Therefore the total RF acting on the solute at the centre of a cavity, which now includes the first shell of solvent molecules, is the sum of $\langle R^2 \rangle_u$ and $x \langle R^2 \rangle$, where x denotes the contribution of $\langle R^2 \rangle_v$ to the total RF. According to Homer and Percival however, $x = (2\pi/3)$ for solutes and solvents of roughly equal volumes;

$$\langle R^2 \rangle \text{ (Total)} = \text{RFT} = \langle R^2 \rangle_u + (2\pi/3) \langle R^2 \rangle_v \qquad (2.19)$$

Their formulation of the two reaction fields is based on a polarizable static dipole approach, the mean-square RF of which is obtained by direct static-to-dynamic mapping ($y = 1$) so that RFT becomes;

$$\text{RFT (erg/cm}^3\text{)} = 13.58 \times 10^{12} \left[\frac{I_u \alpha_u (n_u^2 + 2)^2 (n_v^2 - 1)^2}{V_u^2 (2 n_v^2 + n_u^2)^2} + (2\pi/3) \frac{I_v \alpha_v (n_v^2 + 2)^2 (n_v^2 - 1)^2}{V_v^2 \, 9 \, n_v^2} \right] \qquad (2.20)$$

The functional forms of the refractive index in (2.17) and (2.20) differ due to the polarizable dipole assumption in the latter expression.

In their formulation Homer and Percival approximate $h\nu$ in the oscillating moment expreesion, (A1.4), by 2I. This is twice the London original approximation. Before the test of (2.20) a comment on the nature of this approximation appears to be an apt digression.

This is an empirical approximation [150] based on Pitzer[151] work. He treats $h\nu$, in the London formula, as an adjustable parameter to match the experimental data for a number of many-electron atoms and molecules. He finds that $h\nu/I$ ranges from 1.2 for He, to 2.82 for Cl_2. Pitzer[152] attributes the need for $h\nu > I$ to the possible partial contribution of more tightly-bound electrons to the London dispersion energy. Here some of the $h\nu$ values given by Margenau[71], and the ionization potentials are reproduced to show the superiority of the London approximation;

Species	H	Ne	Ar	Kr	Xe	H_2	N_2	CO_2	CH_4	Cl_2	NH_3
$h\nu$ (ev)	24.5	25.7	17.5	14.7	12.2	14.5	15.8	15.5	14.1	12.7	11.7
I (ev)	24.5	21.5	15.7	14.0	12.1	15.4	15.6	13.8	13.0	11.5	10.1

It is shown in Chapter 3 that treating polyatomic molecules as polarizable spheres causes the low calculated dispersion energies, for the offset of which the $2I = h\nu$ approximation is resorted to. This can be seen from table 3.7 where the calculated heats of vaporization for polyatomic molecules by London formula fall short of the experimental values by a factor of three, making $h\nu = 2I$ a preferable approximation.

The Homer and Percival total RF is analysed for the available σ_w data in tables 2.4 to 2.9.

Table 2.3. Physical Constants of the Species

Species	Molar Vol. $cm^3/mole$ (30 °C)	Ref.	I (ev)	Ref.	α (A^3)	Ref.	n^2 (20 °C)	Ref.
1,2,3 $C_6H_3(CH_3)_3$	139.0	158	8.43	158	15.4	137	2.248	158
p-$C_6H_4(CH_3)_2$	125.2 (35 °C)	27	8.44	16	14.27	16	2.210	a
p-$CH_3C_6H_4F$	111.0	158	8.80	b	12.28	c	2.1606	158
p-$C_6H_4F_2$	99.8 (35 °C)	165	9.15	c	10.29	c	2.054	a
$(CH_3)_2C{=}C(CH_3)_2$	118.9	158	8.31	158	11.74	a	1.9943	158
$CH_3C{\equiv}CCH_3$	78.3	158	9.94	158	7.45	c	1.9380	158
$Si(OCH_2CH_3)_4$	224.0 (35 °C)	163	9.25	d	20.40	c	1.8961	160
$Si(OCH_3)_4$	150.3 (35 °C)	163	9.25	d	12.90	c	1.8301	160
$Si(CH_2CH_3)_4$	191.3 (35 °C)	163	9.81	159	19.2	159	2.0357	158
$Si(CH_3)_4$	146.5	159*	9.80	159	11.9	159	1.8266	143
$SiCl_4$	117.2 (35 °C)	163	11.6	16	11.4	159	1.990	158
SiF_4	62.7	158	16.94	246	3.33	246	1.464	a
CS_2	61.4 (35 °C)	163	10.08	16	8.56	16	2.6631	158
CH_4	33.6 (m.p.)	69	12.99	16	2.55	16	1.710	a
CF_4	66.8	158	17.81	246	2.89	246	1.2863	a
CH_2Cl_2	64.9	157	11.35	158,164	6.82	173,174	2.02937	158,176
$CHCl_3$	81.1	157	11.42	158,164	8.53	174,177	2.0906	158
CCl_4	98.3 (35 °C)	163	11.44	16	10.24	16	2.1144	158
CH_3Br	56.6 (20 °C)	158	10.53	158	5.61	168,169	2.02151	158
CH_2Br_2	70.3	157	10.48	158,164	8.68	170,171	2.37715	175
$CHBr_3$	88.22	157	10.4	158,164	11.84	170,172	2.5523	158
CBr_4	112.0(100 °C)	158	10.4	b	15.07	a	2.54144	158
CH_2ClBr	66.9 (20 °C)	158	10.77	158	7.58	a	2.20166	158
$CHClBr_2$	86.4	178	10.5	b	10.88	a	2.3969	158
CCl_3Br	99.7	179	10.88	b	11.7	a	2.26894	158
CH_3I	63.0	157	9.54	158,164	7.59	164,168	2.34555	176

(Table 2.3 continued)

CH_2I_2	81.3	157	9.3	b	12.9	170,171	3.03143	175
$C(CH_3)_4$	131.4	159*	10.36	159	10.2	159	1.7902	143
$C(CH_2CH_3)_4$	171.9	27	10.36	e	17.5	c	2.041	a
n-C_5H_{12}	115.2 (20 °C)	158	10.35	158	10.02	a	1.8428	158
Cyclo-C_5H_{10}	96.0 (35 °C)	158	10.53	158	9.1	159	1.978	158
C_6H_6	90.5 (35 °C)	158	9.24	16	10.39	16	2.242	158
C_6F_6	117.4 (35 °C)	165	9.97	158	10.1	257	1.8968	166
Cyclo-C_4F_8	116.0 (0 °C)	158	13.3	f	7.66	c	1.5136	162+
C_6H_{12}	110.0 (35 °C)	158	9.88	16	10.87	16	2.0264	158
n-C_6H_{14}	130.5 (20 °C)	158	10.18	158	12.9	c	1.8908	158
n-C_7H_{16}	146.5 (20 °C)	158	9.9	158	14.96	c	1.92559	158
$Ge(CH_3)_4$	138.2	159	9.17	159	12.8	159	1.9088	143
$Sn(CH_3)_4$	138.2	159	8.36	159	14.4	159	2.054	143
$Sn(CH_2CH_3)_4$	199.2 (35 °C)	163	8.36	e	21.7	c	2.1362	a
$Pb(CH_3)_4$	135.9	159	8.24	159	15.9	159	2.2644	143
SF_6	77.7	158	19.32	246	4.53	246	1.570	a
P_4	68.1 (20 °C)	158	7.04	f	14.7	a	4.5967	158,167
Br_2	51.2 (20 °C)	158	10.55	158,69	6.464	a	2.75892	158
Xe	37.0 (solid)	69	12.13	158	4.04	251	2.15094	a

a: Estimated from Lorentz-Lorenz Eq., (1.2), using either ε or n^2.

b: Estimated from data on similar compounds.

c: Estimated from bond polarizabilities given in Ref.[161].

d: Estimated from data on similar compounds by Percival[160].

e: See foot-note "d" to table 3.5.

f: Estimated from the "inert-atom additivity rule" given in chapter three. See also table 3.7.

*: At variance to his temperature-dependent densities Rummens[159] gives 124.6 and 139.5 cm³/mole for the volumes of CMe_4 and $SiMe_4$ respectively. The correct volume of 131.4 for CMe_4 is used by him in a subsequent work[27].

+: This value is calculated by Abraham and Wileman[162].

Table 2.4. Results of comparison between Expt. - σ_w (ppm) at 30 °C[159] and RFT$\times 10^{-12}$ erg/cm^3 (2.20)

	Solute				
Solvent	CMe_4	$SiMe_4$	$GeMe_4$	$SnMe_4$	$PbMe_4$
CMe_4	.217	.255	.260	.280	.285
RFT	.080	.077	.080	.081	.086
$SiMe_4$	.185	.228	.228	.250	.258
RFT	.079	.076	.080	.080	.085
$GeMe_4$	.215	.262	.260	.280	.287
RFT	.098	.095	.099	.100	.106
$SnMe_4$	.222	.270	.275	.297	.302
RFT	.123	.118	.124	.125	.132
$PbMe_4$	.277	.322	.325	.350	.358
RFT	.175	.170	.176	.178	.188
CC	.927	.963	.944	.957	.963
Slope(B)	.774	.844	.832	.865	.834
Intercept	.137	.177	.176	.194	.198

Table 2.5. Results of comparison between Expt. - σ_w (ppm) at 35 °C[163] and RFTx10^{-12} erg/cm^3 (2.20)

	Solute						
Solvent	$Si(OC\underline{H}_2CH_3)_4$	$Si(OCH_3)_4$	$C(CH_3)_4$	$Si(OCH_2C\underline{H}_3)_4$	$Si(CH_3)_4$	$Sn(CH_3)_4$	CH_4
$Si(OEt)_4$	.160	.182	.173	.193	.217	.270	.295
RFT	.059	.067	.070	.059	.067	.072	.186
$Si(OMe)_4$	.155	.198	.190	.190	.252	.272	.310
RFT	.067	.074	.077	.067	.074	.079	.181
$Si(Et)_4$	.162	.170	.197	.193	.250	.292	.305
RFT	.082	.091	.095	.082	.090	.097	.234
$Sn(Et)_4$	.172	.192	.205	.208	.260	.310	.316
RFT	.108	.118	.123	.108	.118	.125	.279
$Sn(Me)_4$	.185	.187	.205	.205	.267	.310	.322
RFT	.107	.116	.121	.107	.116	.123	.263
$SiCl_4$	.188	.200	.223	.228	.298	.325	.346
RFT	.142	.150	.154	.142	.150	.156	.286
CCl_4	.302	.332	.345	.349	.375	.433	.472
RFT	.206	.216	.220	.206	.215	.223	.373
CC	.931	.862	.941	.932	.973	.974	.949
Slope(B)	.940	1.026	1.042	1.041	.960	1.037	.800
Intercept	.085	.098	.091	.109	.160	.186	.110

Table 2.6. Results of comparison between Expt. - σ_w(ppm) at 35 °C[17,163,180] and RFTx10^{-12} erg/cm^3 (2.20)

	Solvent							
Solute	$SnEt_4$	$SiEt_4$	$SnMe_4$	$SiCl_4$	CCl_4	CC	Slope(B)	Intercept
C_5H_{10}	.178	.165	.185	.203	.295			
RFT	.156	.124	.150	.181	.252	.982	1.047	.024
C_6H_6	.273	.240	.277	.293	.443			
RFT	.169	.135	.162	.192	.265	.980	1.578	.014
C_6H_{12}	-	.145	.175	.187	.265			
RFT	.145	.115	.141	.173	.242	.989	.921	.038
$CH_3C{\equiv}CCH_3$	.300	.277	.288	.318	.477			
RFT	.165	.132	.160	.189	.261	.968	1.633	.035
$(CH_3)_2C{=}C(CH_3)_2$	.232	.218	.230	.237	.340			
RFT	.130	.101	.127	.160	.227	.950	.983	.105
$C\underline{H}_3C_6H_4C\underline{H}_3$	.267	.242	.268	.283	.423			
RFT	.139	.109	.135	.167	.235	.970	1.453	.068
$CH_3C_6\underline{H}_4CH_3$	.230	.200	.227	.245	.340			
RFT	.139	.109	.135	.167	.235	.988	1.101	.075
1,3,5 $C_6H_3(C\underline{H}_3)_3$	.272	.250	.278	.295	.417			
RFT	.131	.102	.128	.161	.228	.977	1.333	.102
1,3,5 $C_6\underline{H}_3(CH_3)_3$	.202	.183	.205	.220	.292			
RFT	.131	.102	.128	.161	.228	.989	.862	.092
$F{-}C_6\underline{H}_4{-}F$	.287	.253	.290	.315	.492			
RFT	.150	.119	.145	.176	.246	.979	1.910	.007
$Sn(CH_2C\underline{H}_3)_4$	.207	-	.187	.205	.282			
RFT	.121	.093	.119	.152	.218	.956	.872	.087
$Si(CH_2C\underline{H}_3)_4$	-	.153	.153	.162	.257			
RFT	.113	.086	.112	.146	.211	.922	.864	.061

Table 2.7. Results of comparison between Expt. $^{19}F - \sigma_w$ (ppm) at 35 °C and RFTx10^{-12} erg/cm^3 (2.20)

	Solute					
Solvent	CF_4	SF_6	SiF_4	p-Me-$C_6H_4\underline{F}$	p-$C_6H_4\underline{F}_2$	C_6F_6
$Si(OEt)_4$	5.97	6.36	8.95*	5.74	6.12	6.31
RFT	.082	.110	.108	.087	.090	.077
$Si(OEt)_4$	5.54	5.96	8.31*	5.21	5.77	5.16
RFT	.088	.113	.111	.092	.095	.084
$Si(Et)_4$	6.00	6.35	9.82+	6.98	7.21	7.16
RFT	.109	.143	.140	.115	.119	.104
$Sn(Et)_4$	6.26	6.70	9.12+	7.25	7.43	7.21
RFT	.138	.177	.173	.146	.150	.133
$Sn(Me)_4$	6.82	7.05	10.05	7.61	7.74	7.89
RFT	.135	.170	.167	.142	.145	.130
$SiCl_4$	6.85	7.03	10.10	7.83	7.96	8.45
RFT	.167	.199	.197	.173	.176	.162
CCl_4	7.60	7.98	11.15	8.14	8.27	8.81
RFT	.235	.273	.270	.243	.246	.230
CC	.939	.957	.882	.850	.869	.859
Slope(B)	12.40	11.21	14.60	17.29	15.15	20.59
Intercept	4.74	4.88	7.20	4.50	5.00	4.58

*: Raynes and Raza[165] give 16.32 and 12.36 ppm respectively for SiF_4 in $Si(OEt)_4$ and $Si(OMe)_4$ in variance with their rule that the shifts for SiF_4 can be found from those of CF_4 by multiplying by 1.5. The corresponding entries here are according to this rule.

+: Rummens[17] mistakenly quotes 14.37 and 15.97 for SiF_4 in $Si(Et)_4$ and $Sn(Et)_4$ respectively.

Table 2.8. Results of comparison between Expt. ^{19}F - σ_w (ppm) at 40 °C[162] and RFTx10^{-12} erg/cm^3 (2.20)

	Solvent									
Solute	CCl_4	C_6H_6	n-C_7H_{16}	C_6H_{12}	n-C_6H_{14}	n-C_5H_{12}	c-C_4F_8	CC	Slope(B)	Intercept
CF_4	7.60	6.61[a]	6.08	5.94	5.77	5.44	3.04			
RFT*	.239	.274	.120	.168	.122	.114	.051	.830	15.00	3.45
c-C_4F_8	6.94	-	5.62	5.49	5.34	4.96	2.87			
RFT	.230	-	.114	.161	.116	.108	.049	.914	19.90	2.60
C_6F_6	9.21[b]	-	7.72	7.62[b]	7.38	6.90	3.73			
RFT	.234	-	.116	.164	.118	.110	.049	.886	26.10	3.63

---

a: Ref[187]; b: Cyr et al[188] give 9.09 and 7.40 ppm for C_6F_6 in CCl_4 and C_6H_{12} respectively.

b: The calculated RFTs are for 30 °C. Tabulated volume of c-C_4F_8 is used, table 2.3.

Table 2.9. Results of comparison between Expt. $^{31}P^*$ - σ_w (ppm) at 30 °C[181] and RFTx10^{-12} erg/cm^3 (2.20)

Solvent --->	n-C_5H_{12}	C_6H_{12}	C_6H_6	CCl_4	CS_2	P_4(White phosphorus)	CC	Slope(B)	Inter.
σ_w	21.1	23.5	30.0[+]	30.5	40.4	89.8			
RFT	.207	.299	.450	.388	.994	2.70	.997	26.91	16.55

---

*: Phosphorus vapour below 800 °C consists almost entirely of P_4 (Raman spectroscopy[182], electron diffraction[183], and, recent laser Raman sectroscopy[184]) with tetrahedral structure; P-P-P angle of 60°, and, P-P bond length of 2.21 ± .02 A.

White phosphorus (mp = 44.1 °C) in the liquid has the same structure[185,186].

+: A correction of .5 ppm has been made for the anisotropy effect. No correction is made for the anisotropy of CS_2. Large σ_w values however, render the corrections immaterial.

2.4. Buffeting Interaction

From the results of the regression analysis given in these tables the following inferences can be made.

1- Homer and Percival RF model is the only pure RF formulation for σ_w that apparently works for nearly all the systems (with the exception of some of ^{19}F systems) with reasonable correlation coefficients.

2- The slopes or B values with the overall average of 1.06 ± .3 for ^1H shows that the calculated screenings are of the same order as the data. This overall average is in agreement with the empirical value of 1.06 found by Raynes et al[78] for hydrocarbons.

The B values are not constant and vary by a factor of 2.46 (.774 to 1.91). Some of this variation is due to the site of the H atom in the molecule; compare the ring and CH_3 hydrogens of 1,2,3-$C_6H_3(CH_3)_3$, for example. Correction for the site of the resonant nucleus, as Rummens[153] has shown, reduces this variation to some extent. The B value of $(16.9 \pm 4.4)\times10^{-12}$ cm^3/erg for ^{19}F agrees well with the Kromhout and Linder[138] value of B = 18 for $CF_4...CF_4$ interaction. There is no theoretical or empirical B value available for ^{31}P, but $B = 27\times10^{-12}$ appears reasonable on the basis of the Jameson et al B_o value, because one would expect (see Chapter 5) the value of ^{31}P B to fall somewhere between those of Ne and Ar.

3- The distinctive feature of RFT is the existence of positive intercepts for all the systems as it is typified in Fig. 2.3.

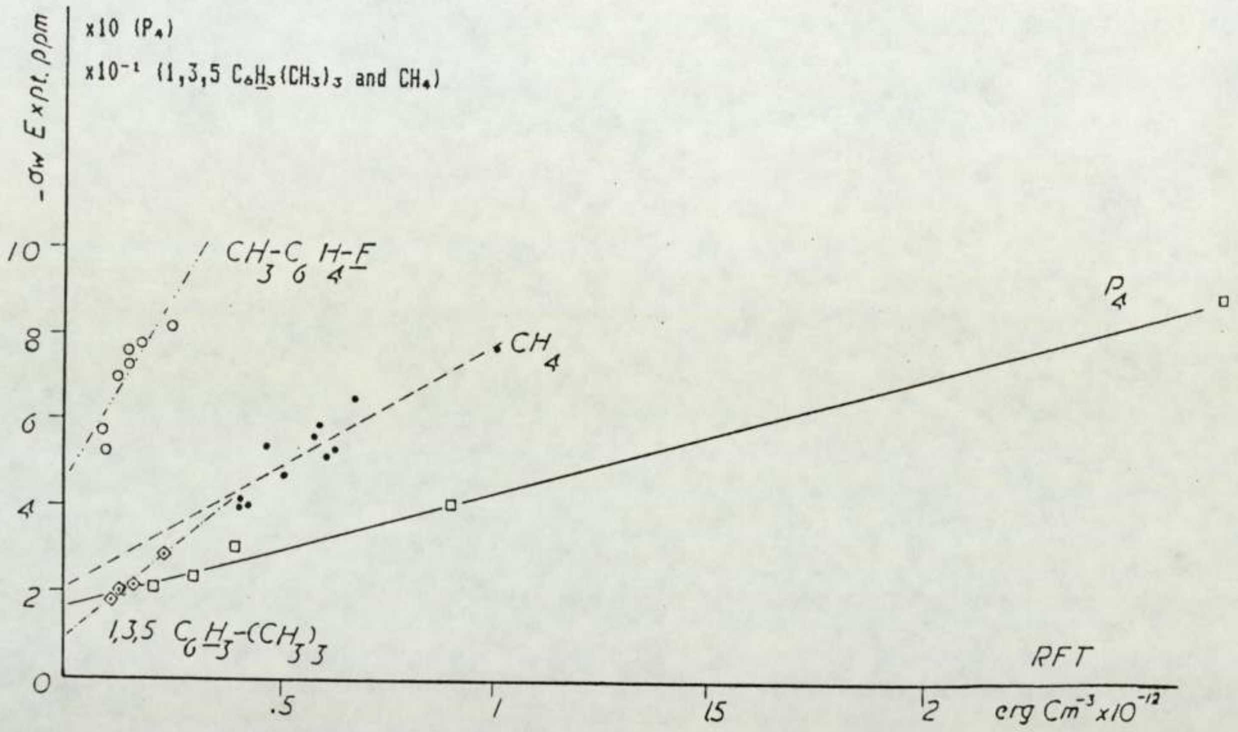

Fig. 2.3 Typical experimental σ_w for the labelled solutes as a function of the Homer and Percival RFT, Eq.(2.20).

These intercepts led Homer and Percival to the re-discovery of a well-known effect in liquid and solid state theories, namely the interaction between the peripheral atoms of the nearest solvents and the solute. They coined this effect as a buffeting interaction according to which the expression for the characterization of σ_w must be changed to;

$\sigma_w = - B \text{ RFT} + \text{Intercept}$, or;

$$\sigma_w = \sigma_{RF} + \sigma_{BI} \qquad \text{for} \quad y = 1 \qquad (2.21)$$

This expression reflects the fact that no pure RF model is capable of adequate formulation of σ_w. In fact the solvent RF, $\langle R^2 \rangle_v$, and the BI together embody the pairwise interactions from which any vdW effect arises as Dickinson's interaction term qM requires

It must be emphasised that (2.20) is based on $y = 1$. The actual value of $y = 1/16$ would nullify the RF part of (2.21) so that;

$$\sigma_w \simeq \sigma_{BI} \qquad \text{for } y = 1/16 \qquad (2.22)$$

Now if (2.22) is true, one might ask, were all the good correlations between the σ_w data and RFT fortuitous? The answer is that the significance levels of mostly < 5% rule out the accidental nature of the correlations. The Homer and Percival RFT owes its good correlation with data to the second term in (2.20). This is the predominant term, except for small solutes such as CH_4, and has the volume of the solvent as the cavity size, which is the solvent cavity idea.

It is shown by Homer and Percival, and also in the next chapter, that the functional form of σ_{BI} is similar to the second term in (2.20) without $f(n_v)$. It is proportional to $I\alpha$ of the solvent atoms, and has the same a^{-6} dependence. Therefore some sort of $\sigma_{EI}-\sigma_w$ linear relationship would be likely that explains the observed correlations between RFT and σ_w.

2.5. The Medium Eeffect Contribution of Permanent Dipoles

When dipolar solutes or solvents are used, the screening effects of their extra field have to be accounted for by addition of more terms to (2.8).

For polar solvents there is a direct field contribution E^2 due to their permanent dipoles so that (2.8) becomes;

$$\sigma_m = \sigma_a + \sigma_b + \sigma_w + \sigma_E \qquad (2.23)$$

Polar solutes give rise to a static Onsager's RF contribution R^2 according to (1.8 and 1.9), therefore (2.23) may be extended to;

$$\sigma_m = \sigma_a + \sigma_b + \sigma_w + \sigma_E + \sigma_R$$

Water as a dipolar solute with $\varepsilon_o = 87.74$ and $\mu = 1.84$ D, has the largest static reaction field value of $R = 2\times10^5$, the square of which (to be used in $\sigma_R = - B_o R^2$) $.04\times10^{12}$ erg/cm^3 is the smallest amongst those of table 2.4 to 2.9.

Other dipolar solutes have even smaller RF values, for example $R^2 = 4\times10^8$ and 8×10^7 for chloroform ($\varepsilon_o = 4.81$, $\mu = 1.15$ D) and nitrobenzene ($\varepsilon_o = 34.82$, $\mu = 4.03$ D) respectively.
These values show the negligible contribution of the dipolar effect of solutes.

Concerning the dipolar effect of solvents, Raynes et al[27,78] have shown that this contribution can be written as;

$$\sigma_E = \sigma_w \frac{2\,\mu_v^2}{3\,\alpha_v I_v}$$

In terms of the expression for the oscillating moment of solvent, this may be written as;

$$\sigma_E = \sigma_w\, \mu_v^2/\langle m^2\rangle_v \qquad (2.24)$$

This contribution is also generally negligible because; $\langle m^2\rangle_v \gg \mu_v^2$. For the two polar solvents considered here; $Si(OCH_3)_4$, and $Si(OCH_2CH_3)_4$, it amounts to the maximum values of;

$$\boldsymbol{\sigma_E\ (Si(OMe)_4) = \sigma_w\ (1.8)^2/335.22 = .0096\ \sigma_w = \left\{\begin{array}{l} .003 \text{ ppm for } ^{1}H \\ .057 \text{ ppm for } ^{19}F \end{array}\right.}$$

$$\boldsymbol{\sigma_E\ (Si(OEt)_4) = \sigma_w\ (1.1)^2/497.30 = .0024\ \sigma_w = \left\{\begin{array}{l} .001 \text{ ppm for } ^{1}H \\ .014 \text{ ppm for } ^{19}F \end{array}\right.}$$

where the values of $\langle m^2\rangle$ are calculated using the I and α data from table 2.3, and the permanent dipoles of $C(OMe)_4$ and $C(OEt)_4$ are used by analogy. Their dipoles respectively are .8[154,155], or, 1.8[176] and 1.1 D[154,156].

The Homer and Percival RFT is further tested on the data obtained by Buckingham et al[22] for methane in polar solvents. Raynes[157] has re-calculated the Buckingham (et al) excess screenings, $\sigma_m - \sigma_b = \sigma_w + \sigma_E$, because the susceptibility data they used to find σ_b were inaccurate. Table 2.10 gives these values except for Br_2 and CBr_4 for which the corrected values of Rummens[27] are given.

We note that Br_2 is excluded from the analysis given in this table, because its point is well off the linear trend which

Table 2.10. Analysis of - σ_w (30 °C) of CH_4 in Polar Solvents

	Dipole moment ergcm^{3}x10^{36}				
Solvent	Permanent μ^2[161]	Transient $\langle m^2 \rangle$	$\frac{\mu^2}{\langle m^2 \rangle}$	RFTx10^{-12} erge/cm^3	- σ_w (ppm) [157]
CH_3Br	3.28	141.52	.023	.405	.397
CH_2Cl_2	2.56	185.78	.014	.417	.407
$CHCl_3$	1.02	233.79	.004	.401	.420
CH_2ClBr	5.58^a	195.93	.028	.506	.475
CH_3I	2.62	173.78	.015	.600	.515
CH_2Br_2	2.04	218.32	.009	.622	.532
CCl_3Br	3.63^b	307.08	.012	.458	.542
Br_2	.0	163.67	.000	1.052	.556*
$CHClBr_2$	4.62^c	274.17	.017	.570	.568
CBr_4	.0	376.15	.000	.582	.594*
$CHBr_3$	.98	295.53	.003	.668	.652
CH_2I_2	4.29^d	287.93	.015	1.026	.767

CC$^+$	.923
Slope(B)	.573
Intercept	.205

a: Calculated (according to the principle of vectorial additivity of dipole moments[161]; $\mu^2 = \mu_1^2 + \mu_2^2 + 2\mu_1\mu_2 \cos\theta$) using θ(Cl-C-Br) = 111° and bond-moment of μ(C-Cl) = 1.87 and μ(C-Br) = 1.8 D[161].

b: Calculated using $\mu(CHCl_3)$ = 1.02, μ(C-Br) = 1.8, and θ(Br-C-Cl) = 111°.

c: Calculated using $\mu(CH_2Br_2)$ = 2.04, μ(C-Cl) = 1.87, and θ(Br-C-Cl) = 111°.

d: Calculated using μ(C-I) = 1.64[161], and θ(I-C-I) = 113°[158].

*: Ref.[17].; +: Correlation coefficient excluding Br_2.

reduces the correlation coefficient to .3. The RFT (2.20) tends to calculate too large a value when solute and solvent are small.

The small ratios of static to dynamic dipoles in the last column of the table justify the use of (2.8) instead of (2.23). The ratio however may be larger for small molecules with large μ values. Water and CH_3CN (μ = 3.44 D), for example, have ratios of .075 and .115 respectively, giving rise to σ_E values about one order of magnitude smaller than their corresponding σ_w. It may therefore be concluded that the electrostatic contribution to the shift of the medium is generally negligible.

2.6 Conclusion

We saw that the excess screening, $\sigma_m - \sigma_b$, in the absence of a magnetic anisotropy effect has been labelled as the vdW screening constant σ_w. In this sense σ_w is interlocked with the concepts of the local and demagnetization fields, from which the theoretical $2\pi/3$ factor arises for cylindrical NMR tubes.

Although the exact value of the $2\pi/3$ factor has not been confirmed by the classical NMR experiments, the recent work of Homer and Al-Daffaee[189], on the determination of χ_v from chemical shifts, gives a direct and positive verification of this theoretical value. Therefore, one may limit the source of uncertainties in the determination of σ_w(expt.) by the $2\pi/3$ χ_v correction to the inaccuracy in χ_v values only.

The B parameter is another source of uncertainty for the calculated σ_w values. Tables 2.4-2.10 show the variability of B and its dependence on the solute-solvent systems. The values of B obtained by the Homer and Percival RR model for heavy nuclei are more akin to those of static theoretical ones. For ^{129}Xe in solid Xe with σ_w = 11800 ppm cm^3/mole[190], for example, one finds RFT = .835 (in units of 10^{12} erg/cm^3) which gives B = 384.3 (in units of 10^{-18} cm^3/erg), in agreement with the Jameson et al static value of 337.3. The calculated field appears to be too high. The revised buffeting theory (Chapter 3) finds a field value of .404 for this system resulting in B = 787, a value close to the Kramhout and Linder dynamic value of 914.

The important fact that the same revised buffeting model finds the right heat of vaporization for Xe verifies B = 787 as a genuine value.The calculated heat of vaporization by the RF model for y = 1 and $h\nu = 2I$, as has been used by RFT here, exceeds the experimental value by a factor of 16. The same is true for ^{31}P B = 27, it is too small because the calculated fields are too large (see Chapter 6 for details).

The Homer and Percival RFT, in accounting for the contribution of the solvent RF to the central molecule, runs parallel with the Kirkwood[141] theory of correcting for the fluctuations in the local dielectric constant. The Kirkwood correction increases the calculated value of ε for water from 31 by Onsager's theory to 55 (ε_0(expt.) = 87).The Homer and Percival theory increases the RF by an order of magnitude.

The crux of the σ_w-RFT analysis is the discovery of the buffeting interaction which has been formulated by Homer and Percival[29] and is the subject of a rigorous investigation in the next chapter.

Chapter 3

Polyatomic London Potential

Introduction

The sphere is an admirable shape, upon which, in hard, soft, and flexible versions, many molecular theories have been based.

The London dispersion potential or the Lenard-Jones potential for example, are quantitative expressions for the forces of attraction (repulsion) between polarizable or flexible spheres assumed to represent molecules.

The macroscopic properties of liquids are mainly related to the properties of the molecules themselves, namely their dynamic behaviour and their arrangement in the liquid state, and more fundamentally, to the nature of their constituent atoms. A potential function inter-relates macroscopic and microscopic properties of molecules; the problem of this inter-relation has remained largely unsolved.

One might therefore legitimately ask:

1- Is there a connection between the inter-relation problem and the approximation of using spheres to represent molecules, as the approximation contradicts their atomic nature?

2- Is it possible to develop a practical potential function for real molecules which accounts for their atomic nature? and

3- Does the new potential accomplish much more than the previous potential? In other words, is mastering the new method worth the time and energy when there is only a slight difference in their numerical results?

The main objective of this chapter is to find a liquid state molecular pair-potential function and answer these questions. However, in achieving this, we find that the passage from a sphere-based potential to a molecular-based one is hindered by three main problems as follows:

1- The conventional problem of determining the inter-molecular distance R in the liquid state. To solve this relevant problem, a simple method of estimating R from molar volumes is adopted here, the validity of which is tested against some available crystalline, van der Waals, and Lenard-Jones R distances.

2- The second problem arises from the recognition of atoms in molecules. The constant thermal rotation of molecules in the liquid state results in the continuous change of the atom-atom distance of two interacting molecules. An average atom-atom distance, as a function of a fixed R and the structure of molecules, is found to account for this fact. The analytical method used proves to be arduous and inadequate. Therefore a simple and efficient numerical method using random numbers for simulating molecular rotation (MONTE CARLO METHOD) is developed here, which also helps to overcome the contentious divergence problem of a series arising from the analytical method. To maintain the continuity of the main presentation, the two methods are relegated to Appendices.

3- As an atom-atom potential deals with atoms in bonds, an obstinate problem arises as to what the ionization potential and the polarizability of the bonded atoms are. The latter problem is solved by the well-known additivity rule for polarizabilities. For the bonded-atom ionization potential, however, a new method based on the "admirable" sphere is developed in which the atom in a bond is approximated to its corresponding (spherical) inert atom. The validity of this supposition is analysed for scores of molecules, and the outcome is a new additivity rule for predicting molecular ionization potentials. This rule is made the basis for the prediction of the ionization potentials of some systems, P_4, S_8, and cyclo-C_4F_8, that are not apparently available. The inert-atom approximation rejuvenates the way we think about dispersion interaction of molecules by replacing their molecular formula C_6H_{12}, for example, by the inert-atom formula Ne_6He_{12}. It is also used for elucidating the structures of some molecules, and reveals the ionic character of SiF_4, SF_6, and CF_4, and the paramagnetism of O_2 and NO.

The circumvention of the afore-mentioned problems, combined with an elegant method due to Homer and Percival in which a text-book field Eq. is converted into a dispersion type field expression, leads to a new molecular or buffeting pair potential function. This function reduces to the London potential formula when the two interacting molecules are sufficiently small or sufficiently far apart. It is in fact a generalized London dispersion potential.

The passage from the buffeting pair-potential, or the two-body potential, to the real liquid is obstructed by the lack of knowledge of the number of nearest neighbours in the liquid state Z_L. This problem is dealt with objectively and leads to an expression for Z_L by which the heat of vaporization of liquids in terms of the pair-potential is formulated.

An analysis of the heats of vaporization for some systems reveals that there is only a small difference between the predictions of the generalized and the London potentials and the observed values for small molecules like H_2. For large molecules such as CCl_4 or $C(CH_3)_4$, however, the sphere-based London potential values fall short of the observed values by a factor of about three, whereas those of the generalized one are substantially in agreement with the data.

The result of such an analysis for water is interesting and unorthodox. The sphere-based potential attributes the standard value of 19% to the dispersion forces whereas the generalized one gives about 47%. The remainding 53% arises from other sources -mainly hydrogen bonding.

3.1. Historical Background

3.1.1. Atom-Atom Interactions and Liquid State Theories

The equilibrium properties (density, thermal expansion coefficient,...) of simple fluids composed of inert atoms, Ar, Kr and Xe, have been satisfactorily described by a Lenard-Jones (6-12) central force potential which is a function of the distance between the centres of the molecules[191].

However, measurements on the various physical properties of symmetric polyatomic molecules such as, CH_4, CCl_4, $C(CH_3)_4$, which gain spherical symmetry by their rapid rotation, have shown that their interactions cannot be interpreted in terms of the (6-12) central potential[192] and the acentric distribution of polarizable electrons necessitates a drastic change of this potential[193].

Experimental evidence found by Hildebrand[194] in 1947 proves that the intermolecular forces between polyatomic molecules arise mainly from the interactions of their peripheral atoms. This means that the effective centres for the interaction potential are now the atoms, well removed from the centres of the molecules[195-197].

As London[81] has pointed out "...only the highly compact molecules can reasonably be treated simply as force centres. For the long organic molecules it seems desirable to try to build up the van der Waals' attraction as a sum of single actions of parts of the molecules."

The assumption of a (6-12) potential for the interaction of atoms belonging to different molecules, for example, results in a potential function which no longer has the spherical symmetric form of the inert atoms (spheres) potential but contains supplementary terms depending on the relative orientations and the geometric structure of the molecules[192]. The structural parameter of the molecule introduced into the potential function shows the marked effect of the structures of molecules on their physical properties.

Although recent theoretical models of properties of polyatomic molecules, from diatomic to biopolymers, are based on the atom-atom interaction between molecules[198-203], its history at least dates back to the work of Miller[204] in 1936 on organic molecular crystals.

3.1.2. Atom-Atom Interactons in NMR

We saw in the two previous chapters how the study of the vdW chemical shift led to the recognition of the difference between corresponding static and dynamic quantities, and the demagnetization field for diamagnetic materials. The same study forced NMR investigators to a recognition of the polyatomic nature of molecules.

The two models for the characterization of the vdW chemical shift are the continuum, and the non-continuum models. In the continuum or the RF treatment, the solute, a polarizable sphere, interacts with a polarizable continuum of solvent. In the non-continuum treatment of vdw effect on the other hand, the polarizable sphere of the solute interacts with the polarizable solvent spheres of the first shell (in a binary or cage-model manner).

The continuum and non-continuum models of a structureless solute and solvent failed to explain the simple experimental fact that different protons in a given solute molecule have different vdW chemical shifts. After the inspection of the experimental data the following explanations were offered.

Bothner-By[134] put forward the argument of the "accessibility" of the solute proton to the field of the solvent molecules, so that different protons with different accessibilities will show different solvent effect.

Raynes and Raza[163] remarked on the "degree of exposure" of the solute protons to the solvent.

Rummens et al[80,159] and Rummens[27] talked about a "site factor" which corrects for the fact that the nuclei measured are not normally located at the centre of the mass of the solute molecule.

De Montgolfier[144,145,205] argued that no molecule is a true point molecule and therefore an atom of the solute molecule in the Onsager cavity would not only experience the RF but also the fields of the bond dipoles of the solute itself.

One notes that the common theme of these explanations is the recognition of the polyatomic nature of the solute.

The effect of solute polyatomicity on σ_w was quantified in terms of a factor called the "site factor" by Rummens et al and Rummens and was incorporated into the continuum[27] and non-continuum[80,159] models.

The next natural step, the recognition of polyatomicity and structure for the solvent molecule, was taken by Raynes[206].

By arguing that "... as two molecules approach each other, it becomes less valid to treat them as point polarizable spheres". He quantified the interaction between polyatomic solute and solvent in terms of a "site-site factor". Raynes' approach however, because of mathematical and modelling problems, has been confined to methane-methane interaction only.

This discrimination between the polyatomic solute and point structureless solvent persisted until recently, when Homer and Percival[29] made a breakthrough by an elegant modelling of the polyatomic interaction between solute and solvent. They argue that there are two distinct mechanisms involved in the characterization of σ_w, the continuum σ_{RF}, and the non-continuum buffeting action of the peripheral solvent atoms on the solute atoms, σ_{BI} (see sec. 2.4).

The effect of solvent-solute structure in Homer and Percival theory is formulated in terms of a "steric" factor, which is more akin to a site-site factor. In their theory of σ_w, unlike the "site factor" school, there is no need for a scale factor to cure the shortfall of experimental values.

The objective of this chapter is to give a rigorous derivation of the Homer and Percival buffeting field expression by which, on the one hand a general form for the London potential is derived here, and on the other hand, the physical significance of their steric factor and its relevance to the site and site-site factors is explored in the next chapter.

3.2. Buffeting Interaction, General Theory

In accordance with the general method of the formulation of chemical screening (2.10), and, (2.11) given in the previous chapter, σ_{BI} in (2.22) should be proportional to some non-zero mean-square fields of the "solvent atoms" at the site of the resonant nucleus[29];

$$\sigma_{BI} = - B \langle E^2 \rangle \qquad (3.1)$$

An evaluation of this mean-square field is intended, for comparison with the Homer and Percival[29] derivation.

3.2.1. A qualitative description of the Buffeting Field, $\langle E^2 \rangle$

Let us consider a pair of molecules, solute and solvent, with a particular mutual orientation as depicted in Fig. 3.1.

As a result of the independent rotations -assuming no special interactions- of the two molecules at the fixed R, the distance between a given pair of atoms, 'i' and 'j', changes with time, as is shown in Fig. 3.1a and 3.1b.

At instance t_o, when i and j are a distance $r_{ij}(t_o)$ apart, the electron cloud of j "buffets" that of the solute atom i as a result of which the electron cloud of i expands. This expansion reduces the shielding of the i's nucleus by its electrons. At instance t_1, when the distance between the buffeting atom j and the "buffeted" atom i has increased to $r_{ij}(t_1)$, the strength of the electronic buffeting of j diminishes. The attraction or expansion of the electronic cloud of i is less and therefore its nucleus is more shielded compared to instant t_o.

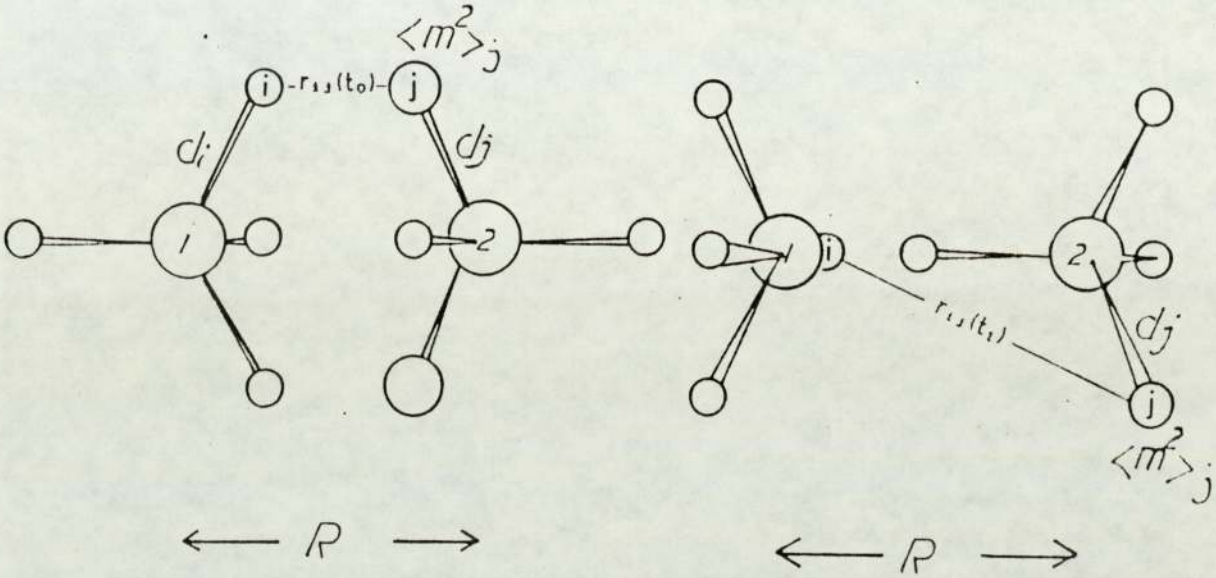

Time t_o

(a)

Time t_1

(b)

(a) A short instantaneous, $r_{ij}(t_o)$, between two interacting atoms i and j results in a strong dispersion attraction between their electron clouds that could mean high "exposure" or "accessibility" of i to j.

(b) A long instantaneous, $r_{ij}(t_o)$, between two interacting atoms i and j results in a weak dispersion attraction between their electron clouds that could mean low "exposure" or "accessibility" of i to j.

Fig. 3.1 Two mutual orientations of two interacting molecules.

Other possible interpretations of situation at t_1, are the "less accessibility" of the solute atom to the solvent atom, "less exposure" of the resonant nucleus to the field of the solvent atom, and, as Homer and Percival put it, less steric accessibility of the solute resonant nucleus to the encounters by the solvent atom.

The implication of adopting the afore-mentioned quotations of different authors as possible interpretations of the situations (a) and (b) (Fig 3.1) is that "accessibility", "degree of exposure", and, "steric accessibility" stem from the relative rotations of the two polyatomic molecules.

Therefore, it is by the formulation of the effect of these mutual orientations that a steric factor, a site factor, or a site-site factor will be incoporated into the effective field $\langle E^2 \rangle$ produced at 'i' by 'j'.

Fixing the intermolecular distance at R while molecules rotate is tantamount to separating the translational and rotational motions. The separation of different molecular motions is based on their relative time scales, which has a key role in the formulation of the effective field, and is discussed below.

In a magnetic field of .2T, for example, the precessional period of the nuclei is of the order of 10^{-7} s, because;
$\omega = B_0 \, g_N \, e/(2m_p) = .2 \text{ (T) } 4.79\times10^7 \text{ (T}^{-1}\text{s}^{-1}\text{)}$
$\omega = 9.58\times10^6 \text{ s}^{-1}$, or the period is;
$\tau = 2\pi/\omega = 6.56\times10^{-7}$ s
This is a very much larger period compared to that of

electronic, vibrational, rotational and translational motions[212];

Motion	Electronic	Vibrational	Rotational	Translational	Precessional
Period s	10^{-16}	10^{-14}	10^{-12}	10^{-10}	10^{-7}

Therefore, one can assume that these motional effects average out before the NMR signal is picked up. The very narrow liquid states NMR lines compared to solids, for example, is a well-known result of the difference in translational and precessional (and other) time scales.

To see how the difference in the time scales simplifies the derivation of the effective field, (1.49) is re-written as;

$$E(t_E,t_R) = \frac{3\ m_j(t_E).\ r_{ij}(t_R)}{r_{ij}^5(t_R)}\, r_{ij}(t_R) - \frac{m_j(t_E)}{r_{ij}^3(t_R)} \qquad (2.2)$$

where $E(t_E,t_R)$ is the oscillating field produced at 'i' by the oscillations of the electrons of 'j', while they are a distant $r_{ij}(t_R)$ apart. Note that the time dependence of the oscillating moment is electronic (t_E) and that of r_{ij} is rotational, and the field is a function of both.

According to the relative electronic and rotational time scales, before $r_{ij}(t_R)$ can change, the electrons in j have performed 10^4 oscillations, averaging out j's moment to zero, $\langle m(t_E)\rangle = 0$. This in turn results in a zero average field while the distance between i and j is still $r_{ij}(t_R)$. We know from Chapter 2 that although the mean moment is zero, its non-zero mean-square value gives rise to a mean-square field at i while the distance is still $r_{IJ}(t_R)$. Putting this differently, at any rotational instant of time the buffeted atom experiences a finite field by (1.50);

$$\langle E^2(t_R)\rangle = 2\ \langle m^2\rangle_J\ r_{IJ}^{-6}(t_R) \qquad (3.3)$$

Note that the electronic time dependence of the field has been averaged out while the rotational dependence still exists.

Now the effect of the vibrational motion can be considered. This motion is about 100 times faster than the rotational one, and therefore at any r_{IJ} distance the corresponding bond-length (or bond-angle) will average out at their observed equilibrium values, which are used for the calculations of the centre-of-mass to the atom distances, d's, in Fig. 3.1. This averaging is in fact equivalent to the rigidity of molecules (see sec. 3.5.2).

Likewise, while the inter-molecular distance R, which is a function of the translational time, is fixed at $R(t_T)$, the two molecules have assumed at least 100 mutual orientations, averaging out the pairwise distance $r_{IJ}(t_R)$. The mean-square field in (3.3) therefore becomes;

$$\langle\overline{E^2}\rangle = 2\ \langle m^2\rangle_J\ \overline{\{r_{IJ}^{-6}(t_R)\}} \qquad (3.4)$$

where bars denote the space averaging and the field is a space-time averaged field independent of both electronic and rotational time (but still dependent on the translational time to be discussed later).

From (3.4) one can see that the difference in the time scales has reduced the problem of finding the effective field to that of finding the average of the inverse-sixth-power distance between i and j. It is by this averaging that the incorporation of the molecular structure parameters, d's into the formulation of the effective field is expected.

Reference to Fig. 3.1 shows that in the limit of $d_i = d_j = 0$ where molecules become points, or equally, when $R >> d_i$ and d_j the averaging reduces to R^{-6};

$$\langle\overline{E^2}\rangle = 2 \langle m^2\rangle_j R^{-6} \qquad \begin{array}{ll} \text{if} & R >> d_i \text{ and } d_j \\ \text{or} & d_i = d_j = 0 \end{array} \tag{3.5}$$

In the absence of such conditions, however, there must be a factor, F, that accounts for the rotation of the two molecules such that; $\overline{\{r_{ij}^{-6}(t_M)\}} = F R^{-6}$. Furthermore, from the condition of (3.5) the functional form of this factor may conceivably be given as; $F = f(d_i,d_j,R)$, and the averaging of (3.4) as;

$$\langle\overline{E^2}\rangle = 2 \langle m^2\rangle_j R^{-6} F(d_i,d_j,R) \tag{3.6}$$

3.2.2. Average Inver-Six-Power Distance

The mathematical derivation of the functional form of F, by the existing conventional methods, which has proved an arduous task detracting from a true understanding of the physics of the problem, is confined to Appendix 3, according to which F is given by;

$$F = f_0 + f_2 + f_4 + f_6 + f_8 + \ldots, \text{ where} \tag{3.7}$$

$$f_0 = 1$$

$$f_2 = \frac{5\ (d_i^2 + d_j^2)}{R^2}$$

$$f_4 = \frac{14\ (d_i^4 + d_j^4) + 100\ d_i^2 d_j^2}{R^4}$$

$$f_6 = \frac{30\ (d_i^6 + d_j^6) + 386\ (d_i^4 d_j^2 + d_i^2 d_j^4)}{R^6}$$

$$f_8 = \frac{55\ (d_i^8 + d_j^8) + 660\ (d_i^2 d_j^6 + d_i^6 d_j^2) + 1122\ d_i^4 d_j^4}{R^8}$$

This analytical form of the F factor or the buffeting factor is a function of d, namely the bond lengths and bond angles of the molecules, and R only.
Note that F is a dynamic factor which fully determines the orientational dependence of any interaction involving free rotations of polyatomic globular molecules.

The concrete meaning of (3.7) is simply that in general; $\overline{(r_{ij}^{-6})} > R^{-6}$ by a factor of F. For two inert atoms that is, is $d_i = d_j = 0$, $F = 1$ and (3.7) reduces to (1.50).

When the two molecules are identical F reduces to the Raynes site-site factor[206], and when either of the molecules is a sphere (point) F becomes the Rummens and Bernstein[17,80] site factor;

$F_6(d_i = d_j, R)$ = Raynes site-site factor

$F_8(di = 0, d_j, R)$ = Rummens and Bernstein site factor

where F_x denotes F until term x.

Expression (3.6) formulates the effective field of a single 'j' at 'i'. If however the solvent molecule consists of X_j species of kind j they would all produce the same effective field at i and by assuming that their fields are additive (see sec. 3.5.4) the mean-square effective field at i becomes;

$$\langle\overline{E^2}\rangle_{ji} = 2\ X_j\ \langle m^2\rangle_j\ R^{-6}\ F(i,j)$$

The term species is used for identical atoms with identical d's. Identical atoms with different d values, that is similar atoms at different locations in a molecule like H of CH_3OH in CH_3 and OH groups, are different species.

For a solvent molecule with different buffeting atoms the effective field, which is a pairwise field between one solvent molecule and the solute, can be written as;

$$\langle\overline{E^2}\rangle(\text{Pair}) = 2\ R^{-6} \sum_j X_j\ \langle m^2\rangle_j\ F(i,j) \qquad (3.8)$$

The total field of Z_L solvent molecules surrounding the solute at a fixed R, assuming the additivity of the fields (see sec. 3.5.3) becomes;

$$\langle\overline{E^2}\rangle(\text{Total}) = 2\ Z_L\ R^{-6} \sum_j X_j\ \langle m^2\rangle_j\ F(i,j) \qquad (3.9)$$

Inspection of (3.9) shows that it incorporates three adjustable parameters and one contentious factor. These are Z_L, the number of nearest neighbours in the liquid, R, the liquid state inter-molecular distance, $\langle m^2\rangle_j$, the bonded atom moment, and the buffeting factor F.

3.3. Adjustable Parameters of the Buffeting Field

In the liquid state (unlike the solid) the exact number of the nearest neighbours Z_L and the nearest neighbours distance R is not generally known. Therefore their values can be adjusted to fit the experimental data for which the theory is given. This for example, is the case with the Debye-Huckle thoery where the ionic size and the solvation number Z are often treated as adjustable parameters[207,208].

The purpose of this section is scrutinization of the parameters of (3.9), by which it is hoped to fix their values or find simple expressions for them.

3.3.1. Slow-Convergent Buffeting Factor

As successive f terms of the buffeting factor (3.7) show, this series is a rapidly increasing function of d/R.

Rummens[17] warns about the divergence of series like F. Raynes[206] combines his site-site factor, F_B, with another series (see sec. 3.3.3, and Chapter 4) to quicken its rather slow convergence.

More recently the risk of the divergence of similar series is avoided by using its first three terms and introducing a "damping factor"[202,209].

Here we consult the vivid language of numbers for the discussion of the divergence of the buffeting series. This has been made possible by the [MONTE CARLO] method developed in Appendix 4, the results of which are compared with those of the analytical series (3.7) in table 3.1. The derivation of the analytical forms of terms beyond f_8, for $d_i \neq d_j \neq 0$, is a formidable task because of the host of integrals involved; over 200 for the f_9 term alone.

Note that the q ratio is defined as; $q = (d_i + d_j)/2R$. Note also from the table that, first, the F values are finite, for the range of q values, and therefore F meets the condition of the convergent series. Second the error of using the analytic F increases with the increase in q. Third, the analytic series is not reliable for $q > .36$ and a best fit to the [MONTE CARLO] F-q curve must be used, which is given in Appendix 4 (Eq. A4.3) and is valid for $0 < q < .43$.

The q ratios depend very much on the values of R (yet to be defined). Fig. 3.2 shows the graphs of F_6, F_8, and the numerical F values as a function of q from table 3.1. It also shows where typical pure systems lie in terms of their q values, which are calculated using their largest d values, that is the peripheral atoms' d values given in table 3.4, and (3.17) for their R (see sec. 3.3.3).

The F values in table 3.1 however give the amount by which $\overline{\{r_{ij}^{-6}\}}$ is larger than R^{-6}. For $q = .428$, for example, the former is about 40 times larger than the latter, stressing the fact that molecules at short inter-molecular distances cannot be mistaken as spheres.

Table 3.1. Comparison between the Numerical and Analytical F

			[MONTE CARLO]* F		------------- Analytical F -------------						
			Number of trials				$f_0 = 1$				Error+
d_i	d_j	R	10000	100000	F	f_2	f_4	f_6	f_8	q	%
0	0	-	1.000	1.000	1.000	.000	.000	.000	.000	.000	0
1	1	5	1.576	1.563	1.665	.400	.205	.053	.006	.200	-6
2	2	10	1.595	1.566	1.665	.400	.205	.053	.006	.200	-6
2	2	7	2.771	2.757	3.239	.816	.853	.452	.117	.286	-17
3	3	10	3.121	3.238	3.716	.900	1.037	.606	.172	.300	-15
2	2	6	4.989	4.873	5.234	1.111	1.580	1.141	.401	.333	-7
3	3	9	4.510	4.639	5.234	1.111	1.580	1.141	.401	.333	-13
1	3	6	5.346	5.922	5.746	1.389	1.580	1.214	.563	.333	3
4	3	10	6.526	6.224	6.305	1.250	1.912	1.534	.610	.350	-1
2	3	7	6.649	6.793	6.864	1.326	2.065	1.737	.735	.357	-1
3	3	8	8.012	9.597	8.280	1.406	2.531	2.314	1.029	.375	14
2	4	8	10.886	10.207	8.609	1.562	2.492	2.360	1.193	.375	15
3	4	9	11.790	11.844	9.760	1.543	2.914	2.887	1.415	.389	17
4	4	10	20.711	15.103	11.009	1.600	3.277	3.408	1.725	.400	27
3	3	7	48.972	38.366	15.306	1.836	4.318	5.155	2.994	.428	60

---

*: Each numerical integration by the [MONTE CARLO] program for 100,000 trials has taken 100 mins. on the [9826 HEWLETT PACKARD] computer. For 10^6 trial it takes about 18 hrs -400 hrs on the Sinclair ZX Spectrum- giving the more accurate results of F (4,4,10) = 15.729, F (3,3,8) = 9.108, F (3,3,7) = 39.267.

+: Error = $(F_{NU} - F_{AN})/F_{NU} \times 100$

3.3.2. Number of Nearest Neighbours in the Liquid State, Z_L

Expression (3.9) shows the influence of Z_L on the calculated values of any equilibrium property based on the mean-square field.

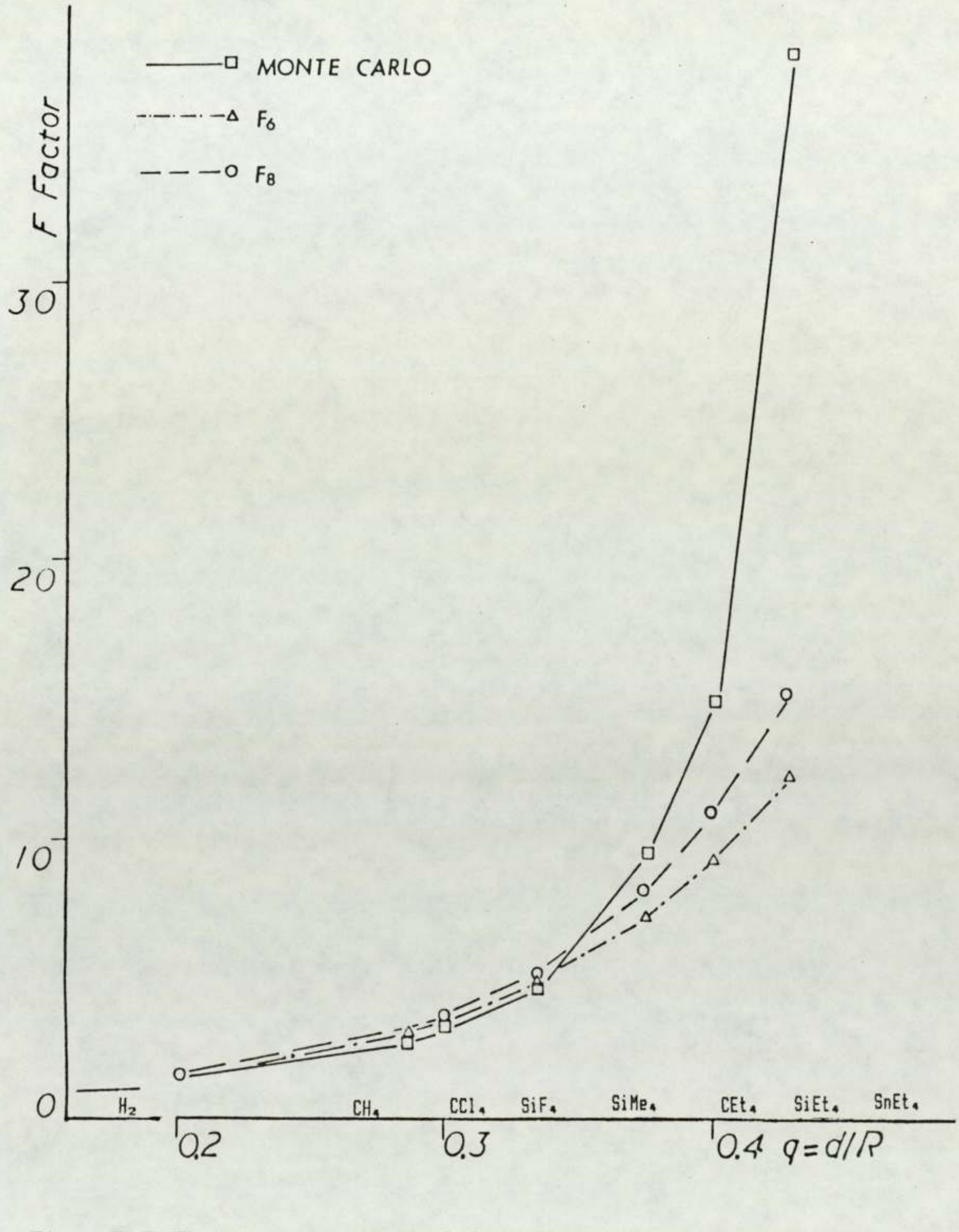

Fig. 3.2 The convergence of the F series. A comparison between the numerical and analytical buffeting factors as a function of q = d/R.

The number of nearest neighbours in the solid state Z_S, is well-known and depends on the packing of molecules. For example for face-centred-cubic (fcc) or hexagonal close-packing (hcp) structures $Z_S = 12$, and for body-centred-cubic (bcc) $Z_S = 8$[69].

Organic molecules are the main concern here for the solid state of which Kitaigorodsky[210] gives the value of $Z_S = 12$ as the common value. sometimes the specific shape of the molecule provides packing with $Z_S = 14$ or 10; like $N_4(CH_2)_6$ (bcc) and urea $O=C(NH_2)_2$ (tetragonal), respectively[210].

It may be noted that a bcc structure for $N_4(CH_2)_6$ has 14 nearest neighbours compared to $Z_S = 8$ of inorganic compounds, and also, a tetragonal structure, which is similar to a simple cubic structure with $Z_S = 6$, shows $Z_S = 10$. It is not therefore difficult to accept $Z_S = 12$ for $Sn(C_6H_4CH_3)_4$, $Sn(C_6H_5)_4$, $Sn(C_6H_4OCH_3)_4$ with tetragonal structures, and, $Sn(C_6H_4OC_2H_5)_4$ with monoclinic structure.

In fact $Z_S = 12$ is explicitly given for $Sn(C_6H_5)_4$ (tet.) by Kitaigorodsky. We have drawn a parallel between these structures and those of $C(Et)_4$, $Si(Et)_4$, $Sn(Et)_4$, and $Si(OEt)_4$ in table 3.2 to arrive at their Z_S.

The significance of the knowledge of Z_S for predicting Z_L is that there is a simple approximate relationship between the two given by Moelwyn-Hughes[211] as;

$$Z_L \simeq Z_S\ (1 - H_f/H_s) \qquad (3.10)$$

where H_f and H_s are the heats of fusion and sublimation respectively.

The underlying assumption in the derivation of (3.10) is the equality of a "pair potential" -which can be related to H_f and H_m- in the solid and liquid states. This implies that it is the Z that changes in transition from the solid to liquid state, and not R. This apparently is an experimental fact. For water, for example, R changes from 2.82 A at 4 °C to 2.94 A[212] at 200 °C, at constant density. X-ray diffraction of liquid white phosphorus P_4, at 48 and 220 °C shows that the first P...P nearest neighbours distance hardly changes from 3.9 A[213] over this temperature range. This is also the case with Hg (see below).

Expression (3.10) may be re-formulated in terms of H_v and H_f as;

$$Z_L \simeq Z_B \, [\, H_v/(H_v + H_f) \,] \tag{3.11}$$

The two expressions give similar results. Table 3.2 contains Z_B and the corresponding Z_L found from (3.10) and (3.11).

However Z_L depends on the temperature and more on the number density of the molecules in the fluid. The values given in this table compare rather well with those found by the x-ray method, for example, Z_L = 11.4 for liquid methane[214] and 7 for Hg[214];

X-ray diffraction results for liquid Hg*

Temp. °C	-36	18	150
Z_L	7.5	6.0	7.7
R A	3.03	3.00	3.10

*: The data are obtained by different experimentalists

Table 3.2. The Solid and Liquid States Next Nearest Neighbours

	Z_S	Packing	H_f	H_v	Z_L
Species		[69]	KJ/mole[215]		(3.11)
He	12	hcp[216]	.008	.084	10.9
He	8	bcc[217]	.008	.084	7.3
H_2	12	hcp	.177	.916	10.0
H_2	12	fcc[216]	.177	.916	10.0
Ne	12	fcc	.330	1.80	10.0
Ar	12	fcc	1.19	6.50	10.0
Kr	12	fcc	1.64	9.05	10.0
Xe	12	fcc	2.29	12.6	10.0
Rn	12	fcc	2.89	16.7	10.0
Hg	8	bcc	2.29	59.3	7.7
H_2O	4	teth[a]	6.01	45.05	3.5 *
CH_4	12	fcc[218]	.941	8.18	10.7
CF_4	12	mon[219]	.699	12.59	11.3
CO_2	12	fcc[220]	8.33	25.23$^+$	8.0
CS_2	12	fcc[b]	4.39	26.73	10.3
SiF_4	8	bcc[221]	9.50	26.48	5.9
SF_6	8	bcc[216]	5.01	23.85$^+$	6.3
CCl_4	12	fcc[222]	2.47	30.00	11.0
C_5H_{10}	12	hex[223]	.606[158]	30.98[158]	11.8
C_6H_6	12	ort[224]	9.94[158]	42.86	9.7
C_6H_{12}	12	fcc[225]	2.63[158]	32.73[158]	11.0
$C(Me)_4$	12	fcc[226]	3.25[158]	23.61[158]	10.5
$C(Me)_4$	12	hex[227]	3.25	23.6	10.5
$Si(Me)_4$	12	tet[c]	6.89	24.23	9.3
$Pb(Me)_4$	12	tet[d]	10.79	32.93	9.0
$C(Et)_4$	12	tet,bcc[e]	–	–	–

(Table 3.2 continued)

$Si(Et)_4$	12	tet$_f$	–	–	–
$Si(OEt)_4$	12	tet$_g$	–	–	–

---

a: teth (tetrahedral cubic); mon (monoclinic); hex (hexagonal); ort (orthorhombic); tet (tetragonal).

b: By analogy with CO_2.

c: By analogy with $Si(C_6H_5)_4$ with tet. structure[210]

d: By analogy with $Pb(C_6H_5)_4$ with tet. structure[210]

e: By geometric analogy between $C(SCH_3)_4$ and $C(CH_2CH_3)_4$[216]. Structure of $C(SMe)_4$ is tet. according to Ref.[216] and bcc according to Ref.[210].

f: By analogy with $C(Et)_4$, or, $Sn(C_6H_4CH_3)_4$.

g: By analogy with $Sn(C_6H_4OEt)_4$.

*: X-ray experimental value is about 4[212].

+: Heat of sublimation used with (3.10).

In the light of this table one can examine (3.12) which is usually used in NMR studies for Z_L[17,159,228];

$$Z_L = \pi \, (r_u + r_v)^2/r_v^2 \tag{3.12}$$

This expression finds $Z_L = 4\pi$ for pure liquids and $Z_L = \pi$ when the solute is considerably smaller than the solvent, $r_v >> r_u$[17]. Derivation of (3.12) is based on the surface areas of the solute and solvent.

It gives small values for small solutes in large solvents, and large values for large solutes in small solvents; 6 for CH_4 in $SnEt_4$, and, 19 for $SnEt_4$ in CS_2 or 16 in CCl_4. Such values necessitate the collapse of the solvent structure around the solute.

It is more likely that the small solute will fit into the abundant cavities or voids of the solvent. Therefore the Z_L value is determined by the structure of the solvent and not the solute. For large solutes in small solvents on the other hand, $Z_L > 12$ (excess close-packing around solute) means that the large solute with its low surface charge density is capable of attracting more solvent molecules around itself and restricting the exchange of the solvent molecules between adjacent solvent layers. This is also unlikely, as the solvation number for Cl ($r = 1.81$ A) with its strong local ionic field is between 6 and 7[212], whereas (3.12), based on the difference of the sizes of the solute Cl and the solvent H_2O, gives $Z_L = 11$.

Comparison between the values of Z_B and Z_L in table 3.2 shows that one can relate the two in a simple practical way as;

$$Z_L \simeq Z_B - 1 \qquad (3.13)$$

This gives the fixed value of 11 for organic compounds considered here. This approximate rule agrees substantially with the x-ray data as was mentioned for water, mercury, and methane, and is observed for nitrogen ($Z_L = 10.0$), oxygen ($Z_L = 10.3$) bromine ($Z_L = 12$)[214] and white phosphorus ($Z_L = 7$); see Chapter 5. Evidently the only exception to this rule is liquid chlorine ($Z_L = 6$, $Z_B = 12$); see Chapter 5.

It should be noted that the experimental values for Z_L are the areas under the pair-correlation function g(r) data curves (to be exact, the curves of $n(r) = 4\pi r^2 \rho\ g(r)$) which could not be obtained with great precision. For P_4, for example, Z_L is somewhere between six and eight.

3.3.3. Nearest Neighbours Distance in the Liquid State

Another adjustable parameter of (3.9) is the liquid state intermolecular distance R. The choice of R, because of its inverse-six power dependence, affects the results of (3.9) considerably. The scrutiny of this subject is therefore worthwhile.

The process of the separation of molecular motions was continued to (3.7) or (3.9), where R was denoted without time dependence. The time dependence of R is however necessary as the translational motion is fast enough compared to the precessional one for R to be averaged out before the MNR signal is picked up. Therefore (3.7) or (3.9) should have been written as;

$$\overline{\langle E^2(t_T) \rangle} = 2\ R^{-6}(t_T)\ \langle m^2 \rangle_J\ F(i,j)$$

Now there remains one further averaging to be performed on the mean-square field. This is usually done by the introduction of the Boltzmann factor;

$$\langle \overline{\overline{E^2}} \rangle = \int \overline{\langle E^2(t_T) \rangle}\ \exp(-\ U/kT)\ d\tau \qquad (3.14)$$

where the second bar on $\langle \overline{E^2} \rangle$ stands for averaging over t_T, the translational time.

This process has been used by Raynes et al[78] in their binary collision gas model. Tackling this integral entails the knowledge of U, the intermolecular potential function, for which the LJ (6-12) function is used. The solution of (3.14) is given in terms of yet another polynomial H_n, as a function of KT and the emperical LJ parameter ϵ ($\epsilon = U_{min}$).

The problems of using such an averaging approach are numerous. First, the troublesome LJ parameters r_o and ϵ, which are obtained by fitting the LJ potential to other experimental data, viscosity for example. Second, incorporating the uncertainties of these parameters into the buffeting field expression. Third, the loss of the simplicity of $\langle E^2 \rangle$ by incorporation of H_n series, not to mention the inconsistency of using LJ central potential function which treats polyatomic molecules as spheres (see sec.3.1.1). This is in fact the inconsistancy in the Raynes site-site factor theory. He takes advantage of the resulting H_n series to accelerate the covergence of his site-site factor by a factor of about two (see Chapter 4).

Alternatively one can use equations comprising the radial distribution or pair-correlation function of the solute-solvent system $g(R_{12})$, with an instantaneous intermolecular distance of R_{12}[229];

$$\langle R^{-n} \rangle = 4\pi\rho \int R_{12}^{(-n+2)}\, g(R_{12})\, dR_{12}$$

The pair-correlation function may be determined for some simple liquids, with serious technical problems (pp 836-854 Ref. 212), from x-ray or thermal neutron diffraction studies[230]. Kielich, by resorting to the Kirkwood[231] radial distribution function for rigid spheres of diameter d and volume $v = \pi d^3/6$ for which[232];

$$g(R_{12}) = \begin{cases} 0 \text{ for } R_{12} < d \\ 1 \text{ for } R_{12} > d \end{cases}$$

derives;

$$\langle R^{-n} \rangle = \frac{4\pi\rho}{n - 3} (\pi/6V)^{(n-3)/3}$$

For n = 6 and in terms of molar volumes V this may be written as; $\langle R^{-6} \rangle = 4\pi^2 (L/V)^2/18 = 2.2 (L/V)^2$. This average inverse-six-power distance, which may be directly used, gives values about 12 times larger than a realistic intermolecular distance. For example, (3.16), written as a function of R^{-6}, gives $.182 (L/V)^2$. Besides, this approach is not suitable for mixtures. Kielich[233] also uses a radial distribution function with tha LJ potential to arrive at an average R^{-6} very similar to that of Raynes et al.

Instead, we resort to the method of obtaining the average R from molar volumes. This method has been used, by Onsager for his cavity size, and with minor changes by Bernstein and Raynes[79], and Rummens et al[159].

The effective molecular radius can be deduced from the average volume available per molecule, $V_M = (M/\rho)L$, by the following expressions;

a: The available volume per molecule[228];

$$r^3 = .238 V_M \quad (3.15)$$

b: The available volume per molecule with a solid like closed packing structure, with the incorporation of a packing factor into (3.15);

$r^3 = .297\ V_M$ [228]

$r^3 = .293\ V_M$ [17,159] (3.16)

c: The available volume per molecules in a liquid with a random distribution of molecules. A probabilistic approach first used by Herts[234] in 1909 and later by Jaffe (Chapter 2) to improve the Onsager's cavity size (3.15). The result of this method in terms of V_M may be written as;

$r^3 = .17\ V_M$ (3.17)

Although based on random packing of particles (3.17) is equivalent to the effective radius of an orderly fcc packing with $r^3 = .1767\ V_M$[69].

Which is the most suitable expression for the effective radius and the intermolecular distance given by $R = r_v + r_u$?

Table 3.3 serves to answer this query by giving the values of R according to (3.15-3.17) using the quoted molar volumes, the vdW distances R_v, the empirical LJ distances R_{LJ}, and the experimental solid state distances R_s.

The vdW distances are found using the vdW radii, r_v[235];

Atom	H	F	O	Cl	S	Half-thickness of aromatic ring
r_v A	1.15*	1.35	1.4	1.8	1.85	1.7

*: This is the in-between value of 1.1[235] and 1.2[158].

and the d values. For CH_4 for example, using the C-H bond length of 1.094 A, one finds $R_v = 2\ (1.15 + 1.094) = 4.488$ A.

We note that a simple trust in $R_v = 2\ (r_v + d)$ also fails for non-globular molecules. For benzene, for example, one finds, $R_v = 2\ (1.15 + 2.46) = 7.22$ A, whereas the solid state structural studies show that aromatics tend to arrange themselves so that the hydrogens of one molecule are near the π-electron of its neighbouring molecule[236]. Based on this fact one finds $R_v = (1.15 + 2.46 + 1.7) = 5.31$ A. In the liquid state where benzene molecules rotate freely one would expect R to be in between the two R_v values; $R = (7.22 + 5.31)/2 = 6.26$ A. This is in agreement with $R_{LJ} = 6.3$, and $R = 6.18$ A we have found using its heat of vaporization (see Chapter 5).

The same argument goes for CS_2 in arrangements (a) and (b);

(a) S C S...S C S $R_v = 2\ (1.85 + 1.558) = 6.81$ A

(b) 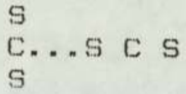
$$\overset{S}{\underset{S}{C}}...S\ C\ S$$
$R_v = 2\ (1.85 + 1.558 + 1.7) = 5.12$ A

where $r_v = 1.7$, by analogy with benzene, is used for the half-thickness of the π-electron of C=S bond. The mean of the two extremes, $R_v = 5.96$ A, is in agreement with 5.86 as found in Chapter 5 from its heat of vaporization.

For water arrangements (a) and (b) give the R_v entries of the table;

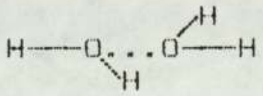

$R_v = 2\ r_v(O) = 2.8$

(a)

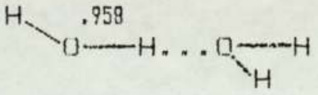

$R_v = (1.15 + 1.4 + .958) = 3.508$

(b)

The value of 2.8 A, agrees with microwave spectroscopy result of 2.98 A [237].

Table 3.3. Comparison between Nearest Neighbour Distances

Species	V cm³/mole Solid or at 30 C	d A [159]	R_s^a (Expt.) A	R_v A	R_{LJ}^b A [161]	------ R(cal.) A ----- (3.17)	(3.15)	(4.16)
He	19.43_s[240,212]	0	2.97[242]	2.44[240]	2.873[212,220]	3.53	3.94	4.25
He	24.7_s[217]	0	3.77[217]^c	-	-	3.82	4.27	4.60
Ne	14.0_s[240]	0	3.16[217,243]	3.20[240]	3.70	3.16	3.54	3.81
Ar	24.12_s[240]	0	3.76[217,244]	3.84[240]	3.89	3.79	4.24	4.56
Kr	27.90_s[240]	0	3.99[217,245]	3.90[240]	4.05	3.98	4.45	4.79
Xe	36.76_s[240]	0	4.33[217,245]	4.36[240]	4.55	4.36	4.88	5.25
Rn	50.45_s[240]	0	-	-	-	4.85	5.42	5.81
H_2	23.31_s[69]	.373[158]	3.78[240]^d	3.05	3.27	3.75	4.19	4.50
H_2O	19.82_s[69]	.958[158]	2.82[212]	2.80,3.51	2.97	3.55	3.97	4.27
CH_4	30.94_s[69]	1.09[158]	4.49[212],4.17[218]	4.49	4.28[159]	4.12	4.6	4.96
SiF_4	48.00_s[247]	1.56[224]	4.68[221]	5.82	5.56[246]	4.77	5.83	6.28
CF_4	66.80[158]	1.33[241]	-	5.36	5.27[241,246]	5.32	5.95	6.41
SF_6	77.70[158]	1.57[241]	-	5.84	6.63[241,246]	5.6	6.26	6.74
CS_2	61[158]	1.56[235]	-	5.11,6.82	4.98	5.16	5.78	6.22
CCl_4	87.90_s[69]	1.76[158]	5.9[222]	7.13	6.48[159]	5.83	6.52	7.02
C_6H_6	77.28_s[69]	2.46	-	5.31,7.22	6.32[159]	5.59	6.25	6.73
C_6H_{12}	109.41[159]	2.21^e	6.2[225]	6.43	6.89[159]	6.27	7.02	7.56
$SiCl_4$	116.5[159]	2.17[158]	-	7.94	7.09[159]	6.40	7.16	7.71
C_6F_6	117.4[165]	2.7^f	-	5.75,8.1	-	6.42	7.19	7.74
$C(Me)_4$	131.42[159]	2.15^g	6.21[226]	6.53	-	6.67	7.46	8.03
$Si(Me)_4$	146.52[159]	2.50	-	7.23	6.78[159]	6.92	7.74	8.33
$Ge(Me)_4$	138.19[159]	2.55	-	7.23	6.70[159]	6.78	7.59	8.17
$Sn(Me)_4$	139.52[159]	2.73	-	7.69	6.84[159]	6.80	7.61	8.20
$Pb(Me)_4$	135.93[159]	2.83	-	7.89	6.96[159]	6.74	7.54	8.12
$C(Et)_4$	171.9[27]	3^f	-	8.3	-	7.30	8.16	8.78
$Si(Et)_4$	190.40[159]	3.25	-	8.73	8.2[159]	7.55	8.44	9.09

Table 3.3 (continued)

$Sn(Et)_4$	198.1[27]	3.5[f]	-	9.3	-	7.65	8.56	9.21

a: Except for H_2O and 4.49 A for CH_4 the quoted R_m values are calculated using the cell length, a, data from quoted Refs. and; $R_m(fcc) = a\ 2^{1/2}/2$; $R_m(bcc) = a\ 3^{1/2}/2$; $R_m(cubic) = a/2^{1/2}$ from Ref.[69,pp 536-540].

b: $R_{LJ} = r_{min} = 2^{1/6} r_o = 1.122\ r_o$[161]. The value of $R_{LJ} = 1.09\ r_o$ is also suggested[250].

c: $R_m = 3.77$ A is for a bcc He at 0 °C with the quoted volume.

d: Theoretical values of 3.69[248] and 3.49 A[249] from differential scattering are also available.

e: This is the mean of d = 2.49 (equitorial) and d = 1.93 (axial) hydrogens[159].

f: Calculated as explained in Appendix 5.

g: The d values of $X(Me)_4$ and $X(Et)_4$ systems belong to the peripheral hydrogens. The d values of other atoms in these molecules can be found in Appendix 5.

The R_v value of CCl_4 (and $SiCl_4$) is not in agreement with the solid state value, possibly because of special arrangements of this molecule in the solid state, or over-estimation of r_v value for chlorine. Zimmermann gives parallel (R = 4.7) and anti-parallel (R = 6.06) arrangements for the liquid state of CCl_4 after failing to describe its experimental pair-distribution function[238], the mean of which, 5.4 A (also given in Ref.[239] as R_m) is considerably smaller than the solid state experimental value of 5.9 A.

As was mentioned previously the liquid state inter-molecular distances are similar to the corresponding solid state ones and the results of table 3.3 show that (3.17) in general, gives a more realistic estimate of these distances from molar volumes. Therefore on this basis and also on the basis of the further evidence found in Chapter 5, where (3.9) is used for the prediction of σ_w and heats of vaporization, we choose (3.17).

It is worth noting that the Onsager's form (3.15), which has often been criticised for being a bad approximation, gives better estimates compared to (3.16) with a packing factor.

3.3.4. Mean-Square Moment of Bonded-Atom

The cornerstone of the buffeting field expression (3.9) is the bonded-atom moment, $\langle m^2 \rangle_j$, without the knowledge of which (3.9) reduces, at its best, to a semi-empirical expression. Defining the properties of atoms in bond has proved to be the main obstacle of developing formulations for polyatomic molecules.

Raynes[206] in the paper on the interacting CH_4 molecules treated bonded atoms as isolated ones whilst realizing that "...this is a severe approximation since it is well known that the electronic environments of nuclei that are chemically bound are substantially different from those of isolated atoms."

Let us use atomic polarizability and ionization potentials in the expression for the moment, $\langle m^2 \rangle = 3\ I\alpha/2$ (Eq. A1.4), and contrast the values so found for molecules with those of the molecular moment, where molecular I and α are used.

For atomic (isolated) H and C we have;

Species	H	C
α A^3[251]	.667	1.76
I eV[158]	13.6	11.25
$\langle m_2 \rangle \times 10^{36}$	21.77	47.52

Hereafter all moments are given in units of 10^{-36} erg cm^3 , $(esu\text{-}cm)^2$ or D^2

Treating hydrogen and carbon of methane, for example, as isolated atoms necessitates the use of these atomic moments in place of $\langle m^2 \rangle_J$ in (3.9), and add to give;

$$\langle m^2 \rangle(CH_4) = 4\ \langle m^2 \rangle_H + \langle m^2 \rangle_C = 134.6$$

The molecular moment using molecular I and α from table 3.4 equals, $\langle m^2 \rangle(\text{mol.}CH_4) = 79.6$. The difference of about 69% signifies the fact that assignment of atomic moments to the bonded atoms conflicts with the molecular property.

For H_2 the molecular moment of 30 shows a discrepancy of 45% compared with the moment of 43.5 for 2 H atoms.

Of course, the argument presumes the intuitive validity of some kind of additivity rule, according to which the sum of the bonded-atom moments balances with the molecular one.

In the search for such an additivity rule one can begin with the fact that bonded atoms in molecules are electronically saturated, that is, they obtain the inert atom configuration, and therefore their electronic environment may be tentatively approximated with that of the corresponding inert atom.

This is consistent with the Kitaigorodsky[210] statement that "...precision x-ray structure studies show that excellent agreement with experiment can be secured by calculations using isotropic atomic factors of x-ray scattering, and that the pattern of electronic density can be represented with experimental accuracy, as the superposition of spherically symmetrical atoms", see Fig. 3.3a.

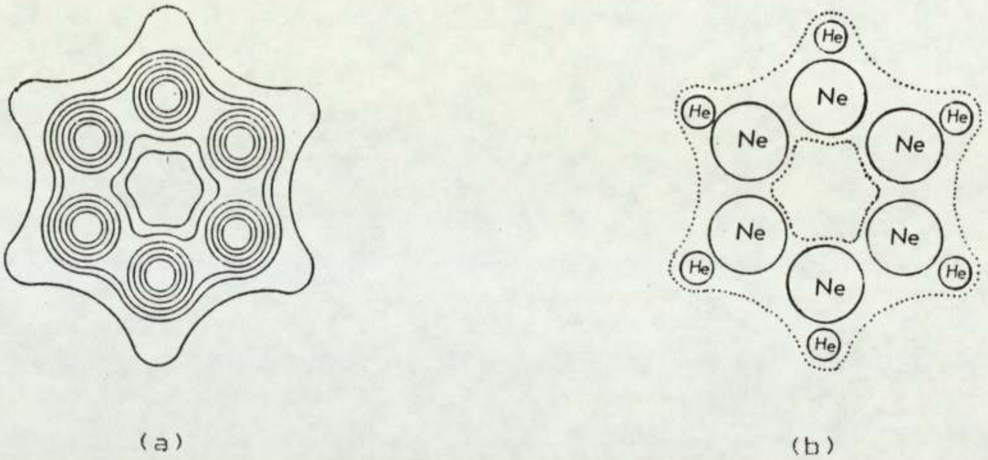

(a) Cross-section of the contours of a constant electron-probability density in C_6H_6 (carbons) as determined by x-ray diffraction data (from Ref.208).

(b) The inert-atom approximation of the electron density pattern of C_6H_6.

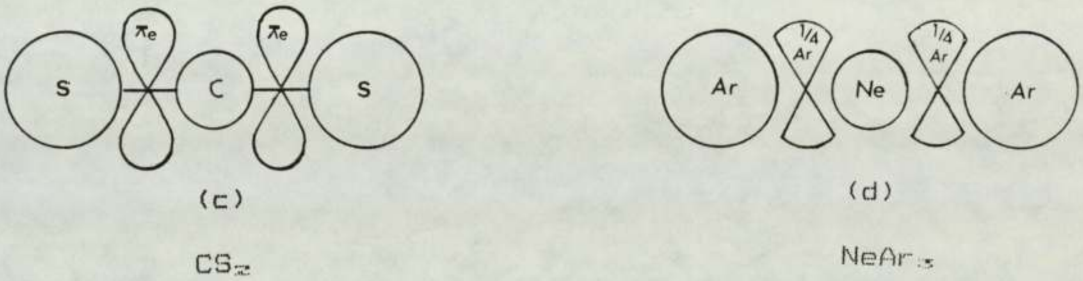

(c) The pi-electron system in CS_2.

(d) The inert-atom model of CS_2. Each pi-electron is equivalent to 1/4 of the corresponding inert atom.

(e) The chlorine anion Cl^-.

(f) The inert atom model of Cl^-.

Fig. 3.3 Species and their inert atom counterpart.

The supposition of the correspondence of the molecular electronic environment, or density pattern, with that of inert atoms is tantamont to approximating a molecule with a collection of inert atoms, as far as $\langle m^2 \rangle$ is concerned. This supposition is more graphically shown in Fig. 3.3b for benzene, and quantitatively may be put as;

$$\langle m^2 \rangle_E = \sum \langle m^2 \rangle_{inert} \tag{3.18}$$

where the summation is over all the corresponding inert atoms. The validity of the formulation of the inert-atom approximation (3.18) can be readily checked by using the values of $\langle m^2 \rangle_{inert}$ given in table 3.4.

For CH_4, for example, by corresponding H to He and C to Ne, one finds from (3.18);

$\langle m^2 \rangle_E = 4 \langle m^2 \rangle_{He} + \langle m^2 \rangle_{Ne} = 4 \times 12.111 + 20.45 = 68.89$
in better agreement with the molecular value of 79.6. The error has reduced from 69%, for isolated-atom additivity, to -13%, for inert-atom additivity. This is also the case for H_2 where (3.18) gives; $\langle m^2 \rangle_E = 2 \langle m^2 \rangle_{He} = 24.22$, compared to the molecular value of 30.03. It is interesting to note that the inert-atom value compares well with the quantum mechanical value of $\langle m^2 \rangle = 3\, a_0^2 e^2 / z = 13.5$, where $z = 1.2$ is the 'hydrogenic atomic charge' for bonded-H compared to $z = 1$ for isolated H atom[29].

Table 3.5 provides more evidence for the validity of (3.18) by comparing its results with the molecular (experimental) moments, (3/2) I(Expt.)α(Expt.).

Table 3.4. Inert-Atom Moments

Atom	I(eV) [252]	α(A^3) [251]	$\langle m^2\rangle_{inert}$* erg cm^{3}x10^{36}
He	24.587	.204956	12.111
Ne	21.564	.3946	20.450
Ar	15.759	1.64	62.112
Kr	13.999	2.48	83.436
Xe	12.130	4.04	117.773
Rn	10.748	5.44$^+$	140.518

*: $\langle m^2\rangle$ (erg cm^3), (esu-cm)^2 or D^2 = (3/2) I(eV)x1.6022x10^{-12} (erg/eV) α (cm^3).

+: Estimated from a graph given by Gerrard[253].

Let us focus our attention on the first error column. What does not escape observation is the presence of large error of molecules with double bonds, such as, N_2, O_2, CO, NO_2, CO_2, and CS_2, the π-electron of which is depicted in Fig. 3.3c.

Accounting for the existence of π-electron system, which affects the electron density pattern of a molecule, appears as a natural step in the refinement of (3.18).

The moment of a π-electron pair appears to be half of the moment of the corresponding inert atom, so that (3.18) becomes;

$$\langle m^2\rangle_E = \sum_{\sigma} \langle m^2\rangle_{inert} + (1/2) \sum_{\pi} \langle m^2\rangle_{inert} \qquad (3.19)$$

Where the summatioms are now over the σ-skeleton and the π-electron.

Table 3.5. Comparison between Molecular and Estimated Moments

Index		---------- Molecular parameters ----------			$\langle m^2 \rangle_e$	Error[a]	$\langle m^2 \rangle_e$	Error
number	Molecule	α Å³[16]	I ev[16]	$\langle m^2 \rangle$	(3.18)	%	(3.19)	%
1	H_2	.81	15.43	30.04	24.22	-19	-	-
2	N_2	1.74	15.58	65.22	40.90	-37	61.35	-6
3	O_2	1.60[254]	12.07	46.37	40.90	-10	51.12	10*
4	Cl_2	4.61	11.48	127.19	124.22	-2	-	-
5	CO	1.93[69]	14.01[158,255]	64.76	40.90	-37	51.12	-21*
6	NO	2.99[251]	9.25[166,255]	66.56	40.90	-38	51.12	-23*
7	HCl	2.56[69]	12.74[158]	78.41	74.22	-5	-	-
8	HBr	3.49[69]	11.62[158]	97.52	95.55	-2	-	-
9	CO_2	2.63	13.79	87.16	61.35	-30	81.8	-6
10	CS_2	8.56	10.08	207.51	144.67	-30	206.78	0
11	SH_2	3.64[69]	10.42[69]	91.25	86.33	-5	-	-
12	NH_3	2.14[69]	10.15[255]	52.32	56.78	8	-	-
13	CH_4	2.55	12.99	79.6	68.89	-13	-	-
14	CF_4	2.89[246]	17.81[246,256]	123.55	102.25	-17	b	3
15	SiF_4	3.33[246]	16.94[246]	135.36	143.91	6	b	-1
16	SF_6	4.53[246]	19.32[246]	210.10	184.81	-12	b	0
17	CCl_4	10.24	11.47	282.35	268.90	-5	-	-
18	$SiCl_4$	11.4[159]	11.6	317.37	310.56	-2	-	-
19	$TiCl_4$	14.99	11.70	421.49	331.88	-21*	-	1
20	C_2H_6	4.39	11.65	122.88	113.56	-7	-	-
21	C_6H_{12}	10.87	9.88	258.1	268.03	4	-	-
22	C_6H_6	10.39	9.24	230.85	195.37	-15	226.04	-2
23	C_6F_6	10.1[257]	9.97[158,258]	241.67	245.40	1	276.07	14*
24	p-C_8H_{10}	14.27	8.44	289.40	284.71	-2	315.38	9*
25	$C(Me)_4$	10.20[159]	10.36[159]	253.96	247.58	-2	-	-
26	$Si(Me)_4$	11.90[159]	9.80[159]	280.27	289.24	3	-	-
27	$Ge(Me)_4$	12.8[159]	9.17[159]	282.09	310.57	10	-	-

Table 3.5 (continued)

28	$Sn(Me)_4$	14.4[159]	8.36[159]	344.90	344.90	19	-	-
29	$Pb(Me)_4$	15.9[159]	8.24[159]	314.87	367.65	17	-	-
30	$C(Et)_4$	17.5^c	10.36^d	435.78	426.27	-2	-	-
31	$Si(Et)_4$	19.2[159]	9.81[159]	452.16	467.93	3	-	-
32	$Sn(Et)_4$	21.7^c	8.36^d	436.17	523.60	20	-	-
33	$CH_3C{\equiv}CCH_3$	7.45^c	9.94[158]	176.91	154.47	-13	174.92	1

a: Error = $[\langle m^2\rangle(\text{Est.}) - \langle m^2\rangle(\text{mol.})]/\langle m^2\rangle(\text{mol.})\times 100$.

b: See the text for the true moments.

c: Calculated using bond polarizabilities given in Ref.[161].

d: Rummens[159] has estimated I of $Si(Et)_4$, by extrapolation from data of related compounds, to be equal to the I of $Si(Me)_4$. We have assumed this to be true for $C(Me)_4$-$C(Et)_4$ and $Sn(Me)_4$-$Sn(Et)_4$ pairs.

*: See the text for the real errors.

For CS_2, for example, the inert-atom counterpart formula would be $NeAr_2$ from (3.18), that is, just the σ-skeleton, and $NeAr_3$ according to (3.19), see Fig. 3.3d. Therefore, using the data from table 3.5, one finds;

Table 3.5. Mole. CS_2 $\langle m^2\rangle = 207.5$

Eq.(3.18)........... $\langle m^2\rangle = \langle m^2\rangle_{Ne}(\text{for C}) + 2\langle m^2\rangle_{Ar}(\text{for S})$

$\langle m^2\rangle = 144.67$ Error −30%

Eq.(3.19)........... $\langle m^2\rangle = 144.67 + 2\,[(1/2)\ \langle m^2\rangle_{Ar}]\ (\text{for } 2\pi)$

$\langle m^2\rangle = 206.78$ Error 0%

The corrected values according to (3.19) and their errors are given in the last two columns of the table. Before consideration of the other observations of the first error column a comment on the meaning and implication of (3.18) and (3.19) is essential.

The frequent use of words "atom" and "inert atom" may give the impression that these expressions deal with atoms. On the contrary there is no implication of atoms in their concrete sense, but rather, atoms as electronic charges with different abilities to interact. Some lend themselves to interactions more easily than others. These are electrons with large "stretchability" reflected by their large $I\alpha$ or $\langle m^2\rangle$ values. For example, one electron of argon is five times more active than one electron of helium; $\langle m^2\rangle_{Ar}/\langle m^2\rangle_{He} = 62/12 \simeq 5$.

When $Ne_{7.5}He_6$ is given for C_6H_6, where the number of Ne exceeds that of C, the existence of some kind of extra electronic reactivity is acknowledged.

It is not difficult therefore to extend the idea to ions, and instead of Cl^- write 1.25Ar, as the greater reactivity of this species with one extra electron than Cl is reflected by 1/4 of an argon moment; Fig 3.3e and f.

In fact the relationship between the inert-atom moments and the Yonemoto Q values given in the next chapter verifies this extension and the value of 1/4 for a single electron.

Discussion of all the informative aspects of the content of this table necessitates a long digression.

Let us begin with molecules containing a benzene ring. It is sometimes argued that molecules with a conjugated π-electron system show a particularly strong dispersion attraction due to the large in-plane polarizability of the π-electron[259,260]. An error of −15% (table 3.5) for benzene shows that π-electron system contributes to the buffeting or dispersion interaction by about 15%, and the 85% is attributable to the contribution of the σ-skeleton. This is in agreement with the Muler and Huiszoon[261] finding that for none of the polarizability components does the π-electron contribution really dominate over the contribution from the σ-skeleton while the π-electron contribution is far from negligible.

For a substituted benzene ring (3.18), with no π-correction, gives less error compared to (3.19), meaning that the π-electron mobility or polarizability somehow vanishes. For C_6F_6 this can be understood, as the π electrons are drawn to the fluorine atoms. For this reason (3.18) is used in calculations involving substituted rings (see table 3.7).

The next aspect to consider is the increase in the positive error of XMe_4 and XEt_4 systems with the increase in the metallic character of the central atom.

The fact that the errors for $SnMe_4$-$SnEt_4$ pair, and $SiMe_4$-$SiEt_4$ pair are the same reinforces the presumption that the error may arise from the use of a <u>full</u> $\langle m^2 \rangle_{inert}$ for the central atom.

This has proved to be the case for mercury where the corresponding inert-atom moment, $\langle m^2 \rangle_{Rn} = 140.5$, exceeds the atomic moment of mercury, $\langle m^2 \rangle_{Hg} = 127.66$, by 10%.

However, these errors, because of the low-buffeting site of the central atom, namely d = 0, have negligible effect on the estimation of properties by the buffeting <u>field</u> expression.

Note that the large negative error of -21% for $TiCl_4$, with a <u>transition</u> central metal distant from inert atoms in the periodic table, conflicts with the afore-mentioned suggestion according to which the estimated moment should exceed the molecular one. The negative error means that the central atom contributes more than its apparent σ-skeleton. Addition of another Kr's moment for Ti, which is equivalent to the contribution of 4 electrons, gives;

$\langle m^2 \rangle_E = 331.88 + 83.436 = 415.31$

with an error of 1% which is given in the table.

From the evidence of this section we come to the conclusion that the adjustable bonded-atom moment $\langle m^2 \rangle_J$ in (3.9) may, with reasonable accuracy, be fixed at the known corresponding inert atom moment, given in table 3.4.

However, the unexplained large errors of CF_4 and SF_6, or, CO, NO, and O_2 even after π-correction cast doubt on this conclusion to some extent. The investigation into these anomalies presented in the next two subsections is motivated by confidence in the validity of inert atom additivity expressions.

<u>3.3.4.1. Pauling " 3-Electron Bond"</u>

The inert-atom additivity expressions (3.18) and (3.19) appear to be sensitive to the pecularities of the chemical bonds. For example, the moments of CO and NO even after π-correction fall short of the molecular ones by about -22%. This shortfall indicates that there is some unaccounted electron density in the bondings of these molecules.

In 1931, Pauling[262] introduced the concept of "3-electron bond", A...B, to help describe the electronic structures of a number of molecules such as, NO, NO_2, and O_2, the ground states of which are paramagnetic at room temperature. Harcourt[263] displys the paramagnetic NO and O_2 as;

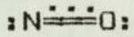

$:N\overset{\cdots}{\equiv}O:$

(a)

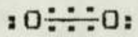

$:O\overset{\cdots}{\underset{\cdots}{-}}O:$

(b)

The value of 51.12 in the table was found for N=O; the paramagnetic structure (a) demands an extra .75 $\langle m^2\rangle_{Ne}$ for the three electrons;

$\langle m^2\rangle_{e}(N\overset{\cdots}{\equiv}O) = 51.12 + .75\ \langle m^2\rangle_{Ne} = 66.45$

which is almost exactly the molecular moment of 66.56 found from the experimental I and α.

For oxygen, Harcourt-Pauling representation increases the already positive error of 10% found on the basis of the conventional O=O structure. Instead, we suggest the resonance structure;

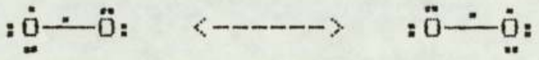

$:\underset{\cdot\cdot}{\dot{O}}\overset{\cdot}{-}\ddot{O}: \longleftrightarrow :\ddot{O}\overset{\cdot}{-}\underset{\cdot\cdot}{\dot{O}}:$

(c)

according to which the exact molecular moment of 46.37 may be calculated;

$\langle m^2\rangle_{e}(:O...O:) = 2\ \langle m^2\rangle_{Ne} + (1/4)\ \langle m^2\rangle_{Ne} = 46.01$

It must be noted that the Harcourt-Pauling form (b) is challenged here by the form (c). A structure of type (b) necessitates a much larger polarizability for O_2 than the observed value of 1.6 A^3. This can be seen by the comparison between N=O and $^{-}C\equiv O^{+}$ where the former has a polarizability 1.5 times larger than the latter.

Spectroscopy studies provide a more direct proof of the superiority of (c) to (b). A comparison of the force constants for N_2 (triply bonded), CO (triply bonded, see (d) below), and O_2 shows that a structure of type (b); $:O\overset{\cdot\,\cdot}{\equiv}O:$, is unlikely;

Species	N_2	CO	O_2
Force constant N/m[264]	2294	1902	1177

For CO, a diamagnetic at room temperature, a structure of type (d) is suggested on the ground of its permanent dipole moment, the direction of which corresponds to (+) on oxygen[263];

$$^{-}:C\equiv O:^{+}$$

(d)

This structure also explains the formation of complexes with transition metals such as $Ni(CO)_4$. If structure (d) as compared with conventional C=O, for which 51.12 was found, is used, one finds;

$$\langle m^2\rangle_E(^{-}:C\equiv O:^{+}) = 51.12 + (1/2)\ \langle m^2\rangle_{N\equiv} = 61.34$$

short of the molecular value of 64.76 by 5% compared with 21% of the conventional structure.

3.3.4.2. Fluorine Compounds and "4-Electron 3-Centre bond"

The large negative errors in estimated moments of CF_4 and SF_6 together with the confidence in the reliability of (3.18) for small molecules forced us to verify the accuracy of the I and α values given by Mohanty and Bernstein[246].

Evidently the fluorine derivatives of hydrocarbons have smaller α than the corresponding hydrocarbons;

Species	CH_4 (CH_2F_2, CHF_3)	C_2H_6 (C_2F_6)	C_6H_6 (C_6F_6)
α A^3	2.55 (2.48[201], 2.40[201])	4.47[254] (3.98[201])	10.4 (10.1)

Therefore the value of $\alpha = 2.89$ for CF_4 is likely to be in error. More recent measurements[201] give 2.31 as compared to 2.89[241], and 3.67 A^3[265].

By using this new value one finds;

$\langle m^2\rangle(\text{Mol. } CF_4) = 98.7$,

to be compared with,

$\langle m^2\rangle_E = 5\ \langle m^2\rangle_{Ne} = 102.25$,

with 3% error as given in the last column.

For SF_6, on the other hand, the ionization potential of 19.32 given in the table appears to be too large as this has the highest polarizability in the series CF_4, SiF_4, and SF_6. Siegbahn[266] gives a more accurate value of 16 eV, therefore;

$\langle m^2\rangle(\text{Mol. } SF_6) = 174$, and;

$\langle m^2\rangle_E = \langle m^2\rangle_{Ar}(\text{for S}) + 6\ \langle m^2\rangle_{Ne}(\text{for F}) = 184.81$

with 6% error, which equals the error of SiF_4.

The ionic or the "4-electron 3-centre" bonding of these compounds with structures of type (a), (b), and (c) is discussed in detail in Chapter 5, according to which the electronic charge from the central atom is shifted to the peripheral high-buffeting ones;

$F_3C^+F^-$	$F_3Si^+F^-$	$F_5S^+F^-$
(a)	(b)	(c)

This fact affects the estimated moments of SiF_4 and SF_6, as the corresponding inert atoms of the central and the peripheral atoms are different. It was mentioned that a single non-σ electron is equivalent to $\pm(1/4)\ \langle m^2\rangle_{inert}$, where negative is used for cations (lacking electron) and positive for anions (extra electron). Therefore one finds;

$$\langle m^2\rangle_E(F_3Si^+F^-) = .75\ \langle m^2\rangle_{Ar}(Si^+) + 3\ \langle m^2\rangle_{Ne}(F) + 1.25\ \langle m^2\rangle_{Ne}(F^-)$$

$\langle m^2\rangle_E = 133.49$, $\langle m^2\rangle(\text{Mol.}) = 135.36$, Error = -1%

and likewise for SF_6;

$\langle m^2\rangle_E = 174.39$, $\langle m^2\rangle(\text{Mol.}) = 174.00$ Error = 0%

Table 3.6 gives the estimated and the molecular moments of some more fluorine compounds (asuumed to be covalent).

3.3.4.3. Inert-Atom Additivity Rule

From the evidence of the last two sections one may express an additivity rule (omitting the (3/2) factor of $\langle m^2\rangle$) as;

$$I\ \alpha(\text{Mol.}) = \Sigma\ I\alpha\ (\text{inert}) \pm (1/4)\ \Sigma\ I\alpha\ (\text{inert}) \qquad (3.20)$$

where the summations are over σ- and non-σ-skeleton.

Table 3.6. Analysis of the moments of Halofluorocarbons

Index number	Molecule	I eV	Molecular Parameters[201] α Å^3	$\langle m^2 \rangle$	$\langle m^2 \rangle_e$ (3.18)	Error %
34	CF_3Cl	13.0	4.31	134.47	143.91	7
35	CF_2Cl_2	12.3	6.56	193.65	185.57	-4
36	$CFCl_3$	11.9	8.42	240.47	227.23	-5
37	CF_2Br_2	11.2	8.6	231.17	207.72	-10
38	$CFBr_3$	12	11.90	342.72	291.2	-15
39	CF_2HCl	12.6	4.6	139.10	138.36	0
40	$CFHCl_2$	12	6.5	187.20	180.02	-4
41	CFH_2Cl	11.7	4.48	124.95	132.8	6
42	CH_2Cl_2	11.4	6.51	178.11	170.46	-4
43	C_2F_5Cl	13	6.46	201.55	205.26	2
44	$C_2F_4Br_2$	11.4	10.72	293.3	289.57	-1
45	$C_2F_3Cl_3$	11.8	10.47	296.51	288.58	-3
46	C_2F_3HClBr	11.2	9.37	251.86	262.70	4

Non-σ-skeleton includes the π-electron and the anion-cation systems.

The implication of the second term is that one can define ionization potential and polarizability for electrons in a molecule.

Given the molecular polarizability one can now estimate the ionization potential (IP) and vice versa from (3.20). The latter option is not attractive because of the abundance of methods for estimating molecular polarizability with reasonable accuracy, such as bond polarizability, contribution polarizability, and Lorentz-Lorenz Eq., (1.2), which requires the refractive index and the density.

The option of estimating IP however, is particularly intersting as apparently there exists no prediction method for the molecular <u>(1st) ionization potential</u>.

The ionization potential is a prime molecular quantity that measures the ease with which a molecule can be oxidized. The wide range of uses for this important quantity warrants the test of (3.20).

Table 3.7 gives the experimental and estimated IP values by (3.20). The majority of the molecular polarizabilities are calculated using refractive indices from Ref.[158] and (1.2) the equation of which can be given as;

$$\alpha_E(A^3) = .3964\ V \frac{(n^2 - 1)}{(n^2 + 2)} \tag{3.21}$$

where the molar volume should be in cm^3/mole. Combining this with (3.20) gives an equation for the estimation of IP from the refractive index and molar volume as it is used in the table;

$$I_E(eV) = 1.051\ V \frac{(n^2 - 1)}{(n^2 + 2)} \sum_{\sigma,\text{non-}\sigma} \langle m^2 \rangle_{\text{inert}} \tag{3.22}$$

Notice that the inert-atom moments as entered in table 3.4 are to be used in (3.22).

For the calculations of I for electron rich molecules, O_3, SO_2 N_2O, and HCN, the following structures are used;

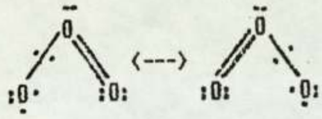
(a)

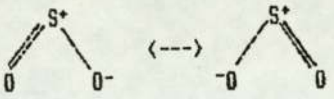
(b)

$H^+C^-\equiv N$

(c)

$N\equiv N=O$

(d)

Structure (a) for O_3 is given by Harcourt. The traditional Lewis type sructures (e) used in (3.22) gives I_E = 10.47 eV, in disagreement with the experimental value, signifying the sensitivity of inert-atom approximation to the structural types of electron rich molecules. The traditional O=S=O structure for SO_2 gives I_E = 13.6 eV.

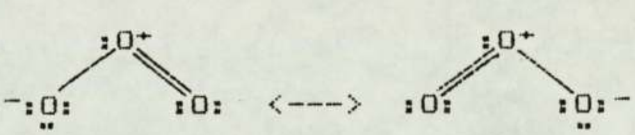
(e)

It must be added that S_8, S_7, and S_6 are assumed to be purely covalent, inspite of the belief[267] that there are delocalized electrons in S_8 sulphur ring. This model of delocalized electrons, or as it is known 'non-σ' electrons, explains the colour of sulphur. One could verify the existence of delocalized electrons in the ring if the experimental I for S_8 were available. This subject is further discussed when the solubility of S_8 in CS_2 is analysed in the last chapter.

Notice the poor agreement between I(Esti.) and I(Expt.) for $AsCl_3$. From the comparison between the experimental ionization potentials (IP) of entries 74 and 76 together and then between 73 and 75, one can see that I(Expt.) for $AsCl_3$ is likely to be erroneous.

Table 3.7 Experimental and Estimated Ionization Potentials

Index number	Species	α Å^3 (3.21)	I(Expt.) [158] ev	I(Esti.) (3.22)	Index number	Species	α Å^3 (3.21)	I(Expt.) [158] ev	I(Esti.) (3.22)
47	HF*	.813	16.06[214]	16.75	70	$CHCl_3$	8.53	11.42	10.68
48	HI	5.199[69]	10.39[16]	10.39	71	CH_2ClBr	7.58	10.77	10.44
49	H_2O	1.444[69]	12.6	12.87	72	P_4	14.7	-	7.04
50	H_2O_2	2.336	11.0	11.61	73	PCl_3	10.4	9.91	9.94
51	O_3	2.845[69]	12.3	11.96	74	$P(C_6H_5)_3$	34.66	7.36	7.34
52	CH_3OH	3.23[49]	10.84	11.50	75	$AsCl_3$	11.68	11.7^7	9.61
53	SO_2	3.774[69]	12.34	11.33	76	$As(C_6H_5)_3$	36.67	7.34	7.18
54	N_2O	2.921[69]	12.894	13.11	77	S_6	16.69^a	9.7	9.29
55	C_6H_6O	11.098	8.51	8.10	78	S_7	19.47^a	9.2	9.29
56	$C_4H_{10}O$	11.045	9.14	10.35	79	S_8	23.82	-	8.68
57	$C_6H_5NO_2$	12.92[214]	9.92	8.55	80	PH_3	4.1^a	9.98	10.00
58	$(Me)_2NCOH$	7.896	9.12	10.4	81	Cyclo-C_4F_8	6.72	-	15.18
59	$(Et)_2NCOH$	11.455	8.89	10.4	82	C_6H_5Cl	12.25[214]	9.07	8.36
60	C_2H_2	3.33[49]	11.4	10.69	83	HCN	2.487[69]	13.8	12.99
61	C_2H_4	4.26[49]	10.4	9.72	85	CH_3CN	4.27	12.2	11.52
62	C_3H_8	6.29[49]	11.1	10.47	86	CH_3CH_2CN	6.067	11.84	11.18
63	C_5H_{10}	9.1[159]	10.44[159]	10.21	87	N_2H_4	3.50	8.74	10.6
64	CH_3Br	5.61$^+$	10.53$^+$	10.40	88	$(CH_3)_3N$	7.767	7.82	10.23
65	CH_2Br_2	8.68	10.48	10.14	89	$(Et)_3N$	13.39	7.5	10.10
66	$CHBr_3$	11.84	10.4	9.94	90	$(C_6H_5)_3N$	27.24	6.86	8.72
67	CH_3I	7.59	9.54	9.57	91	C_6H_7N	12.13	7.7	7.83
68	CH_2Cl_2	6.82	11.35	10.30^b	92	C_5H_5N	9.42	9.3	9.34

*: Refs.[49] and [214] give the erroneous value of α = 2.46 Å^3 for HF.

+ : I and α of 64 to 71 are from table 2.3.

a: Estimated using the polarizability contributions of S, P, and H given in Appendix 6.

b: I(Est.) = 10.80 for α = 6.51 from table 3.6.

The inert-atom approximation that supplies reasonable estimates for the IP of many systems fails for some of N-containing molecules. This is where the Koompson approximation (the i-th IP is given by the negative of the i-th orbital energy) also fails. In fact this problem is associated with the N-lone pair and is fully discussed in von Niessen's work[268].

From the inspection of the IPs of $(Me)_3N$, and $(Et)_3N$, however it appears as if the ionization is taking place out of the N-lone Pair orbitals, because the latter with about twice the polarizability shows the same IP. When N is attached to electro-negative groups there is a better agreement between I(Esti.) and I(Expt.). The exploration of these effects is beyond the scope of this work and requires quantum mechanical techniques.

This section ends with the estimation of IP for cyanogen C_2N_2 and dicyanoacetylene C_4N_2 for which the Koopmans' approximation fails, and which are considered by von Niessen.

The polarizabilities of these molecules are estimated using that of (HCN - H) and (HCCH - 2H) from the table. For H, a polarizability contribution of .43 A^3 is used (see the next section). In this way one finds the approximate values of;
$\alpha(N{\equiv}C{-}C{\equiv}N) = 4.1$, $\alpha(N{\equiv}C{-}C{\equiv}C{-}C{\equiv}N) = 7.29\ A^3$.
which using (3.20) give;

		C_2N_2	C_4N_2
(3.20)..........	I(Esti.)eV	12.58	10.52
Quantum Mechanical...	I(Theor.)[268]	13.20	11.88
	I(Expt.)[268]	13.36	11.84

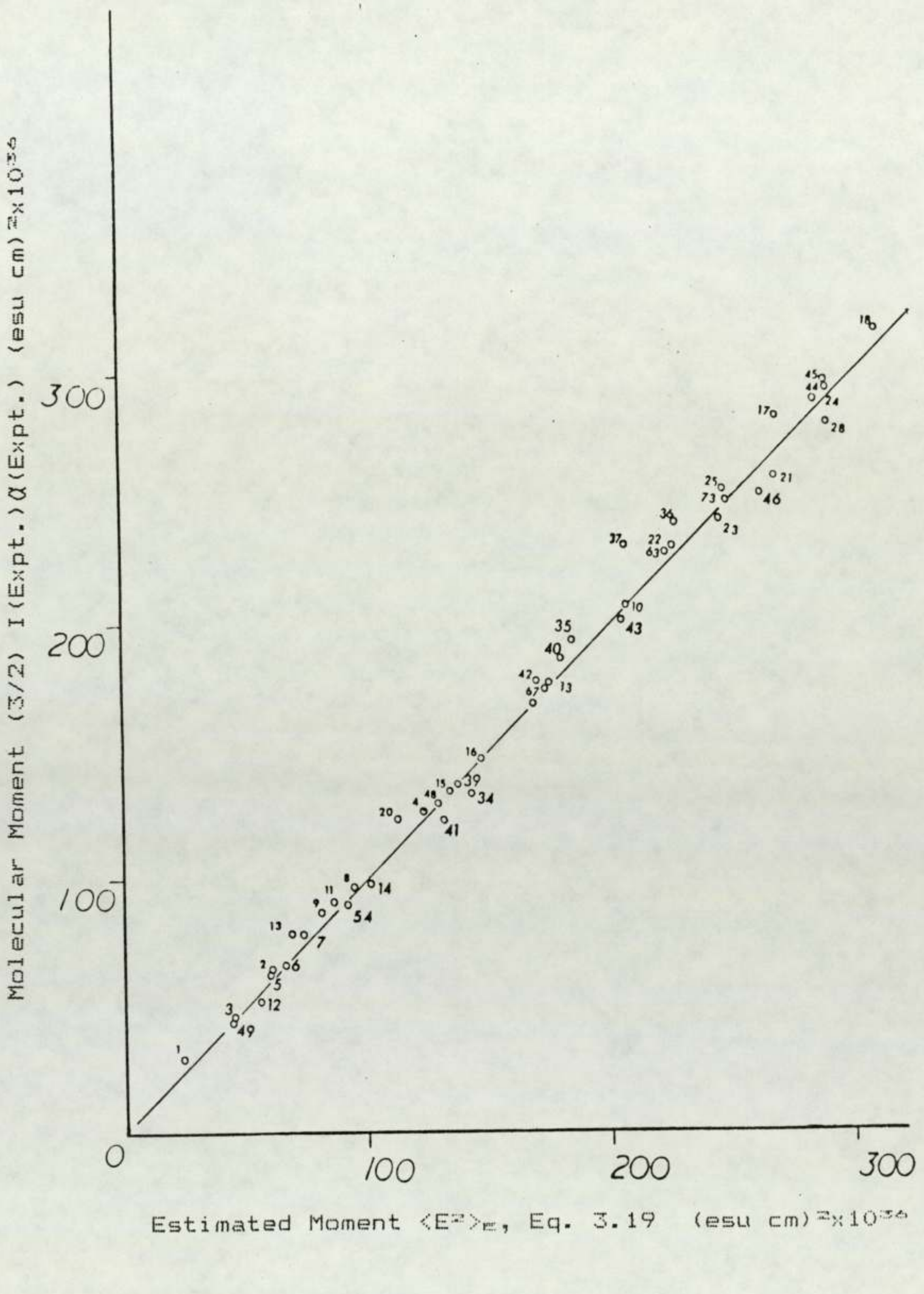

Fig. 3.4 Relationship between the molecular and estimated moments of selected molecules as indexed in tables 3.5, 3.6 and 3.7.

The substantial agreement between the available experimental and estimated IPs reinforces the validity of the use of $\langle m^2\rangle_{inert}$ in place of the bonded-atom moment $\langle m^2\rangle_j$ in (3.9) and also estabilishes (3.20-3.22) as an approximate additivity rule for estimation of IP.

A graphical presentation of selected molecular and estimated moments from the last three tables is given in Fig. 3.4.

3.4. Polyatomic or Generalized London Dispersion Potential

The workability of (3.9), now a combination of reasonably well-defined parameters, Z_L, $\langle m^2\rangle_{inert}$, F, and R, needs to be tested. The calculation of heats of vaporization (HV) provides the most straightforward verification of this field expression.

This section is devoted to the derivation of a polyatomic potential function that can be used to find HV.

To convert a mean-square field to a potential form, use is made of the unorthodox relation (1.51) found in the first chapter;

$U_{i,j} = -\ (1/8)\ (\alpha_i\langle E^2\rangle_j + \alpha_j\langle E^2\rangle_i)$

This shows the mean mutual interaction potential between an atom i of polarizability α_i in the oscillating field of atom j. In terms of the moment of j, using (3.6), this becomes;

$$U_{i,j} = -\ (1/4)\ R^{-6}F(i,j)\ [\alpha_i\langle m^2\rangle_j + \alpha_j\langle m^2\rangle_i] \qquad (3.23)$$

Implicit in this Eq. is the fact that i and j now belong to two interacting molecules a distance R apart. Letting $F(i,j) = 1$ and $i = j$, it becomes the London dipersion formula (1.48) between two identical atoms a distance R away.

One immediately realizes the problem that arises when atom i becomes part of a molecule; α_i becomes the bonded-atom polarizability.

Fortunately the concept of bonde-atom polarizability or as it is called the 'polarizability contribution' (Pc) is well-known. A short list of Pcs and the isolated atom polarizabilities shows their difference (see Appendix 6 for a fuller list);

Group ---------------->	H	C	C=	C≡	O (R-O-H)	F	Cl	I
Pc α_i A^3[161]	.43	.93	.58	.86	.59	.38	2.28	5.11
Atomic α A^3[212]	.667	1.76	-	-	.802	.557	2.18	3.9

By using the Pcs given here one can find accurate molecular polarizabilities, for example;

$\alpha(CH_4) = 4.43$ <------ atomic -----> $\alpha(CF_4) = 3.16$

$\alpha(CH_4) = 2.65$ <------ Pc ---------> $\alpha(CF_4) = 2.45$

$\alpha(CH_4) = 2.66$ <------ Expt. ------> $\alpha(CF_4) = 2.31$

Therefore for α_i in (3.23) the Pc values should be used.

For a pair of molecules with X_i atoms of the same species i (belonging to one molecule) and X_j atoms of same species j (belonging to the other molecule) the pair potential can be written as;

$$U(\text{pair}) = -(1/8)\, R^{-6}\, X_i X_j F(i,j)\, [\alpha_i \langle m^2 \rangle_j + \alpha_j \langle m^2 \rangle_i]$$

which for two molecule containing different species becomes;

$$U(\text{pair}) = -\,(1/8)\,R^{-6}\sum_{i}\sum_{j} X_i X_j F(i,j)\,[\alpha_i\langle m^2\rangle_j + \alpha_j\langle m^2\rangle_i]$$

This may be regarded as a Polyatomic London Dispersion formula It reduces to that of London for two interacting atoms.

3.4.1. Heat of Vaporization

Let us derive an expression for the heat of vaporization (HV) (or sublimation) in terms of the polyatomic pair potential (3.24) according to a method due to Moelwyn-Hughes[69, p.315].

In a mole of compound with Z nearest neighbours, the number of neighbourly pairs that can be formed is (1/2)ZL. If it is assumed that the greater part of the total potential energy, that is the molar potential energy, is due to the immediate interactions between nearest neighbours one can write;

$U(\text{molar}) = (1/2)LZ\,U(\text{pair})$

where U(molar) is the total interaction potential and U(pair) is the molecular pair potential (3.24).

The U(molar) approximately equals the heat of vaporization when Z_L is used;

$$H_v(\text{kJ/mole}) \simeq -7.53Z_L R^{-6}\sum_{i}\sum_{j} X_i X_j F(i,j)\,[\alpha_i\langle m^2\rangle_j + \alpha_j\langle m^2\rangle_i] \qquad (3.25)$$

where R in A, α in A^3, $\langle m^2\rangle$ in units of 10^{-36} erg cm^3 from table 3.4 give H_v in KJ/mole.

The preliminary analysis of the HVs given in table 3.8 serves to verify this expression. For R the solid state experimental values are tentatively used. The H_v values according to the

Table 3.8. Comparison between experimental and calculated heats of vaporization

Compound	Z_L	R(Expt.) A Table 3.3	H_v(Expt.) KJ/mole[240]	H_v KJ/mole Polyatomic (3.25)	H_v KJ/mole London (1.48)	Polyatomic H_v / London H_v	q* = d/R
He	7[a]	3.77	.100	.091	.091	1.00	0
Ne	11	3.16	1.740	1.34	1.34	1.00	0
Ar	11	3.76	6.288	5.97	5.97	1.00	0
Kr	11	3.99	9.187	8.49	8.49	1.00	0
Xe	11	4.33	12.643	11.96	11.96	1.00	0
Rn	11	4.44[b]	16.76[b]	16.53	16.53	1.00	0
H_2	11	3.78	1.05[c]	1.25	1.38	.90	.098
CH_4	11	4.17	8.898[c]	10.86	6.38	1.70	.261
CCl_4	11	5.90	34.52[c]	34.52	11.34	3.04	.299
H_2O[d]	4	2.82	40.62[c]	19.32	7.55	2.56	.339
$C(Me)_3$	11	6.21	22.36[c]	25.46	7.47	3.40	.346
C_6H_{12}	11	6.20	32.73[c]	34.77	8.17	4.25	.356

a: For bcc He with Z_m = 8. The good agreement between H_v(Expt.) and H_v(Cal.) is marred by strong quantum effects in He.

b: The value of R = 4.44 A is found from an excellent α-R linear relationship for inert atoms without He. The H_v value is from Ref.[255].

c: From Ref.[158]

d: The centre of mass of water molecule is not at oxygen. For the calculations d_O = .0065 and d_H = .920 A are used from Appendix 5. Note that in table 3.3, for simplicity it was assumed that d_O = 0.

*: The q ratios are for the outer atoms, indicating the size of the molecules.

London formula are also given by using U_L (1.48) for U(pair) in the derivation of (3.25).

The table, more than anything else, verifies the buffeting field expression and the main features of its underlying assumptions.

There are many noteworthy aspects in this comparison. First, the departure of the polyatomic values from those of the sphere-based London values as the number of atoms in the molecule increases. As the q ratio approaches zero, the factor F approaches unity and the polyatomic potential becomes the London potential, in other words, London potential is the asymptotic form of (3.24). Note that the q values for these molecules do not exceed the limit at which the analytical F series is invalid.

The inclusion of water in this table is heuristic. The calculated value is based on the assumption that the four nearest neighbours and the central molecule rotate freely. The table shows that the text-book[49,214] dispersion contribution of 19% for water originates from the London formula; 7.55/40.6 ×100 = 18.6; the polyatomic value is about 47%. The remainder of 21.3 KJ/mole arises from non-dipersion sources, mainly H-bonding.

It is shown in Chapter 5 that the entire heat of vaporization for CH_3CN (μ = 3.44 D) is calculable by (3.25) signifying the negligible contribution of dipolar interactions to the total cohesion energy.

The larger value of the London H_v compared to the polyatomic one for H_2 is intriguing. It stems from the fact that; $2 \langle m^2\rangle_{H-} < \langle m^2\rangle_{H2}$, as the -19% error of table 3.5 shows. In the London formula the molecular moment is used, which explains the anomaly.

It must be emphasised that all the atoms of the two interacting molecules, as (3.24) shows, contribute to the pair potential, the d values of which can be found in Appendix 5. In table 3.8 only the largest d values, that is the d values of the peripheral atoms which show the molecular size, are used for q.

3.4.2. A Brief Survey of Polyatomic Potentials

The simplicity and versatility of the buffeting approach would be appreciated if similar works on the interaction of polyatomic are outlined. Let us first recapitulate the main problems of dealing with polyatomic molecules. These are;

1- Definition of the mean inter-atomic distace for rotating molecules which was solved by the F factor.
2- Definition of IP for bonded-atom which was solved by the inert-atom approximation.

There are two groups of workers, namely those who treat molecules as polarizable points[269-271], and those who treat molecules as polyatomic system[202-204,210].

The former group is not plagued with the afore-mentioned problems but to cure the undercalculated values uses some disguised scale factor. Slater and Kirkwood[270] for example, introduced the $z^{1/2}$ factor into the London formula, where z is the number of electrons in the outer shell of the molecule, which for CCl_4, for example, amounts to 32. This involvement of 32 electrons in the dispersion interaction implicitly undermines the concept of the first ionization potential used for approximating $h\nu$ in the moment expression.

In the latter group, Muller[204] has pioneered the polyatomic interaction for crystals of organic molecules. He could calculate the atom-atom distances (of $n-CH_2$ chain) from crystalographic data. To overcome the problem of bonded-atom parameters he took advantage of the Kirkwood[271] expression for the London dispersion in terms of susceptibilities;

$U = 6\ mc^2\ \chi_1\chi_2/(\chi_1/\alpha_1 + \chi_2/\alpha_2)$

where for $I = 4\ mc^2\ \chi/\alpha$ this expression becomes the London formula.

Such an expression, therefore, helps define a bonded-atom ionization potential by using the additivity of the susceptibility -already a well-known concept. The IP values so obtained are larger than hv or the ionization potentials, even for inert atoms (except for He) for which this method should work best. For Xe for example it is larger than $h\nu$ or I(expt.) by a factor of three.

More recently Claverie[203] avoids the problem of bonded-atom parameters by considering the dispersion interaction of the <u>bonds</u> i and j, rather than atoms, of two interacting molecules.

Mathematically his formulation involves the Traces of the polarizability tensors and physically the anisotropy of the bond polarizability. This approach lacks simplicity and creates the problem of the ionization potential for bond, the centre of interaction for bond, and the anisotropy in the bond polarizability.

Regarding the problem of rotation of the molecules, or bonds in this case, which involves the bond-bond distances and R, a series in terms of Legendre′s polynomial is derived[202]. In the view of the inverse-Sixth-Power dependence of the distance the series, as it is shown in Appendix 3, should be in terms of the Gegenbauer polynomial. However, three terms of the series are used to avoid the risk of divergence, and instead a damping is introduced[209].

4.5. Implicit Assumptions of the Buffeting Field Expression

The derivation of the total buffeting field expression (3.9) was based on a number of well-known assumptions which are outlined in this section.

3.5.1. Multiple Approximation Assumption

The cornerstone expression of the buffeting field is the dipolar field (3.3) which results in dipole-dipole interaction. The multipole field expression can be written as;

$\langle E^2 \rangle = F(i,j)\ R^{-6}[A + B\ R^{-2} + C\ R^{-4} + \ldots]$

where A, B, and C are constants involving respectively, mean-square dipole, mean-square quadrupole, and mean-square octapole. Margenau[272] has shown, for London dispersion, that even constant B is only a relatively small fraction of A, the term of which is further reduced by R^{-2} to a negligible contribution, justifying the dipolar approximation.

3.5.2. Rigid Molecule Assumption

This assumption was made on the grounds of the differences in the time scales of the vibrational and other molecular motions. It is a valid assumption as the dispersion forces are much weaker than the forces holding the nuclei together (the bond forces[201]).

3.5.3. The Inter-molecular additivity assumption

The pairwise field was converted to the total field for Z nearest molecules by assuming the additivity of fields.

This is the well-known additivity problem of the London dispersion formula. It has been shown, by extending the second order perturbation theory to the third order[273], that there would be a 3-body component and so the strict additivity vanishes. Nevertheless, the effect of the non-additivity was found to be negligible for crystals of inert gases[273,274].

More rigorous use of the perturbation theory to a group of molecules has shown that the London type potential is approximately additive[275]. Quantum mechanical treatment of non-additivity effects in $(H_2O)_3$[276], $H_2O...CH_3OH$[277], $CH_4...CH_4$[278] and inert gases[279] show that this effect is fairly small. This problem is more extensively discussed by Margenau and Kestner[71], and Claverie[203].

3.5.4. Intra-molecular Additivity Assumption

For a molecule with X_j atoms of species j, the field of a single j atom (3.7) was multiplied by X_j. This is a sort of intra-molecular additivity rule which is less well-known and it has been taken for granted by many workers, especially those dealing with molecular crystals[204,210].

However, recent quantum mechanical computations show that this approximation works reasonably[202]. In the case of C_2H_4 (and also benzene and azobenzenes[280]), this assumption fitted to quantum mechanical data, gives fairly realistic results for the equilibrium structure such as unit cell parameters, molecular orientations in the cell[281,282], and the cohesion energy[283].

These computations for the properties of N_2 crystal, such as equilibrium structure and cohesion energy, show that the intra-molecular additivity rule works much better for $N_2...N_2$ than $C_2H_4...C_2H_4$[284]. In general not much is yet known about this additivity but we may safely assume that it holds as good as the inter-molecular additivity rule.

3.5.5. Free Rotation Assumption

The derivation of the F series is based on the assumption of free molecular rotation, so that the atoms fully span their spherical surfaces.

Work on plastic crystals has made available massive data on the orientational freedom of the systems considered here. In fact, the existence of orientational freedom is the property that distinguishes plastic crystals -orientational disordered crystals- from other molecular solids[210,216,285].

A possible criterion for the existence of essentially free-rotational behaviour in plastic crystals is a nearly spherical, or globular, molecular form[286], which is seen in spherical methane derivatives[287]. For example, neutron scattering studies of $C(CH_3)_4$, in the liquid crystalline state, show the presence of isotropic rotational motion in which on a time average a molecule has no preferred orientations in space with rotational period of $.4\times10^{-12}$ s $< \tau <$ $.8\times10^{-12}$ s[288].

The isotropic rotational motion of C_6H_{12} (mp 270 °K) and C_5H_{10} in the plastic phase has been proved by the same method with $\tau \simeq 2\times10^{-12}$ and 10^{-12} s respectively[289]. Raman and infra-red line shape methods[290] give a rotational period of 1.6×10^{-12} s for <u>liquid</u> C_6H_{12} (296 °K) slightly shorter than that of the plastic phase as one would expect.

Studies of fluorinated cyclohexane, $C_6F_{11}H$, and $C_6F_9H_3$, show the presence of preferred orientations, and anisotropic rotational motion in the <u>plastic</u> phase[290].

For pivalic acid, $(Me)_3CCOOH$, a combination of NMR, dielectric and light scattering studies has established that the molecules are randomly dimerised with one of the <u>12</u> nearest neighbours. The molecules re-orientate themselves by making and breaking H-bonds with a period of about 10^{-8} s in the <u>plastic</u> phase[216]. These facts justify the assumption of free rotations in the liquid state, perhaps even for water with strong H-bonding.

3.6. Conclusions

The general idea that brought together the range of the problems discussed in this chapter was the atom-atom potential model. The model is undoubtedly approximate but rather successfully deals with the problems of structured molecules and their macroscopic properties. Furthermore the formulations are simple and require no experimental information except for the readily accessible density, bond-length and bond-angle.

One of the the major problems of theoretical studies, specially the new computer simulation techniques of the equilibrium and dynamic behaviour of molecules, is the statement of the correct pair-potential function. It was shown that a sphere-based potential function is an irrational choice and unlikely to work for liquids. This fact has forced investigators to introduce more adjustable parameters into the existing potential functions to account for the shape and molecular rotation. Molecules have been categorized as, rigid convex, ellipsoidal, sphero-cylindrical, oblate sphero-cylindrical, prolate sphero-cylindrical, generalized sphero-cylindrical, four-centre and so forth[49]. The buffeting model, according to which the interactions occur between the spherical inert atoms properly located in the molecule to account for its shape, supersedes such artificial classifications.

The buffeting pair-potential therefore offers itself as an alternative attraction potential function for the prediction of macroscopic properties.

The potentiality of quantifying the interaction between electrons, electron lone pairs, and in general any fraction of the electronic charge, is another important feature of this potential function. It therefore lends itself to the study of the aligned forces like hydrogen bonding and chemical reactivity.

The inert-atom approximation proved useful in the prediction of the molecular first ionization potential. Table 3.7 shows that the estimated IP values are (on average) within about 5% of the available experimental values for the majority of the 45 molecules considered.

An important use of the ionization potential additivity rule is for estimation of the *IP of functional groups* in molecules. This is of importance because it links the inert-atom approximation to the *reaction mechanism* and chemical activity studies. A molecular functional group of low IP value is more reactive and therefore determines mechanism of the reaction.

No explanation for the correspondence of $1/4 \langle m^2 \rangle_{inert}$ and a single non-σ electron was given as this is strictly a quantum mechanical matter.

A more extensive use of the buffeting field and potential functions for the study of the heats of vaporization and vdW nuclear screenings is deferred until Chapter 5.

In the following chapter the connection between the buffeting field and that of Homer and Percival will be explored.

Chapter 4

Comparison between the Site-Factor and Buffeting Theories of the van der Waals Nuclear Screening

Introduction

The sensitivity of the vdW nuclear screening to the site of the resonant nuclei in the molecule has forced investigators to recognize structure and polyatomicity of molecules when developing their theoretical models for σ_w.

Rummens et al, for example, assigned a factor to the molecule under study as a measure of the off-centricity of each of its resonant nuclei. The attachment of this factor, a site-factor, to the body of the existing sphere-based formulations appears to have improved their theory of σ_w. To obtain agreement between theory and observation they bring in yet another factor with unknown origin. This indispensable factor, called a scale factor proved to be a variable depending on the solute-solvent systems, and an irrepressible disadvantage of the site-factor theories of σ_w.

In this area of work, the solvent remained a polarizable sphere until Raynes introduced the concept of atom-atom interactions for nuclear screening, and therefore regarded both interacting molecules as polyatomic, a fact reflected in his $\text{site}_{\text{solute}}$-$\text{site}_{\text{solvent}}$ factor. The Raynes atom-atom interaction model unlike the Rummens et al theory was limited to the case of two interacting methane molecules and for mathematical and physical problems has not been extended to other systems.

The site-factor and site-site factor theories have been succeeded by the buffeting theory of Homer and Percival in which the structure and polyatomicity of both interacting molecules are accounted for by a geometric or steric-factor obtained from simulation of the molecular encounters using molecular models. This theory supersedes the previous theories of σ_w, due to its independence of the scale factors and its universality.

The purpose of this chapter is to use the buffeting theory of the preceding chapter as an intermediary and seek the common and contrasting features of the three theories of σ_w.

It is shown that the Rummens et al cage model scale-factor is necessary to account for the effect of the structure of the solvent (assumed to be point) because the use of our F factor in place of their site-factor improves this theory and renders the scale-factor obsolete.

A critical study of the outlines of the binary gas collision model of Rummens et al for σ_w reveals that the use of this model for the liquid state is unjustified and that its scale factor is not associated with the polyatomicity of the solvent, but is an artifact of this model.

Comparing the Homer and Percival buffeting theory with that implicit in Chapter 3 shows the close relationship between their geometric factor and the F factor. This indicates the fact that all the factors -site, site-site, steric, and F- are a common feature among the models.

It is further shown that there is almost exact correspondence between the Homer and Percival semi-empirical K constant and the inert-atom moment, and an excellent correlation between the latter and the Yonemoto's quantum mechanical Q values, which also correlate with K.

4.1. Homer and Percival Buffeting Theory

The buffeting field derived by Homer and Percival[29,160] is essentially similar to (3.9) given in the previous chapter. Their approach is unique, compared to the prevalent treatment of interacting rotating molecules, in the sense that it outwits the problems of the nearest number of molecules, the number of peripheral atoms, the intermolecular distance, and the rotational averaging which gives rise to the F series. This however, is achieved at the expense of difficulties in defining and deriving their geometric factor $(2\beta - \xi)^2$, by using molecular models.

In the next two sections the relationship between the two fields is investigated.

4.1.1 The Homer and Percival K constant and $\langle m^2 \rangle_{inert}$

The space-time averaged buffeting field derived by Homer and Percival (Eq. 38, Ref.29, denoted here by $\langle E^2 \rangle$) (4.1) has the same form as (3.9) which for a solvent containing one species of buffeting atom may be re-arranged as (4.2);

$$\langle E^2\rangle = \frac{2\,\langle m^2\rangle}{r_v^6}\,(2\beta - \xi)^2 \tag{4.1}$$

$$\overline{\langle E^2\rangle} = \frac{2\,\langle m^2\rangle_J}{R^6/Z_L X_J}\;F(i,j) \tag{4.2}$$

where r_v, is the sum of the vdW radii of the buffeting atom j and the buffeted atom i, and $(2\beta - \xi)^2$ like F is a geometric factor. A comparison between (4.1) and (4.2) shows that the Homer and Percival field is independent of Z_L, X_J, R. Instead, they realistically have assumed that the buffeting and the buffeted <u>atoms</u> are <u>at all times</u> a well defined distance apart, which is characterized by the sum of their vdW radii; $r_v = r_v(j) + r_v(i)$.

This makes the quantitative comparison between the two fields, as a whole difficult, because r_v is fixed but R depends on the solute-solvent systems. Generally, for the peripherial atoms one can write;

$\overline{\langle E^2\rangle} \simeq \langle E^2\rangle$ for R from (3.16)

$\overline{\langle E^2\rangle} > \langle E^2\rangle$ for R from (3.15), (3.17), or R_v

The comparison between the bonded-atom moments, $\langle m^2\rangle$, and $\langle m^2\rangle_J$ and the geometric factors, however is possible. For bonded hydrogen, as was mentioned in the previous chapter, Homer and Percival suggest the quantum mechanical value of $\langle m^2\rangle_H = 13.5$ (in units of $(\text{esu-cm})^2\times10^{36}$), which compares well with $\langle m^2\rangle_{H\infty} = 12.11$.

For buffeting atoms other than H, they include the bonded-atom moment of (4.1) in an adjustable parameter K (or Q) and write;

$$\langle E^2 \rangle = K\, r_v^{-6}\, (2\beta - \xi)^2 \qquad (4.3)$$

where K is a buffeting constant depending on the buffeting atoms (of the solvent) only.

It will be remembered from Chapter 3 that different buffeting atoms differ in their moments by their corresponding inert-atom moments. The heavier the buffeting atom -the larger its $\langle m^2 \rangle_{inert}$- the greater the field it produces at the site of the buffeted or resonant nuclei, and the larger the attraction or deshielding. This natural outcome of (4.1) or (4.2) has been proved quantum mechanically by Yonemoto[77], Marshall and Pople[137], and Musher[301], using perturbation theory.

According to Yonemoto, if the (buffeting) field produced by a H atom may be assumed to be unity, the field of a heavier atom is larger by a factor Q. He writes " a precise calculation of Q is difficult because no accurate molecular wave function is available that describes the state of ionization, hybridization, or the state of inner and lone-pair electrons of a heavier atom in a bond". Nevertheless he gives some Q values for halogens and their ions which are used by Homer and Percival to correlate with their emperical K or Q values obtained from (4.3).

The Homer and Percival K values are found using the experimental vdW shifts of (a solute containing) hydrogen in a number of solvents containing different heavy peripheral atoms such as O, F, Cl, and Br.

Table 4.1. Comparison of the Q values and normalized moment

Buffeting species	Q_Y [77]	Q_{HP} [29]	$\frac{\langle m^2\rangle_{inert}}{\langle m^2\rangle_{He}}$
H	1.0	1.0	1.00
F	3.1	2.1	1.69
F^-	3.6	–	2.11
O	2.8^a	2.3^b	1.69
Cl	10.2^c	6.5	5.13
Cl^-	12.5	–	6.41
Br	14	8	6.89
Br^-	18	–	8.61
CC*	.999	.996	

a: This is an extrapolated value from the Yonemoto Q values by Homer and Percival[29].

b: This is the mean value of single (Q = 3.4) and double (Q = 1.2) bond oxygens given by Homer and Percival. Strictly speaking, only Q of a singe bond oxygen can be compared to that of Yonemoto, because the Q values are sensitive to the bond state of the atom, like moments; $\langle m^2\rangle$ (=O) = 1.5 $\langle m^2\rangle_{Ne}$, $\langle m^2\rangle$ (-O) = $\langle m^2\rangle_{Ne}$.

c: It is not given by Yonemoto, it is estimated from the mean value of 1.22 = Q_{ion}/Q_{atom}.

*: Correlation coefficient between the Q values and normalized moments.

Table 4.1 gives the Q values of Yonemoto, those of Homer and Percival, and the normalized values of the moments, namely, the corresponding inert-atom moments divided by the moment of 'He'. For the anions, as was mentioned in Chapter three, 1/4 of the inert-atom moment, equivalent to one electron, is added to that of the atom. The content of this table is shown graphically in Fig. 4.1.

The good correlation coefficient of .999 (intercept -.93, slope 2.16) between the Q values of Yonemoto and the normalized moments once more strengthens the inert-atom approximation, and also the extension of that concept to anions.

This linear relationship between the moments and the Q values, computed by Hartee-Fock wave functions[77] -the Hartee method approximates the total wave function of a system of N electrons Ψ in terms of one electron orbital wave functions Φ such that $\Psi \simeq \Phi_1\Phi_2...\Phi_N$[302]- indicates the possible association of the quantum mechanical approximation with the inert-atom approximation.

The good relationship between the Homer and Percival empirical Q values and the normalized moments (CC = .996, interc. = .096 slope = 1.18) on the other hand, signifies their strong relationship and the fact that K in (4.3) is best equated with the corresponding inert-atom moment; $K \simeq \langle m^2 \rangle_{inert}$.

4.1.2. Comparison between $(2\beta - \xi)^2$ and F

The key to the circumvention of R, Z_L, and X_J in the Homer and Percival buffeting theory is their method of handling the

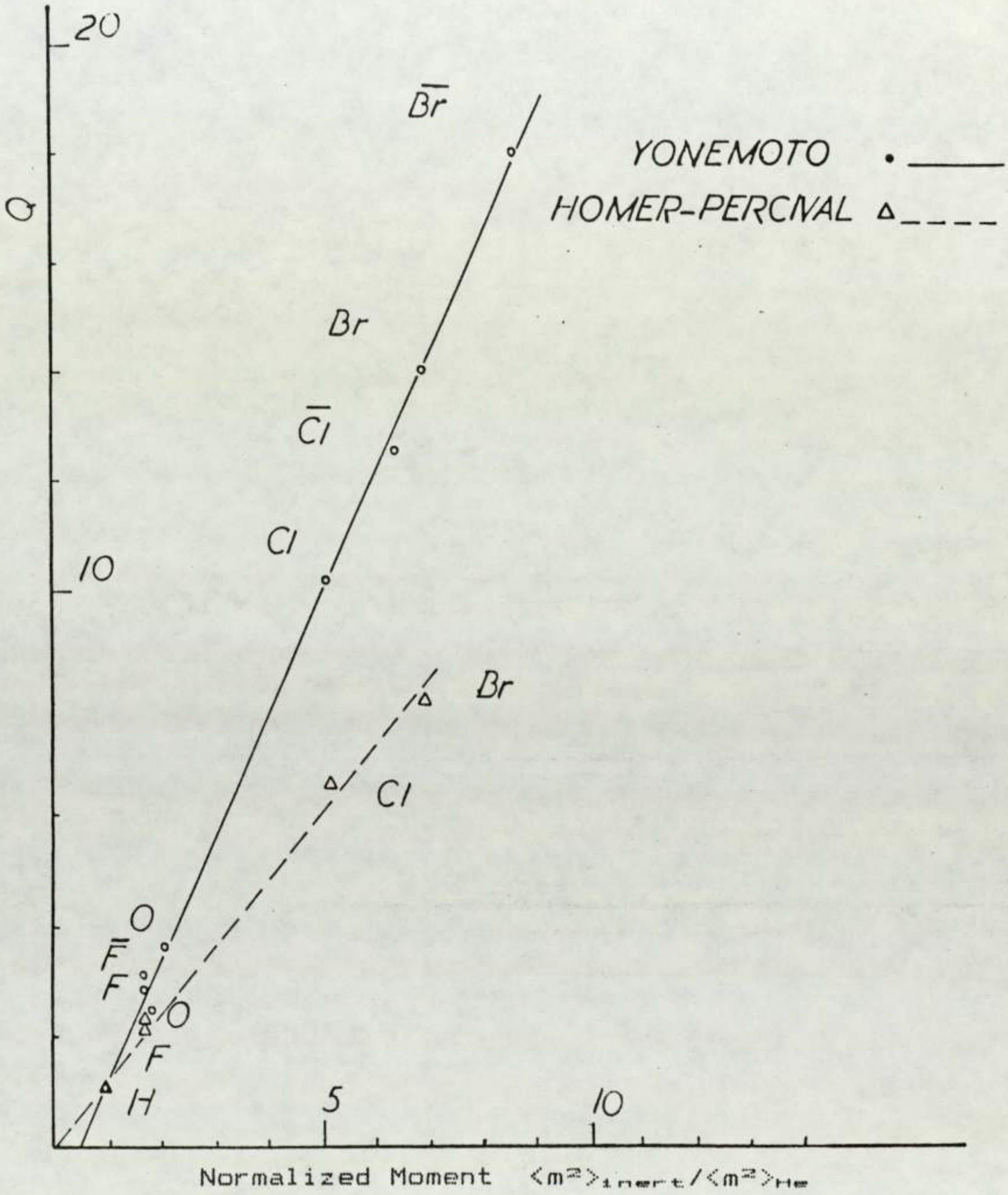

Fig. 4.1 Relationship between the Q values and normalized moment.

interaction between rotating molecules. This method can be outlined as follows.

Let us consider a particular volume (one octant, for example) between a solvent and a solute. The solute atoms are successively and continuously encountered by the solvent buffeting atoms. A "snapshot" of the situation, at any instant of time, shows a solute atom at a finite distance from the buffeting atom. This distance may be approximated by the sum of vdW radii of the two atoms. Exactly the same condition exists for other parts of the solute molecule, because on average it is in (vdW) contact with other surrounding solvent molecules. Two parameters β and ξ are then introduced to describe the effectiveness of the accessibility of the buffeted atom to the buffeting one as a result of their pairwise encounters. Two inert atoms, for example, can maintain full contact in the referred-to octant, and the value of unity is assigned to β and the value of two to ξ so that, $(2\beta - \xi)^2 = 0$. For two bonded atoms, that is when the atoms are parts of two interacting molecules, the full contact is no longer possible.

This condition results directly from the formation of bonds by the atoms in question and their consequent polyatomicity. Now the full penetration or contact of the two atoms is hindered by the steric hindrance action of the remainder of their molecules so that $\beta < 1$, $\xi < 2$, and $(2\beta - \xi)^2 > 0$.

One can therefore attribute the values of $(2\beta - \xi) > 0$ to the polyatomicity of the interacting solute and solvent, and infer that this factor should increase with the increase in the size

of the solute-solvent system. This inference about the Homer and Percival factor is in agreement with the analogous trend in the values of F as shown in table 3.1.
Concerning the interactions between the inert atoms (4.1) gives a zero field for $(2\beta - \xi)^2_{inert} = 0$, and therefore conflicts with the existence of the dispersion energy between these systems. This anomaly is justified in the context of the Homer and Percival buffeting theory in which (4.1) should be used with the (non-zero) RFT contribution, (2.20).

In table 4.2 the relationship between $F' = F/10$, and the available $(2\beta - \xi)^2$ values found by using molecular models, is analysed. For the values of R in the calculations of F, (3.16) is used. It can be shown that the choice of the expression for R; (3.14),(3.16), or (3.17) does not affect the correlation of the two factors. The values of F divided by 10, F′ in this table, are roughly of the same order of magnitude as $(2\beta - \xi)^2$. The d values of the peripheral atoms used in F expression (3.7) are from table 3.3.

Inspection of this table shows that there are a number of inconsistencies in the values of $(2\beta - \xi)^2$. First, according to the concept of this factor, one would expect to find the smallest value for the smallest system, that is, CH_4 in C_6H_6. Instead, CF_4 in C_6H_{12} and SiF_4 in CCl_4 show the smallest value of .096. Second, although the values of this factor are equal for CH_4 in C_6H_{12} and C_6H_6, this is not observed for CF_4 in these solvents. Third, SiF_4 has different values in $SiEt_4$ and $SnEt_4$, whereas the corresponding values of C_6F_6 are equal causing the poor correlation of .75 between the values of

Table 4.2. Comparison between $F' = F/10$, and $(2\beta - \xi)^2$

System	Ref.	Solvent or Solute						CC
$C_6H_6(v)$	29	CH_4	CMe_4	$SiMe_4$	$SnMe_4$			
$(2\beta - \xi)^2$		.123	.230	.270	.285			.97
F'		.244	.371	.434	.518			
$C_6H_{12}(v)$	29	CH_4	CMe_4	$SiMe_4$	$SnMe_4$			
$(2\beta - \xi)^2$		.123	.230	.270	.285			.97
F'		.191	.296	.344	.404			
$XMe_4(v)^+$	29	CMe_4	$SiMe_4$	$GeMe_4$	$SnMe_4$	$PbMe_4$		
$\overline{(2\beta - \xi)^2}$		.225	.270	.275	.295	.300		.97
$\overline{F'}$		.324	.383	.402	.445	.475		
$CF_4(u)$	160	C_6H_{12}	$SnMe_4$	C_6H_6	$SiEt_4$	$SnEt_4$		
$(2\beta - \xi)^2$		.096	.102	.09	.144	.152		.95
F'		.214	.236	.275	.430	.466		
$SF_6(u)$	160	CCl_4	$SiCl_4$	$SnMe_4$	$SiEt_4$	$SnEt_4$		
$(2\beta - \xi)^2$		.360	.360	.449	.518	.533		.96
F'		.201	.207	.263	.469	.51		
$SiF_4(u)$	160	CCl_4	$SiCl_4$	$SnMe_4$	$SiEt_4$	$SnEt_4$		
$(2\beta - \xi)^2$		.096	.096	.144	.176	.194		.96
F'		.200	.205	.261	.466	.505		
$C_6F_6(u)$	160	CCl_4	$SiCl_4$	$SnMe_4$	C_6H_{12}	$SiEt_4$	$SnEt_4$	
$(2\beta - \xi)^2$		.577	.577	.593	.608	.608	.608	.75
F'		.352	.377	.477	.442	.776	.844	

+: These are the mean values of the two factors for each solute in the series of XMe_4 solvents.

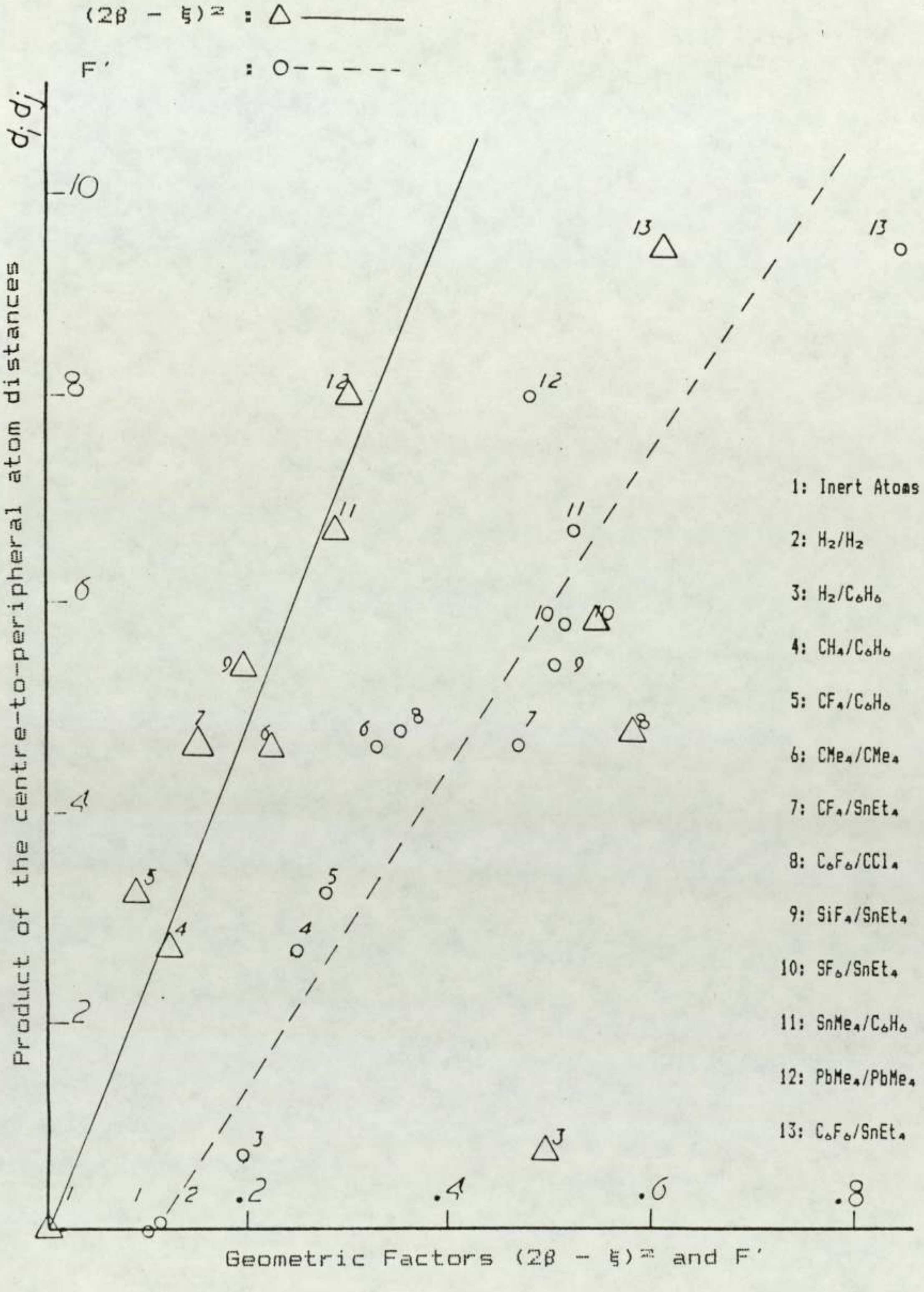

Fig. 4.2 Increase in the geometric factors $(2\beta - \xi)^2$ and F′ with the increase in molecular size, $d_i d_j$.

F′ and $(2\beta - \xi)^2$. The equal values of this factor for different solutes in C_6H_6 and C_6H_{12}, might have been caused by the difficulties in modelling and simulating the encounters of these systems accurately by molecular models.

The analyses in this table, in spite of the statisically small number of data in each case, serve to show that the formula for F replaces the molecular modelling of $(2\beta - \xi)^2$. This is in spite of their apparently different physical interpretations and the belief[160] that "... an entirely general formulation of β and ξ appears to be impossible...".

One notes from this table the trend of the increase in F′ and $(2\beta - \xi)^2$ with the increase in the sizes of the solute and solvent. A quantitative way of depicting this trend is to plot the values of these factors against some quantity representing the sizes of the solute-solvent system, for example $d_i.d_j$, Fig. 4.2.

The straight lines in this Fig. are only trend lines showing the direction of the increase in the factors and d_id_j more clearly. Note the smaller scatter of the F′ values compared to those of $(2\beta - \xi)^2$. The point for H_2 in C_6H_6 from the Homer and Percival work[29] markedly departs from the trend line of their factor. They have treated hydrogen gas as a unique case. The value of their factor for this gas is four times larger than that of CH_4 in the same solvent, contradicting the fact that as molecules shrink in size and approach mono-atomicity they may be mistaken by points for which the value of $(2\beta - \xi)^2$ equals zero. In other words, this factor should have the lowest value for H_2 after inert atoms, signifying the fact that small molecules may be approximated by spheres as was shown in Chapter 3.

The Homer and Percival theory, however, for the first time in NMR, considers both the solute and the solvent as polyatomic molecules and gives a working formula for the effective field between polyatomic molecules. Their effective field was re-derived, (3.9), in the previous chapter and the comparison between them here shows that one can write;

$\langle m^2 \rangle_{inert} \simeq K$; $F' \simeq (2\beta - \xi)^2$; and,

$R^6/(10\ Z_i X_j) \simeq r_v^6$ For R given by (3.16)

4.2. Rummens et al Site-Factor theory

Inspired by the experimental fact that different hydrogen species in a given solute molecule have different chemical shifts, for example, $C\underline{H}_2$ and $C\underline{H}_3$ in $X(CH_2CH_3)$, Rummens and Bernstein[80] developed the "solute site factor" model in which the solute assumes polyatomicity but the solvent remains a point. In this section a parallelism is drawn between the site factor and the buffeting factor F.

4.2.1. Rummens et al Site-Factor of the Cage Model

Two solute site factors have been incorporated into the non-continuum models of σ_w by Rummens et al[159]. These are S^c_6 (c for cage and 6 for dispersion forces only, that is the 6 in the LJ (6-12) potential), and S^c_g (g for gas) for the cage model and binary gas collision model respectively. The cage model is more akin to our approach as the same model was used in Chapter 3 in the transition of the pair-field to the total field of Z nearest neighbours. Therefore, this model is considered first.

The cage model site-factor is given as[159];

$S_\xi = (1 + q^2)/(1 - q^2)^4$

where $q = d_1/R$. The values of this factor and those of F with their ratios for XMe_4 systems are given in table 4.3.

Table 4.3. Comparison between S_ξ and F

Solute	S_ξ	$\overline{F}$	$\overline{F}/S_\xi$
$C(CH_3)_4$	1.445	3.25	2.25
$Si(CH_3)_4$	1.59	3.83	2.41
$Ge(CH_3)_4$	1.655	4.02	2.47
$Sn(CH_3)_4$	1.777	4.45	2.50
$Pb(CH_3)_4$	1.878	4.75	2.53
CC	.999	mean =	2.43

As S_ξ is a solute-factor, one has to find the mean value of F; $\overline{F}$, for a particular solute in different solvents to be comparable with S_ξ. To be consistent with the authors' approach their expression for R, namely (3.16), is used throughout this section.

They have found that[159] all their calculated chemical shifts fall short of the experimental values by a constant factor of 2.55 for XMe_4 systems. They called this factor the cage model scale factor, $K_\xi = 2.55$, with unkown origin. From the table one can see that the values of S_ξ are smaller than those of $\overline{F}$ by nearly this factor, which is reflected in their ratios. By using the mean ratio of 2.43 from this table one can write;

$$F = 2.43\ S_\xi; \quad \text{or} \quad F \simeq K_\xi\ S_\xi \tag{4.4}$$

In other words, the unkown scale factor arises because the solvent molecules are treated as points, and their scale factor is indeed a compensating factor for the effects of the solvent polyatomicity.

The authors[159] made an attempt to attribute some sort of temperature dependence to the scale factor as $K_\xi = a + bt$, and thus explain the temperature dependence of σ_w. They say that "... K may be temperature dependent since it presumabley corrects, at least partly, for the absence of an intermolecular potential in the cage model". Table 4.3 (and 4.4) clearly show that K_ξ corrects for the absence of structure for the solvent rather than lack of the potential function.

One might legitimately ask how σ_w could be found if the intermolecular potential is absent in the expression for σ_w? In fact the intermolecular potential exists in their expression but for a spherical solvent, see (4.5).

When they used S_ξ and its scale factor of 2.55 for systems other than XMe_4 it was found that the use of a single-valued scale factor cannot fit all the σ_w data, see table 4.4. Column five of this table contains the calculated screenings found by replacing $S_\xi K_\xi$ by the F factor. One notes the marked increase

Table 4.4. Comparison between the cage models of $S_\xi K_\xi$ (K_ξ = 2.55) and F

		σ_w Hz (Expt.) 30 °C[159]	---- σ_w(cal.) ---- [159]		--- Factors ---	
Solvent	Solute		$S_\xi K_\xi$	F	S_ξ	F
CMe_4	CMe_4	12.6, 13.3	14.2	10.7	1.47	2.81
$SiMe_4$		11.1, 12.7	13.2	11.1	1.44	3.10
CCl_4		17.5, 20.2	23.6	15.5	1.50	2.52
$SiCl_4$		13.2	20.4	14.6	1.48	2.71
C_6H_{12}		14.6, 11.5	17.6	14.4	1.49	3.12
C_5H_{10}		11.8	19.2	13.4	1.32	2.71
CMe_4	C_6H_6	16.9	23.9	17.7	1.76	3.34
$SiMe_4$		14.6	19.1	15.9	1.72	3.67
CCl_4		23.8	40.4	28.4	1.86	3.33
$SiCl_4$		16.7	33.4	24.2	1.79	3.31
C_6H_{12}		15.8	29.3	25.3	1.81	3.99
CMe_4	C_6H_{12}	11.2	16.1	11.9	1.53	2.90
$SiMe_4$		10.9	13.9	11.5	1.50	3.20
CCl_4		16.0	13.9	11.5	1.50	2.90
$SiCl_4$		11.1	23.7	17.3	1.54	2.87
C_6H_{12}		12.1	20.5	17.6	1.56	3.43
CMe_4	C_2H_4	13.8	22.9	14.1	1.27	2.01
CCl_4		22.3	39.2	22.6	1.30	1.91
C_6H_{12}		12.7	29.2	20.2	1.29	1.97
C_5H_{10}		13.0	32.0	19.7	1.31	2.06
CMe_4	CH_4	13.0	23.5	14.0	1.16	1.76
CCl_4		24.2	39.5	21.8	1.18	1.65
$SiCl_4$		15.8	33.9	19.7	1.16	1.72
C_6H_{12}		16.6	29.4	18.8	1.17	1.96
C_5H_{10}		14.7	32.1	18.9	1.18	1.77

in the agreement between the experimental and the theoretical values as a result of this replacement.

This table is also represented graphically in Fig. 4.3, where an ideal line through the origin eases the comparison between the cage model of F and that of S§K§.

4.2.2. Solute Site-Factor in the Binary Gas Collision Model

Rummens et al[159] have also used the solute site-factor with binary gas model of Raynes et al[78] with marked superiority compared to the cage model.

For the discussion of this model, it is helpful to know that the binary gas model, as used for the formulation of σ_w, is a compendium of conflicting concepts. It is a binary (two-body) gas collision model and thus misused for liquids where the interaction is intrinsically many-body and involves at least the Z nearest neighbours.

In this model, as in the cage one, the general (sphere based) expression[78];

$$(\sigma_w)_{pair} = - B \langle E^2 \rangle = - B\ 2 \langle m^2 \rangle_{SOLVENT}\ R^{-6} \tag{4.5}$$

links the screening with the intermolecular field.

When the R values of (3.16) were used in (4.5) it gave rise to the scale factor of the cage model, therefore the authors made an attempt to find smaller R values for (4.5) to remedy this shortcoming, by using (3.14) as;

$$\sigma_w = \int (\sigma_w)_{pair} \exp(-U/kT)\ d\tau \tag{4.6}$$

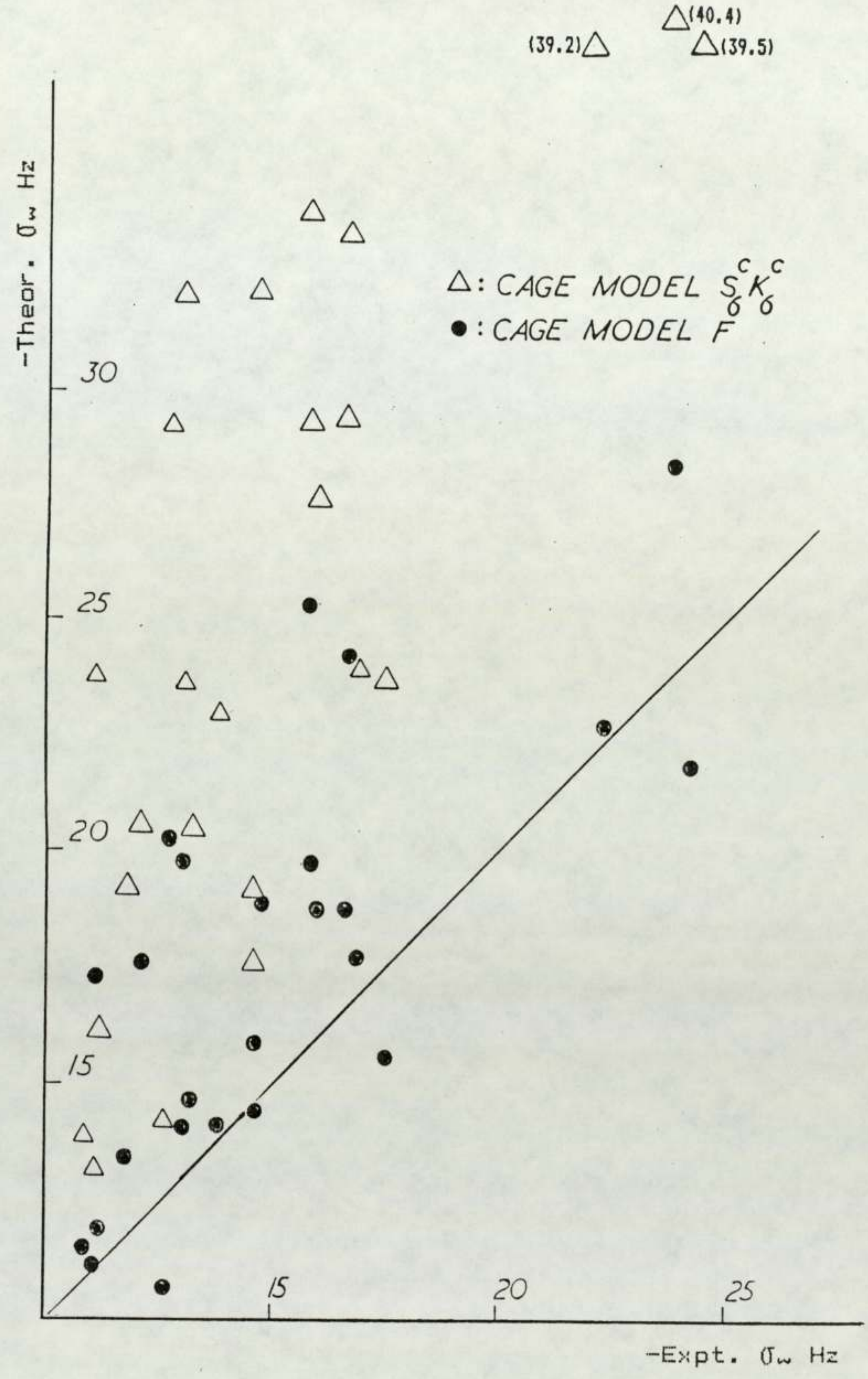

Fig. 4.3 A comparison between the Rummens et al cage model of σ_w with their site-factor scale-factor $S_\delta K_\delta$ and our buffeting factor F.

where $d\tau$ is the coordinate space element. Now a question arises as to the nature of the intermolecular potential U in (4.6). They use a LJ (6-12) potential for U and, in doing so, contradict the important fact that inherent in (4.5) is a dispersion intermolecular potential function. Therefore one might ask if there are two potential functions governing the intermolecular forces. If a LJ potential is used for U in (4.6) the same function, in the form of a field, should be used in (4.5) to characterize σ_w.

Nevertheless, by incorporating the site-factor into (4.5) and using (4.6) a gas model site-factor is obtained that is written as;

$$S_g = 1 + 3.45\, q_0^2 + 7.42\, q_0^4 + 12.9\, q_0^6 + 19\, q_0^8 + \ldots \qquad (4.7)$$

where $q_0 = d_1/r_0$, and r_0 is the distance in the LJ potential at which the repulsion begins, that is, when $U = 0$. Furthermore (4.5) is now written in terms of r_0 instead of R.

As $R > r_0$ (table 3.3 shows that in general $r_0 = R - 1$, for example, for CH_4, $r_0 = 3.8$ A, and $R = 4.96$) the calculated shifts turn out to be about 6 times larger than those of the model based on (4.5), therefore the Z nearest neighbours of the cage model no longer could be used. The new expression without Z is thus a tow-body formulation which is called the <u>binary</u> gas model.

Of course, there are other conceptual problems in this model. For example, the LJ potential which is an empirical potential function requires the adjustment of its parameters r_0 and ϵ to fit the experimental data, and automatically accounts for the polyatomicity of molecules and therefore renders the use of a site factor unwarranted.

However this model again requires a scale factor $K_\gamma = 1.65$, to improve the calculated values of σ_w specially for small solutes. The gas model scale factor unlike the cage model one is not related to the polyatomicity of the solvent. Apparently it compensates (together with the stated factor of about 6) for absence of Z; $1.65 \times 6 \simeq 10$.

It must be mentioned that the values of S_γ are somewhat larger than the corresponding S_δ values, for CH_4 in CCl_4, for example, using $r_0 = (r_0(u) + r_0(v))/2$, one finds $S_\gamma = 1.222$ and $S_\delta = 1.177$. The graphs of the two factors given by the authors[159] show otherwise, namely, $S_\delta > S_\gamma$.

The solute site-factor in the form of $S_{cont.} = 1/(1 - q^2)$ is also used in the continuum model of σ_w by Rummens[27]. The conceptual and the mathematical problems of using this site factor in the RF model are discussed in detail by Homer and and Percival[29] and need not be reiterated here.

4.3. Raynes Site-Site Factor

In a paper dealing with the NMR nuclear screening of methane, Raynes[206] introduced the concept of the atom-atom interaction and therefore accounted for the polyatomicity of both interacting methane molecules. It will be remembered from the preceding chapter that the atom-atom interaction model entails the knowledge of the mean inverse-six power of atom-atom distance, the mean intermolecular distance, and the properties of the bonded-atom.

The atom-atom distance averaging process in the Raynes work results in a geometric factor which is a special case of the F series; $F_6(d_i=d_j,R)$, as was mentioned in Chapter 3.

For the average R, Raynes resorts to (4.6) which brings in the Buckingham and Pople[303] H_n series as a function of ϵ/kT, and R becomes in terms of r_0. The amalgamation of the F_6 series and H_n gives another series with about twice the rate of convergence of the F_6 series. This procedure of course is analogous to that used by Rummens et al in obtaining S_6^r from S_6^R and replacing R in (4.5) by r_0. The use of the F factor or site-site factor, for the interacton of two methane molecules in the gaseous state, which involves a binary gas collision, appears to be questionable for the following reason.

If one assumes that the rotational motion period for molecules in the gaseous state is similar to that in the liquid state, and therefore of the order of 10^{-12} s, one would expect the collision of the two methane molecules to last at least about 10^{-12} s for the fulfilment of their full rotations during the collision. At normal temperature the translational speed of a methane molecule is about 4×10^4 m/s. Now if a stationary methane molecule is approached by another molecule at this speed, it takes about 5×10^{-15} s to travel a distance of about 2 A during which the attraction forces are operative.
A conservative estimate by Matheson[304] for a typical

translational speed of 5×10^{2} m/s and travelling distance of 1 A puts the collision time at 4×10^{-13} s. This is a shorter time than the time a methane molecule requires for full rotation in order to justify the use of the F or site-site factor for binary gas collisions. In other words, site or site-site factors are characteristics of the liquid state where the translation motion is slower than the rotational one which allows the rotational averaging while R is fixed.

Regarding the properties of the atoms in bonds, Raynes acknowledged the severe approximation of treating bonded-atoms as isolated ones. To understand his approach it is helpful to draw a parallel with the buffeting field. The nuclear screening of the H atom in two interacting CH_4 molecules in terms of the buffeting field can be written as;

$$\langle E^2\rangle \text{ (total field at resonant H)} = 4\,\langle E^2\rangle_{HH} + \langle E^2\rangle_{CH} \qquad (4.8)$$

The screening parameter B converts the field into the screening so that (4.8) becomes (regardless of the signs);

$$\sigma = 4\,B\,\langle E^2\rangle_{HH} + B\,\langle E^2\rangle_{CH};\ \text{or}\ \sigma = 4\,\sigma(H,H) + \sigma(C,H) \qquad (4.9)$$

where $\sigma(H,H)$ and $\sigma(C,H)$ are respectively the screenings caused by H and C atoms. Raynes begins with an expression similar to (4.9) and therefore calculating the screening of H requires the chemical screening of two interacting H atoms $\sigma(H,H)$, and that of a carbon and H atoms $\sigma(C,H)$. For the former he uses the result of the Marshall and Pople[137] work for two isolated H atoms. For the latter however, Raynes assumes the proportionality between the shielding and the atomic polarizability and writes;

$$\frac{\sigma(C,H)}{\sigma(H,H)} \simeq \frac{\alpha(C)}{\alpha(H)} \qquad (4.10)$$

then by using the <u>theoretical</u> isolated atom polarizability values of $\alpha(H) = .59$, and $\alpha(C) = .135\ A^3$ (Expt. values are respectively .666 and 1.67), given by Hirschfelder et al[49], arrives at an irrational estimate of $\sigma(C,H) = .23\ \sigma(H,H)$.

It is clear that the shielding caused by a carbon atom should be larger than that by hydrogen atom, because of (4.10) and the fact that $Q(C) > Q(H)$ or $\langle m^2\rangle_C > \langle m^2\rangle_H$. The correct estimate, using the bonded-atom or contribution polarizabilities, is $\sigma(C,H) = 2.2\ \sigma(H,H)$. However, because carbon has a low buffeting location ($d_C = 0$), its contribution to the total shielding does not exceed 15% and the error thus introduced is not considerable.

One notes that by assuming (4.10), Raynes implicitly accepts general proportionality of the screening and the field; $\sigma = -B\langle E^2\rangle = -B\, I\alpha\, R^{-6}$; according to which even (4.10) is not strictly true because of the involvement of R and I. The Raynes method lacks the features of a practical generalizable theory because;

1- It depends on theoretical values of σ, which is available for H...H only.

2- The expression for the F series is useable for the case of $d_i = d_j$ only.

3- The problems of bonded-atom properties are unsolved.

Nevertheless, by using $r_o = 3.8$ A and the isolated-atom nuclear screening Raynes calculates the value of $-\sigma_w = 6$ to be compared with the experimental values of 7.6 ± 2, 5.6 ± 2, 6.6 ± 3, 7.7 ± 1, 9.4, 5.4 ± 2 ppm cm^3/mole[17].

4.4. Conclusions

It was shown that although the Homer and Percival buffeting and the buffeting field derived in Chapter 3 are not wholly equal their main parameters are equivalent.

The almost one-to-one correspondence between the normalized moments and the K constant is interesting when one notes that the latter is obtained by the Homer and Percival buffeting field only, using a shift difference technique that cancels the RF contribution[29].

Another important finding here was the considerable correlation between the Q values of Yonemoto and the normalized moments which once more reinforces the "inert-atom bonded-atom" correspondece from a different theoretical view point, for the fact that Q is a quantum mechanical quantity. This correlation also suggests that a further scrutiny of the budding concept of "inert-atom bonded-atom" relationship by quantum mechanical techniques could prove fruitful.

The study of the binary gas collision mode bears out the fact that one could, to the benefit of the buffeting theory, use the generalized London potential in place of U in the Boltzmann factor in (4.6) or (3.14) and combine the kT factor with the buffeting formulations. This is important as it gives the generalized London potential and the buffeting field a direct temperature dependence through the kT factor. This will remedy the absence of kT in the buffeting model and enhance its flexibility.

The nature of the scale factors in the Rummens et al theories was elucidated and it was shown that the common element in their models, the Raynes model, and the Homer and Percival theory is their geometric factors.

In the following chapter the buffeting field expression is used for calculations of vdW nuclear screenings and heats of vaporization.

Chapter 5

Polyatomic Dispersion Field and van der Waals Nuclear Screening Constant

Introduction

The preliminary calculations of the heats of vaporization using the polyatomic potential function in Chapter 4 verified the underlying assumptions of the buffeting model.

The key expression in the derivation of this potential function was the polyatomic or buffeting mean-square field, a direct verification of which is possible by the calculation of the vdW screening constant. The passage from the mean-square field to nuclear screening is achieved by the operation of the ambiguous B parameter on the field; $\sigma_w = - B \langle E^2 \rangle$.

A preliminary analysis shows that the experimental vdW screenings may be calculated, with accuracies within the experimental errors, using the polyatomic field and a fixed value of B ^{1}H = .54, without the need for adjustable parameters or scale factors. This value of B for ^{1}H is in agreement with the quantum mechanical calculations and empirical findings.

At an ensuing stage this fixed value of B and experimental σ_w are used to find some realistic liquid state inter-molecular distances. These distances, used with the polyatomic potential function, calculate heats of vaporization for the systems which are in excellent agreement with the experimental values.

In fact in this chapter the calculations of σ_w and H_v are concurrent with one verifying the other and together substantiating the claim that the buffeting theory provides an authentic liquid state inter-molecular force function.

The combined use of the <u>field-potential</u> is then applied to adverse systems, which provides valuable information on the liquid state molecular structure and dynamics; in other words, a major use is found for the vdW site-sensitive screening effect.

The analysis of the screening constants for $C\underline{H}_2$ in pure $X(CH_2CH_3)_4$ systems by the polyatomic field leads, to the mechanism of their behaviour and encounters in the liquid state. It is shown that the separation of rotational and translational motions and the key assumption that the former motion is much faster than the latter is unrealistic for large systems. This, together with the fact that the q ratios of these systems exceed .43 -beyond which the F series diverges- renders the buffeting model inappropriate.

This limitation however is viewed as a source of information which could address the fundamental concept of the *additivity of the inter-molecular potential.*

The satisfactory accord between the experimental screenings and the calculated ones validifies the use of the polyatomic field for the cases where more than one solvent effect is present, namely the solvent magnetic anisotropy, the calculated values of which for some anisotropic solvents are found to be in agreement with the literature values.

The calculations of the B parameters for ^{19}F, ^{129}Xe, and ^{31}P provide a more subtle test for the polyatomic field expression and give respective values of 11 ± 1.6, 786 ± 1, and 120 ± 36.

The quantum mechanical predictions of the solvent dependence of B, although not observed for ^{1}H and ^{19}F, are salient for the B values of ^{31}P and ^{129}Xe in different solvents, possibly because of their very large σ_w values compared to those of ^{1}H and ^{19}F.

A simple criterion for the order of magnitude estimation of the B values for <u>any</u> nucleus, based on the B values of the inert atom nuclei, is also suggested.

Moreover it is shown that liquid state structural information such as the number of nearest neighbours and inter-molecular distances can be obtained from the polyatomic field-potential formulation and data on σ_w or H_v. The cases of liquid Hg, liquid Cl_2, liquid P_4, $SiCl_4$, CF_4, SiF_4, SF_6, and C_6H_{12} are used to exemplify this approach.

3.1. The Polyatomic Field and the vdW Screening Constant

In view of the fact that both cohesion energy and vdW nuclear screening are manifestations of inter-molecular forces, one would expect the buffeting model to work for the latter as it did for the former. The purpose of this chapter is to use (3.9) for the calculation of σ_w and throw light on the nature of the proportionality constant B between $\langle E^2 \rangle$ and σ_w.

5.1.1. Nuclear Screening Due to the Polyatomic Field

Expression (3.9) according to (2.11) produces a nuclear screening for the resonant nucleus i in the solute molecule that can be written as;

$$\sigma_P = - B \langle E^2 \rangle = - 2 B Z_L R^{-6} \sum X_j \langle m^2 \rangle_j F(i,j) \qquad (5.1)$$

where σ_P is the screening due to the Polyatomic field (5.1), and other symbols have their usual meanings.

Let us expand (5.1) for a specific molecule like $FH_2CCFHBr$ as was done for CH_4 in (4.8). We note that such a (solvent) molecule has four kinds of atoms but seven species $X_j = 7$, because the centre-of-mass to the atom distances d, for C's, F's and H's are different;

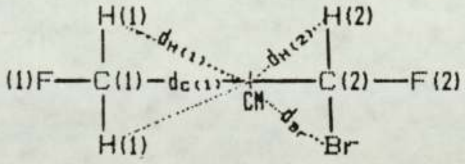

which result in different F values for the same atom. Therefore (5.1) may be expanded as;

$$\sigma_P = - 2Z_L B R^{-6} \{ \langle m^2 \rangle_C [F(C_1,i) + F(C_2,i)] + \langle m^2 \rangle_H [F(H_1,i) + F(H_2,i)] + \langle m^2 \rangle_F [F(F_1,i) + F(F_2,i)] + \langle m^2 \rangle_{Br} F(Br,i)\}$$

We see that the solute resonant nucleus 'i' contributes to the field by its location, d_i, in the $F(d_i,d_j,R)$ factor. The values of d can be calculated for each species by using the bond length-angle and the law of the lever. This is explained in Appendix 5 where a table provides all the d values needed in this work, that can be calculated with reasonable accuracy.

For $.43 > q > .36$ the best-fit polynomial (A4.3) is used in place of the analytical F series (3.7). For the moments, the corresponding inert-atom moments from table 3.4 should be used.

Equation (5.1) for R in A, $\langle m^2\rangle_{inert}$ in units of 10^{-36} erg cm^3 (that is, just the entries of table 3.4) and B in units of 10^{-12} ppm cm^3/erg (that is, just the value of .54, for example) give σ_F in ppm.

It is noteworthy that (5.1) differs from the Homer and Percival σ_{EI} by accounting for the field of <u>all</u> the constituent atoms of the solvent molecule rather than the peripheral ones. The contribution of the central atoms, $d \simeq 0$, affecting the third decimal places, is negligible in the calculation of the screening -but not in the calculation of the cohesion energies.

5.2. Polyatomic Screening Constant for Pure Compounds

As has been mentioned previously, the accurate calculation of molecular properties using polyatomic formulations entails the knowledge of accurate R values. The test of the generalized London potential (GLP) by the preliminary calculations of H_v was based on R_e values. It is instructive to repeat that procedure here for the test of (5.1).

In table 5.1 are given the results of such a procedure in which the empirical value of B = .54 found by Rummens[153] is tentatively used to convert field into screening. Uncertainties in the experimental values of σ_w are generally large as highlighted here and throughout tables in this chapter. A single entry for σ_w in these tables should not imply its accuracy, but rather the lack of further data; the reason for this is two-fold at least.

First, there are experimental difficulties especially in determining σ_a. Second, σ_w are not a direct data but results from processed data; it is processed in that, from the experimental gas-to-liquid screenings σ_m, σ_a, and σ_b are subtracted to obtain;

$\sigma_w = \sigma_m(\text{Expt.}) - \sigma_a(\text{Expt.}) - 2\pi/3(\text{Theo.})\chi_v(\text{Expt.})$

Therefore unlike solubility and to some extent H_v, σ_w data are not strictly suitable for a stringent test of a theory.

Nevetheless, from the study of the preliminary analysis of this table one can draw the following conclusions:

(1) The B value of .54 appears to be suitable for the preliminary calculations and compares well with the quantum mechanical values of .59 and .54 found respectively by Kromhout and Linder[138] for $CH_4...CH_4$ and Yonemoto[77] for $H_2...H_2$.

(2) The calculated and experimental screening constants of CMe_4 and C_6H_{12} can be matched for larger R values. The respective values of 6.3 and 6.34 A, intutively more realistic liquid state inter-molecular distances, give σ_r = .219, and σ_r = .201 ppm for the two systems. To find these screening values using the static B_o = .74 (see Chapter 2), R should be increased to 6.49 A for CMe_4, for example. One might ask what ensures the superiority of 6.3 over 6.49 A, and simultaneously that of B = .54 over .74? The confirmation can be found by comparing the cohesion

Table 5.1. Experimental[a] and Preliminary Calculated vdW Screening Constants for Pure systems (Z_L = 11)

Compound	CH_4	C_6H_{12}	$C(CH_3)_4$
R_B A (table 3.3)	4.17 (bp -164 °C)	6.20	6.21
$\langle E^2 \rangle$ Eq. 5.1[*]	.651	.457	.465
$-\sigma_P$ ppm (B = .54)	.351	.246	.250
$-\sigma_w$ ppm	.176[+] (-106.1 °C)	.203 (30 °C)	.228 (30 °C)
	.230[b] (-184 °C,mp)	.192 (30 °C)	.217 (30 °C)
		.143 (35 °C)	

a: The Expt. σ_w values given in this chapter are from Ref.[17] unless otherwise quoted.

b: Calculated by extrapolating the gaseous data $-.482\rho$ to liquid methane at its melting point with volume V = 33.6 cm^3/mole. Rummens[17,153] argues that such extrapolation calculates a value for σ_w which is about a factor of 1.65 too small. Multiplying .230 by this factor gives .379 in agreement with σ_P = .351. This extrapolation is discussed later in this chapter.

*: The fields and B parameter hereafter are given in units of 10^{12} erg cm^{-3} and 10^{-12} cm^3 erg^{-1} ppm respectively.

+: For liquid methane.

energies based on these R values with those found experimentally. Inclusion of more systems will substantiate such analysis. Therefore we first find the R values of the remainder of XMe_4 system by treating R in (5.1) as an adjustable parameter to match σ_P with σ_w;

Compound (pure)	$SiMe_4$		$GeMe_4$	$SnMe_4$		$PbMe_4$
$-\sigma_w$ ppm	.228	.205	.260	.297	.310	.358
$-\sigma_r$ ppm (5.1)	.226	.205	.260	.294	.313	.360
R (Cal.) A (5.1)	6.72	6.77	6.72	6.94	6.91	7.01

Exclusion of liquid methane from this list is justified by ambiguous σ_w data -one for liquid methane at $T \gg T_{bp}$ which may not allow the use of $Z_L = 11$, and the other one an estimation from gaseous data.

Instead R_L for methane is found from the more reliable H_v data as given in table 5.2, for which (5.1) calculates; $-\sigma_r$ (Liquid methane) = .276 ppm (B = .54).

Table (5.2) compares the calculated and experimental heats of vaporization for which (except for CH_4) the above R values are used.

Table 5.2. Calculated (by Eq. 3.25) and Experimental Cohesion energies H_v (Z_L = 1)*

compound	CH_4	C_6H_{12}	CMe_4	$SiMe_4$	$GeMe_4$	$SnMe_4$	$PbMe_4$
H_v(Expt.) KJ/mole	8.18	30.05	22.36	26.91	29.76	33.01	36.96
Ref.	[215]	[158]	[158]	[158]	[158]	[158]	[158]
H_v(Cal.) KJ/mole	8.0	29.89	22.45	25.12	30.03	33.70	40.75
R A	4.3	6.34	6.3	6.72	6.72	6.94	7.01

*: The use of $Z_L = 11$ is justified by the fact that $Z_s = 12$ for these compounds, see (3.13).

The fact that the polyatomic potential using R values deduced from σ_w and B = .54, calculates the cohesion energies in excellent agreement with the data, corroborates B ^1H = .54, and at the same time indicates the potential of this method in estimation of B for other nuclei. We now come to the third conclusion.

(3) The R values found here appear to match those of table 3.3 calculated from volumes on the basis of the random distribution of particles, that is (3.17);

$$R_{.17} = 2\ (.17\ V_M)^{1/3} \qquad (5.2)$$

where V_M is the molecular volume. In the remainder of this chapter more evidence is provided to support $R_{.17}$ as a reasonable estimate of the liquid state intermolecular distance from density.

The cases of large $X(CH_2CH_3)$ and solute-solvent systems of different sizes are examined in the following two sections.

5.2.1. Polyatomic Screening Constant for Tetraethyl Systems

According to the buffeting model the vdW nuclear screening of a peripheral atom must exceed that of the non-peripheral one because $d_{peri} > d_{non-peri}$ which results in $F_{peri} > F_{non-peri}$ and larger F values means larger screening by (5.1).

Table 5.3 contains the results of testing (5.1) on pure XEt_4 systems. As there is no R_B for the compounds, the R values are adjusted so that $\sigma_F(CH_3) \simeq \sigma_w(CH_3)$. These values of R are then used in (5.1) to calculate $\sigma_F(CH_2)$ for comparison with $\sigma_w(CH_2)$. The d values of the species are given in table (A5.1).

Table 5.3. Calculated (by Eq. 5.1) and Experimental $\sigma(CH_2)$ ppm, for Pure XEt_4 systems

Compound	$C(CH_2CH_3)_4$	$Si(CH_2CH_3)_4$			$Sn(CH_2CH_3)_4$	
$-\sigma_w(CH_3)$	.184	.145	.153	.197[a]	.184	.207
Tem. °C	38	38	35	30	30	35
$-\sigma_w(CH_2)$	.139	.109		.155[a]	.156	
Tem. °C	38	38		30	30	
$-\sigma_r(CH_3)$	.186	.146		.198	.186	.208
$-\sigma_r(CH_2)$	.092	.076		.093	.080	.086
R (Cal.) A (5.1)	7.7	8.23		8.06	8.48	8.42

a: Ref.[159]

The considerable disagreement in the experimental data for $SiEt_4$ is striking. It could not have been caused by the difference in the temperature of the measurement because the change in volume for this compound over 8 °C could hardly change the third decimal figure of any quantity with R^{-6} dependence;

Tem. °C	30	35	38
V cm^3/mole	190.4	191.3	191.8

We see that the calculated screenings for CH_2 are consistently smaller than the experimental values. The deliberate increase of $d_H(CH_2)$, which would increase its F factor, suggests itself as a possible remedy. This solution proves fruitless for two reasons. First, d_H of CH_2 cannot be increased far beyond the corresponding value of $d_H(CH_3)$ for $X(CH_3)_4$ systems, and second, any increase in d_H of CH_2 affects the calculated R and σ_r, resulting in an endless loop of alterations.

Alternatively, one can re-examine the inherent assumptions of the buffeting model when dealing with <u>large molecules</u>. Let us assume that, instead of the "on the spot" rotations of the molecules according to the buffeting model, the (peripheral atoms of) solvent molecule can momentarily penetrate the open structure of the large solute molecule and buffet the CH_2 group to an extent more than the mathematics of the model allows. As Rummens[17] puts it "... for $X(CH_2CH_3)_4$ in any of its possible conformations at least one of the CH_2 groups will be just as exposed as the CH_3 groups...".

If this is true one would expect the difference;

$\Delta = \sigma_w(CH_3) - \sigma_w(CH_2)$

to increase as the size of the peripheral buffeting atoms of the solvent increases, or as the size of the central atom X decreases, because in both cases the penetration is more hindered. The data supports this supposition as borne out below;

Experimental Δ values

Increase in the Size of the Peripheral atom of the solvent ---------------->

		$Sn(CH_3)_4$	C_6H_{12}	CCl_4	$SiBr_4$
Increase	CEt₄	.043	.045	.067	.075
in size	SiEt₄	.034	.038	.052	.053
of X ↓	SnEt₄	.027	.023	.043	.040

This effect is also observed for zig-zag-like molecules. For $Si(OCH_2CH_3)_4$ the difference between $\sigma_P(CH_2)$ = .077 and σ_w = .16 ppm is even larger because of its even more open structure. Therefore one is forced to the conclusion that the basic assumption of the separation of translational and rotational motions is invalid for large molecules, in which;

v(Trans.) > v(Rot.). This is because the moment of inertia $I = \Sigma m d^2$ in v(Rot.) $\propto (kT/I)^{1/2}$ is much larger than m in v(Trans.) $\propto (kT/m)^{1/2}$. Therefore the solvent can "translate" towards the solute and penetrate it while the latter is still in one of its rotational conformations.

This effect cannot be incorporated in the mathematics of the buffeting model at this stage without the introduction of some sort of factor which accounts for the extra buffeting. However, one cannot help thinking about an extreme situation in which a small solute can be envisaged to be buffeting all the constituent atoms of a large molecule independently.

The tentative acceptance of such a situation brings about far-reaching consequences for the buffeting theory. First, the concept of the intermolecular distance loses its meaning and attraction. The R distance, between a small solute and the atoms in the solvent, would be more like vdW distances almost always fixed -note the emergence of the Homer and Percival buffeting model from the argument. Even the solvent d values lose their importance for the fact that the atoms or groups in the solvent are fixed to it and appear static during the interaction with the fast-rotating small solute.

This idea is tested for the solubility of small solute (CO_2) in a number of large alcohols in the following chapter with interesting results which stimulate further investigation.

At this point a serious criticism of one aspect of the Homer and Percival buffeting theory should be mentioned, but which may fortunately be justified in the light of the foregoing argument.

It will be recalled that the distance r_v in their buffeting field expression (4.1) is defined as the sum of the vdW radii of the peripheral interacting atoms. This, of course is correct for the outer atoms, but for the interaction of the peripheral atom of the solvent and CH_2 of the solute the distance is larger by the amount by which the CH_2 group is away from the surface of the solute molecule.

Homer and Percival in their successful treatment of the CH_2 shifts of $SiEt_4$, and $Si(OEt)_4$ have used the same $2\ r_v$ of the outer situation, which results in larger calculated values. In other words the assumption of the full penetration of the buffeting atom into the solute structure is implicit in their treatment so that $2\ r_v$ of the outer situation is maintained.

Note that the calculated R values from screenings in table 5.3 disagree with $R_{.17}$ values in table 3.3. For $R_{.17}$ values the ratio $q = d_H(CH_3)/R_{.17}$ exceeds .43 for $SiEt_4$ and $SnEt_4$ rendering even the best-fit F expression inefficient. Comparison between the available experimental and calculated heats of vaporization for $SiEt_4$ shows that the R values of table 5.3 are too large;

H_v(Expt.) = 41.35[158]; H_v(Cal. R = 8.23) = 22.49; H_v(Cal. R = 8.06) = 29.32 KJ/mole

The experimental heat of vaporization can be calculated for R = 7.85 A, a value still larger than $R_{.17}$ = 7.55 given in table 3.3.

5.3. Polyatomic field screenings of small solutes

In the treatment of the binary mixtures the question of the cavity size arises. Correlational analyses of the RF model of σ_w in Chapter 2 clearly supported the solvent cavity size concept, which is tested in this section for the polyatomic model of σ_w.

It is instructive to test the solvent cavity concept on mixtures of some similar size molecules first. Table 5.4 gives the results of such test in which the solvent cavity idea; $R = R_v$ if $R_v > R_u$, is used.

Table 5.4. Expt. and Calculated (5.1) vdW Screenings (ppm) based on the Solvent Cavity Size(Z_L = 11)

Solvent----->	CCl_4 (R = 5.9)		C_6H_{12} (R = 6.34)		CMe_4 (R = 6.3)		$SiMe_4$ (R = 6.72)	
Solute	σ_w	σ_r	σ_w	σ_r	σ_w	σ_r	σ_w	σ_r
C_6H_6	.394	.394	.257	.310	.268	.291	.243	.220
(R = 6.18)	.420[a]		.203					
	.443							
C_6H_{12}	.267	.278	.202[a]	.200	.187	.223	.182	.175
(R = 6.34)	.265		.192[a]					
			.143					
$C(CH_3)_4$	.290	.273	.230	.233	.222	.219	.185	.168
(R = 6.3)	.307		.220		.217		.212	
	.320		.187					
$Si(CH_3)_4$	.267	.270	.233	.239	.240	.216	.228	.230
(R = 6.72)	.299		.270		.255		.205	
	.322		.282					
	.360							

a: Ref.[27]

The R values of CCl_4 and C_6H_6 given in this table are from tables 3.3 and 5.9 respectively.

The good agreement between the experimental and calculated values supports the solvent cavity size and $B\ ^1H = .54$. The solute cavity size for C_6H_6 in $SiMe_4$ gives $-\sigma_F = .387$ ppm, for example.

Let us now test the solvent cavity size for a small solute like CH_4 in a large solvent like CCl_4 for which R = 5.9 A. Expression (5.1) gives $-\sigma_F = .16$ ppm, which compares poorly with the observed values of $-.473$ and $-.443$ ppm.

Clearly the concept of a centre-retained solute for a small mass like methane with a critical temperature very much lower than the temperature of measurement ($\simeq$ 30 °C) is unrealistic. However on the grounds of its relatively fast movements; $v(\text{Trans. } CH_4) \simeq 3\ v(\text{Trans. } CCl_4)$, a methane molecule inside the solvent cavity would have a high collision rate and appear to be in the vicinity of the surrounding solvent molecules for most of the time. Fig. 5.1 illustrates this situation.

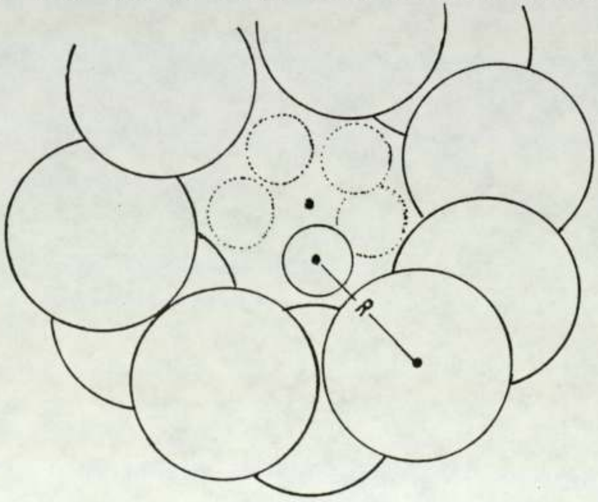

Fig. 5.1. Solvent cavity concept for small gaseous solute with apparent inter-molecular distance $R \simeq (R_u + R_v)/2$ and $Z_L = Z_L(\text{solvent})$.

The inter-molecular distance is now more like;

$$R \simeq (R_u + R_v)/2 \tag{5.3}$$

than the solvent size $(R_v + R_v)/2$. Note that the size of the cavity, and therefore Z_L, are still governed by the solvent. Table 5.5 compares the calculated and experimental screening constants and heats of vaporization for systems of table 2.10.

Table 5.5. Analysis of H_v of Pure Solvents and Screenings of CH_4 in the Solvents ($B = .54$, $Z_L = 11$)

Solvent	$R_{.17}$ A (5.2)*	H_v(Expt.) KJ/mole	Ref.	H_v(Cal.) KJ/mole (5.25)	$-\sigma_w$ ppm [27]	$-\sigma_P$ ppm (5.1)
CH_2I_2	5.68	-		79.04	.769, .767^a	.765
$CHBr_3$	5.83	40.43	158	48.39	.652^a, .646	.641
CBr_4	6.32	45.02	158	45.62	.594	.592
Br_2	4.82	29.45	215	27.92	.556	.502
CH_3I	5.22	28.16	158,215	b	.505, .547^a	.562
$CBrCl_3$	6.08	-		34.81	.533, .542^a	.541
CCl_4	5.9	34.52	158	34.36	.443, .472^c	.540
CH_3Br	5.04	24.77	158	b	.355, .445^a	.486
$CHCl_3$	5.67	29.71	215	27.33	.407, .420^a	.458
CH_2Cl_2	5.27	31.65	158	33.07	.398, .407^a	.527
$SiCl_4$	6.40	28.49	215,255	28.70	.301, .347^c	.481

*: Calculated (except for CCl_4) using molar volumes of table 2.3 in (5.2).

a: Ref.[157]; b: The q ratios for hydrogens exceed .43 (see Appendix 5 for d_H).

c: Ref.[17].

The considerable agreement between the calculated values and the data particularly in view of the fact that no parameter is treated as adjustable corroborates, the value of .54 for ^1H, the inert-atom approximation, $R_{.17}$ (3.17) or (5.2) for nearest neighbour distance, (5.3) for binary mixture of small solutes.

Note that these results are obtained by using the densities and bond length-angle of the systems <u>only</u>.

The rather poor agreement between σ_w and σ_P for $SiCl_4$ has initiated the investigation of section 5.6.1 into the liquid structure of this solvent.

Table 5.6 gives the results of similar analysis for three more gaseous solutes for two of which σ_w data is available.

Table 5.6. Analysis of vdW Screening Constant and Cohesion Energy of Pure Liquids (Z_L = 11*, B = .54)

	H_2	Ref.	C_2H_6	Ref.	C_2H_4	Ref.
Mp °C	-259.2	158	-88.63	158	-103.71	158
Vol. Cm^3/mole	26.15	69	52.57	158	49.56	255
At Tem. °C	-259.2		-108		-102	
$R_{.17}$ A (5.2)	3.89		4.914		4.819	
H_v(Expt.)KJ/mole	.903	69,255	14.7	255	14.44	158
	1.05	158	15.63	158	13.53	255
H_v(Cal.)KJ/mole	1.00		15.66		13.44	
$-\sigma_w$ ppm	-		.257	153	.291	305
			.279	305		
$-\sigma_P$ ppm (5.1)	.092		.324		.290	

*: The Crystalline structures of fcc, hexagonal[306], and orthorhombic[306] all with Z_B = 12, for H_2, C_2H_6, and C_2H_4 respectively justify Z_L = 11 according to (3.13). Note that $R_{.17}$ for H_2 compares well with R_B in table (3.3)

The agreement between the data and calculations is impressive in view of the fact that again no parameter is adjusted to obtain the results. Note that the magnetic anisotropy effect for C_2H_4 is assumed to be zero.

The screening constant of liquid hydrogen in the form of; $\sigma_m = .092 \times V = .092 \times 26.15 = 2.4$ ppm cm^3/mole may be crudely compared with the available gaseous value of 4.6 ± 2.

The <u>liquid</u> state dependence of σ_w on density for C_2H_6 and C_2H_4 is given by Gordon and Dailey[305] as $.488\rho$ and $.515\rho$ ppm respectively, from which the data in table 5.6 are found by using the volumes at the quoted temperatures.

Rummens[153] has studied C_2H_6 in the gas and liquid states down to −55.6 °C at $\rho = .502$ gr/cm^3. He argues that the liquid state shifts cannot be found by direct extrapolation from the corresponding gaseous state. We have checked this by using his results on C_2H_6, which shows that the shift at −55.6 °C for ($\rho = .233$ gr/cm^3), for example, may be found from the gaseous shift at 35 °C ($\rho = .233$ gr/cm^3) by extrapolation in good agreement with his experimental value.

Accordingly from his data at −55.6 °C we find −.257 ppm for the screening constant of C_2H_6 at −108 °C ($\rho = .572$) which agrees with the Gordon and Dailey result of .279 ppm.

The gas-to-liquid screening of liquid H_2 cannot be found from the available gaseous data of Dayan and Widenlocher[307] because they have not quoted the densities.

The results of the analysis of the screening constant of these gases in two available solvents are given in table 5.7. The $R_{.17}$ values found in table 5.6 are used in (5.3) to obtain σ_F values.

Table 5.7. Analysis of the Screening Constants of H_2 , C_2H_6, and C_2H_4 ($B = .54$, $Z_L = 11$)

	Solvent			
	CCl_4 ($R = 5.9$)		C_6H_{12} ($R = 6.34$)	
Solute	$-\sigma_m$ ppm	$-\sigma_F$ (5.2)	$-\sigma_m$ ppm	$-\sigma_F$ (5.2)
H_2	.485	.474	.285, .300	.391
C_2H_6	.305, .310	.470	.195, .210	.413
C_2H_4	.345, .370	.500	.225, .240	.439

Note the correct trend but the rather poor agreement between the existing data and calculated values, particularly for cyclohexane. The polyatomic field appears to predict consistantly large values for small solutes in cyclohexane. For methane in this solvent it gives $-.475$ compared with the data of $-.225$, $-.285$[17] and $-.270$[27] ppm. This anomaly is not observed for similar size systems of table 5.4.

The possibility of non-zero neighbour anisotropy effect for C_6H_{12} as a cause of the anomaly is examined in the following section.

In spite of the stated anomalies the evidence provided so far authenticates and proposes the buffeting formulas for more subtle uses like the study of the magnetic anisotropy, the B parameter of nuclei other than ^1H, and molecular structure in the liquid state.

5.4. Neighbour Anisotropy Screening, σ_a

The historical introduction to Chapter 2 showed that the anomaly of aromatic solvents in the experimental verification of the theoretical shape factor $2\pi/3$, was attributed to the magnetic anisotropy of the solvent by Bothner-By and Glick.

The expression for the screening of the medium (2.8) upon σ_b correction and re-arrangement becomes;

$$\sigma_a = \sigma(\text{Expt.}) - \sigma_w \qquad (5.4)$$

In other words σ_a comes to existence if the experimental screening of the medium after correction for the bulk susceptibility has a residue which either is too small to be a genuine σ_w or is a positive value.

Consider the gas-to-liquid screening of methane in $C(NO_2)_4$ and C_6H_6 , for example. In the former, the residue shift is too small -.053 ppm to be a genuine σ_w, and in the latter it is +.124 ppm, a positive value or up-field.

The neighbour anisptropy effect arises as a result of the secondary magnetic field produced by the solvent at the site of the resonant nuclei in the solute. The secondary magnetic field results from the interaction of the external field and the solvent.

It is shown by Buckingham et al[22] that this secondary field or its screening constant is proportional to the anisotropy in the diamagnetic susceptibility $\Delta\chi = \chi_\parallel - \chi_\perp$ of the solvent or the groups belonging to the solvent.

It is also the orthodox view that[22,308-314] a σ_a shift is positive (high-field) for disk-shaped molecules like C_6H_6 and negative (low-field) for rod-shaped ones like CS_2 or CN group of CH_3CN. The anisotropy screening may be estimated from (5.4) assuming that $\sigma_w \simeq \sigma_r$;

$$\sigma_a \simeq \sigma(\text{Expt.}) - \sigma_r \qquad (5.5)$$

The results of such estimations are given in table 5.8 for some anisotropic solvents.

Table 5.8. Neighbour Anisotropy Screenings (ppm) for Anisotropic Solvents (B = .54, Z_L = 11)

Solvent--->	C_6H_6			$C(NO_2)_4$			CS_2			CH_3CN		
Solute	σ(Expt.) [27]	σ_r (5.1)	σ_a (5.5)	σ(Expt.) [27]	σ_r (5.1)	σ_a (5.5)	σ(Expt.) [163]	σ_r (5.1)	σ_a (5.5)	σ(Expt.) [163]	σ_r (5.1)	σ_a (5.5)
CH_4	.124	-.432	.556	-.053	-.580	.530	-.583	-.353	-.229	-.416	-.317	-.099
C_6H_6	.235	-.379	.614	-.120	-.447	.327	-	-.260	-	-.452	-.394	-.058
C_6H_{12}	.272	-.225	.497	.043	-.298	.341	-.398^a	-.185	-.213	-.285	-.241	-.044
$C(CH_3)_4$	.213	-.218	.431	.028	-.292	.264	-.426	-.181	-.245	-.317	-.234	-.083
$Si(CH_3)_4$	.151	-.229	.380	.035	-.290	.255	-.520	-.178	-.342	-.343	-.237	-.106
Mean σ_a		.495			.343				-.257			-.078

a: Ref.[27].

Table 5.9. Calculated R values for Anisotropic Solvents using Heats of Vaporization (Z_L = 11*)

	CS_2	Ref.	CH_3CN	Ref.	C_6H_6	Ref.	$C(NO_2)_4$	Ref.
R (Cal.) A	5.86		4.80		6.18		6.57	
H_v (Expt.)	26.74	215,315	31.35	255,315	30.79	255,315	41.16	158
	28.37	158			30.79	69		
					34.05	158		
H_v(Cal.)	26.64		31.28		30.53		41.53	

*: This value for CH_3CN is based on the Kitaigorodsky observation that organic molecules have Z_B = 12 (see Chapter 3). Appendix 6 gives the details of the calculations of H_v.

The R values which, when used in (3.25) give the right cohesion energies for the solvents, ensure the reliability of caculated σ_F and σ_m. These are found in table 5.9 and used in table 5.8. This results in calculated screenings consistent with the cohesion energies.

The R values of CH_3CN and $C(NO_2)_4$ compare well with respective $R_{.17}$ values of 4.9 and 6.48 A found from their volumes at 20 °C. The R value of 6.57 A for $C(NO_2)_4$ based on its H_v(Expt.) is less attractive because it exceeds $R_{.17}$ = 6.48 A at 20 °C. However such a difference in R's has little effect on σ_F and H_v. For example, one finds σ_F = −.543 ppm for CH_4 in this solvent and H_v(Cal.) = 46.78 KJ/mole for pure solvent when $R_{.17}$ = 6.48 is used.

The values of R for disk-shaped benzene and rod-shaped CS_2 are troublesome. These values do not comply with $R_{.17}$ formula (5.2) as was discussed in Chapter 3. It appears that for non-spherical molecules R is best found from the mean (or the geometric mean) of R_v values given in table 3.3. The geometric means are 6.18 and 5.9 A respectively, which compare very well with those of table 5.9.

Let us now return to the discussion of the results of table 5.8. First, the values of σ_m have the orthodox signs, positive for benzene and $C(NO_2)_4$, and negative for CS_2 and CH_3CN. Second, the proportionality of σ_m with $\Delta\chi$ is borne out below. Third, Rummens[27] finds no evidence for a significant value of σ_m for CS_2 based on his site-factor RF model of σ_w, although he finds a mean value of −.14 ppm for CH_3CN. His findings do not show the proportionality of σ_a with $\Delta\chi$;

Molecule	C_6H_6	CS_2	CH_3CN	CH_3I	CH_3Br	CH_3Cl
$-\Delta\chi = \chi_\parallel - \chi_\perp$ erg $gauss^{-2} \times 10^{27}$	9.91[a]	5.00[b]	2.24[c]	1.82[c]	1.41[c]	1.32[c]
Mean σ_a	.495	-.257	-.078			

a: Ref.[316]; b: Ref.[22]; c: Ref.[317]

Fourth, the large permanent dipole of CH_3CN; $\mu = 3.44$ D[318]), according to (2.24), results in the dipolar screening of; $\sigma_E = .094\ \sigma_w$ for this solvent. If this value is subtracted from the anisotropy screenings the average σ_a reduces to the smaller value of .o51 ppm.

Fifth, the vdW screenings of $C(NO_2)_4$, which because of its tetrahedral structure is expected to have no anisotropy effect, are too small to be genuine σ_w. This molecule, as has been mentioned in detail by Raynes and Raza[163], on the grounds of its four disk-shaped NO_2 groups, gives rise to substantial anisotropy shifts. The average value of .345 ppm compares well with that of Percival[160], .35 ppm, found on the basis of the Homer and Percival buffeting theory. It compares poorly with Rummens'[27] average value of .239 ppm.
The average σ_a for benzene is in agreement with those of Homer and Redhead[319]; .407, Rummens[27]; .55, and Becconsall[314] .50 ppm.

Concerning the shifts of gaseous solutes in cyclohexane, the evidence in table 5.7 suggest a sizable $\sigma_a \simeq .20$ ppm for this solvent. This however can be supported neither by the evidence in table 5.4 nor by its presumeably vanishing small $\Delta\chi$.

5.5. Empirical Determination of B

In this section the buffeting model is used for the study of the B parameters of F, P, and Xe.

5.5.1. Determination of ^{19}F B parameter

The lack of knowledge about ^{19}F B has forced workers to empirical determination of this parameter. The values so obtained show outstanding sensitivity to the solute-solvent system. Empirical values as small as 10 and as nonsensically large as 782 have been found for ^{19}F B, depending on the model of $\langle E^2 \rangle$. Here the same method is adopted in which (5.1) and the experimental screenings would be used to find B.

A preliminary calculation of the heat of vaporization for CF_4, a conventional solute of ^{19}F shift studies, showed that the value of $R_{.17}$ = 4.662 A, found from its molar volume at the mp, gave H_v(Cal.) = 9.15, short of the experimental value by 3.5 KJ/mole. Another conventional solute, SiF_4, showed the same pattern when its R_B(Expt.) = 4.68 A was used in (3.25).

As R cannot be decreased beyond the solid state values to increase the calculated values of H_v, these shortcomings were viewed as the reflection of some sort of structural peculiarities of the compounds.

In fact the special bonding character of them is the root of the variances. Pauling[318] has shown that CF_4, for example, is best described as a resonance hybrid of 12 structures of type (a), four of type (b) and one of the traditional covalent type (c) which was used in the calculation of H_v by (3.25);

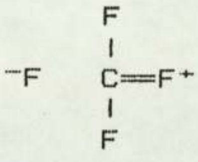

(a)

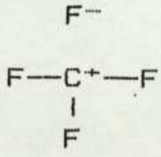

(b)

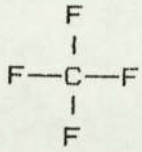

(c)

Recently Maclagan[320] has discussed the bonding for SF_6 and has concluded that ionic Lewis structures such as (d) should have larger weights than type (e);

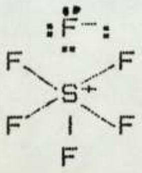

(d)

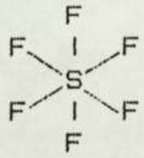

(e)

New developments of the Pauling "3-electron bond" theory shows that a more suitable representation of the ionic structures is provided by what is called "4-electron 3-centre bonding". For SF_6 Harcourt[262] gives the following forms where the "4-electron 3-centre bonding" is in resonance with other locations;

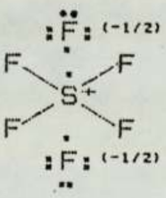

(f)

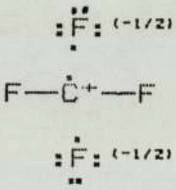

(g)

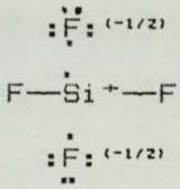

(h)

The new representation is also adopted for CF_4 and SiF_4 in (g) and (h).

The existence of ionic character in molecules has a bearing on the buffeting model, as was clearly shown in Chapter 3 for the estimated moments $\langle m^2 \rangle_E$.

The buffeting formulas (3.25) and (5.1), via $\langle m^2 \rangle_E$, are capable of differentiating between the covalent and ionic types.

One notes that the ionic type, by analogy with inorganic ionic compounds, should have enhanced inter-molecular forces and therefore larger cohesion energies.

By accounting for the ionic structure (see Appendix 6) the calculated heat of vaporization for CF_4, for example, increases to 11.6 (Exp. = 12.6) KJ/mole with the difference of;
11.6 - 9.15 = 2.45 KJ/mole being due to the ionic character.

Table 5.10 gives the R values of some fluorine solutes found from their volumes at the quoted temperatures by (5.2) and by (3.25) using the experimental H_v values. The agreement between them is remarkable bearing in mind that for disk-shaped C_6F_6 realistic R cannot be found from (5.2), as was mentioned previously. For SF_6, R = 5.15 A is a better inter-molecular distance for the liquid state because $R_{.17}$ = 5.06 A is calculated from the volume at -91 °C, well below its melting point.

Ionic structures equivalent to those of (f) to (h) are also assigned to C_6F_6, and C_4F_8 as; $C_6^+F_5F^-$ and $C_4^+F_7F^-$ because there is no reason to believe that they should not have ionic character.

Table 5.11 contains the results of the analysis of fluorine screening constants for both polar and non-polar solutes and solvents. The solute CF_2Cl_2 (mp -158 °C) is also included simply by using its $R_{.17}$ = 5.38 A from V = 69.1 cm_3/mole at -115°C. Many more solutes including CF_2Br_2, CF_2ClBr, CF_3Cl CF_3CCCF_3, FClCCFCl from the work of Abraham et al[162] could have been analysed if the molar volumes were available.

Table 5.10. Calculated R values from molar volumes (5.2) and Cohesion Energies (Z_L = 11)*

Compound	Mp °C	V (At °C) cm^3/mole	Ref.	$R_{.17}$ (5.2)	R (Cal.) A (3.25)	H_v(Cal.) (3.25)	H_v(Expt.) KJ/mole	Ref.
CF_4	-184	44.89 (-184)	158	4.66	4.66	11.60	12.6	158,215
SiF_4	-90	48.0 (-98)	247	4.77	4.75	18.45	18.6	a
SF_6	-51	57.3 (-91)	247	5.06	5.14	17.77	17.08	255
c-C_4F_8	-38^c	116.0 (0)	158	6.39	6.42^b	23.79	23.32	255
C_6F_6	3.7	115.8 (25)	214	6.39	6.58	31.42	31.64	255
$CFCl_3$	-110^d	91.94 (17)	225	5.92	5.76	26.26	26.85	158

*: See section 5.6.2. on the Z_L for SiF_4 and SF_6.

a: It is generally true to write $H_v \simeq H_m - H_f$ which for SiF_4 gives $H_v \simeq 26.48 - 9.498 = 16.98$. The same expression gives $H_v = 23.85 - 5.02 = 18.83$ (data from Ref.[215]) for SF_6 in agreement with the experimental values. The experimental value of 18.6 for SiF_4 is from an unidentified Ref.

b: For $R_{.17} = 6.39$ Eq. (3.25) gives $H_v = 25.32$ KJ/mole still in considerable agreement with the experimental value. c: Bp = -4 °C; d: Bp = 23.7 °C.

The rather unorthodox ^{19}F B values found in table 5.11, being lower than what is normally suggested, are interesting in that they are independent of the solvents and also show small variations over the range of the solutes considered.

The variations in B values for different solutes however appear to be genuine. Petrakis and Bernstein[241] argue that in the series CF_4, SF_6, and SiF_4, there is an increasing double bond character. In other words the increase in the electropositivity of the central atom from C to Si guarantees the increased enrichment or "swelling" of the fluorine bond with electrons. This increased ionic character means larger shielding of F nuclei which in turn necessitates a larger B value.

Table 5.11. Calculated ^{19}F B parameter from (5.2) and σ_w(Expt.) of tables 2.7 and 2.8

		Solvent					
Solute		CCl_4	$SiCl_4$	$CFCl_3$ [162]	C_6H_{12}	$SnMe_4$	Mean B
CF_4	$\langle E^2\rangle$	.906	.792	.816	.797	.812	
	B	8.38	8.64	7.50	7.45	8.41	8.07 ± .5
SiF_4	$\langle E^2\rangle$	1.019	.884		.890	.899	
	B	10.93	11.42	*	*	11.17	11.17 ± .2
SF_6	$\langle E^2\rangle$	.751	.660		.661	.671	
	B	10.60	10.64	*	*	10.50	10.58 ± .1
$CFCl_3$	$\langle E^2\rangle$	.484		.432	.429		
	B	12.60	*	11.85	11.91	*	12.11 ± .3
CF_2Cl_2	$\langle E^2\rangle$	.536		.478	.475		
	B	11.69	*	11.00	10.77	*	11.15 ± .4
c-C_4F_8	$\langle E^2\rangle$	.614		.550	.549		
	B	11.29	*	10.53	10.00	*	10.60 ± .6
C_6F_6	$\langle E^2\rangle$	.660	.583	.592	.623	.520	
	B	13.94	14.50	12.96	12.22	15.17	13.7 ± 1.2

Overall Mean B = 11.0 ± 1.6

*: No σ_w available.

Likewise, judging from the large B value of C_6F_6, the fluorine bond appears to be "glutted" by electrons from the electron-rich ring. Overall, these conclusions suggest that one can relate the B parameter to the ionic character of the bond as shown in Fig. 5.2.

Decrease in the ionic character of bond.

$\dashrightarrow$

Species $C_6F_6 > CFCl_3 > SiF_4 \approx CF_2Cl_2 > SF_6 \approx C_4F_8 > CF_4$

B $13 > 12 > 11 > 10 > 8$

$\dashrightarrow$

Decrease in the values of B.

Fig. 5.2. Ionic character of bond and the B value.

Note the consistency in the order of the B values and the ionic character. For methane derivatives it follows the natural direction of $CFCl_3 > CF_2Cl_2 > CF_4$ because as the number of F atoms increases the charge density per atom decreases. Judicious use of order relationships such as this help reduce the error in predicting σ_w of ^{19}F compounds by finding a suitable B value rather than indiscriminate use of the overall average of 11 ± 1.6. For example, in the case of CF_2Br_2, Fig 5.2 and the fact that 2Br provide more electrons for F than 2Cl, suggests the value of B $\simeq$ 12.

Note that the solvent cavity size for C_6F_6 in $SnMe_4$ has caused the large B value of 15.17, otherwise, using (5.3) B equals 10.3.

The average value of 11 in itself merits some discussion. If the concept of crude proportionality of B with the electron

charge density is grafted onto the concept of the correspondence of inert atoms with atoms in bond, a criterion may be set for deciding the value of B for different nuclei as follows:
The B value of nucleus falls somewhere between the B values of its corresponding inert gas nucleus and that of the inert nucleus of the next row in periodic table. For ^{19}F, for example, the B value accordingly has to be larger than that of Ne and smaller than the B value of Ar.

This criterion is based on the fact that fluorine in the bond appears to have a larger polarizability than Ne, and therefore is more shielded. The fact that the polarizability of fluorine in bond is larger than that of Ne is shown below;

Species	Ne	F—X	F^-
α $Å^3$	.395	.38*	.985[321]

*: This the polarizability contribution of bonded F.

Fig. 5.3 summarizes this criterion.

Species	He	[H]	Ne	[C, N, O, F]	Ar	[Si, P, S, Cl]	Kr	[Ge, As, Se, Br]	Xe
B_o	.075*		5.6		41.3		124.7		337.3
B	.17		4.1		?		252		914

$$.17 < \text{H B} < 4.1\ (5.6) < \text{(C, N, O, F) B} < ?(41.3) < \text{(Si, P, S, Cl) B} < 252(124) < \text{(Ge, As, Se, Br) B} < 914(337)$$

Fig. 5.3. A Criterion for the order of magnitude estimation of B for different Nuclei.

*: This value of Jameson et al is not reliable (see Rummens[17]).

The B (dynamic) values are from Kromhout and Linder (see Chapter 2).

The theoretical and empirical B values for H and F follow the order of Fig. 5.3. Some of the Mohanty and Bernstein[246] empirical values of B = 262 ($CF_4...CF_4$) and 782 ($SF_6...SF_6$) for example, found from gas phase studies with the inclusion of repulsion in the inter-molecular potential appear nonsensical and out of place.

This, together with the fact that any repulsion term for the poyatomic potential-field formulation must contain empirical parameters, which cripples the practicality of the model, justifies the exclusion of a repulsion-type contribution from this attractive model.

5.5.2. Determination of ^{31}P B parameter

^{31}P NMR has been increasingly popular because of its biochemical applications. There is very little information on ^{31}P solvent effects and virtually none on its B value[17].

The ^{31}P NMR solvent effects are very large, about 100 times larger than for protons and about five times larger than for ^{19}F, therefore new phenomena may be observable in the analysis of its data.

For the analysis of the screening data of phosphorus given in table 2.9, Z_B and R must be known.

Early studies on white phosphorus at −35 °C report a cubic structure with a = 7.17 A[322]. The same structure is reported in the 'Handbook of X-ray Analysis' by Mirkin[323], with a = 7.18 A. For a cubic unit cell of this size, one finds;

R_B = 5.0 A. However later studies on a single crystal[324-326] categorically reported a bcc lattice with a = 18.51 A.

The x-ray diffraction on liquid white phosphorus at 48 °C by Thomas and Gingrich[327] confirms the cubic structure. Their radial distribution curve shows three peaks at distances 2.25, ~ 3.9, and ~ 5.9 A from a particular phosphorus atom, with areas equivalent to 3, ~ 8, and ~ 32 phosphorus atoms.

The first three nearest neighbour atoms are consistent with the P_4 molecular structure of white phosphorus. The second eight nearest neighbour atoms, have to be viewed in the light of the fact that x-ray diffraction takes place in $t < 10^{-15}$ s[238] during which time no translational or rotational motion takes place. This suggests that the second radial distribution peak represents 8 nearest P atoms belonging to 8 molecules, namely $Z_L \simeq 8$. This is in agreement with the cubic Z_B = 8 and (3.13).

To ease the calculation of the nearest neighbour distance, R, that is the centre-of-mass of a P_4 to the corresponding centres in the neighbouring molecules, from P...P distance of ~ 3.9 A the P_4 is depicted as a circle in Fig. 5.4.

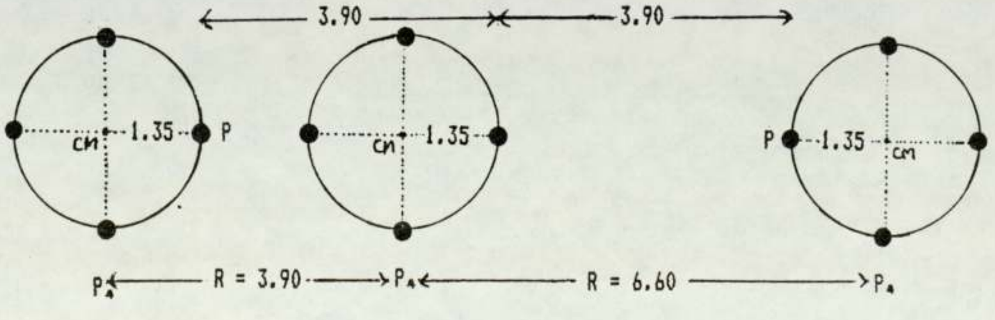

$\overline{R}$ = (3.90 + 6.60)/2 = 5.25 A

Fig. 5.4. An x-ray 'snapshot' of the nearest neighbours distance in liquid P_4.

The average value of R = (6.6 + 3.9)/2 = 5.25 A compares well with $R_{.17}$ = 5.35 from the volume at 20 °C. Note that 1.35 A is the d_P value given in Appendix 5. Also note that the observed 32 P atoms of the third peak can be explained if some molecules of beyond the second molecular shell can momentarily join the second shell.

This R value is used in table 5.12 for the calculation of H_v. The agreement between the data and the calculated value is impressive.

Table 5.12. Calculated and Experimental cohesion energy for white phosphorus (Z_L = 8)

V cm³/mole		$R_{.17}$ A	R_L A	H_v(Expt.)	KJ/mole	H_v(Cal.)
At 20 °C	Ref.	(5.2)	(Fig. 5.3)		Ref.	(3.25)
67.77	255	5.35	5.25	52.36	158,215	51.95
				52.67	328	

The usual value of Z_L = 11 and $R_{.17}$ in (3.25) would give H_v = 62 KJ/mole, about 10 KJ/mole larger than the experimental value. This signifies the sensitivity of the polyatomic formulas to the liquid state structure (see sec. 5.6.2).

In the absence of x-ray data on liquid P_4 the over-estimated H_v value could have been used to find a more realistic Z_L and via that surmise, on the liquid and solid state structures of P_4.

The buffeting fields and the calculated B values for P_4 in five solvents are given in table 5.13. For all the solvents except CS_2, because of its small size compared to P_4, the solvent cavity idea is used. The R values for the solvents are those previously given in this chapter.

Table 5.13. Empirical B values of ^{31}P (Z_L = 8, R = 5.25 A, $\emptyset_w$ data from table 2.9)

Solvent	$\langle E^2 \rangle$ (5.1)	B	B ($I_u + I_v$)	$I_u/(I_u + Iv)$
P_4	.479	187	2625	.50
C_6H_6	.236	127	2062	.43
CS_2	.386	104	1790	.41
C_6H_{12}	.238	98	1658	.41
CCl_4	.368	84	1549	.38

B = 120 ± 36 CC = .93

One notes the sensitivity of the B parameter to the solvent. Mohanty and Bernstein[246] also observed such a prominent solvent-dependence behaviour for their ^{19}F B values.

The Kromhout and Linder theory predicts the solvent-dependence of the B parameter as;

$B = c\ (3\ I_u + 2\ I_v)/(I_u + I_v)^2$

where c is a constant for a given solute and I_u and I_v are the ionization potentials of the sol<u>u</u>te and the sol<u>v</u>ent respectively.

Mohanty and Bernstein, by re-arranging this expression as;

$B\ (I_u + I_v) = c + (1/2)c\ I_u/(I_u + I_v)$

made an attempt to find the linear relationship that should exist between $B\ (I_u + I_v)$ and $I_u/(I_u + I_v)$. They found no simple linear relationship.

Table 5.13 shows that a rather good linear relationship exists between the values of the last two columns. Such solvent dependence behaviour of B is probably evident for phosphorus because of its very large screenings, which magnify the effect. The average B value of 120 ± 36 and the individual B values are in accord with the inert-atom-B value criterion shown in Fig. 5.3.

The B value of P_4/P_4 system however is larger than that of Jameson et al for Kr, signifying that the dynamic values of Kromhout and Linder are probably more realistic. This is checked for Xe in the following section.

5.5.3. Determination of ^{129}Xe B

In table 5.14 are given the screening data for ^{129}Xe in solid and liquid states in ppm cm^3/mole which are converted to ppm by dividing them by the solvent's molar volume. For solid Xe, $Z_s = 12$ and for the liquid $Z_L = 11$ are used.

The calculated B values are akin to the Kromhout and Linder values and in reasonable agreement with the empirical value of 837 foud by Jameson et al in contrast to their theoretical static value of 337. The B value found here for ^{129}Xe is, as one would expect, fixed, because the solvent is constant.

From gas phase studies Jameson et al have found empirical solvent dependent B values for ^{129}Xe. In fact we extrapolated their gas phase data to liquid phase by the crude method of dividing them by the liquid state volumes of the solvents and found distinct solvent dependent B values. A correlational analysis similar to that of P_4 in table 5.13 shows a good correlation coefficient of .98 fo ^{129}Xe.

Table 5.14. Empirical ^{129}Xe B value

Solvent ------->	Solid Xe	Liquid Xe
	$Z_S = 12$	$Z_L = 11$
V cm^3/mole	37.09*	42.69*(mp)
$R_{.17}$ A	4.37	4.58
$-\sigma_w$(Expt.)	11800 (ppm cm^3/mole)	9360
$-\sigma_w$(Expt.)	318 (ppm)	219
$\langle E^2 \rangle$ (5.1)	.404	.279
B	787	785

*: Ref.[69].

5.6. Liquid State Structural Problems

This section typifies the sort of liquid state problems that can be studied by the buffeting model.

5.6.1. σ_w for $SiCl_4$

Comparison between the σ_w data of CCl_4 and $SiCl_4$ shows that shifts produced by the former are always larger than those of the latter.

Raynes and Raza[163] observed this and wrote "... the shifts produced for CCl_4 are 40-50% greater than those produce by $SiCl_4$. In contrast to this are the polarizabilities, $SiCl_4$ has a polarizability some 10% larger than that of CCl_4. Thus we are forced to the conclusion that local effects principally determine σ_w. In the present case the chlorine atoms of $SiCl_4$ are probably very much less polarizable than those of CCl_4 due to the presence of structures such as $Si{=}Cl^+$ ...".

Pauling[318] gives structures of type (a) and (b) for $SiCl_4$;

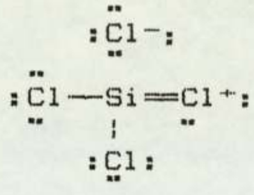

$$:\ddot{\mathrm{Cl}}-\underset{:\ddot{\mathrm{Cl}}:}{\overset{:\ddot{\mathrm{Cl}}^-:}{\mathrm{Si}}}=\mathrm{Cl}^+:$$

(a)

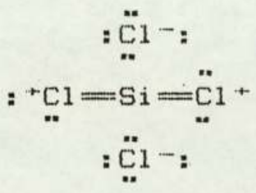

$$:{}^+\mathrm{Cl}=\underset{:\ddot{\mathrm{Cl}}^-:}{\overset{:\ddot{\mathrm{Cl}}^-:}{\mathrm{Si}}}=\ddot{\mathrm{Cl}}^+$$

(b)

These structures do not show the transfer of electronic charge from the high-buffeting chlorine to the low-buffeting silicon as Raynes and Raza suggest by $Si=Cl^+$.

The buffeting model offers the concept of the solvent cavity as a plausible alternative explanation of the observed effect. The cavity size provided by $SiCl_4$ for the solute is larger than that of CCl_4; 6.4 A ($SiCl_4$) > 5.9 A (CCl_4), which explainsthe the observation. Note also that the inter-molecular forces in CCl_4 are stronger than those of $SiCl_4$, a fact reflected in their cohesion energies. One therefore should not expect larger shifts for the latter on the grounds that it has a larger <u>molecular</u> polarizability than the former. The <u>atom-atom</u> interactions between molecules determine the inter-molecular forces and not the molecules as a whole. Table 5.15 contrasts the buffeting screenings of some solutes in the two solvents to show that in all cases; $\sigma_r(CCl_4) > \sigma_r(SiCl_4)$ are in accord with the observation. The solvent cavity size is used if $R_v > R_u$.

Table 5.15. Comparison between the Screening Constants (ppm) for $SiCl_4$ and CCl_4 ($Z_L = 11$, $B = .54$)

Solute ------>	C_5H_{10}	C_6H_6	C_6H_{12}	MeC≡CMe	$Me_2C=CMe_2$
R A	$R_{,17} = 6.00$	$R = 6.18$	$R = 6.34$	$R_{,17} = 5.6$	$R_{,17} = 6.45$
$SiCl_4$ $-\sigma_r$ $(-\sigma_w)$	.185 (.203)	.236 (.272,.293)	.235 (.187)	.300 (.318)	.302 (.237)
CCl_4 $-\sigma_r$ $(-\sigma_w)$	.277 (.295)	.394 (.394)	.278 (.265)	.519 (.477)	.345 (.340)

5.6.2. Number of Nearest Neighbours in the Liquid State

It may have been noted that throughout this chapter a fixed value of 11 (except for P_4) has been used for Z_L.

The crystalline structure of the compounds justifies the value of 11, as was discussed in Chapter 3. This however is not true for SiF_4 and SF_6 with bcc structures, Z_S = 8 (see table 3.2). For Z_L = 7, the cohesion energies calculated by (3.25) fall short of the experimental values by 7 and 6 KJ/mole respectively. The fact that (3.25) works so well for so many compounds by using Z_L = 11, suggest that 11 might be a <u>scale factor</u> rather than a genuine nearest number of neighbours.

Table 5.16 verifies this suggestion in which the calculated heats of vaporization for two extreme cases of mercury and liquid chlorine, with known Z_L from x-ray studies, are given.

Table 5.16. Calculated and Experimental heats of Vaporization for Hg and Cl_2

	V cm³/mole	Ref.	$R_{.17}$ A (5.2)	H_v(Cal.) KJ/mole	H_v(Expt.) KJ/mole	Ref.	Z_L	Ref.
Hg	14.65 (mp)	69	3.21	61.60	59.06	255	7*	214
					59.66	69		
CL_2	34.75 (solid)	240	4.28	17.20	20.33	215,255,69	6*	214
					18.38	240		

*: For Z_L = 11 one finds H_v = 96.8 and 31.52 J/mole for Hg and Cl_2 respectively.

For Z_L = 7, Eq. (3.25) gives H_v(Cal.) = 20.05 KJ/mole for Cl_2.

The results of this table rule out the possibility of 11 being a scale factor, because for such a value the calculated H_v are about twice the experimental ones. The results also reiterate the workability of the buffeting model and ratify $R_{.17}$ as the best expression for estimating liquid state intermolecular distances.

It is worth noting that the close-packing orthorhombic (Z_S = 12) structure of Cl_2, unlike Br_2, is not exhibited in the liquid state[214]. This makes chlorine a unique liquid compared to N_2, O_2 and Br_2. Chlorine is also polar in the liquid state; μ = 1.07 D, a peculiarity due to its unique liquid state structure[214].

However both the liquid state close-packing of Br_2 (we used Z_L = 11 in table 5.5) and the peculiarity of Cl_2 have been satisfactorily explained by the polyatomic field-potential formulas.

Concerning SiF_4 and SF_6, as table 5.10 shows, a close-packing structure in the liquid state (Z_L = 11) is required by the buffeting potential to give H_v(Cal.) $\simeq$ H_v(Expt.), whereas the the crystalline structures are bcc (Z_L = 8). The calculated H_v values for SiF_4, with Z_L = 7 and R_S = 4.68 A (table 3.3) and SiF_6, with Z_L = 7 and $R_{.17}$ = 5.06 A (table 5.10), are compared with the experimental values in Fig. 5.5. The relationship between the experimental and calculated cohesion energies of systems for which no adjustable parameter is used (non-refined) is also shown in Fig. 5.5.

5.7. Conclusions

The results of this chapter support the conclusion that the

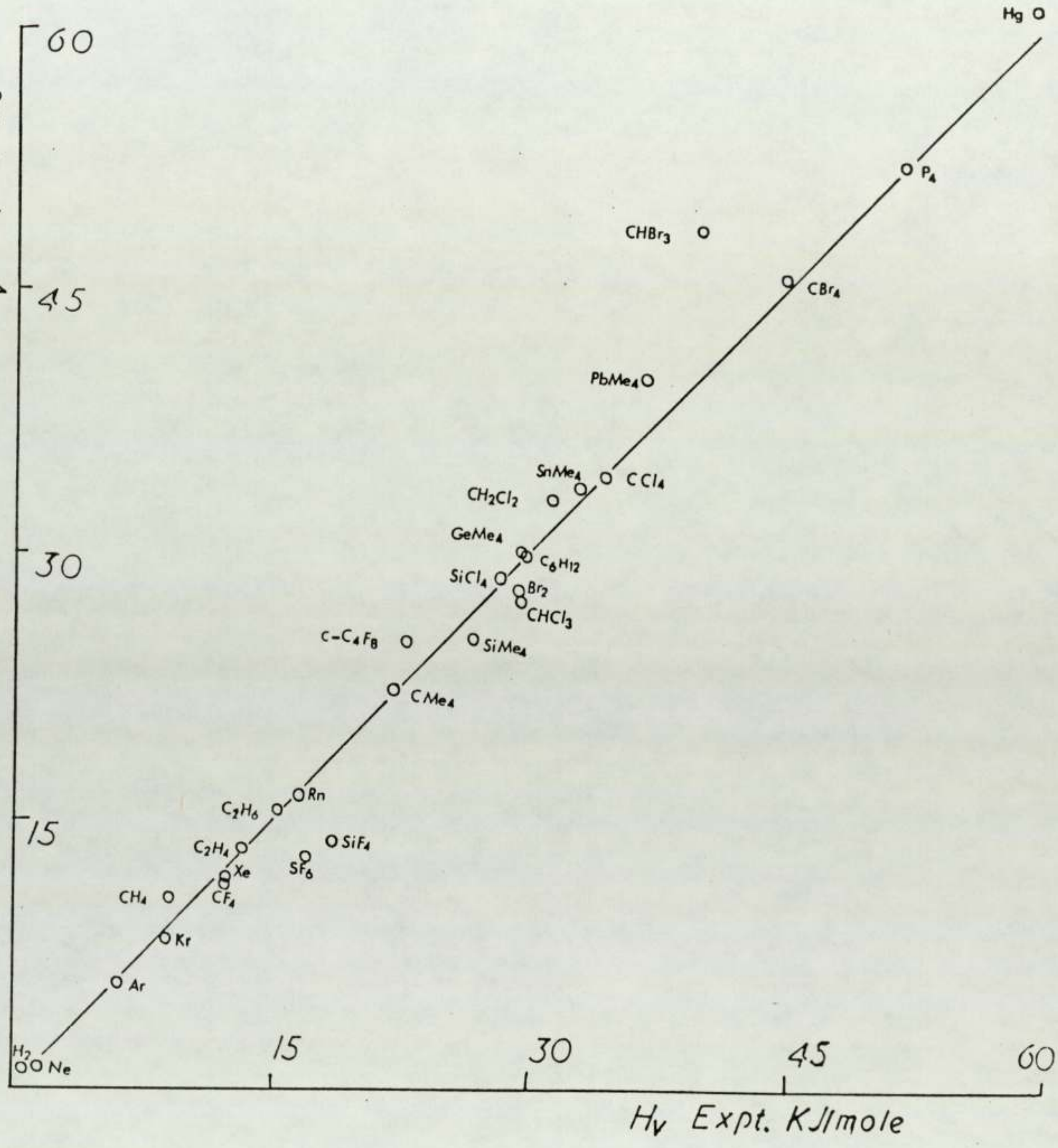

Fig. 5.5 Comparison between (non-refined) calculated and experimental heats of vaporization.

polyatomic model provides a genuine and practical intermolecular attraction force function for the liquid state.

This model, in spite of its simplicity and lack of benefit from tools of statistical mechanics and thermodynamics, efficiently explains the vdW screening constant, the heat of vaporization, and some liquid state structural problems.

It is however conceivable that the model, now in its infancy, can be improved by being subject to further testing in the light of the wealth of liquid state experimental facts.

The evidence shows that its critical parameter, namely the inter-molecular distance, for pure globular systems, can be obtained from molar volumes by (5.2) for all practical purposes.

The definition of R for mixtures of small gas molecules in liquids, judging by the analysis of table 5.7 however, appears to be more subtle than the simple characterization by (5.3).

The B values found here are regarded as genuine nuclear screening parameters because of their inter-calculations and consistency with the corresponding cohesion energies.

The inefficiency of the model for large non-globular molecules, which stems from the invalidity of its assumptions for such systems, initiates the ensuing natural step in the development of the atom-atom potential function for large molecules.
This subject is touched upon in the last section of the following chapter.

Chapter 6

The Buffeting Interaction and Solubility of Gases in Liquids

Introduction

The subject of the solubility of gases in liquids has been a troublesome one. There have been many theoretical and semi-empirical attempts to cope with this problem.
The multitude of terms invented and used indicate the extent to which these attempts have comprehensively coped with this vast subject. Term such as *ideal, non-ideal, real, regular, active, inactive, inert, reactive, non-active, partially active, physically reactive, chemically reactive, associative, non-associative, solvation, hydration, hydrogen bond formation, positive deviation, negative deviation, activity coefficient, internal pressure*, and many more are prevalent in this field.

The subject therefore affords a test case for the buffeting idea and its underlying assumptions. In fact the pi-electron refinement of the inert-atom approximation and the importance of the centre of mass of asymmetric molecules were obtained from the correlational analysis of gas solubility in terms of the pair buffeting field given in this chapter. In other words, the study of the solubility of gases has been the first test case for the buffeting field for which a heuristic pair potential function, different from (3.24), has been derived here to circumvent the problems of Z_L and polarizability contribution which were then unsolved.

The correlational analysis of gas solubility and the heuristic potential has provided grounds on which to discuss the contentious subject of *chemical reactions* as a cause of solubility. A criterion for the concept of "likeness" in the "like dissolves like" maxim is also found in terms of the inert-atom moment rather than the conventional structural likeness concept. The topic of group contribution which points to the possibility of calculating macroscopic properties like solubility from the independent contributions of functional groups in molecules is briefly studied first in terms of the buffeting field and in the last section by Eq. (3.24) where its results are compared with those of the UNIFAC method.

The remarkable variety of uses for gas-liquid solubilities in medical research, anaesthesiology, pharmacology, oceanography aerosol practice, biotechnological engineering, chemical engineering, and, environmental pollution[253] calls for further in-depth study of this subject. The correlational analysis given here is to stimulate such a careful investigation by the polyatomic or buffeting method.

6.1. Background Information

Ideal Solutions

In the conventional treatment of the subject of solubility ideal solutions are those which obey Raoult's law[253] at all temperatures. This means that in a mixture of a gas u (solute) and a liquid v (solvent) at any temperature the mole fraction of u, x_u^i, is given by;

$$P_u = P^o_u \, x^i_u \qquad (6.1)$$

where P_u is the actual pressure of gas u at t °C and P^o_u is the vapour pressure of u over the liquid u at t °C. This mole fraction has come to be called the _ideal_ solubility. Of Course P^i_u is not a measurable quantity if the critical temperature of gas u is above the temperature of the solubility measurement because gas u cannot exist as pure liquid[253].

Hildebrand[331,332] however, accepts a fictitious value for P^o_u by extrapolating the vapour pressure above the critical temperature which is used for a rough calculation of the ideal solubilities of gases. Therefore, for all gases P^o_u is the vapour pressure of the liquified gas, or its equivalent. Hildebrand's ideal solubility of gas is for P_u = 1 atm. and therefore (6.1) becomes[253,333];

$$x^i_u = 1/P^o_u \qquad (6.2)$$

Real Solutions

No known liquid solutions are ideal[334], in fact ideal solutions particularly for gases do not exist[253], but as the components of a solution approach one another in molecular shape, size, chemical type (electronic configuration), and mass, the behaviour of all components in solution approaches (6.1) as a limit. In terms of the buffeting concept, this means that when d's, $\langle m^2 \rangle$'s, and V's of the components of a solution are similar -rare for gas solutions- their behaviour approaches (6.1). Solutions of xylene isomers, for example, deviate from the ideal condition by about 2%[335,336].

However, great deviations are observed in almost all other solutions in which the components have an even greater difference in size, shape, and chemical nature. The deviations from ideal condition are quantified by the activity coefficient γ as;

$$\gamma = \frac{P_u}{x_u P_u^o} \qquad \text{where} \quad \begin{array}{l} \gamma = 1 \ \text{ if } x_u = x_u^i \\ \gamma < 1 \ \text{ if } x_u > x_u^i \\ \gamma > 1 \ \text{ if } x_u < x_u^i \end{array} \tag{6.3}$$

Raoult's law is inseparable from the concept of ideality. If the mixture is ideal it will then obey this law, otherwise there is no significant virtue in Raoult's law[253].

6.2. Early computational Difficulties

6.2.1. Buffeting Field and Gas Solubilities

From the argument of real solutions a pattern emerges for a quantitative discussion of solubility, namely the assumption that if u and v have similar intermolecular potentials in their pure states, then u will exert similar forces on the molecules of v that it exerts on u resulting in their mutual solubilities. This is the fundamental idea underlying the Hildebrand[333] and Bradford[337] internal pressure (cohesion) theory which leads to the concept of the solubility parameter. There are other functions of the intermolecular potentials that may be used as a measure of solubility of u in v. For example, there is the gain in potential energy, ΔPE, on making one dissimilar pair "uv" from two isolated pairs "uu" and "vv"[69];

$$\Delta PE = PE(uv) - (1/2)\ PE(uu) - (1/2)\ PE(vv) \tag{6.4}$$

Gerrard[253] contends that the tendency of a gas u to condense, characterized by PE(uu), is the prime factor to consider with respect to any liquid. The second factor relates to the intermolecular structure of v, PE(vv), and the third one emerges from the inevitable interaction between u and v, PE(uv). As higher PE(uu) and PE(vv) means higher PE(uv) one might use only the interaction potential between u and v, PE(uv), as a measure of their solubility which contains the three factors mentioned by Gerrard. It may equally well be argued that the difference between PE(vv) and PE(uv) governs the tendency of v for u as compared to v;

$$\Delta PE = PE(uv) - PE(vv) \qquad (6.5)$$

What function of the potential energy is the most suitable as a measure of the solubility needs further scrutiny.
To see if the buffeting idea in its main features is pertinent to the solubility problems, use is made of the field expression (3.8) for the preliminary study of systems given in table 6.1. The difference between the fields of uv, when u is in the cavity of v and pure v, as given in (6.6) by analogy with (6.5) is used for the correlational analysis of table 6.2;

$$\Delta\langle E^2\rangle = \langle E^2\rangle_{uv} - \langle E^2\rangle_{vv} \qquad (6.6)$$

The activity coefficients in table 6.2 are found from the ratio of the ideal and observed solubilities given in table 6.1.
The fields are calculated according to the method explained in the preceding chapter. The calculation of the d values for some of the solvent molecules is simplified by taking a suitable atom as the rough centre-of-mass (CM); carbon atom of the "C=O" group

Table 6.1. Solubilities of gases (Mole Fraction x10^4) at 25 °C and 1 atm.[333]

Gas ----------->		CO_2	N_2O	CH_4	O_2	CO	N_2	H_2
Ideal Solubility ----->		257	202	35	13.2	12.8	10	8
Solvent	µ D[161]	0 °C	0 °C					
$(Et)_2O$	1.1	-	-	45.3	19.8	16.90	12.52	5.52
C_6H_{12}	.0	-	-	28.3	-	-	7.22	3.80
CCl_4	.0	100	-	28.6	12.0	8.86	6.42	3.27
m-$C_6H_4(Me)_2$	.36	102	-	25.8	-	9.12	6.14	4.13
CH_3COOCH_3	1.7	-	-	20.0	9.08	8.65	5.97	3.07
CH_3COCH_3	2.8	209	185	22.3	9.25	8.54	5.92	2.31
C_6H_6	.0	91	-	20.7	8.16	6.63	4.48	2.61
CCl_3H	1.1	123	182	-	7.38	6.45	4.45	2.20
C_6H_5Cl	1.69	-	-	20.8	7.91	6.32	4.31	2.66
CH_3OH	1.7	71	53	7.1	3.18	3.25	2.35	1.57
CS_2	.0	22	-	-	-	2.06	1.45	.93
H_2O	1.9	7	5	.24	.23	.18	.12	.15
C_5H_5N	2.21[a]	129	120	-	-	-	-	-
CH_2BrCH_2Br	1.1[b]	125	100	-	-	-	-	-
CH_3COOH	1.73	121	-	-	-	-	-	-
$C_6H_5CH_3$	.37	107	-	-	-	-	-	-
CH_3CH_2OH	1.7	70	72	-	-	-	-	-

a: Ref.[338]; b: Ref.[339] at 163 °C

Table 6.2. Results of comparison between γ and $\Delta\langle E^2\rangle$ in 10^{-10} erg cm^{-3} from (6.6)

Gas	CO_2		N_2O		CH_4		O_2		CO		N_2		H_2	
Solvent	Δ	γ	Δ	γ	Δ	γ	Δ	γ	Δ	γ	Δ	γ	Δ	γ
H_2O	175.4	36.7	175.4	40.4	152.4	145.8	49.0	57.3	50.0	71.1	42.0	83.4	24.8	53.3
CS_2	50.0	11.7	-	-	-	-	-	-	12.9	6.2	10.4	6.9	4.1	8.6
CH_3OH	45.2	3.6	45.2	3.8	39.3	4.9	11.1	4.1	11.4	3.9	9.1	4.2	3.7	9.1
CH_3CH_2OH	14.7	3.7	14.7	2.8	-	-	-	-	-	-	-	-	-	-
C_6H_6	17.4	2.8	-	-	15.3	1.7	4.7	1.6	4.8	1.9	3.9	2.3	2.0	3.9
CCl_4	15.2	2.6	-	-	13.2	1.2	3.1	1.1	3.9	1.4	3.2	1.5	1.5	2.5
$m-C_6H_4(Me)_2$	14.7	2.5	-	-	12.9	1.4	-	-	3.9	1.4	3.2	1.6	1.5	1.9
$C_6H_5CH_3$	16.5	2.4	-	-	-	-	-	-	-	-	-	-	-	-
CH_3COOH	35.1	2.1	-	-	-	-	-	-	-	-	-	-	-	-
CCl_3H	21.1	2.1	21.1	1.1	-	-	5.4	1.8	5.5	2.0	4.4	2.2	2.0	3.6
CH_2BrCH_2Br	29.0	2.1	29.0	2.0	-	-	-	-	-	-	-	-	-	-
C_5H5N	20.0	2.0	20.0	1.7	-	-	-	-	-	-	-	-	-	-
CH_3COCH_3	22.2	1.2	22.2	1.1	19.4	1.6	5.8	1.4	5.9	1.5	4.8	1.7	2.3	3.7
C_6H_5Cl	-	-	-	-	16.7	1.7	4.8	1.7	5.0	2.0	4.0	2.3	1.8	3.0
C_6H_{12}	-	-	-	-	11.0	1.2	-	-	-	-	2.7	1.4	1.2	2.1
CH_3COOCH_3	-	-	-	-	15.9	.7	4.6	1.4	4.7	1.5	3.8	1.7	1.7	2.6
$(Et)_2O$	-	-	-	-	10.0	.8	2.9	.7	3.0	.8	2.4	.8	1.0	1.4
CC*	.978		.990		.986		.994		.987		.987		.999	

*: Correlation coefficient.

in acetone for example. One notes that the nearly equal values of d for CO_2 and N_2O (see Appendix 5) result in the equal values of field differences given in table 6.2. This is in accord with the Kunerth[340] argument that "... because they have the same number and arrangement of electrons, they should therefore exhibit little if any difference in their solubilities". Fig 6.1 typifies a graph of the activity coefficient γ against $\Delta\langle E^2\rangle$ for hydrogen gas. The results of this correlation analysis, and similar ones for reaction fields $\langle R^2\rangle_1$, $\langle R^2\rangle_2$, and RFT, led to the following findings.

(1) There is no correlation between the activity coefficients (or solubilities) and either of the reaction fields.

(2) There is no correlation between static dipole μ, dielectric constant, refractive index, polarizability (or any function of these solvent's parameters) and activity coefficients or solubilities. The lack of linear correlation of the solubilities with dipole moment and dielectric constant has been clearly shown by Gerrard[341]. There appears therefore to be no relation between the solubility and the bulk properties of solvents.

(3) The large deviations of CS_2 and CH_3OH from the line (open circles in Fig. 6.1) led us to the contribution of double bond electrons in the interactions of the former and the significance of the CM for the latter. Correction for the effect of pi-electron in CS_2, by assigning half the Ar moment to each pi-pair, on the one hand enhanced the buffeting field of this solvent (full circle in Fig. 6.1), and on the other hand improved the inert-atom approximation

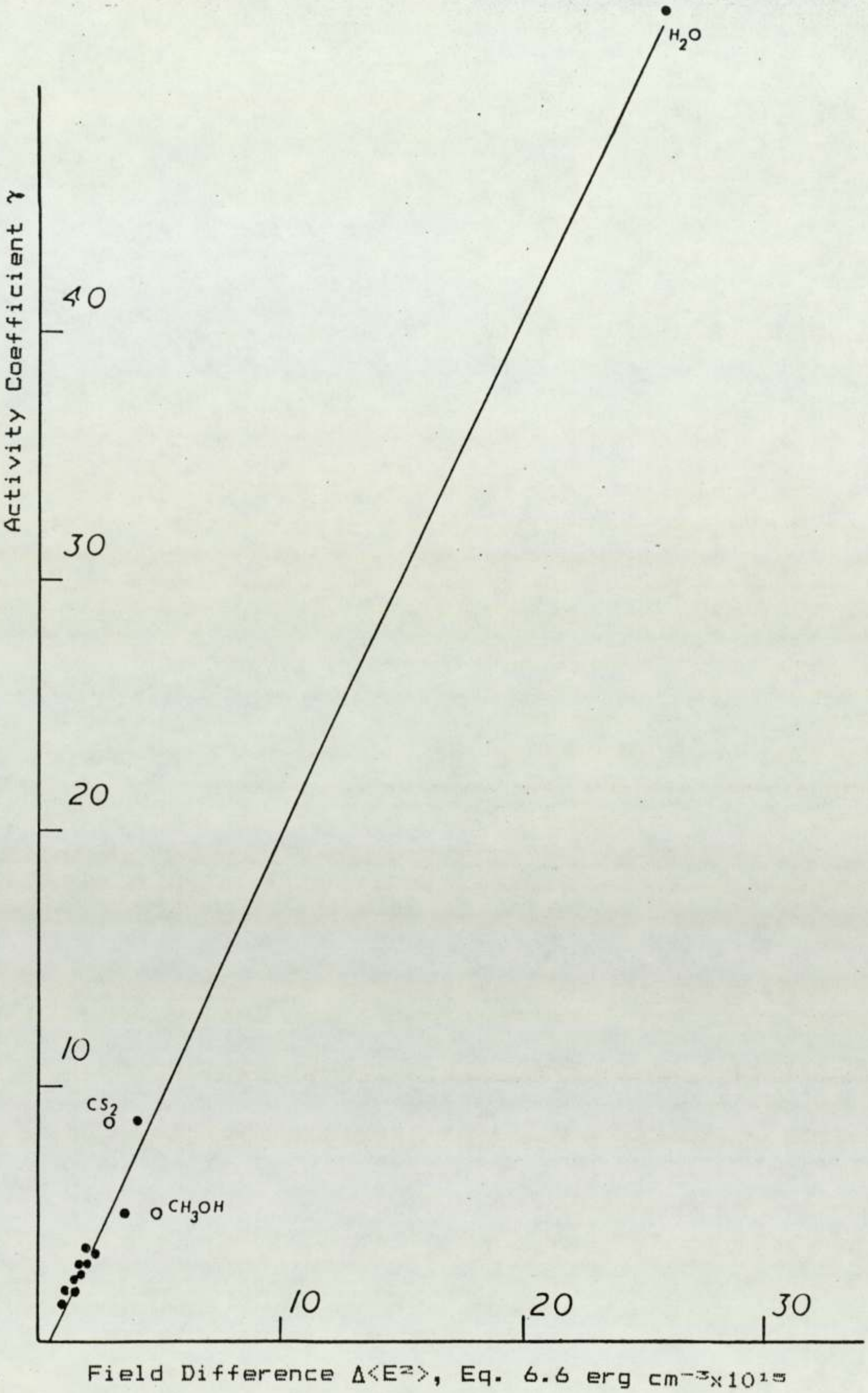

Fig. 6.1 Solubility of H_2. Relationship between the activity coefficient and the buffeting field difference.

as explained in Chapter 3. Correction for the CM in methyl alcohol, which originally was assumed to be on the carbon atom ($d_C = 0$, $d_O = 1.43$, $d_H = 2.05$ A) decreased its buffeting field (full circle in Fig. 6.1) because the right CM ($d_C = .738$, $d_O = .668$, $d_H = 1.35$) lowers the buffeting power of H(OH) and "O".

(4) As the calculations of the pair fields involved the atomic fields, it appeared as if the field contributions of identical atoms in different solvents were equal. This has initiated the important topic of <u>group contribution</u> in the next section.

6.3. Group Contributions

A group is an identifiable structural unit in a molecule such as CH_3 in a paraffin hydrocabon or OH in an alcohol. A few kinds of groups make up a vast variety of molecules of interest. Langmuir[342] suggested the premise that the forces about any particular group is characteristic of that group and is independent of the nature of the rest of the molecule. He called this premise the principle of <u>independent action</u>.
This principle focuses attention on the segments of the molecules and states that many of these segments in different molecules behave in much the same way in their contributions to molecular interactions[334].

According to the buffeting or polyatomic field expression what makes the field contribution of identical atoms different in different molecules is their locations, d, and the molecular volumes. Accounting for these two factors should, in principle, equalize the field contributions of identical atoms. In table

6.3 are given the field contributions of similar groups in different solvents for CO_2. These are in fact the uv fields used in the calculations for the entries in table 6.2 with and without corrections for the differences in the molecular volumes of the solvents.

Table 6.3. Buffeting field $\langle E^2 \rangle_{uv}$x10-14 erg cm^{-3} of group

solvent	V 20 °C gr cm^{-3}	CCl	C_6H_5	CH_3	OH
H_2O	18.9				27.67
$CHCl_3$	80.5	3.37(2.62)*			
CCl_4	96.5	2.19			
C_6H_5Cl	101.7	3.86(=CCl)	4.9(5.6)		
C_6H_6	88.8		6.91(7.62)		
C_5H_5N	80.7		8.71		
$C_6H_5CH_3$	106.2		4.40(4.32)	2.98(2.3)	
m-$C_6H_4(Me)_2$	122.3		3.14	2.00	
CH_3COCH_3	73.5			3.59	
CH_3COOH	57.2			4.75(4.61)	3.83(3.7)
CH_3CH_2OH	58.4			4.53	3.63

*: Entries in the brackets are the corrected values for the volume differences. For example, CCl contribution of $CHCl_3$ (3.37) compares with 2.19x96.5/80.5 = 2.62 which is the CCl contribution of CCl_4 when it is in the same volume as $CHCl_3$.

As this table shows, correction for volume differences, that is multiplying the uv field by the volume ratio of the two solvents with similar groups, improves the agreement between contributions. However the agreement is poor which stems from the approximate nature of the calculations and more importantly from the fact that fields are used instead of potential functions to characterize the solubility. This subject is further discussed in terms of the polyatomic potential in the last section.

6.4. A Heuristic Potential Function

The solute-solvent interaction is best characterized by a potential rather than a field used in the previous sections. A potential function like (3.24) would involve the contribution polarizability which was originally avoided here by using $\langle m^2 \rangle$ instead of α. The result is the following heuristic pair potential analogous to that of Keeson's[81], $(2/3)\mu_1^2\mu_2^2R^{-6}/kT$ for dipole-dipole interaction;

$$PE(uv) \propto -\sum_i\sum_j X_i X_j \langle m^2\rangle_i \langle m^2\rangle_j F(i,j)R-6 \qquad (6.7)$$

where the symbols have the same meaning as in (3.24).

In the subsequent sections (6.7) is used for the correlational analysis of the solubility data.

6.5. Significance of the Solubility of Gases as Molecular Probes

Solubility of gases in liquids provides an ideal testing ground for the underlying assumptions of the polyatomic model.
In other words, the gas can be used as a molecular probe for the study of the intermolecular forces and processes under different conditions of pressure and temperature.
We begin with inert gases for which the solubilities, boiling points -as a measure of their tendency to condense- and PE(uv)

according to (6.7) are given in table 6.4.

6.4. Solubilities of inert gases at 25 °C and 1 atm[343]

Solvent ------>		------------- H_2O -------------			------------- C_6H_6 -------------		
Solute	bp °K	$x_u \times 10^4$	Ln x_u	- PE(uv)	$x_u \times 10^4$	Ln x_u	- PE(uv)
He	4	.069	-11.884	.458	.785	-9.452	.132
Ne	27	.083	-11.699	.772	1.07	-9.142	.222
Ar	87	.300	-10.414	2.342	9.66	-6.942	.672
Kr	121	.470	-9.965	3.148	27.2	-5.907	.904
Xe	166	1.040	-9.171	4.419	111.	-4.500	1.268
Rn	211	1.850	-8.595	5.483	392.	-3.239	1.574
CC			.997			.999	

Hereafter solubilities, x_u, are in mole fraction.

From this table one notes that for a series of solutes in one solvent there is no linear relationship between x_u and either of PE(uv) or bp. There is however an excellent linear relationship between the logarithm of x_u, Ln x_u, and both PE(uv) or bp, see Fig. 6.2. The logarithmic relation is more akin to the thermodynamic methods of estimating the solubility; as for example by the solubility parameter method of Hildebrand[333].

Eley[344] gives a theory of solubility for inert gases in which two consecutive stages are involved; the formation of a cavity and the entrance of the gas molecule into the cavity. This is a theory of making holes and filling holes[345,346]. Eley writes of the "...anomalous factors in the solubility of the inert gases in water". Fig. 6.2 shows that there is no significant

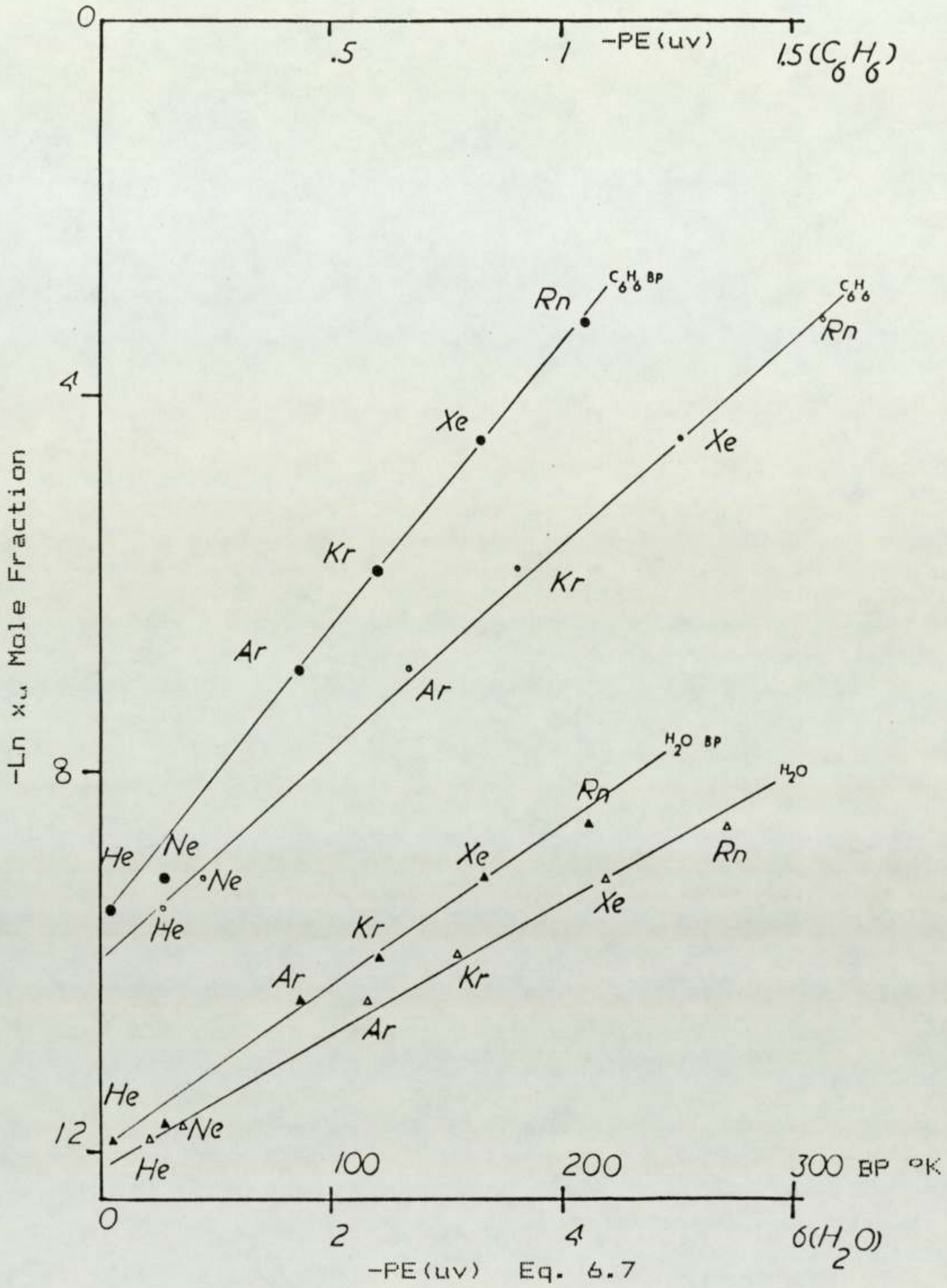

Fig. 6.2 Solubilities of inert gases in water and benzene. Relationship between the logarithm of solubility and the buffeting potential energy and boiling point.

departure from the line for any of the gases in the solvents as has been found by other workers[347] also. According to (6.7) water-gas interactions are purely dispersion with no dipolar effects.

The solubility of ^{222}Rn in waters (drinking water, spring water, rivers and sea) and in biological fluids is of interest because of its radioactivity. Some spring waters like those at Hot Springs, Arkansas, have dissolved radon. The solubility of Rn in heavy water, D_2O, the neutron moderator in nuclear reactors with natural uranium fuel, is also of importance. Vadovenko et al[348] have found that the solubility of Rn in D_2O is slightly higher than in water. They only give the ratios of the absorption coefficients K as;

$K_{Rn}(D_2O)/K_{Rn}(H_2O)$	1.09	1.08	1.07
Tem. °C	6.0	10.0	15.0

The distinguishable features of the two waters are the molar volumes and the d distances, properties like bond length-angle, 'I', and α are the same. In table 6.5 are given the available volumes at two different temperatures, calculated PE(uv), and ΔPE(uv) according to (6.4).

Table 6.5. Rn-D_2O and Rn-H_2O Potential Functions

Solvent	-- V Cm³/mole --		- PE(uv)		-ΔPE(uv)		d A
Tem. °C	15	25	15	25	15	25	
H_2O	18.036	18.073	6.177	6.090	.561	.582	d_H = .920; d_O = .065
D_2O	18.121	18.136	6.013	5.997	.629	.642	d_D = .893; d_O = .117

Molar voluems are from Ref.[158].

Judging by the PE(uv) values, Rn should have slightly higher solubility in water than in heavy water. If however, the values of ΔPE(uv) are accepted as the characterizing potential function for a solute in <u>a series of solvents</u> the order of the solubilities reverses. The ratios of the potential differences can then be used for comparison with the K ratios;

$\Delta PE(D_2O)/\Delta PE(H_2O)$	1.12	1.10
Tem. °C	15	25

which indicates the decrease in the solubility ratio with increase in temperature. The ratios compare well with those of Adovenko et al. The solubility of Rn in T_2O, tritium oxide, would be slightly higher than in H_2O and D_2O according to ΔPE. Note that the d values of water given in this table were used in table 6.4.

The analysis of the solubilities of other gases provides a still better test for the polyatomic model and would be more informative compared with the inert gases. Table 6.6 gives the solubilities of nine distinct gases in three distinct solvents and the results of their analysis. The d values of the species are given in Appendix 5. From this analysis one notes the improvement of the correlation between PE and Ln x_u from H_2O to CCl_4. Graphical presentation of the PE-Ln x_u relationship in Fig. 6.3 however discloses more subtle facts about the nature of the interactions.

If one is contented with the <u>statistical</u> analysis of the data and its good correlation (dashed lines in Fig. 6.3) given in the table, the contribution of the so-called chemical reactions of CO_2 and SO_2 to their solubilities that so many authors believe, can not be justified[349-355];

$$CO_2 + 2\ H_2O \Longleftrightarrow CO_3^{-}H + H_3^{+}O$$
$$SO_2 + 2\ H_2O \Longleftrightarrow SO_3^{-}H + H_3^{+}O \qquad (6.8)$$

Table 6.6. Analysis of the Solubility data of gases at 25 °C and 1 atm.[333]

Solvent		H_2O			C_6H_6			CCl_4		
solute	bp °K	$x_u \times 10^4$	Ln x_u	- PE(uv)	$x_u \times 10^4$	Ln x_u	- PE(uv)	$x_u \times 10^4$	Ln x_u	- PE(uv)
He	4	$.067^a$	-11.913	.458	.77	-9.471	.132	-	-	.122
H_2	20	$.14^a$	-11.176	.968	2.61	-8.251	.271	3.27	-8.026	.309
N_2	77	$.115^a$	-11.330	1.739	4.4	-7.728	.472	6.42	-7.351	.432
CO	82	.18	-10.925	2.226	6.63	-7.318	.596	8.86	-7.029	.547
Ar	87	.25	-10.596	2.342	9.6^a	-6.948	.675	13.5^b	-6.607	.625
O_2	90	$.227_a$	-10.693	2.230	8.16	-7.111	.597	12.0	-6.725	.548
CH_4	111	$.28^c$	-10.483	3.667	20.7	-6.180	.883	28.6	-5.857	.801
CO_2	194	7.0	- 7.264	4.643	96.2^a	-4.644	1.08	100.0	-4.605	.976
SO_2	263	434.0	- 3.137	6.844	2300.0^b	-1.469	1.603	1500.0^b	-1.897	1.45
CC			.940			.990			.995	

a: Ref.[343]; b: Ref.[253]; c: Ref.[356] and Ref.[333] give .24, Ref.[343] gives .225.

However, the intrigue of the deviation of helium in water from the statistical best-line along with the inspiration from Fig. 6.2 would suggest a <u>physical best-line</u> based on the inert atoms which passes through the inert points (solid lines in Fig. 6.3). The <u>inert-best-line</u> offers a guideline by which the behaviour of other gases may be judged. Inspection of Fig. 6.3 in the light of the inert-atom guideline reveals the following points.

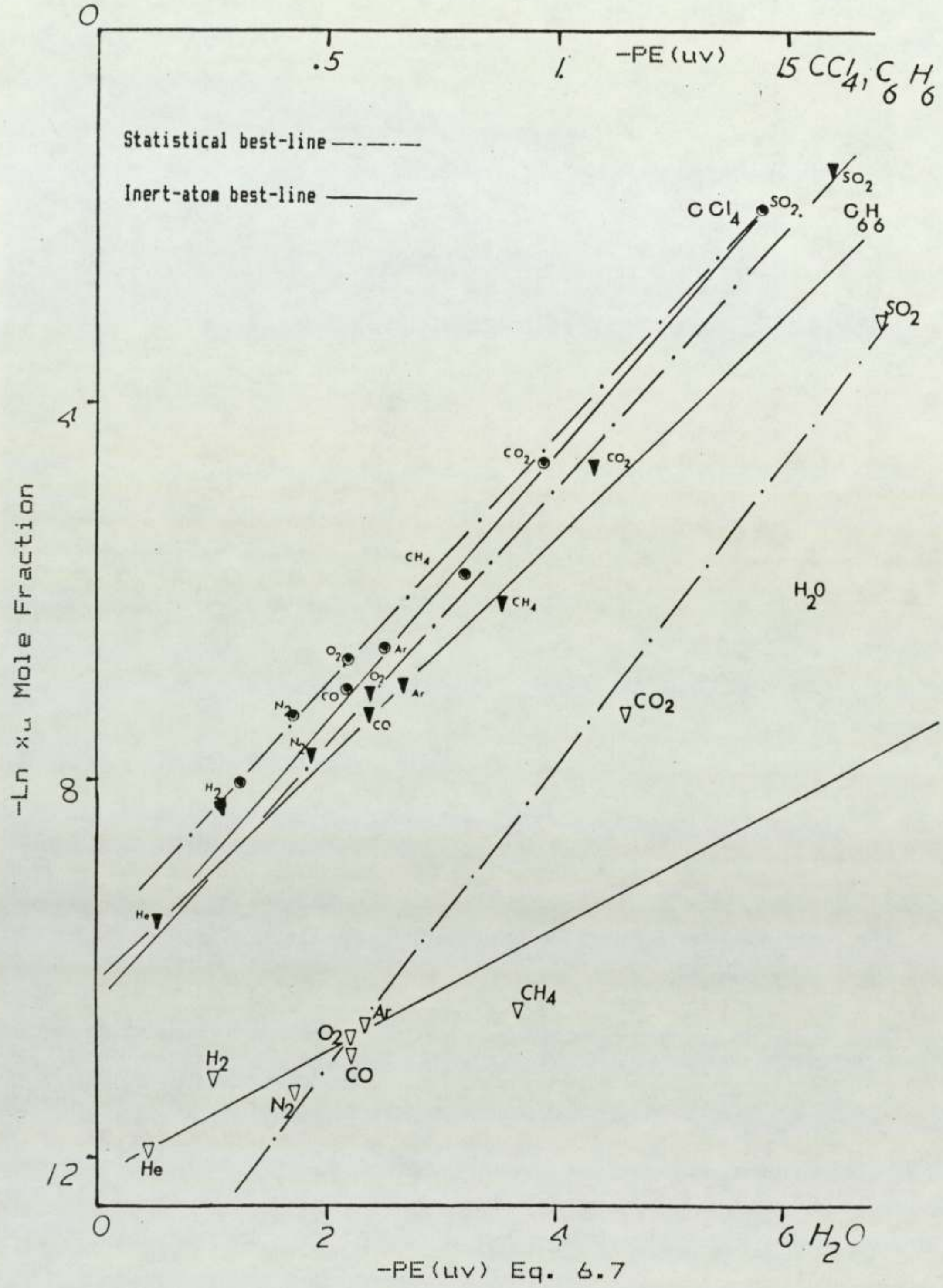

Fig. 6.3 Solubilities of the labelled gases in water, benzene and carbon tetrachloride. Plots of the logarithm of solubility against the buffeting potential energy.

(1) The solubilities of CO_2 and SO_2 in water can partly be explained by PE(uv) because the inert-line falls below these points imposing the conclusion that there must be some kind of specific interaction of type (6.8) to explain the excess solubilities.

(2) In the absence of reactions of type (6.8) one would expect the inert-line to coincide with the statistical line. This is the case in Fig. 6.3 where the two lines approach each other for C_6H_6 and CCl_4. We note the departure of SO_2 from the inert-line in benzene which indicates the possibility of SO_2-pi-electron interaction. A question arises here about the nature of the reactions resposible for the excess (on the basis, of course, of the inert-line) solubility of oxygen containing gases. Data in general and those in table 6.1 in particular show the enhanced solubility of CO_2 in solvents containing "-O-" and "=O" groups. Compare the solubility of acetone with that of carbon disulfide, benzene and ethyl alcohol, for example. Ethyl alcohol and acetone are isomers and the former offers a smaller cavity to the gas but still has much lower dissolving power than the latter. It appears that the rule of *like dissolves like* is operative between "=O" of CO_2 and "=O" of CH_3COCH_3. This points to some sort of <u>likeness</u> interaction between like groups distinct from the reactions of type (6.8). Note that "=O" groups in solute-solvent system have identical $\langle m^2 \rangle$ that could be interpreted as identical frequencies for the motion of electronic charge.

One might ask why such interaction is absent for O_2 and CO in water. It may be recalled from Chapter 3 that the "O" group in these gases is different from a typical "=O". The moment of the former is 1.25 $\langle m^2 \rangle_{Ne}$ and that of latter equals 1.75 $\langle m^2 \rangle_{Ne}$ whereas the moment of "=O" in CO_2, SO_2 and acetone is more like 1.5 $\langle m^2 \rangle_{Ne}$.

Gerrard[253] is a critic of resorting to chemical reactions as an explanation for the high solubilities of CO_2 and SO_2. He believes that the high solubilities of these gases is solely determined by their tendency to condense. In Fig 6.4 a graph of bp against Ln x_u shows the characteristics of Fig. 6.3. Here again if one is prepared to accept the large deviation of helium from the statistical line in water, the absence of chemical reactions or otherwise is justifiable. The presence or absence of interactions other than dispersion as a cause of solubility cannot be rigorously verified unless the proportionality factor of pair potential-solubility is known.

Comparison between Figs. 6.3 and 6.4 shows the superiority of PE to bp as a measure of solubility. The foregoing prolonged argument however should not conceal the role of the gas as a molecular probe for the elucidation of molecular interactions.

6.6. Solubilities of Solids; I_2, S_8, and SnI_4

In this section the potential function (6.7) is used to analyse the solubilities of these solids in a series of simple solvents. Table 6.7 give the solubilities and the PE(uv) values. The d values of the systems can be found in Appendix 5. For the moment of $TiCl_4$(V = 110.5 cm^3/mole), as was discussed in Chapter 3, 2 $\langle m^2 \rangle_{Kr}$ + 4 $\langle m^2 \rangle_{Ar}$ is used in the caculations in this table. One notes that in this case the good correlation exists between

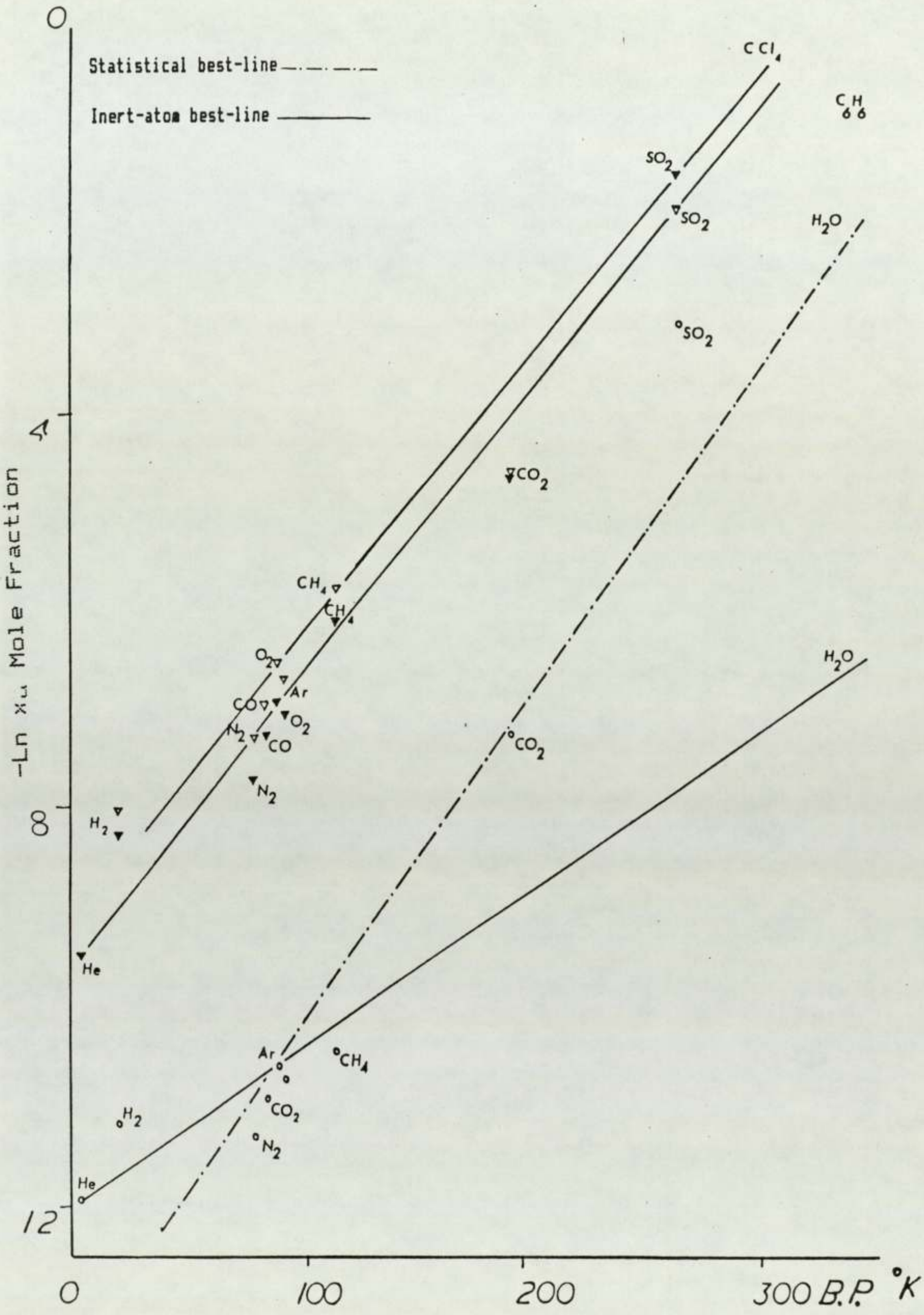

Fig. 6.4 Solubilities of the labelled gases in water, benzene and carbon tetrachloride. Plots the logarithm of solubility against boiling point.

PE and the solubilities.

The interesting point to note is the excess solubility of sulphur in CS_2. The statistical analysis has again veiled this aspect of the molecular interaction and should warn of the risk of unquestioning trust in the use of <u>statistical methods</u>. The ratio of the PE values for sulphur in benzene and carbon disulfide is about 2.3 whereas that of solubilities is 21.5, pointing to the existence of the "likeness" interaction between "=S" of CS_2 and "-S" of S_8. The *like dissolves like* maxim appear operative here. Of course the likeness is in the moments of S in CS_2 and that of S in S_8. Such a large solubility ratio is not observed for SnI_4 or I_2. It will be remembered from Chapter 3 that some experimental evidence support the existance of double bonds in the S_8 ring. This kind of likeness can not be found between SnI_4 and XCl_4 in spite of their structural similarity which suggest their conventional "likeness" and therefore, higher solubility.

Table 6.7. Analysis of the Solubility of Solids at 25 °C and 1 atm.[333]

Solid --->	----- I_2 -------		---- S_8 -------		-----SnI_4 ------	
Solvent	Mole%	PE(uv)	Mole%	PE(uv)	Mole%	PE(uv)
$SiCl_4$	.499	2.67	-	-	.382	12.04
CCl_4	1.147	3.13	.50	9.86	1.459	14.76
$TiCl_4$	2.15	3.96	-	-	-	-
CCl_3H	2.28	3.81	.57	12.47	1.692	19.19
C_6H_6	-	-	.64	11.50	2.181	17.50
CS_2	5.46	7.558	13.8	27.22	14.64	43.98
CC	.991		.991		.991	

6.7. Solubilities of Hydrides of group IV in Water

This section serves to illustrate the possibility of finding bond lengths from solubility data.

The available solubilities of methane, germane, and stannane are given in table 6.8, that of silane is estimated from the Ln x_u-PE linear relationship.

The bond lengths in GeH_4 and SnH_4 were not accessible and are estimated from the linear relationship by adjusting the value of d in the F factor until the calculated PE from (6.7) matches the solubility data. These estimated values are in considerable agreement with those found from covalent radii of H, Ge, and Sn given in the footnote to the table.

Table 6.8. Analysis of the solubilities of Hydrides of group IV[253]

Solute	bp °K	d_{X-H} A	$x_u \times 10^4$	Ln x_u	- PE(uv)
CH_4	111	1.09	.252	-10.58	3.667
SiH_4	161	1.48	.593*	-9.73	6.468
GeH_4	184	1.51*	.755	-9.49	7.400
SnH_4	220	1.85*	2.19	-8.4	10.563
CC				.999	

*: Estimated values from the covalent radii of H = .3 A, Ge = 1.225 A, and Sn = 1.511 A one finds; d_{Ge-H} = 1.525, and d_{Sn-H} = 1.811 A. The Ge-H bond length in GeH_3Cl is 1.52 A[158].

6.8. Additivity of Molecular Potential Energy

The analysis of the chemical screening constants in the previous chapter showed that the polyatomic field and potential formulations are inadequate for large non-globular molecules for which the separation of the rotational and translational motions and also the F series are invalid.

In this section the premise of the additivity of the molecular potential is tested for the solubility of CO_2 in large solvents.

Let us assume that the small solute gas buffets, according to the buffeting model, the constituent atoms of a large molecule independently. That is the fast rotating small solute interacts with the relatively stationary atoms of the solvent at a well-defined distance. The atoms of the solvent appear static because they are attached to the relatively slow rotating solvent molecule. In this situation the centre-to-atom distance d_j, for the atoms of the solvent equals zero, because it is interacting as a separate spherical entity and the buffeting factor reduces to the "solute-site-factor"; $F(d_j=0,d_i,R)$. This considerably simplifies the calculations of the potential energy as the evaluation of the d values becomes more difficult as the size of the solvent increases. The intermolecular distance of such a system is also independent of the size of the solvent molecule and depends on the sizes of the solute and the atom in question. To define R, one can use vdW r values or calculate it from the volumes of the solute and the atom.

There are a number of additivity methods available for estimating the molecular volume from the atomic volumes. The method of Le Bas[357], for example, attributes the following volume increments to the atoms that may be used for our preliminary test;

Species	C	H	O(O=)	O(Me-O-)	O(Et-O-)	Ring(6-membered)
Vol. Increment cm^3/mole	14.8	3.7	7.4	9.1	9.9	-15.0

These volumes and the volume of the solute can be used in (5.2) for example, to find the R for the interacting system.

Table 6.9 gives the potential energies of the CO_2-atom and CH_4-atom systems calculated using expression (3.25), according to the method explained in Appendix 6. The volumes of both solutes are calulated from the Le Bas increments to be 29.6 cm^3/mole.

Table 6.9. The Atom-Solute System Potential Increment

	Potential Increment (3.25) KJ/mole				
Solute	PE(H,u)	PE(C,u)	PE(C^{***},u)	PE(cyclo-C,u)	PE(O,u)
CO_2	.072	.041	.074	.049	.063
CH_4	.039	.025	.045	.029	.036

Now the potential between CO_2 and CH_3OH, for example, can be found by adding the atomic increments as;

$PE(uv) = 4\ PE(H,u) + PE(c,u) + PE(O,u) = .392$ KJ/mole

and for the methyl alcohol homologues, $CH_3(CH_2)_nOH$ it simply is; $PE(uv) = n\ PE(CH_2,u) + .392 = nx(.185) + .392$ KJ/mole

Such an additive method is based on the assumption that all the constituent atoms of a molecule are equally accessible to the solute, so that in general one may wtite;

$$PE(uv) = \Sigma\ PE(Atom,u) \tag{6.9}$$

where the summation is over all the atoms of the solvent, with

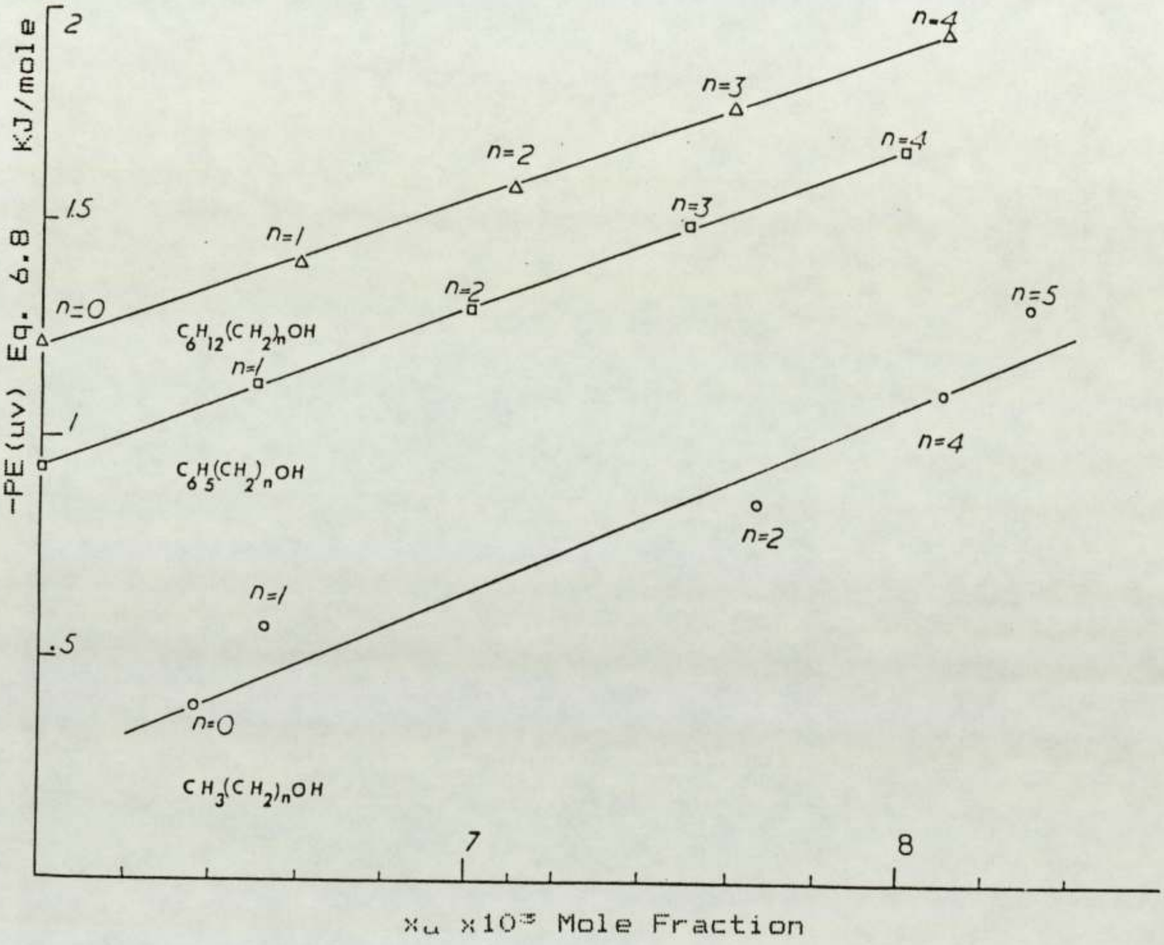

Fig. 6.5 The additivity of molecular potential energy. Relationship between molecular potential energies and solubilities of CO_2 in the labelled alcohols estimated by the UNIFAC method[263].

equall weighting factor, showing their equall accessibility. Note that the potential increment of cyclo-carbon is different from that of benzene ring because of their different polarizability contributions (see Appendix 6) and inert-atom moments.

Fig. 6.5 shows the relationship between the PE(uv) values found from this table and the solubilities of CO_2 in a series of alcohols estimated by a semi-empirical group contribution technique[258-260] called UNIFAC[261,262].

The validity of this potential additivity method, (6.9), cannot be tested unless the absolute prediction of solubility by (3.24) is possible.

6.9. Conclusions

Solubility problems have possibly until now eluded satisfactory explanation, even the simple rule-of-thumb that *like dissolves like*. The significant correlations between the solubility data and the heuristic potential form throughout this chapter suggests the potentiality of the polyatomic or buffeting theory in solving these problems.

It appears that the bulk effects, formulated by the reaction field techniques, have no significant role in determining the solubility.

From the analysis of the solubility-potential relationship it is evident that such a relationship takes different forms for different systems. It is of the form; Ln x_u-PE, for different gases in one solvent, and of the form; x_u-PE, for one solid in different solvents. It might also take the latter form for a gas in a series of solvents.

The new concept of "likeness" in terms of the likeness of the inert-atom moments focuses on the likeness of groups between two molecules rather than the traditional over-all molecular similarity. In this sense it is related to the concept of reactivity and reaction mechanism discussed in the conclusion to Chapter 3.

It may be possible to quantify the concept of likeness when the proportionality factor between solubility and the pair potential is known and thus elucidate whether or not non-dispersion, or chemical reaction type contributions are important to the solubility of species.

The brief study of the concept of potential additivity points to the possibility of treating molecular potential energies, like other additive molecular properties, as an additive quantitiy. Further examination of this fundamental concept extends the versatility of the buffeting model to large molecules for which by virtue of its inherent assumptions it is inadequate.

Appendix 1 The Mean-Square Moment

The mean fluctuations of an instantaneous dipole moment can be derived using the semi-classical equation of motion of a damp-free harmonic oscillator;

$$x_v(t) = (2\,E_v/m\omega_v^2)^{1/2} \cos \omega_v t \ \{\text{or, } \sin \omega_v t,\ \sin(\omega_v t + 0)\}$$

where $E_v = (v + 1/2)\,\hbar\omega_o$ are the quantised energy levels.

The moment is $m_x(t) = e.x_v(t)$, which for the ground state or zero-point fluctuations of charge, $E_{v=o} = \hbar\omega_o/2$, becomes;

$$m_x(t) = (e^2\,\hbar/m\omega_o)^{1/2} \cos \omega_o t$$

The mean and the mean-square values of this moment are;

$$\langle m(t)\rangle_x = (e^2\,\hbar/m\omega_o)^{1/2} \lim_{T\to\infty} \frac{1}{2T} \int_{-T}^{+T} \cos \omega_o t\, dt = 0$$

$$\langle m^2\rangle_x = (e^2\,\hbar/m\omega_o) \lim_{T\to\infty} \frac{1}{2T} \int_{-T}^{+T} \cos^2 \omega_o t\, dt = (e^2\hbar/m\omega_o).1/2$$

$$\langle m^2\rangle_x = 1/2(e^2\,\hbar\omega_o/m\omega_o^2)$$

This expression in terms of $\alpha(0)$ from (1.47) becomes;

$$\langle m^2\rangle_x = (1/2)\,\hbar\omega_o\,\alpha(0) \qquad \text{(A1.1)}$$

For isotropic molecules or atoms one can write;

$\langle m^2\rangle_x = \langle m^2\rangle_y = \langle m^2\rangle_z$; and, $\langle m^2\rangle = \langle m^2\rangle_x + \langle m^2\rangle_y + \langle m^2\rangle_z$

or, $\langle m^2\rangle = 3\,\langle m^2\rangle_x = 3\,\langle m^2\rangle_y = 3\,\langle m^2\rangle_z$ (A1.2)

Combination of the last expression and (A1.1) gives the required mean-square moment;

$$\langle m^2\rangle = (3/2)\,\hbar\omega_o\,\alpha(0) = (3/2)\,h\nu_o\,\alpha(0) \qquad \text{(A1.3)}$$

or using the London approximation $h\nu_0 = I$

$$\langle m^2 \rangle = (3/2)\ I\ \alpha(0) \qquad \text{(A1.4)}$$

Appendix 2 The Mean-Square Moment-field relationship

Referring to (1.49) and Fig. 1.4, for the field components produced at B by A, one may write;

$E(t,A)_z = 2\ m(t,A)_z\ R^{-3}$ .... For the fluctuations of moment in the Z-direction

$E(t,A)_x = -\ m(t,A)_x\ R^{-3}$ .... For the fluctuations of moment in the X-direction

$E(t,A)_y = -\ m(t,A)_y\ R^{-3}$ .... For the fluctuations of moment in the Y-direction

The mean-square components are therefore;

$\langle E^2 \rangle_{A,z} = 4\ \langle m^2 \rangle_{A,z}\ R^{-6}$

$\langle E^2 \rangle_{A,x} = \langle m^2 \rangle_{A,x}\ R^{-6}$

$\langle E^2 \rangle_{A,y} = \langle m^2 \rangle_{A,y}\ R^{-6}$

Adding up the mean-square components of the field and using Eqs. (A1.2) one finds (1.50) as;

$\langle E^2 \rangle_A = 6\ \langle m^2 \rangle_{A,x}\ R^{-6} = 6\ \langle m^2 \rangle_{A,y}\ R^{-6} = 6\ \langle m^2 \rangle_{A,z}\ R^{-6}$

or;

$$\langle E^2 \rangle_{A \text{ on } B} = 2\ \langle m^2 \rangle_A\ R^{-6} \qquad \text{(A2.1)}$$

Appendix 3 Average Inverse-Six^th^-Power of Distance, $\overline{\langle r_{ij}^{-6} \rangle}$

Since the distance between two interacting atoms i and j, r_{ij} changes with time, as a result of the molecular rotations, it has to be averaged in terms of the known molecular parameters R, d_i, and d_j.

The averaging procedure given here is an adaptation of a method usually used in liquid state theories[191,192,199,291].

Let us fix the centres of two symmetric polyatomic molecules at the centres of two polar coordinate systems a distance R away, as is depicted in Fig. A3.1.

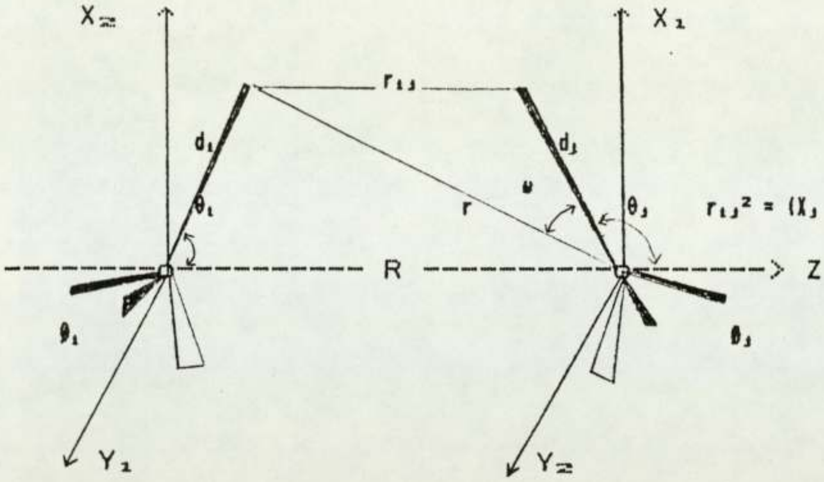

$x = d \sin\theta \cos\emptyset$

$y = d \sin\theta \sin\emptyset$

$z = d \cos\theta$

$r_{ij}^2 = (X_j - X_i)^2 + (Y_j - Y_i)^2 + (R + Z_j - Z_i)^2$

$\cos\omega = \cos\theta_i.\cos\theta_j + \sin\theta_i.\sin\theta_j.\cos\emptyset_i.\cos\emptyset_j + \sin\theta_i.\sin\theta_j.\sin\emptyset_i.\sin\emptyset_j$

or, $\cos\omega = \cos\theta_i.\cos\theta_j + \sin\theta_i.\sin\theta j.\cos(\emptyset_i - \emptyset_j)$

Fig. A3.1. A particular mutual orientation of two interacting molecules in a polar coordinate system.

For asymmetric molecules the centre of mass of the molecules is at the centre of the coordinate systems.

At some instance of time d_i and d_j make angles θ_i, θ_j and, $\emptyset_i$, $\emptyset_j$ with the axes respectively. The cosine rule for the triangle with sides r_{ij}, d_j and r gives;

$$r_{ij} = (r^2 + d_j^2 - 2rd_j\cos\omega)^{\frac{1}{2}}$$

or

$$r_{ij} = r[1 - 2(d_j/r)\cos\omega + (d_j/r)^2]^{\frac{1}{2}} \qquad (A3.1)$$

The inverse of any variable may be expressed in terms of some polynomial, for example, it is well-known that;

$$\frac{1}{x-1} = 1 + x + x^2 + x^3 + \ldots = \sum_{n=0}^{\infty} x^n$$

Let us begin with this simple example and manipulate it to get the form of (A3.1), by fist writing it as; $[(x-1)^2]^{\frac{1}{2}} = [x^2 - 2x + 1]^{\frac{1}{2}}$

or in general as; $[x^2-2xt+1]^{\frac{1}{2}}_{t=1}$ and then in the form;

$$\frac{1}{(x-1)} = \frac{1}{[x^2-2tx+1]^{\frac{1}{2}}_{t=1}} = \sum_{n=0}^{\infty} x^n = \sum_{n=0}^{\infty} P_n(t)x^n = \sum_{n=0}^{\infty} P_n(1)x^n$$

where P_n are the Legendre polynomials with the property $P_n = 1$. This is why $\Sigma\, x^n$ is arbitrarily expressed as $\Sigma\, P_n(1)x^n$. Replacing t by cos ω in the last expression gives[292];

$$\frac{1}{[x^2-2x\cos\omega+1]^{\frac{1}{2}}} = \sum_{n=0}^{\infty} P_n[\cos\omega]x^n \qquad (A3.2)$$

where $$P_n(x) = \frac{1}{2^n n!}\frac{d^n}{dx^n}(x^2-1)^n$$

Therefore, the inverse-first-power of r_{ij} may be expressed in terms of the Legendre polynomial (A3.2). Likewise other inverse powers of r_{ij} may be expressed as a function of other polynomials.

The generalized form of (A3.2) is given as[291,293-296];

$$\frac{1}{[x^2-2x\cos\omega+1]^u} = \sum_{n=0}^{\infty} C_n^u(\cos\omega)x^n \qquad (A3.3)$$

where C_n^u are the Gegenbauer polynomials. Comparison between (A3.2) and (A3.3) shows that; $C_n^{\frac{1}{2}}(\cos\omega) = P_n(\cos\omega)$ or in general[291];

$$C_n^{(P-2)/2}(x) = \binom{n+P-3}{n} P_n(x)$$

Also (A3.3) for u = 0, becomes;

$$\frac{1}{(x^2-2x\cos\omega+1)^0} = 1 = \sum_{n=0}^{\infty} x^n C_n^0(\cos\omega) = C_0^0 + xC_1^0 + x^2C_2^0 + \dots$$

from which it may be deduced that; $C^0_{\underset{n>0}{n}}(\cos\omega) = 0$, $C_0^0(\cos\omega) = 1$, and in general[291];

$$C_n^u(x) = \sum_{P} (-1)^P \frac{(n+u-P-1)!}{P!(u-1)!(n-2P)!}(2x)^{n-2P} \qquad (A3.4)$$

A list of C_n^u polynomials, derived from (A3.4) is given in table A3.1.

Now the inverse-sixth-power of r_{ij} from (A3.1) according to (A3.3) when u = 3, is;

$$\frac{1}{r_{ij}^{6}}=\frac{1}{r^{6}[1-2(d_j/r)\cos\omega+(d_j/r)^{2}]^{3}} = r^{-6}\sum_{n=0}^{\infty} C_n^3(\cos\omega)\left(\frac{d_j}{r}\right)^{n} \qquad (A3.5)$$

The value of r in (A3.5) is also unkown and has to be written in terms of R and d_i by using the cosine rule, this time for the triangle with sides R, d_i, and r (Fig. A3.1);

$$r = (R^{2}+d_i^{2}-2d_iR\cos\theta_i)^{\frac{1}{2}}$$

Therefore r^{-6} and r^{-n} of (A3.5), by analogy with (A3.5) may be written as;

$$r^{-6} = R^{-6}\sum_{K=0}^{\infty} C_K^3(\cos\theta_i)(\frac{d_i}{R})^{K} \qquad (A3.6)$$

$$r^{-n} = R^{-n}\sum_{m}^{\infty} C_m^{n/2}(\cos\theta_i)(\frac{d_i}{R})^{m} \qquad (A3.7)$$

By replacing (A3.6) and (A3.7) into (A3.5) one obtains the desirable form of r_{ij}^{-6} at the expense of the daunting expression;

$$r_{ij}^{-6} = R^{-6}\sum_{n}\sum_{m}\sum_{K} \frac{d_i^{K+m}\, d_j^{n}}{R^{n+m+K}} \quad C_n^3(\cos\omega)\, C_m^{n/2}(\cos\theta_i) C_K^3(\cos\theta_i) \qquad (A3.8)$$

The space-average of r_{ij}^{-6}, when the two atoms span the whole surfaces of their two spheres, in accord with the mean-value theorem of functions may be written as;

$$\overline{(r_{ij}^{-6})} = \frac{\int_0^{\pi}\int_0^{\pi}\int_0^{2\pi}\int_0^{2\pi} r_{ij}^{-6}\,dt_i\,dt_j}{\int_0^{\pi}\int_0^{\pi}\int_0^{2\pi}\int_0^{2\pi} dt_i\,dt_j} \qquad (A3.9)$$

where $dt_K = \sin\theta_K d\theta_K \varphi_K$

Substituting for r_{ij}^{-6} from (A3.8) into this integral, replacing the denominator with its value of $(4\pi).(4\pi) = 16\pi^2$ and factoring out the constant R one obtains;

$$\overline{(r_{ij}^{-6})} = \frac{R^{-6}}{16\pi^2} \int\int\int\int \sum_n \sum_m \sum_K \frac{d_i^{K+m} d_j^n}{R^{n+m+K}} C_n^3(\cos\omega) C_m^{n/2}(\mathrm{Cos}\,\theta_i) C_K^3(\cos\theta_i) dt_i dt_j \qquad (A3.10)$$

Such a formidable expression for expressing a physical fact shows the unsuitability of the mathematical method. This method however appears elegant compared to the technique of 4-variable Taylor's series expansion used by Raynes[206]. An alternative analytical method is suggested in the following Appendix.
The solution of this integral involves hundreds of integrations resulting from the expansion of the C_n polynomial and their subsequent products which are all of the form;

$$\int_0^{\pi}\int_0^{\pi}\int_0^{2\pi}\int_0^{2\pi} \cos^n\omega \cos^m\theta_i \; dt_i dt_j = \begin{cases} \dfrac{16\pi^2}{(m+1)(n+1)} & \text{for n and m even} \\ 0 & \text{for n or m odd} \end{cases} \qquad (A3.11)$$

This is the generalized form of the numerical integrations performed by the [MONTE CARLO] program developed in Appendix 4. For example, the coefficient of term $(d/R)^{10}$ in the F series can be found easily using (A3.11) and C_{10}^3 from table A3.1;

$$\int\int\int\int C_{10}^3(\cos\theta_i) dt_i dt_j = \frac{67584}{11} - \frac{126720}{9} + \frac{30640}{7} - \frac{20160}{5} + \frac{1680}{3} - 21 = 91$$

We note that the factor $16\pi^2$ in (A3.11) cancels with that of (A3.10) to give 91 as the coefficient of d^{10}.
The F series of (3.7) is the result of the integration of

(A3.10) using this approach. The calculation of the coefficients of terms beyond d^8 when $d_i \neq d_j \neq 0$ is quite impractical. This together with the absence of alternative methods for handling (A3.10) has given rise to speculations about the divergence of such series.

In complete contrast to the inefficient analytical technique we have developed two numerical methods based on random numbers, which conveniently handle the problem of inverse-six-power averaging (see Appendix 4).

Table A3.1 Gegenbauer Polynomials (from Eq. A3.4)

$C_1^1(x) = 2\ x$

$C_1^2(x) = 4\ x$

$C_1^3(x) = 6\ x$

$C_2^1(x) = 4\ x^2 - 1$

$C_2^2(x) = 12\ x^2 - 2$

$C_2^3(x) = 24\ x^2 - 3$

$C_3^1(x) = 8\ x^3 - 4\ x$

$C_3^2(x) = 32\ x^3 - 12\ x$

$C_3^3(x) = 80\ x^3 - 24\ x$

$C_4^1(x) = 16\ x^4 - 12\ x^2 + 1$

$C_4^2(x) = 80\ x^4 - 48\ x^2 + 3$

$C_4^3(x) = 240\ x^4 - 120\ x^2 + 6$

$C_5^1(x) = 32\ x^5 - 32\ x^3 + 6\ x$

$C_5^3(x) = 672\ x^5 - 480\ x^3 + 60\ x$

$C_6^1(x) = 64\ x^6 - 80\ x^4 + 24\ x^2 - 1$

$C_6^3(x) = 1792\ x^6 - 1680\ x^4 + 360\ x^2 - 10$

$C_8^3(x) = 11520\ x^8 - 16128\ x^6 + 6720\ x^4 - 840\ x^2 + 15$

$C_{10}^3(x) = 67584\ x^{10} - 126720\ x^8 + 80640\ x^6 - 20160\ x^4 + 1680\ x^2 - 21$

Appendix 4 MONTE CARLO Methods for Average Inverse-Sixth-Power

For the numerical averaging of r_{ij}^{-6} one can begin with (A3.9) in which the integrand, r_{ij}^{-6}, is the instantaneous distance between i and j on the surfaces of two spheres the radii of which are fixed at d_i and d_j, but the angles θ and ϕ change with time, Fig. A3.1. The distance r_{ij} may be formed in terms of these angles which can be chosen randomly.

The inverse-six-power distance is then formed and the integral in (A3.9) solved by approximating it with its arithmetic mean. This method of integration may be described as[36,297-299];

$$\frac{1}{n}\sum_{i=1}^{n} f(x_i) = \frac{\int_a^b f(x)dx}{(b-a)}$$

or

$$\int_a^b f(x)dx = (b-a)\left[\frac{1}{n}\sum_{n} f(x_i)\right] \qquad (A4.1)$$

For multiple integrals (A4.1) becomes;

$$\int_a^b\int_c^d\int_e^f \ldots f(x,y,z,\ldots)dxdydz\ldots = (b-a)(d-c)(f-e)\ldots\left[\frac{1}{n}\sum f(x,y,z,\ldots)\right] \qquad (A4.2)$$

In solving multiple integrals no conventional numerical method rivals the MONTE CARLO technique in accuracy and simplicity. The method is based on the use of random numbers, in this case random variation of the angles θ and ϕ in the intervals $[0,\pi]$ and $[0,2\pi]$ respectively.

The program [MONTE CARLO] listed below solves the integral in (A3.9) according to the algorithm of (A4.2). The program gives

$\overline{\{r_{ij}^{-6}\}}$ directly which upon multiplying by R^6 the value of F series can be obtained as given in table 3.1. The accuracy of the MONTE CARLO method is believed to be of the order of $n^{-1/2}$ where n is the number of trials[300]. Therefore one has to use large values for n which explains its time-intensive nature.

We note that the concept of integration as given by (A3.9) is involved in this program. Program [SIMULATION] however, handles the problem in a more natural way by finding the arithmetic mean of the values of r_{ij}^{-6}.
This program takes the following steps in finding the average.

(1) Simulates the rotation of i and j by generating two random points on the surfaces of the two spheres which are a distance R away; lines 60 and 80.
(2) Finds the Cartesian coordinates of the two points; lines 70 and 90.
(3) Computes the distance r_{ij}^2 between the two points; line 100.
(4) Raises this distance to power 3 to give r_{ij}^6; line 110.
(5) Adds all the inverse-six-power distances together; line 120
(6) Finally finds the average by dividing the sum by the number of times in which the addition is made; line 140, and obtains the F factor; line 150.

We note that to find points with uniform distribution on the surface of a sphere cosine of θ must be randomized instead of θ itself as shown in lines 60 and 70. The reason for this is explained in Ref.[300, p. 60].

Both programs give similar results. The programs were also used for the numerical integration of (A3.11).

In Fig. A4.1, are given two best-fit to the F-q data obtained by the programs. As an alternative to the analytical F series the simple polynomial of the best-fit (b), which can also be wtitten as (A4.3) and is valid for $0 < q < .43$, may be used.

$$F^{-1}(q) = 1 + .727\,q - 17.509\,q^2 + 24.550\,q^3 \qquad (A4.3)$$

where $q = (d_i + d_j)/2R$.

It was found, from the programs, that r_{ij} values have a normal distribution with mean value R. This fact can be used for an alternative analytical method of handling the average inverse-six-power distance, simply by finding the probability function of r_{ij}, $P(r_{ij})$, and then using the mean value theorem as;

$$\langle r_{ij}^{-6}\rangle = \int r_{ij}^{-6}\, P(r_{ij})\, dr_{ij}$$

This method should, in principle, give an exponential function in terms of q, or R, d_i, and d_j. For the probability function to be defined only the width or the standard deviation of the normal distribution has to be found which can be done by the programs given here.

```
10  [MONTE CARLO]
20  INPUT "Number of trials ?",n
30  INPUT "di,dj,R ?",di,dj,R
40  sum = 0
50  FOR i = 1 TO n
60  ti = RND*PI
70  tj = RND*PI
80  fi = RND*2*PI
90  fj = RND*2*PI
100 x = R + dj*SIN (tj)*COS (fj) - di*SIN (ti)*COS (fi)
110 y = dj*SIN (tj)*SIN (fj) - di*SIN (ti)*SIN (fi)
120 z = di*COS (tj) - di*COS (ti)
130 rij6 = (x*x + y*y + z*z)^3
140 sum = sum + SIN (ti)*SIN (tj)/rij6
150 NEXT i
160 PRINT "av.-inverse-six-power=", sum*PI*PI/4/n
170 PRINT "F series=", sum*PI*PI/4/n*(R^6)
```

```
10  [SIMULATION]
20  INPUT "Number of trails ?",n
30  INPUT "di,dj,R ?",di,dj,R
40  sum = 0
50  FOR i = 1 TO n
60  fi = 2*RND : costi = 2*RND - 1 : sinti = SQR (1 - costi*costi)
70  xi = di*sinti*COS (fi) : yi = di*sinti*SIN (fi) : zi = di*costi
80  fj = 2*RND : costj = 2*RND - 1 : sintj = SQR (1 - costj*costj)
90  xj = dj*sintj*COS (fj) : yj = dj*sintj*SIN (fj) : zj = dj*costj
100 rij2 = (R + xj - xi)^2 + (yj - yi)^2 + (zj - zi)^2
110 rij6 = rij2^3
120 sum = sum + 1/rij6
130 NEXT i
140 PRINT "AV.inverse-six-power=", sum/n
150 PRINT "F series=", sum/n*(R^6)
```

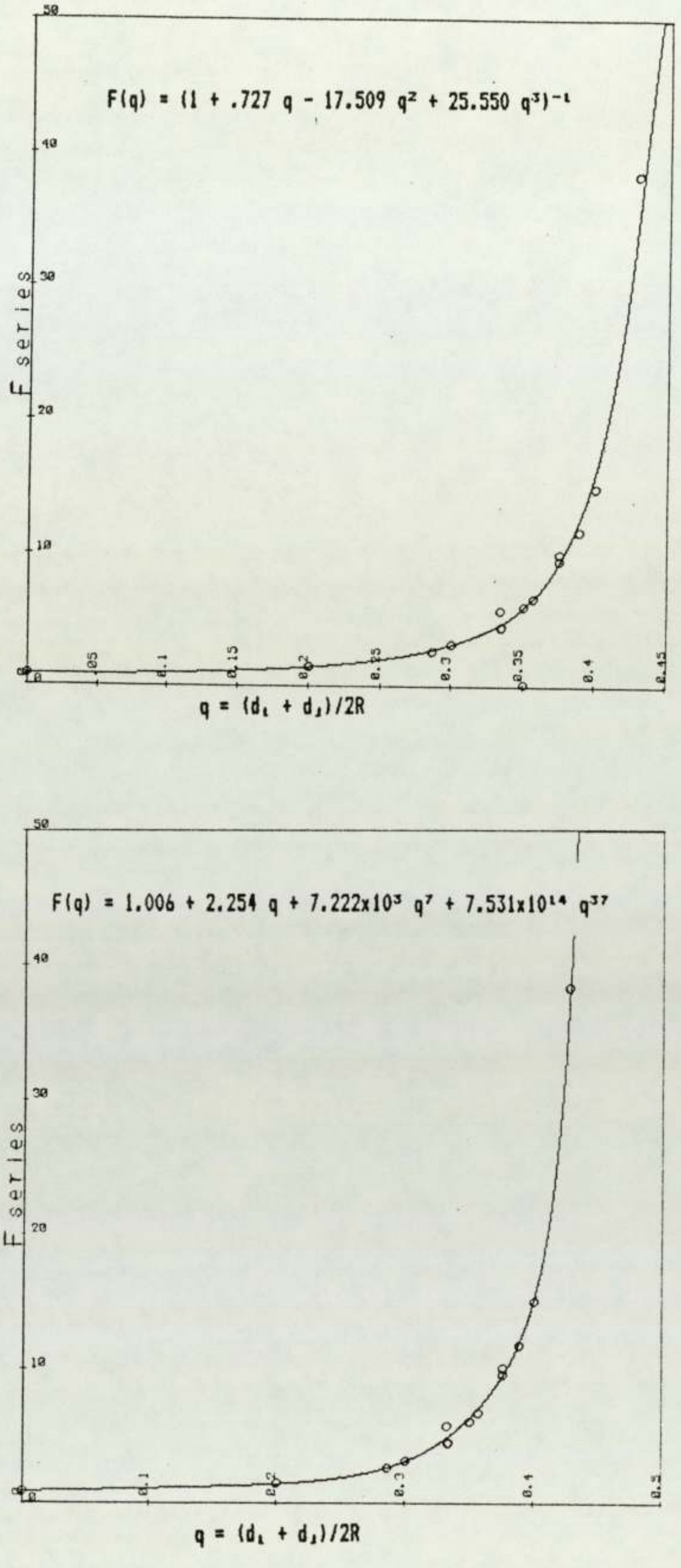

Fig. A4.1. The best-fit to the F-q data from table 3.1.

Appendix 5 The Centre-Of-Mass to Atom Distance, d

The distance from the centre-of-mass of a molecule to the buffeting, d_j, or buffeted, d_i, atom is the only structural or molecular shape parameter in the polyatomic formulations. This distance distinguishes the location of the atom from the CM of the molecule because the CM is assumed to be the centre of molecular rotation.

For diatomic molecules X_2, d equals half of the X-X bond length. For diatomic molecules of type XY, of bond length r the law of the lever gives;

d_x d_y
X----------|-------Y $m_x d_x = m_y (r - d_x)$
m_x CM m_y
<------- r ------>

from which d_x and d_y can be worked out. For CO of r = 1.13 A for example, this procedure gives the values given in table table A5.1. The bonds length of the symmetric molecules like XY_4, XY_3, XY_2 equals d_y and that of d_x equals zero (the values of $d_x = 0$ are not given in table A5.1).

For molecules like X_4, CX_3Y and $X(CH_3)_4$ the d values can be calculated exactly using bond lengths and bond angles (from Ref. 158) and a method given by Moelwyn-Hughes[69,pp. 501-510].

The d values of more complicated molecules such as $X(CH_2CH_3)_4$ hydrocarbons, and CX_2Y_2 can be found by approximate graphical methods as depicted in Fig. A5.1 for $SnEt_4$.

Table A5.1 gives the d values used in the calculations of H_v and σ_r, and the simple molecules of Chapter 6.

Table A5.1. The Centre-Of-Mass to the Atom Distance, d^*

Molecule	d_* A	Molecule	d_* A	Molecule	d_* A	Molecule	d_* A
H_2	.373	CH_3Br		CH_2BrCl		CH_3OH	
N_2	.549	H	2.19	H	2.2	H (OH)	1.35
O_2	.604	Br	.316	Br	.92	H (CH_3)	1.32
CO		C	1.621	Cl	2.08	O	.688
C	.646	CH_2Br_2		C	1.25	C	.738
O	.484	H	2.25	$CHClBr_2$		CH_3CN	
N_2O		Br	1.62	H	2.1	H	1.82
N	1.19	C	1.18	Cl	2.8	C (CH_3)	1.28
N	.10	$CHBr_3$		Br	1.8	C (CN)	.159
O	1.12	H	1.633	C	1.0	N	1.317
H_2O		Br	1.834	CCl_3Br		$C(NO_2)_4$	
H	.92	C	.565	Cl	1.97	O	2.3
O	.065	CH_3I		Br	1.442	N	1.47
D_2O		H	2.446	C	.494	c-C_5H_{10}	
D	.892	I	.231	CF_2Cl_2		H	1.9
O	.117	C	1.899	F	1.38	C	1.54
SO_2		CH_2I_2		Cl	.42	C_6H_{12}	
O	1.30	H	2.3	C	.63	H	2.21
S	.358	I	1.8	$CFCl_3$		C	1.54
Cl_2	.994	C	1.3	Cl	1.722	C_6H_6	
Br_2	1.145	CH_2Cl_2		F	1.609	H	2.46
I_2	1.331	H	2.2	C	.169	C	1.39
P_4	1.353	Cl	1.5	C_2H_4		c-C_4F_8	
S_8	2.124^+	C	.81	H	.50	F	2.48
$TiCl_4$	2.426	$CHCl_3$		C	.668	C	1.10
SnI_4	2.736	H	1.572	C_2H_6		CH_3CCCH_3	
CBr_4	1.93	Cl	1.673	H	1.52	H	2.50
		C	.502	C	.768		

(continued)

Molecule	d_* A	Molecule	d_* A	Molecule	d_* A	Molecule	d_* A
Me_2CCMe_2		CMe_4		$SiMe_4$		$GeMe_4$	
H	2.55	C (CH_3)	1.54	C	1.865	C	1.98
$SnMe_4$		$PbMe_4$		$C(CH_2CH_3)_4$		$Si(CH_2CH_3)_4$	
C	2.143	C	2.29	H (CH_3)	2.9	H (CH_3)	3.25
$Sn(CH_2CH_3)_4$		$Si(OCH_3)_4$		H (CH_2)	2.15	H (CH_2)	2.5
H (CH_3)	3.45	H	3.0	C (CH_3)	2.6	C (CH_3)	2.85
H (CH_2)	2.73	C	2.5	C (CH_2)	1.54	C (CH_2)	1.865
C (CH_3)	3.0	O	1.504	$Si(OCH_2CH_3)_4$			
C (CH_2)	2.143			H (CH_3)	3.75		
				H (CH_2)	3.0		
				C (CH_3)	3.37		

*: Note that the d values of peripheral atoms given in table 3.3 are not reproduced here.

+: This is the S-S bond length from Ref.[330], which by the symmetry of S_8 ring also equals d_S.

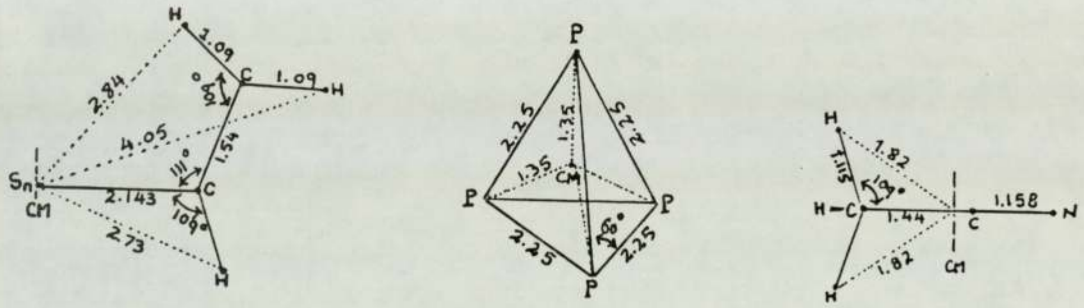

$Sn(CH_2CH_3)_4$

$d_H(CH_2)$ = 2.73 A

$d_H(CH_3)$ = (2.84 + 4.05)/2 = 3.45 A

P_4

d_P = 1.35

CH_3CN

d_H = 1.82

d_C = .16; d_C = 1.28

d_N = 1.317

(a) (b) (c)

Fig. A5.1. The CM to atom distance, d (dotted lines).

(a): A 2-dimentional graphical method

(b) and (c): A geometric method due to Moelwyne-Hughes.

Appendix 6 Attributes of the Interacting Bonded Atoms

According to the atom-atom potential model each species, namely bonded-atom, π-electron, or lone-pair electron, takes part in the dispersion interation with three attributes. These are its location in the molecule d, its moment $\langle m^2\rangle_{inert}$, and its share of the polarizability or the polarizability contribution (Pc). The two former attributes have been previously discussed. The latter attribute, Pc, however, deserves some amplification.

Let us take the case of P_4 which has a molecular polarizability of $\alpha = 14.7\ A^3$ (found from its refractive index). The share of the polarizability of each bonded phosphorus atom is obviously $Pc(P) = 3.675\ A^3$. This value now can be used with $Pc(Cl) = 2.305$ found from $\alpha(Cl_2) = 4.61\ A^3$, for example, to estimate the molecular polarizability of 10.59 for PCl_3, in agreement with $\alpha = 10.4\ A^3$ (from table 3.6).

Once the Pc of a species is found, it can generally be used for that species in differentmolecular environments. The Pc values in table A6.1 supplement the list given in sec. 3.4 for the computations of the molecular potentials; For the buffeting fields, as expressions (3.9) and (5.1) show, there is no need for Pc's.

Note that the values given in this table have been found from the molecular polarizabilities (with the exception of those given in sec. 3.4 and those of F^-, C^-, and S^-; the Pc values of Cl^- and S^- are given for completeness only).

For Si, Ge, Sn, and Pb, for example, the values of $\alpha(X(CH_3)_4)$

have been used with the values of Pc for H and C as;

$Pc(X) = \alpha(X(CH_3)_4) - 4\ Pc(C) - 12\ Pc(H)$

where X = Si, Ge, Sn, and Pb.

Table A6.1. Polarizability Contributions of some Species

Species	H	C	$C^+(CF_4)$		$C=$	$C\equiv$	$C^{\cdots}$	N	N^-	O (O-H)
Pc A^3	.43	.93	.185		.58	.86	1.302	1.03	1.865	.59
Species	O (R-O-R)	O (C=O)	F	F^-	Si	Si^+	P	S	S (C=S)	$S^+(SF_6)$
Pc A^3	.64	.84	.38	.985*	3.02	1.205	3.675	2.82	3.99	1.645
Species	S^-	Cl	Cl^-	Ge	Br	Sn	I	Pb	Hg	
Pc A^3	8.94+	2.305	3.60+	3.92	3.39	5.52	5.11	7.02	5.1	

*: Refs.[321,331]; +: Ref.[331]

The Pc of the aromatic carbon ($C^{\cdots}$) is found from $\alpha(C_6H_6)$ and Pc(H). For ions like C^+, Si^+, and S^+ in $F_3C^+F^-$, $F_3Si^+F^-$ and $F_5S^+F^-$, the molecular polarizabilities, Pc(F) and Pc(F^-) are used. The Pc of C^+ in CF_4 ($F_3C^+F^-$), for example, can be found as;

$Pc(C^+) = \alpha(CF_4) - 3\ Pc(F) - Pc(F^-)$

$Pc(C^+) = 2.31 - 3\times.38 - .985 = .185\ A^3$

The Pc values of the table should be used judiciously for accurate calculations of H_v. The value of Pc(H) = .43 A^3, a reasonable value for hydrocarbon for example, is unsuitable for H_2, because it gives $\alpha(H_2) = .86$ in poor agreement with the experimental value of .82 A^3. In this case (and also for Cl_2, Br_2, and CCl_4) α(Expt.) is used to arrive at Pc(H) = .41.

The same is true for the Pc(C^+) in C_4F_8 and C_6F_6 in which case

$Pc(C^+)$ = .325 and .655 A^3 are found respectively.

Calculations of H_v and σ_w

It will be recalled from Chapter 3 that the moment attribute of a species with ionic character (anion/cation) changes by a factor of 1/4 for each electron.

For example, $F_3C^+F^-$ with '3 species' has the following attributes;

Molecule	Species	----------- Attributes ---------		
		$\langle m^2\rangle_{inert}$	Pc A^3	d A
CF_4	C^+	$.75\langle m^2\rangle_{Ne}$	.185	0
	F^-	$1.25\langle m^2\rangle_{Ne}$	.985	1.33
	F	$3\langle m^2\rangle_{Ne}$	.38	1.33

The attributes for some of the molecules with extra electrons, along with some comments are given below.

CS_2	(a)	C	$\langle m^2\rangle_{Ne}$	.93	0
		S	$3\langle m^2\rangle_{Ar}$	3.99	1.558

Comments: There are 2S atoms plus two pairs of π-electron equivalent to one $\langle m^2\rangle_{Ar}$. Two points should be noted here. First, the centre of the π-electron is assumed to be at the S atom, which explains the use of $d_\pi = 1.558 = d_S$. This is not strictly correct; for more accurate calculations the centre of the π-electron should coincide with that of the C-S bond;

CS_2	(b)	C	$\langle m^2\rangle_{Ne}$	.93	0
		S	$2\langle m^2\rangle_{Ar}$	2.82	1.558
		π	$\langle m^2\rangle_{Ar}$	1.99	.779

where $Pc(\pi) = 1.99$ A^3 is found from $\alpha(CS_2)$, Pc(C) and Pc(S).

The second point concerns the moment of π-electron which for CS_2 is assumed to be equivalent to that of Ar. For SO_2 the moment of π-electron is that of the Ne, the outer atom, because in this way the molecular moment can be calculated with accuracy from the inert-atom moments.

It therefore appears that the dispersion power of the π-electron depends on the nature of the atoms in the double bond.

It is interesting to note that (3.25) with the attributes in (b) for the R value of 5.86 A, found from H_v(Expt.) and the attributes in (a), gives H_v(Cal.) = 12.00 KJ/mole. This is short of the experimental value by 14 KJ/mole, showing the importance of the buffeting location of the π-electron system. The experimental H_v can be calculated for the attributes in (b) and R = 5.3 A, a value close to $R_{.17} = 5.16$. This argument goes equally well for benzene for which the π-electron system is centred at the cabon atom.

CH_3CN	H	$3\langle m^2\rangle_{He}$	.43	1.82
	C (CH_3)	$\langle m^2\rangle_{Ne}$	.93	1.28
	C (CN)	$\langle m^2\rangle_{Ne}$	.93	.159
	N	$2\langle m^2\rangle_{Ne}$	1.03	1.317

Comments: Here again the π-electron is located at N. The molecular plarizability of $\alpha = 4.274$[69], 4.45[214], 4.35 (from refractive index) and I(ev) = 12.2[158] give;

$\langle m^2\rangle$(Mole.) $\simeq$ 125.14

which compares well with those calculated from inert-atom rule on the basis of structures;

$CH_3-C\equiv N$ $\langle m^2\rangle_E = 118.13$

$H^+CH_2=C=N^-$ $\langle m^2\rangle_E = 120.20$

Using the above attributes and R = 4.75 or 4.8 A (in agreement with $R_{.17}$ = 4.9 A from molar volume at 20 °C) with (3.25) the exact experimental heat of vaporization can be calculated, which signifies the minor role of dipolar effects in the cohesion energy in the <u>absence of hydrogen</u> bonding.

$C(NO_2)_4$	C	$\langle m^2\rangle_{Nw}$	.93	0
	N	$4\langle m^2\rangle_{Nw}$	1.03	1.47
	O	$11\langle m^2\rangle_{Nw}$	.84	2.3

Comments: The molecular α = 12.5 A^3 (from its refractive index) and I(ev) = 10.94[158] give;

$\langle m^2\rangle$(Mole.) = 328.12

Type (a) $\langle m^2\rangle_E$ = 347.6

Type (c) $\langle m^2\rangle_E$ = 327.12

where structure (c) with $.75\langle m^2\rangle_{Nw}$ for the π-electron system gives the exact molecular moment and is therefore suggested as an alternative to the conventional resonance types (a) and (b) with $1\langle m^2\rangle_{Nw}$ and $.5\langle m^2\rangle_{nw}$ for the π-system respectively;

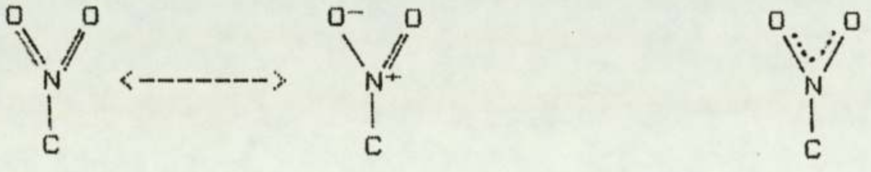

(a) (b) (c)

C_2H_4	C	$2.5\langle m^2\rangle_{N-}$	1.72	.668
	H	$4\langle m^2\rangle_{H-}$	.43	1.5

Comments: The Pc(C=) = 1.72 A^3 for double bond carbon, at variance with that given in table A6.1 from Ref.[161], is found from the molecular polarizability of 4.26[49] using Pc(H) = .43. For R = 4.82 A the double bond contributes about 2.25 KJ/mole to the total cohesion energy of C_2H_4 (for π-electron at C).

C_6H_{12}	C	$6\langle m^2\rangle_{N-}$	.93	1.54
	H	$12\langle m^2\rangle_{H-}$	.43	2.21

Comments: The d value of 2.21 A is the mean of d_H(Equt.) = 2.49 and d_H(Axial) = 1.93. Such attributes for R = 6.34 A give H_v = 26.83 KJ/mole, about four units short of the experimental value. The d attributes assume a flat molecule whereas the real molecule at any instance of time has the well-known chair (and boat) conformations with six equatorial hydrogen at a larger distance from the CM. By accounting for this fact and treating hydrogens as different species the correct cohesion energy can be found (29.89 KJ/mole), once again showing the sensitivity of the polyatomic potential to the liquid state structure.

References

1. Van Vleck J.H. "The Theory of Electric and Magnetic Susceptibilities" Oxford University Press, Oxford, 1965.
2. Partington J.R. "An Advanced Treatise on Physical Chemistry" Longmans, Green and Co., London, 1953, Vol. 4.
3. Bottcher C.J.F. "Theory of Electric Polarization" Elsevier, Amsterdam, 1973, Vol. 1.
4. Partington J.R. "An Advanced Treatise on Physical Chemistry" Longmans, Green and Co., London, 1954, Vol. 5.
5. Lorentz H.A. "Theory of Electrons" Dover, New York, 1952, P. 78.
6. Drude P.K.L. "Theory of Optics" Longmans, Green and Co., London, 1933.
7. Cook O. "The Theory of Electromagnetic Field" Prentic-Hall, Englewood Cliffs, 1975.
8. Good JR R.H. and Nelson T.J. "Classical Theory of Electric and Magnetic Fields" Academic Press, New York, 1971.
9. Debye P. "Polar Molecules" Dover, New York, 1945, pp. 78, 116.
10. Van Vleck J.H. "Phys. Rev." 29, 727, 1927; 30, 31, 1927.
11. Fowler R.H. "Statistical Mechanics" Cambridge University Press, 1966.
12. Zahn C.T. and Miles J.B. "Phys. Rev." 32, 502, 1928.
13. Van Arkel A.E.V. and Snoek J.L. "Trans. Faraday Soc." 30, 707, 1934.
14. Onsager L. "J. Amer. Chem. Soc." 58, 1486, 1936; see also, Van Vleck J.H. "J. Chem. Phys." 5, 320, 1937; Wilson J.N. "Chem. Rev." 25, 377, 1939.
15. Martin A.R. "Phil. Mag." 8, 550, 1929; "Trans. Faraday Soc." 33, 191, 1937; "Trans. Faraday Soc." 34, 742, 1938; Bell R.P. "Trans. Faraday Soc." 31, 1553, 1931.
16. Linder B. "J. Chem. Phys." 33, 668, 1960.
17. Rummens F.H.A. "Van der Waals Forces in NMR Intermolecular Shielding " Vol. 10 of NMR Basic Principles and Progress. Edi. by Diehl P., Fluck E. and Kosfeld R. Springer-Verlag, Hieldelberg 1976.

18 Linder B. "J. Chem. Phys." 37, 963, 1962.

19. Linder B. "Adv. Chem. Phys." 12, 225, 1976
20. Frohlich H. "Theory of Dielectrics" Oxford at Clarendon Press, 1958, 2nd. Edi.
21. Sinaoglv O. and Abdulnur S. "Photochemistry and Biology" 3, 333, 1964.
22. Buckingham A.D., T. Schaefer and W.G. Schneider "J. Chem. Phys." 32, 1227, 1960; Buckingham A.D. "Can. J. Chem." 38, 300, 1960; McRae E.G. "J. Phys. Chem." 61, 562, 1957.
23. Weigang O.E. Jr. "J. Chem. Phys." 41, 1435, 1964.
24. Howard B.B., Linder B. and Emerson M.T. "J. Chem. Phys." 36, 485, 1962.

25. Lumbroso N., Wu T.K. and Dailey B.P. "J. Phys. Chem." 67, 2469, 1963.

26. Rummans F.H.A. "Chem. Phys. Lett." 31, 596, 1975.

27. Rummans F.H.A. "Can. J. Chem." 54, 254, 1976.

28. Barriol J. and De Montgolfier ph. "Compt. Rend. Acad. Soc. Paris" 262C, 1638, 1966.

29. Homer J. and Percival C.C. "J. Chem. Soc. Faraday Trans 2" 80, 1, 1984.

30. Scafe B.K.P. "Complex Permitivity" The English University Press, 1971.

31. Landau L.D., Lifshitz E.M. and Pitaevskii I.D. "Electrodynamic of Continuous Media" Pergamon Press, Oxford, 1984.

32. Feynman R.P., Leighton R.B. and Sands M. "Lectures on Physics" Addison-Wesley, Reading, 1963, Vol. 1.

33. Kreyszig E. "Advance Engineering Mathematics" Wiley and Sons, New York, 1979, 4th. Edi.

34. Schetzen M. "The Voltra and Wiener Theories of Nonlinear Systems" Wiley-Interscience, New York, 1980.

35. DiStephano J.J., Stybberud A.R. and Williams I.J. "The Theory and Problems of Feedback and Control Systems" Schaum's Outline Series, McGraw-Hill, New York, 1967, Chapter 3.

36. Zeldovich Y.B. and Myskis A.D. "Elements of Applied Mathematics" Mir Publishers, Moscow, 1976, Chapter 6.

37. Roach G.F. "Green's Functions" Van Nostrand Reinhold, London, 1970.

38. Chambers L.G. "Integral Equations, a short course" International Textbook Company, London, 1976.

39. Reid J.G. "Linear System Fundations, Continuous and Discrete, Modern and Classic" McGraw-Hill, New York, 1983.

40. Papoulis A. "Circuits and Systems, a Modern Approach" Holt,Rinehart and Winston, New York, 1980.

41. Gaskill J.D. "Linear Systems, Fourier Transforms and Optics" Wiley and Sons, New york, 1978, Chapter 5.

42. Pippard A.B. "The Physics of Vibrations" Cambridge University Press, 1978, Chapter 4.

43. Lifshitz E.M. and Pitaevskii L.P. "Statistical Physics" Pergamon Press, Oxford, 1980, Part 1, 3rd Edi. Chapter 12.

44. Bracenell R.N. "The Fourier Transform and its Applications" McGraw-Hill, New York, 1978, 2nd. Edi.

45. Pathria R.K. "Statistical Mechanics" Pergamon Press, Oxford, 1972, Chapter 13.

46. Lindsay R.B. "Introduction to Physical Statistics" Dover, New York, 1941, p. 13.

47. Reif F. "Fundamentals of Statistical Physics" McGraw-Hill, New York, 1965, Chapter 1.

48. McFanned J.A. "Physical Concepts of Probability" Van Nostrand Reinhold, New York, 1971, Chapter 4.

49. Hirschfelder J.G., Curtiss C.F. and Bird R.B. "Molecular Theory of Gases and Liquids" Wiley and Sons, New York, 1954.

50. Burkhard H. "Dispersion Relation Dynamics" North-Holland Publishing Co., Amsterdam, 1969, Chapter 8.

51. Anderson E.E. "Modern Physics and Quantum Mechanics" W.B. Saunders Co., 1971, Chapter 4.

52. Reichl L.E. "A Modern Course in Statistical Physics" Edvard Arnold Publishers, London, 1980.

53. Ditchburn R.W. "Light" Blackie and Sons, London, 1963.

54. Bendat J.S. "Principles ann Applications of Random Noise Theory" Wiley and Sons, New York, 1958.

55. Titchmarsh E.C. "Introduction to the Theory of Fourier Integrals" Oxford Clerendon Press, 1948, 2nd. Edi.

56. Rayleigh W. "Phil. Mag." Sers. 5, <u>27</u>, 460, 1889.

57. Mitrinovic D.S. "Elementary Inequalities" P. Noordhoff Ltd., Groningen the Netherland, 1964.

58. Hardy G.H., Littlewood J.E. and Polya G. "Inequalities" Cambridge Press, Cambridge, 1952, 2nd. Edi.

59. Lengyel B.A. "Advances in Quantum Chemistry" Edit. by Lowdin P.O., Academic Press, New York, 1968, pp. 1-10.

60. Mikhlin S.G. "Variational Methods in Mathematical Physics" Pergamon Press, Oxford, 1964, Chapter 1.

61. Tsokos C.P. "Random Integral Equations with Application to Life Science and Engineering" Academic Press, New York, 1974, Chapter 1.

62. Schroder J. "Operator Inequality" Academic Press, New York, 1980, pp. 57, 319.

63. Schiff L.I. "Quantum Mechanics" McGraw-Hill, New York, 1955, 3rd. Edi., Chapter 12.

Bohm A. "Quantum Mechanics" Springer-verlag, New York, 1979, Chapters 1 and 2.

Merzbacher E. "Quantum Mechanics" Wiley and Sons, New York, 1961, Chapters 8 and 15.

Shankar R. "Principles of Quantum Mechanics" Plenum Press, New York, 1980, Chapters 1 and 9.

64. Tricomi F.G. "Integral Equations" Wiley-Interscience, New York, 1957.

65. Nylor A.W. and Sell G.R. "Linear Operators Theory in Engineering and Science" Holt, Rinehart and Winston, New York, 1971, Part B, pp. 272-4.

66. Toll J.S. "Phys. Rev." <u>104</u>, 1760, 1956.

67 Haken H. "Light" North-Holland Publ. Co., Amsterdam, 1981, Vol.1, Chapters 1 and 9.

68. Kauzmann W. "Quantum chemistry, an Introduction" Academic Press, New York, 1957, Chapters 15 and 16.

69. Moelwyn-Hughes E.A. "Physical Chemistry" Pergamon Press, Oxford, 1961, 2nd. Revised Edi.

70. Ref.32, Vol. 2. 1964.

71. Margenau H. and Kestner N. R. "Theory of Intermolecular Forces" Pergamon Press, Oxford, 1969, 2nd. Edi.,

72. Prosen E.J.R. and Sachb R.G. "Phys. Rev." <u>61</u>, 65, 1942.

73. Slater J. "Quantum Theory of Matter" McGraw-Hill, New York, 1951, 1st. Edi., p. 251.

74. Mott N.F. and Sneddon I.N. "Wave Mechanics and its Applications" Oxford at Clarandon, 1948, p. 164.

75. Buckingham A.D. "Faraday. Soc. Trns." 52, 1035, 1956.

76. Bothner-By A.A. "J. Mol. Spectroscopy" 5, 52, 1960.

77. Yonemoto T. "Can. J. Chem." 44, 223, 1966.

78. Raynes W.T., Buckingham A.D. and Bernstein H.J. "J. Chem. Phys." 36, 3481, 1962.

79. Bernstein H.J. and Raynes W.T. "Presented at the NMR Symposium Boulder (Colorado)" July 1962; (Ref. 43 in Ref. 17).

80. Rummens F.H.A. and Bernstein H.J. "J. Chem. Phys." 43, 2971, 1965.

81. London F. "Trans. Faraday Soc." 33, 8, 1937.

82. Jackson J.D. "Classical Electrodynamics" Wiley and Sons, New york, 1967, p. 226.

83. Landau L.D. and Lifshitz E.M. "The Classical Theory of Fields" Pergamon Press, Oxford, 1975.

84. Hirschfelder J.D. and Meath W.J. "Adv. Chem. Phys." 12, 63, 1967.

85. McChesney M. "Thermodynamics of Electrical Processes" Wiley-Interscience, New York, 1971, Chapter 6.

86. Johnson J.B. "Nature" 119, 50, 1927; "Phys. Rev." 29, 367, 1927.

87. Johnson J.B. "Phys. Rev." 32, 97, 1928.

88. Nyquist H. "Phys. Rev." 32, 110, 1928.

89. Gopal E.S.R. "Statistical Mechanics and Properties of Matter" Ellis Horwood Ltd., Chichester, 1974, p. 284.

90. Jamieson J.A. "Infrared Physics and Engineering" McGraw-Hill, New York, 1963, Chapter 10.

91. Van der Ziel A. "Noise in Measurements" Wiley-Interscience, London, 1976, p. 41.
"Noise, Sources, Characterization, Measurement" Prentice-Hall, Englwood Cliffs, N.J., 1970, PP. 24, 39.

92. Hoult D.I. and Lauterbur P.C. "J. Mag. Res." 34, 425, 1979.

93. Lerski R.A. (Edit.) "Physical Principles and Clinical Applications of Nuclear Magnetic Resonance" The Hospital Physicist Association, London, 1985, P. 35.

94. Hoult D.I. and Richards R.E. "J. Mag. Res." 24, 71, 1976.

95. Beck A.H.W. "Statistical Mechanics, Fluctuations and Noise" Edward Arnold, London, 1976.

96. Wax N. (Edit.) "Selected Papers On Noise and Statistical Processes" Dover, New York, 1954.

97. Einstein A. "Investigations on the Theory of the Brownian Movement" Edit. by Furth R. , Dover, New York, 1956.

98. Bacertein R. "Atoms and Information Theory" W.H. Freeman & Co., San Fransisco, 1917.

99. Kubo R. "Statistical Mechanics" North Holland Publ. Co., Amsterdam, 1965.

100. Callen H.B. and Walton T.A. "Phys. Rev." 83, 34, 1951; Kubo R. "J. Phys. Soc. Japan" 12, 570, 1957.

Takahashi H. "J. Phys. Soc. Japan" 7, 439, 1952; Bernard W. and Callen H.B. "Rev. Mod. Phys." 31, 1017, 1959; For a critical study of FDT see Ref. 101.

101. Case K.M. "Trans. Theory and Stat. Phys." 2, 129, 1972.

102. Perrin J. "Brownian Motion and Molecular Reality" Taylor and Francis, London, 1910.

103. Barnes R.B. and Silverman S. "Rev. Mod. Phys." 6, 162, 1934.

104. Landsberg P.L.T. (Edit.) "Problems in Thermodynamics and Statistical Physics" Pion Ltd., London, 1971.

105. Welton T.A. "Phys. Rev." 74, 1157, 1948; Weissokopf V.F. "Phys. Rev." 56, 72, 1939.

106. Louisell W.H. "Quantum Statistical Properties of Radiation" Wiley and Sons, New York, 1973, Chapter 4.

107. Jehle H., Jerrold M.Y. and Bade N.L. "Phys. Rev." 110, 793, 1958.

108. McConnell J. "Rotational Brownian Motion and Dielectric Theories" Academic Press, London, 1980.

109. Dickinson W.C. "Phys. Rev." 81, 717, 1951.

110. Dickinson W.C. "Phys. Rev." 80, 563, 1950.

111. Anderson H.L. "Phys. Rev."76, 1460, 1949.

112. Debye P. "Physik. Z." 13, 97, 1912.

113. Slichter C.P. "Principles of Magnetic Resonance" Harper and Row, London, 1963, p. 100.

114. Elliott R.S. "Electromagnetics" McGraw-Hill, New York, 1966, Chapter 6 and 7.

115. Brown W.F. "Micromagnetics" Wiley and Sons, New York, 1963, Chapter 1.

116. Bozorth R.M. "Feromagnetism" Van Norstrand, New Jersey, 1951, Chapter 19.

117. Watson R.E. and Freeman A.J. "Phys. Rev." 123, 2027, 1961.

118. Brown W.F. and Morrish A.H. "Phys. Rev." 105, 1198, 1957.

119. Mattis D.C. "The Theory of Magnetsm, Statics and Dynamics" Springer-Verlag, New York, 1981, Chapter 5.

Heck C. "Magnetic Materials and Their Applications" Butterworths, London, 1974, p. 82.

120. Cullity B.D. "Introduction to Magnetic Materials" Addison-Wesley, Reading, 1972, p. 49.

121. Andrew E.R. "Nuclear Magnetic Resonance" Cambridge at the University Press, 1955, PP. 78 and 79.

122. Bloembergen N. and Dickinson W.C. "Phys. Rev." 79, 179, 1950.

123. Ayant Y. "C.R. Acad. Sci. Paris" 232, 1203, 1951; 232, 1298, 1951; 232, 1094, 1951.

124. Chelkowski A. "Dielectric Physics" Elsevier, Amsterdam, 1980, PP 15, 30, 367.

125. Livens G.H. "Phil. Mag." 25, 817, 1913; 26, 535, 1913; 27, 468, 1914.

Van Vleck J.H. "J. Chem. Phys." 5, 556, 1937; Darwin "Proc. Roy. Soc." 146, 17, 1934.

126. Rayleigh W. "Phil. Mag." 34, 481, 1892; Van Rysselberghe P. "J. Phys. Chem." 36, 1152, 1932;

Brown G.B. "Phil. Mag."34, 26, 1943.

127. Bothner-By A.A. and Glick R.E. "J. Chem. Phys." 26, 1647, 1957.

128. Bothner-By A.A. and Glick R.E. "J. Amer. Chem. Soc." 78, 1071, 1956.

129. Bothner-By A.A. and Glick R.E. "J. Chem. Phys." 26, 1651, 1957.

130. Glick R.E., Kates D.F. and Eherson S.J. "J. Chem. Phys." 31, 567, 1959.

131. Stephen M.J. "Mol. Phys." 1, 223, 1958.

132. Dailey B.P. and Shoolery J.N. "J. Amer. Chem. Soc." 77, 3977, 1955.

133. Glick R.E. and Eherenson S.J. "J. Chem. Phys." 62, 159, 1958.

134. Bothner-By A.A. "J. Mol. Spec." 5, 52, 1960.

135. Marshall T.W. and Pople J.A. "Mol. Phys." 1, 199, 1958.

136. Stephen M.J. "Mol. Phys." 1, 223, 1958.

137. Marshall T.W. and Pople J.A. "Mol. Phys." 3, 399, 1960.

138. Kromhout R.A. and Linder B. "J. Mag. Resonance" 1, 450, 1969.

139. Jameson A.K., Jameson C.J. and Gutowsky H.S. "J. Chem. Phys." 53, 2310, 1970.

140. Potter D. "Computational Physics" Wiley and Sons, New York, 1973, p. 136.

141. Kirkwood J.G. "J. Chem. Phys." 7, 911, 1939.

142. Jaffe G. "J. Chem. Phys." 8, 879, 1940.

143. Rummens F.H.A. "J. Chim. Phys." 72, 448, 1975.

144. De Montgolfier P. "J. Chim. Phys." 64, 639, 1967.

145. De Montgolfier P. "J. Chim. Phys." 66, 685, 1969.

146. Chenon M. "J. Chim. Phys." 67,1252, 1970.

147. McRae E.G. "J. Phys. Chem." 61, 562, 1957.

148. Eyring H. (Edit.) "Physical Chemistry, an Advanced Trearise" Academic Press, New york, 1971, Vol. 8A, P. 336.

149. De Montgolfier P. "Compt. Rend. Acad. Sci. Paris" 263c, 505, 1966.

150. Sinanoglu O. "Adv. Chem. Phys." 12, 283, 1967.

151. Pitzer K.S. "Adv. Chem. Phys." 2, 59, 1959.

152. Pitzer K.S. "J. Am. Chem. Soc." 78, 4565, 1956.

153. Rummens F.H.A. "Mol. Phys." 21, 535, 1971.

154. Williams J.W. "Phys. Z." 29, 686, 1928.

155. Williams J.W. "J. Am. Chem. Soc." 59, 2350, 1928.

156. Huggins M.L. and Hendricks S.B. "J. Am. Chem. Soc." 48, 164, 1926.

157. Raynes E.T. "J. Chem. Phys." 51, 3138, 1969.

158. "Handbook of Physical Chemistry and Physics" CRC Press, Cleveland, Ohio, 1972-1973, 53rd. Edi.

159. Rummens F.H.A., Raynes W.T. and Bernstein H.J. "J. Phys. Chem." 72, 2111, 1968.

160. Percival C.C. "Ph.D. Thesis" University of Aston in Birmingham, 1981.

161. Bretsznajder S. "Prediction of Transport and other Physical Properties of Fluids" Pergamon Press, Oxford, 1971.

162. Abraham R.J., Wileman D.F. and Bedford C.R. "J. Chem. Soc." Perkin II, 1027, 1973.

163. Raynes W.T. and Raza M.A. "Mol. Phys." 17, 157, 1969.

164. Watanabe K. "J. Chem. Phys." 26, 541, 1957.

165. Raynes W.T. and Raza M.A. "Mol. Phys." 20, 555, 1971.

166. Gordow A.J. and Ford R.A. " The Chemist's Companion" Wiley-Interscience, New York, 1972.

167. Condon E.u. and Odishaw H. "Handbook of Physics" McGraw-Hill, New York, 1967.

168. Lefevre C.G. and Lefevre R.J.W. "Revs. of Pure and Applied Chem." 5, 261, 1955.

169. Stuart H.A. and Volkmann H. "Ann. Phys." 18, 121, 1933.

170. Vogel A.I. "J. Chem. Soc." 1833, 1948.

171. Izsak D. and Lefevre R.J.W. "J. Chem. Soc." B, 102, 1966.

172. Lefevre R.J.W. and Ritchie G.L.D. "J. Chem. Soc." 4933, 1963

173. Stuart H.A. and Schiezl S.V. "Ann. Phys." 2, 321, 1948.

174. Ramaswamy K.L. "Proc. Indian Acad. Sci." A4, 675, 1936.

175. Timmermans J. "Physico-chemical Constants of Pure Organic Compounds" Elsevier, New York, 1950.

176. Weissberger A. "Organic Solvents" Wiley-Interscience, New york, 1955, 2nd. Edi.

177. Bridge N.J. and Buckingham A.D. "Proc. Roy. Soc." A295, 334, 1966.

178. Hine J., Dowell A.D. and Singley J.E. "J. Am. Chem. Soc." 78, 479, 1956.

179. Miller R.C. and Smyth C.P. "J. Chem. Phys." 24, 814, 1956.

180. Raza M.A. and Raynes W.T. "Mol. Phys." 19, 199, 1970.

181. Heckmann G. and Fluck E. "Mol. Phys." 23, 175, 1972; "Naturforschung" B24, 1092, 1969; B26, 63, 1971.

182. Venkateswaran C.S. "Proc. Indian Acad. Sci." A2, 260, 1935.

183. Maxwell L.R., Hendricks S.B. and Mosley V.M. "J. Chem. Phys." 3, 699, 1935.

184. Beattie I.R., Ozin G.A. and Perry R.O. "J. Chem. Soc." A, 2071, 1970.

185. Cotton F.A. and Wilkinson G. "Advanced Inorganic Chemistry" Wiley-Interscience, New York, 1972, P. 370.

186. Corbridge D.E.C. "Phosphorus" Elsevier, Amsterdam, 1978, chapter 2.

187. Frei K. and Bernstein H.J. Table 39 in Ref. 17.

188. Cyr N., Raza M.A. and Reeves L.W. "Mol. Phys." 24, 459, 1972.

189. Homer J. and Al-Daffaee H.K. "J. Chem. Soc. Faraday Trans. 2" 81, 803, 1985.

190. Brinkmann D. "Phys. Rev. Letters" 13, 187, 1964.

191. Trappeniers N. "Physica" 17, 501, 1951.

192. Balexu R. "Physica" 2, 224, 1956.

193. Flory P.J. "J. Am. Chem. Soc. " 87, 1833, 1965.

194. Hildebrand J.H. "J. Chem. Phys." 15, 727, 1947.

195. Pitzer K.S. "J. Am. Chem. Soc." 77, 3427, 1955.

196. Hamaan S.D., McManamey W.J. and Pearse J.F. "Trans. Faraday Soc." 49, 351, 1953.

197. Rowlinson J.S. "J. Chem. Phys." 20, 337, 1952.

198. Lowden L.J. and Chandler D. "J. Chem. Phys." 61, 5228, 1974.

199. Lowden L.J. and Chandler D. "J. Chem. Phys." 59, 2742, 1973.

200. Lowden L.J. and Chandler D. "J. Chem. Phys." 59, 6587, 1973; 57, 1930, 1972.

201. Dewar M.J.S. "Topics in Current Chemistry" Springer-Verlag, New York, 1980, Vol. 93.

202. Clementi E. "Computational Aspects of Large Chemical Systems" Springer-Verlag, New york, 1980, Vol. 19 of "Lecture Notes in Chemistry", PP. 59-85.

203. Claverie P. "Intermolecular Interactions, from Diatomic to Biopolymer" Edit. by Pullman B., Wiley, New York, 1978.

204. Muller A. "Proc. Roy. Soc." A154, 624, 1936.

205. De Montgolfier P. "Compt. Rend. Acad. Sci. Paris" 295C, 2831, 1964.

206. Raynes W.T. "Mol. Phys." 17, 169, 1969.

207. Robinson R.A. and Stokes R.H. "Electrolyte Solutions" Butterworth, London, 1959.

208. Levine I. "Physical Chemistry" McGraw-Hill, New York, 1983, 2nd. Edi.

209. Duguette G., Ellis T.M., Scolies G., Watts R.O. and Klein M.L. "J. Chem. Phys." 68, 2544, 1978.

210. Kitaigorodsky A.I. "Molecular Crstals and Molecules" Academic Press, New York, 1973.

211. Moelwyn-Hughes E.A. "Chemical Statics and kinetics of Solutions" Academic press, New York, 1971.

212. Berry R.S., Rice S.A. and Ross J. "Pysical Chemistry" Wiley and Sons, New York, 1980.

213. Thomas G.D. and Gingrich N.S. "J. Chem. Phys." 6, 659, 1938.

214. Marcus Y. "Introduction to Liquid State Chemistry" Wiley and Sons, New York, 1977.

215. "American Institute of Physics Handbook" McGraw-Hill, New York, 1972, 3rd. Edi.

216. Sherwood J.N. (Edit.) "The Plastically Crystalline State" Wiley-Interscience, Chichester, 1979.
(See table 5.6 for the structure of SF_6).

217. Pollack G.L. "Rev. Mod. Phys." 36, 1748, 1964.

218. McLennan J.C. and Plummer W.G. "Phil. Mag." 7, 701, 1929.
Herzey J. and Stoner R.E. "J. Chem. Phys." 54, 2284, 1971.

219. Bolshutkin D.N. "Acta. Crystal." B28, 354, 1972.
Greer S.C. and Meyer L. "J. Chem. Phys." 51, 4583, 1969.

220. Stillwell C.W. "Crystal Chemistry" McGraw-Hill, New York, 1938.

221. Atoji M. and Lipscomb W.N. "Acta. Crystal." 7, 597, 1954.

222. Post B. "Acta. Crystal." 12, 349, 1959.

223. Post B., schwartz R.S. and Fankuchen I. "J. Am. Chem. Soc." 73, 5113, 1951.

224. Wyckoff R.W.G. "Crystal structure" Wiley-Interscience, New york, 1969, 2nd. Edi. Vol.II (SiF_4) and
Vol. VI (C_6H_6).

225. Hassel O. and Sommefeldt A.M. "Z. Phys. Chem." 40B, 391, 1938.
Murti G.S.R.K. "Indian J. Physics" 32, 460, 1958.

226. Mones A.H. and Post B. "J. Chem. Phys." 20, 755, 1952.

227. Rudmen R. and Post B. "Mol. Cryst." 5, 95, 1968.

228. Homer J. "Appl. Spect. Rev." 9(1), 1, 1975.

229. O'Kowski L.T. (Edit.) "Molecular Electro-optics" Marcel Dekker, New York, 1976, Part 1.

230. Pings C.J. "Physics of Simple Fluids" North Holland, Amsterdam, 1968;
Rahman A. "Phys. Rev." 136A, 495, 1964 , on g(R) by MONTE CARLO method;
Narten A.H. "J. Chem. Phys." 56, 5681, 1972, on g(R) of D_2O;
Woodcock L. "Chem. Phys. Letters" 10, 257, 1971, on g(R) of LiCl by MONTE CARLO method.

231. Kirkwood J.G. "J. Chem. Phys." 4, 592, 1936.

232. Kielich S. "Chem. Phys. Letters" 2, 112, 1968.

233. Kielich S. "Chem. Phys. Letters" 7, 347, 1970.

234. Hertz P. "Math. Ann." 67, 387, 1909.

235. Brand J.C.D. and Speakman J.C. "Molecular Structure, the Physical Approach" Edward Arnold, London, 1961.

236. Fox D., Labes M.M. and Weisserger A. "Physics and Chemistry of the Organic Solid State' Wiley-Interscience, New York, 1963.

237. Curtiss L.A. and Pople J.A. "J. Mol. Spect." 55, 1, 1975;

Dyke T.R. and Muenter J.S. "J. Chem. Phys." 60, 2929, 1974

Fredin L., Nelander B. and Tribbecard G. "Chem. Phys. Letters" 36, 375, 1975.

238. Buckingham A.D., Lippert E. and Ratos S.B. (Edits.) "Organic Liquids; Structure, Dynamics, and Chemical Properties" Wiley-Interscience , Chichester, 1978, P. 4.

239. Hart-Davis A. "Solids, an Introduction" Mcgraw-Hill, New York, 1975, p. 35.

240. Samsonov G.V. (Edit.) "Handbook of Physio-Chemical Properties of Elements" Oldbourne Book, London, 1968.

241. Petrakis L. and Bernstein H.J. "J. Chem. Phys." 38, 1562, 1963.

242. Burgmans A.L.J., Farrar J.M. and Lee Y.T. "J. Chem. Phys." 64, 1345, 1976.

243. Farrar J.M., Lee Y.T., Goldman V.V. and Klein M.L. "Chem. Phys. Letters" 19, 359, 1973.

244. Parson J.M., Siska P.E. and Lee Y.T. "J. Chem. Phys." 56, 1511, 1972.

245. Baker J.A., Watts R.D., Lee J.K., Schafer T.P. and Lee Y.T. "J. Chem. phys." 61, 3081, 1974.

246. Mohanty S. and Bernstein H.J. "J. Chem. Phys." 54, 2254, 1971.

247. Van Itterbeek A. "Physics of High Pressure and Condense Phase" North Holland, Amsterdam, 1965

248. Jaszunski M., Kochanski E. and Seigbahn P. "Mol. Phys." 33, 139, 1977.

249. Farrar J.M. and Lee Y.T. "J. Chem. Phys." 57, 5492, 1972.

250. Venkataraman G., Feldkamp L.A. and Sahni V.C. "Dynamics of Perfect Crystals" The MIT Press, Cambridge Mass., 1975.

251. Miller T.M. and Bederson B. "Adv. At. Mol. Phys." 13, 1, 1977.

252. Ahrens L.H. "Ionization Potentials" Pergamon Press, Oxford, 1983.

253. Gerrard W. "Gas Solubilities, Widespread Applications" Pergamon Press, Oxford, 1980.

254. Denbig K.G. "Trans. Faraday Soc. " 36, 936, 1940.

255. "Lange's Hanbook of Chemistry" McGraw-Hill, New York, 1979, 12th. Edi.

256. Goldstein L. " Ann. Phys. Paris" 9, 723, 1938.

257. Lefevre C.G. and Lefevre R.J.W. "Rev. of Pure and Applied Chem." 5, 261, 1955.

258. Bralsford R., Harris P.V. and Price W.E. "Proc. Roy. Soc." A258, 459, 1960.

259. Cohan N,V., coulson C.A. and Jamieson J.B. "Trans. Farady Soc." 53, 582, 1957;

260. Schweig A. "Chem. Phys. Letters" 1, 163, 1967.

261. Muler F. and Huiszoon C. "Mol. Phys." 34, 1215, 1977.

262. Pauling L. "J. Am. Chem. Soc." 53, 3225, 1931.

263. Harcourt R.D. "Qualitative Valence-Bond Descriptions of Electron-Rich Molecules; Pauling "3-Electron Bonds" and "Increased-Valence" Theory. Springer-Verlag, New york, 1982, Vol. 30 of "Lecture Notes in Chemistry".

264. Murrell J.N., Kettle S.F.A. and Tedder J.M. "The Chemical Bond" Wiley and Sons, Chichester, 1985, 2nd. Edi. p. 96.

265. Thomaes G. "J. Chim. Phys." 49, 323, 1952.

266. Siegbahn K. "ESCA Applied to Free molecules" North holland, Amsterdam, 1969.

267. Oae S. (Edit.) "Organic Chemistry of Sulfur" Plenum Press, New york, 1977.

268. Bargon J. (Edit.) "Computational Methods in Chemistry" Plenum press, New York, 1980, p. 65.

269. London F. "J. Chem. Phys." 46, 395, 1942.

De Bore J.H. and Heller G. "Physica" 4, 1045, 1937.

270. Slater J.C. and Kirkwood T.G. "Phys. Rev." 37, 682, 1931.

271. Kirkwood J.G. "Phys. Z." 33, 57, 1932.

272. Margenau H. "Rev. Mod. Phys." 11, 1, 1939.

273. Axilrod B.M. and Teller E. "J. Chem. Phys." 11, 299, 1943.

274. Jansen L. "Phys. Rev." 125, 1798, 1962.

275. Born M. and Huang K. "Dynamical Theory of Crystalline Lattices" Oxford at Clarendon Press, 1954.

276. Hankins D. "J. Chem. Phys." 53, 4544, 1970;

Del Bene J.E. and Pople J.A. "J. Chem. Phys." 58, 3605, 1973.

277. Del Bene J.E. "J. Chem. Phys." 55, 4633, 1971.

278. Kistenmacher H., Lie G.C., Popkie H. and Clemanti E. "J. Chem. Phys." 61, 545, 1974.

279. Novaro O. and Beltran-Lopez V. "J. Chem. Phys." 56, 815, 1972;

Novaro O. and Yanez F. "Chem. Phys. Letters" 30, 60, 1975;

kolos W. and Les A. "Int. J. Quantum Chem." 6, 1101, 1972.

280. Steed J.M., Dixon T.A. and Klemperer W. "J. Chem. Phys." 70, 4940, 1979.

281. Wasiutynski T., Van der Avoird A. and Berns R.M. "J. Chem. Phys." 69, 5288, 1978.

282. Van Nes G.J. and Vos. A. " Acta. Cryst." B33, 1653, 1977.

283. Egan C.J. and Kemp J.D. "J. Am. Chem. Soc." 59, 1264, 1937.

284. Raich J.C. and Gillis N.S. 'J. Chem. Phys." 66, 846, 1977.

Berns R.M. and Van der Avoird A. "J. Chem. Phys." 72, 6107, 1976.

285. Pauling L. "Phys. Rev." 36, 430, 1930; Frenkel J. "Acta. Physiochem. USSR" 3, 23, 1935.

286. Smyth C.P. "Physics and Chemistry of the Organic Solid State" Wiley-Interscience, New York, 1963, Edit. by Fox. D.; Davis M. 'J. Chem. Phys." 63, 67, 1966.

287. Smyth C.P. "J. Phys. Chem. Solids" 18, 40, 1961.

288. Lechner R.E. "Solid state Comm." 10, 1247, 1972;

Mansson T., Olsson L.G. and Larson K.E. "J. Chem. Phys." 66, 5817, 1977.

289. Egelstaff P.A. 'J. Chem. Phys.' 53, 2590, 1970.

290. London F. "Z. Phys. Chem. Abt." B11, 22, 1930; "Z. Phys." 63, 245, 1930.

291. Prigogine I. "The Molecular Theory of Solutions" North Holland, Amsterdam, 1957, Chapter13.

292. Koshlyakov N.S., Smirnov M.M. and Gliner E.B. "Differential Equations and Mathematical Physics" North Holland, Amsterdam, 1964.

293. Hochsladt H. "The Functions of Mathematical Physics" Wiley-Interscience, New york, 1971.

294. Abramowitz M. and Stequm I.A. "Handbook of Mathematical Functions" Dover, New York, 1965.

295. Eyring H., Henderson D. and Jost W. "Physical Chemistry an Advance Treatise" Academic Press, New York, 1975, Vol. XIA.

296. Carson B.C. "Special Functions of Applied Mathematics" Academic Press, New York, 1977.

297. Boas M.L. "Mathematical Methods in Physical Science" Wiley and Sons, New york, 1966.

298. Sched F. "Numerical Analysis" McGraw-Hill, New York, 1968, Schaum's Outline Series, p. 405.

299. Sansone G. 'Orthogonal Functions' Wiley-Interscience, New York, 1959.

300. Sobol I.M. "The Monte Carlo Method" The University of Chicago Press, Chicago, 1974.

301. Musher J.I. 'J. Chem.Phys.' 41, 2671, 1964.

302. Hartee D.R. "The Calculation of Atomic Structures" Wiley and Sons, New York, 1957.

Herman F. and Skillman R. "Atomic Structure Calculations" Prentice-Hall, Englewood Cliffs N.J., 1963.

303. Buckingham A.D. and Pople J.A. "Trans. Farady Soc." 51, 1173, 1955.

304. Matheson A.J. "Molecular Acoustics" Wiley-Interscience, New York, 1971.

305. Gordon S. and Dailey B.P. 'J. Chem. Phys." 34, 1084, 1961.

306. Ref. 224, 1966, Vol. V.

307. Dayan E. and Widenlocher G. "Compt. Rend. Acad. Sci. Paris" 257B, 883, 1963.

308. Bernstein H.J. "Pure. APPl. Chem." 32, 79, 1972.

309. Schug J.C. "J. Phys. Chem." 70, 1816, 1966.

310. Abraham R.J. "Mol. Phys." 4, 369. 1961.

311. Malinowski E.R. and Weiner P.H. "J. Chem. Soc." 92, 4193, 1970.

312. Weiner P.H., Malinowski E.R. and Levinston A.R. "J. Phys. Chem." 74, 14537, 1970.

313. Weiner P.H. and Malinowski E.R. "J. Phys. Chem. " 75, 1207, 1971.

314. Becconsall J.K. "Mol. Phys." 18, 337, 1970.

315. Reid R. and Sherwood T.K. "The Properties of Gases and Liquids" McGraw-Hill, New York, 1958, p. 156.

316. Sutter D.H. and Flygare W.H. "J. Am. Chem. Soc." 91, 6895, 1969.

317. Flygare W.H. and Benson R.C. "Mol. Phys." 20, 225, 1971.

318. Pauling L. "The Chemical Bond" Cornell University Press, New York, 1967.

319. Homer J. and Redhead D.L. "J. Chem. Soc. Faraday Trans. II" 68,1049, 1972.

320. Maclagan R.G.A.R. "J. Chem. Edu." 57, 428, 1980.

321. Zhadanov G.S. "Crystal Physics" Oliver and Boyd, Edinburgh, 1965, p. 252.

322. Natta G. and Passerini L. "Nature" 125, 207, 1930.

323. Mirkin L.I. "Handbook of X-Ray Analysis of Polycrystalline Matter" Consultants Bureau, New York, 1964, p. 419.

324. Corbridge D.E.C. and Lowe E.J. "Nature" 170, 629, 1952.

325. Sugawara T., Sakamoto Y. and Kanda E. "Sci. Rep. Res. Insts. Tokyo Univ." A1, 29, 1949.

326. Sugawara T. and Kanda E. "Sci. Rep. Res. Insts. Tokyo Univ." A1, 153, 1949.

327. Shinoda K. "Principle of Solutions and Solubility" Marcel Dekker Inc., New York, 1974, p. 68.

328. Ref. 224, 1966, Vol. I, p. 51.

329. "Encyclopedia of Chemistry" McGraw-Hill, New York, 1983, p. 1011.

330. Sirkin and Dyatkina "Structure of Molecules" Butterworth Scientific Publ., London, 1950.

331. Hildebrand J.H. "J. Am. Chem. Soc." 38, 1452, 1916.

332. Hildebrand J.H. "Phys. Rev." 21, 46, 1923.

333. Hildebrand J.H. and Scott R.L. "The Solubility of Nonelectolytes" Dover, New York, 1964.

334. Chao K.C. and Greenkorn R.A. "Thermodynamic of Fluids, an Introduction to Equilibrium Theory" Marcel Dekker, Inc., New York, 1975.

335. Redlich D. and Kister A.T. "J. Am. Chem. Soc." 71, 505, 1949.

336. Ellis J.A. and Chad K.C. "Am. Inst. Chem. Eng. J. " 18, 70, 1972.

337. Bradford D. "Phil. Mag." 38, 696, 1919.

338. Minkin V.I., Osipov O.A. and Zhdanov Y.A. "Dipole Moments in Organic Chemistry" Plenum Press, New York, 1970.

339. Oriani R.A. and Smyth C.P. "J. Chem. Phys." 17, 1174, 1949.

340. Kunerth W. "Phys. Rev." 19, 512, 1922.

341. Gerrard W. "J. Appl. Chem. Biotechnol." 22, 623, 1972.

342. Langmuir J. "Third Colloid Symposium Monograph" Chemical Catalog Co., New York, 1925.

343. De Lingny C.L. and Van der Veen N.G. "Chem. Eng. Sci." 27, 391, 1972.

344. Eley D.D. "Trans. Faraday Soc." 35, 1281, 1939.

345. Pierotti R.A. "J. Phys. Chem." 67, 1840, 1963.

346. Karasz F.E. and Halsey G.D. " J. Chem. Phys." 29, 173, 1958.

347. Barton J.R. and Hsu C.C. "Chem. Eng. Sci." 1313, 27, 1972.

348. Vdovennko V.M. Gurikov Y.V. and Legin E.K. "Radiokhimiya" 12, 670, 1970.

349. Moor W.J. "Physical Chemistry" Longman, London, 1972.

350. Pauling L. "Science" 1, 134, 1961.

351. Wood C.W., and Holliday A.K. "Physical Chemistry" Butterworths, London, 1967.

352. Hudson J.C. "J. Chem. Soc." 127, 1332, 1925.

353. Kobatake Y. and Hildebrand J.H. "J. Phys. Chem." 65, 331, 1961.

354. Burrows G. and Preece F.H. "J. Appl. Chem." 3, 451, 1953.

355. Hildebrand J.H. and Lamoreaux R.H. "Ind. Eng. Chem. Fundam." 13, 110, 1974.

356. Glaussen W.F. and Polglase M.F. "J. AM. Chem. Soc." 74, 4817, 1952.

357. Ref. 315., 1977, 3rd. Edi. p. 57.

358. Pierotti G.J., Derr E.L. and Deal C.H. "Ind. Eng. Chem." 51, 95, 1959.

359. Deal C.H. and Derr E.L. "Ind. Eng. Chem." 60, 28, 1968.

360. Wilson G.H. and Deal C.H. "Ind. Eng. Chem. Fundam." 1, 20, 1962.

361. Gmehling J., Rasmussen P. and Fredenslund A. "Ind. Eng. Chem. Process Des. Dev." 21, 118, 1982.

362. Anlunes C. and Tassios D. "Ind. Eng. Chem. Process Des. Dev." 22, 457, 1983.

363. Sitthiosoth S. "First Year Report" Chem. Eng. Dep., Aston University, 1985.

A Simple, General Method for Predicting the Relative Intensities of First-Order, NMR Spin-Spin Coupled Multiplets

John Homer and Mansour Sultan-Mohammadi
The University of Aston in Birmingham, Gosta Green, Birmingham B4 7ET, England

Preliminary undergraduate instruction in the principles of nuclear magnetic resonance spectroscopy normally includes discussion of the analysis of first-order, spin-spin coupled multiplets. It is well known that the number of multiplet lines is given by $2nI+1$ when n magnetically equivalent nuclei of spin I are adjacent to the resonant nucleus and cause the splitting of its resonance.[1] Similarly well known are the principles for predicting the distribution of line relative intensities in first-order multiplets.[1] Because these can be tedious to implement per se it proves advantageous to have simple rules that can be used speedily to predict the line relative intensities. While such rules for spin $\frac{1}{2}$ nuclei are often referred to, there appears to have been little reference to a general rule that permits the rapid evaluation of the relative intensities of the components of first-order multiplets that arise from coupling with any number of equivalent nuclei of any spin. The intention here is to present such a general rule.

Fundamentally, both the number of multiplet lines and their relative intensities depend on the possible combinations, $\Sigma_i\, m_i$, of the allowed spins of each nucleus, i; for each nucleus the quantum number m can adopt the values $I, I-1, I-2 \ldots. -I$. Consequently, the number of lines arising from coupling to n equivalent nuclei is $2nI + 1$ and the relative intensities of these is given by the number of times each value of $\Sigma_i\, m_i$ occurs. In the case of coupling to n spin $-\frac{1}{2}$ nuclei the relative intensities can be generated rapidly from the coefficients of the binomial series or, probably more popularly, using Pascal's triangle. The relevance of the latter (Fig. 1(b)) can be appreciated by reference to Fig. 1(a) which is the result of assuming that each additional nucleus splits each line in the preceding pattern into two. This is mirrored in Fig. 1(b) where each of the elements of any row are obtained by summing the two numbers directly above it and to its left. This is a specific case of a general rule.

When first-order multiplets arise from coupling to n nuclei of spin I the relative intensities of the components can be deduced by deriving appropriate Pascal-type "triangles". For this, *each element of a particular row is deduced by summing the 2I + 1 numbers above and to the left in the preceding row.* This is illustrated in Figure 2 for the case of $I = 3/2$. It can be seen from this that, for example, when $n = 3$, the ^{1}H resonance of $Na^+\, B_3H_8^-$ will occur as a 1:3:6:10:12:12:10:6:3:1 decet due to coupling with the three ^{11}B nuclei.[2]

With the availability of multinuclear-pulsed F-T NMR spectrometers and the consequent accessibility to a multitude of resonance spectra it is inevitable that students must be acquainted with the principles of analyzing spectra involving a variety of nuclear spins. It is possible that the triangulation rules outlined above may prove helpful in the analysis of first-order spin-coupled multiplets.

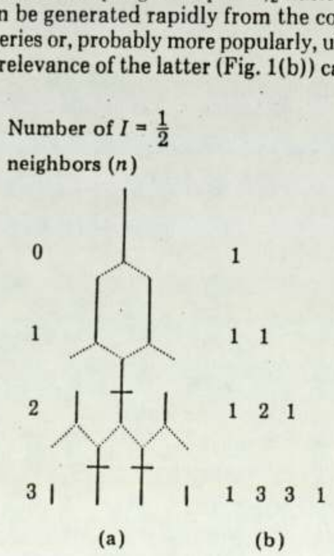

Figure 1. (a) The relative intensity distribution of first-order multiplet lines caused by coupling to n nuclei of spin $\frac{1}{2}$. (b) Pascal's "triangle."

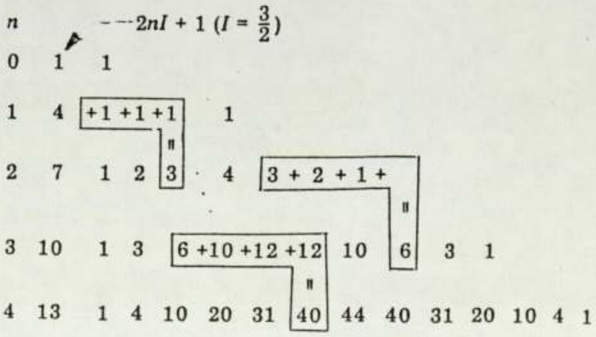

Figure 2. Construction of Pascal-type "triangle" for n nuclei of spin 3/2. In this example, $2I + 1 = 4$ so that four numbers from the preceding row must be added to obtain an item for the row below, as indicated.

---

[1] Akitt, J. W., "N.M.R. and Chemistry," Chapman and Hall, New York, **1973.**

[2] Jesson, J. P., and Muetterties, E. L., "Dynamic Nuclear Magnetic Resonance Spectroscopy," (*Editors:* Jackman, L. M., and Cotton, F. A.), Academic Press, New York, **1975.**